DISSERTATION

NEW APPROACHES TO THE IDENTIFICATION OF BIOMARKERS OF INFECTION

AND NERVE DAMAGE IN LEPROSY

Submitted by

Reem Al-Mubarak

Department of Microbiology, Immunology and Pathology

In partial fulfillment of the requirements

For the Degree of Doctor of Philosophy

Colorado State University

Fort Collins, Colorado

Spring 2012

Doctoral Committee:

       Advisor: Varalakshmi Vissa
       Co-Advisor: Patrick Brennan

       Michael McNeil
       James Bamburg

ABSTRACT

NEW APPROACHES TO THE IDENTIFICATION OF BIOMARKERS OF INFECTION
AND NERVE DAMAGE IN LEPROSY

Leprosy is an ancient disease and the first disease discovered to be caused by a bacterium, *Mycobacterium leprae*. *M. leprae* is an obligate intracellular pathogen that targets the Schwann cells in the peripheral nerves. As a result of this infection nerve damage and deformity occur.

There are three main obstacles that slow the progress in *M. leprae* research and diagnosis. The first obstacle is the absence of a good animal model to study host-pathogen interaction. The second is the absence of good biomarkers for leprosy diagnosis and sub grouping. The third obstacle is the inability to cultivate *M. leprae in vitro*, due to the extreme decay of the *M. leprae* genome and the resulting decline in the maintenance of metabolic pathways. This research thesis addresses each of these issues in turn.

The first goal of this study was to improve using the only available animal model, the nine-banded armadillo (*Dasypus novemcintus*), by studying its molecular response to infection by *M. leprae* (host-pathogen interactions). Several molecular techniques were applied based on the new technology of "omics" and the availability of the partial genome

sequence of the armadillo. Proteomic and lipidomic mass spectrometric profiles of infected and uninfected armadillo tissue (nerve, liver and spleen) were compared. The first partial armadillo nerve protein library was developed. The protein profile showed increased amounts of immunoglobulins IgG and IgM in the infected nerve. A decrease in a 15 kD protein that could be myelin P2 was observed in the infected nerve. We also detected antibodies against myelin P2 in the sera of leprosy patients. The lipid profile of armadillo tissues showed an increase in certain lipid groups, mainly neutral triacylglycerols (TAGs). These TAGs contained acyl chains of specific lengths and unsaturation (mono-and di-unsaturation) in all three types of infected tissues in comparison to naïve tissues. The lipidomics finding was supported by the detection of increased expression of several genes for unsaturated fatty acids and TAG synthesis such as stearoyl-CoA desaturase 9 (SCD9), elongase 5 (ELOVL5), diacylglycerol acyltransferase (DGAT) and fatty acid desaturase (Δ5d) in the infected tissues.

The second study focused on identifying needed biomarkers for the diagnosis of leprosy and differentiates between leprosy sub-groupings. In this case a mass spectrometric metabolomics approach was used to study the circulatory biomarkers in the sera of newly diagnosed untreated leprosy patients. We found a significant increase in the abundance of certain polyunsaturated fatty acids (PUFAs) and phospholipids in the high-bacterial index (BI) patients, when compared with the levels in the low-BI leprosy patients. These PUFAs are known to exert anti-inflammatory properties that may promote *M. leprae* survival. This finding is in agreement with the overall phenotype (increase anti-inflammation and high bacterial load) in the high-BI leprosy patients.

The third part of this study addressed the inability to grow *M. leprae* in culture. Here the hypothesis was that a test of viability (using molecular genetics techniques), in the presence or absence of particular nutrients, would lead to identifying a medium or nutrients required for the *in vitro* maintenance of *M. leprae.* Based on the *M. leprae* genome and the genome-based metabolic databases (Metagrowth), several genes were found to be lost from major metabolic pathways in *M. leprae*. Therefore, the objective was to provide in the medium those metabolites missing because of the pathway disruption. Different culture media were tested to maintain *M. leprae in vitro*. The viability of the bacteria in different media formulations was compared based on testing expression of several *M. leprae* transcripts and the 16S rRNA using quantitative real-time PCR (qRT-PCR). Surprisingly, the results from all of these media trials demonstrated that the simple addition of 2% glycerol to 7H12 media supported *M. leprae* viability up to 21 days, compared to the basal medium (7H12) that showed a decrease in *M. leprae* viability after 7 days. On the other hand, the addition of 0.1% sodium thioglycolate to 7H12 media reduced *M. leprae* viability by 3 and 7 days.

Many leprosy patients suffer irreversible peripheral nerve damage resulting in blindness or other disabilities as a consequence of *M. leprae* infection. Until now the mechanisms of nerve damage have not been fully elucidated due to lack of *in vitro* condition to cultivate *M. leprae* and animal model to study host-pathogen interaction.

In this research dissertation progress was made to understand *M. leprae*-pathogen

interaction. Using new approaches (metabolomics, proteomics and lipidomics) helped in

finding marker (s) for the infection and nerve damage in leprosy.

ACKNOWLEDGEMENTS

I would like to graciously thank my adviser Dr. Varalakshmi Vissa, who guided me
through the whole process and taught me so many things that cannot be learned in class or
from a book. I am deeply grateful to my graduate committee: Drs. Patrick Brennan,
Michael McNeil and James Bamburg for their guidance and patience in assisting me with
my research and thesis work and in helping me to achieve my academic goals.

I am grateful to my colleagues in the mycobacterial and leprosy research laboratories.
I would like to thanks my family for their support and pushing me to do my best and for
always being there to help me along the way.

TABLE OF CONTENTS

CHAPTER 1
Literature Review Page

CHAPTER 2
SERUM METABOLOMICS REVEALS HIGHER LEVELS OF
POLYUNSATURATED FATTY ACIDS IN LEPROMATOUS LEPROSY:
POTENTIAL MARKERS FOR SUSCEPTIBILITY AND PATHOGENESIS

CHAPTER 3
THE LIPIDOME OF *M. LEPRAE* INFECTED TISSUES: ACCUMULATION OF UNSATURATED TRIACYLGLYCEROLS IN LEPROSY

CHAPTER 4

Approaches to the Identification of Biochemical Markers of Infection and Nerve Damage in Leprosy; Proteomics and Humoral immune response of *M. Leprae* infected tissue

CHAPTER 5
STUDIES ON THE EFFECT OF *IN VITRO* GROWTH MEDIA ON GENE EXPRESSION AND DNA CONTENT IN *M. LEPRAE*, AND IDENTIFICATION OF GENETIC MARKERS SUITABLE FOR MEASURING VIABILITY OF *M. LEPRAE* USING MOLECULAR METHODS

5.3. MATERIALS AND METHODS

CHAPTER 6

LIST OF TABLES

LIST OF FIGURES

LIST OF ABBREVIATIONS

SCs	Schwann cells (SCs)
PIM	Phosphatidylinositol mannosides
LAM	Lipoarabinomannan
TLRs	Toll-like receptors
LL	Lepromatous
BT	Borderline tuberculoid
BB	Borderline
BL	Borderline lepromatous
AFB	Acid fast bacilli
PB	Paucibacillary
MB	Multibacillary
BI	Bacterial indices
NF	Neurofilament
MS	Mass spectrometry
TOF	Time-of-flight
ESI	Electrospray ionization
RT	Retention time
UPLC	Ultrahigh pressure liquid chromatography
MS	Mass spectrometry
PUFAs	Polyunsaturated fatty acids
EPA	Eicosapentaenoic acid
AA	Arachidonic acid
DHA	Docosahexaenoic acid
PCA	Principal Component analysis
ROC	Receiver operating characteristic
TAG	Triacylglycerols
LDs	Lipid droplets
2DE	Two-dimensional gel electrophoresis
PAS	Periodic acid Schiff
PNS	Peripheral nervous system
IG	Immunoglobulin
RR	Radiorespirometry
qRT-PCR	Quantitative Real time PCR

CHAPTER 1

Literature Review

1.1. *MYCOBACTERIUM LEPRAE* (*M. LEPRAE*)

M. leprae was first observed by Dr. G. Armauer Hansen (1874) in Bergen, Norway

through examining the leprosy nodules in skin lesions and named *Bacillus leprae*. It was

first assigned to the genus *Mycobacterium* by Lehmann and Neumann in 1896 **(Lehmann**

K., 1896). The bacillus is an obligate intracellular pathogen and it is the only bacterium

known to infect the peripheral nerve. The bacilli are usually located within endothelial and

perineural, Schwann cells (SCs) and macrophages in the cooler areas of the body. The

bacilli can be in a single or clump (globi) form inside these cells **(Meyers W., and Marty**

A., 1991). The bacillus can be classified as Gram-positive, acid-fast because the high lipid

contents in the cell wall (mycolic acid) makes it resistant to decolourization by acid-

alcohol using the Ziehl-Neelsen stain.

M. leprae has an extremely long generation time (2 weeks); this causes the long

incubation periods (2–10 years) of the disease. *M. leprae* has never been cultivated *in vitro*

and *in vivo* model systems its growth has been very limited. In 1960 progress was made by

Shepard, when he observed limited multiplication of *M. leprae* after injection into mouse

footpads **(Shepard C., 1960).** The inoculated nude mouse footpads develop macrophages

full of live bacilli within 6 months. The mouse granuloma model has been used to study

the response of immune cells to infection by *M. leprae* **(Chehl S., 1983 and Adams L.,**

2002). Also, in 1971 the nine-banded armadillo (*Dasypus novemcinctus*) showed susceptibility to *M. leprae* and to develop a systemic infection. **(Kirchheimer W., 1971).** These two approaches of infecting mouse footpads and armadillo became valuable sources for *in vitro* studies of live *M. leprae.*

Moreover, in 2001 the availability of *M. leprae* genome sequence enables genomic comparison. Comparing the genome of *M. leprae* (3.27Mb) to that of *M. tuberculosis* (4.41Mb), showed extreme reduction in the *M. leprae* genome. There are high levels of inactive or pseudogenes (41%) as only about half the genome encode functional genes **(Cole S., 2001).** Recently, it was shown that a large number of *M. leprae* pseudogenes were transcribed during growth in the nude mouse foot pad. The transcription of these genes were based on association with gene clusters or located downstream of functional ORFs. However, the majority of these pseudogenes were nonfunctional, "silenced" inactivated genes **(Williams D., 2009).**

1.1.1 *M. leprae* Structure

M. leprae like other mycobacteria is characterized by a complex cell wall structure rich in lipids (30–60% of dry weight). This envelope is organized into three layers (i) the plasma membrane, (ii) the cell wall and (iii) the capsule **(Figure 1.1).** The plasma membrane is composed of phospholipids in a bi-layer arrangement and proteins. The most common phospholipids are phosphatidylglycerol, diphosphatidylglycerol, phosphatidylethanolamine and various forms of phosphatidylinositol mannosides (PIMs). PIMs are the base for the lipoglycans that are anchored in the plasma membrane and the

2

outer surface of the cell wall: lipoarabinomannan (LAM) and lipomannan (LM). LAM is made of a linear chain of α-D-mannose units linked in a (1→6) linkage and an arabinan part that is linked to the mannose chain and is composed of α-D-Ara-furanose units linked in a 1→5. In mycobacteria there are three types of LAM differing by their capping structure. These include the Man-capped LAM (ManLAM) in slow growing mycobacteria, phosph-myo-inositol-capped LAM (PILAM) in fast growing mycobacteria or non-capped LAM (AraLAM). *M. tuberculosis* is capped with ManLAM (around seven caps per molecule) while *M. leprae* is very weakly capped, with only one cap per molecule. The cell wall skeleton of all mycobacteria is composed of a peptidoglycan composed of a series of N-acetylglucosamine and N-muramic acid (glycolylated or acetylated) units. However, the muramic acid residues of *M. leprae* are only N-acetylated, unlike *M. tuberculosis* that has both N-acetylated and N-glycolylated versions **(Bhamidi S., 2011).** The muramic acid is associated with tetrapeptide chains of L-alanine or glycine (in the case of *M. leprae)*, D-isoglutaminyl, meso-diaminopimetyl (DAP), D-alanine to allow the link between sugar chains. The peptidoglycan is covalently attached to arabinogalactan (AG) esterified with mycolic acids at the nonreducing end of the arabinan. The AG is composed of D-Ara-furanosyl linked in a (1→5) linkage and attached to the galactan core through the C-5. The galactan part of AG is linked to the peptidoglycan at C-6 of some muramyl residues via the linker disaccharide (Rha-GlcNAc)-P at the reducing end. The mycolic acids are composed of two chains: the α-chain and the β-hydroxy meromycolic chain that vary in chain length, modifications and branching based on the species **(Daffe and Draper, 1998, Guenin-Macé, L´., 2009).** Recently it has been shown that *M. leprae* has lower amounts of galactofuranose and arabinofuranose in the AG compared to *M. tuberculosis*. The cell wall

of *M. leprae* has more AG molecules per PG molecule compared to *M tuberculosis*. Bahamidi *et al*. also confirmed that *M. leprae* is lacking methoxy mycolate and only has α- and keto-mycolates **(Bhamidi S., 2011).**

Beside these lipids, some mycobacterial species also contain some non-covalently linked lipids such as trehalose and phthiocerol lipids. Trehalose is formed by two glucose units linked in α,α-(1→ 1) linkage. Sulfolipid 1 (SL-1) is a sulphated trehalose that is esterified by four fatty acids. Diacyltrehaloses (DAT) are composed of a stearic acid at position 2 and a methyl fatty acid at position 3 of the trehalose. The phthiocerol lipids comprise phthiocerol dimycocerosates (DIM), and phenolphthiocerol dimycocerosates or phenolic glycolipids (PGL), which are only present in slow growing mycobacteria. Some *M. tuberculosis* strains have PGL-tb, which consists of the trisaccharide 2,3,4-tri-O-methyl L-fucosyl-α(1→3) L-rhamnosyl-α(1→3)-2-O-methyl L-rhamnosyl attached to the phenol hydroxyl group of phenolphthiocerol dimycocerosate. All *M. leprae* strains have PGL-1 with the tri saccharide 3,6-dimethyl-β-D-glucosyl (1→4) 2,3- dimethyl-α-l-rhamnosyl (1→2) 3-methyl-α-l-rhamnosyl linked to the phenolphthiocerol lipid core **(Brennan P., 1984).** The capsule is mainly composed of proteins and polysaccharides such as glucan, arabinomannan and mannan. The glucan is composed of five or six repeating units of (1→4) linked α-D-glucose and substituted at position 6 by a mono or diglucosylated unit. The major proteins of the capsule include the19 kD protein, and the proteins of the antigen 85 complex, which mediate mycolic acid transfer onto arabinogalactan and trehalose **(Daffe and Draper, 1998, Guenin-Macé, L´., 2009).** **Figures 1.1** illustrates the structure of *M. leprae* cell wall.
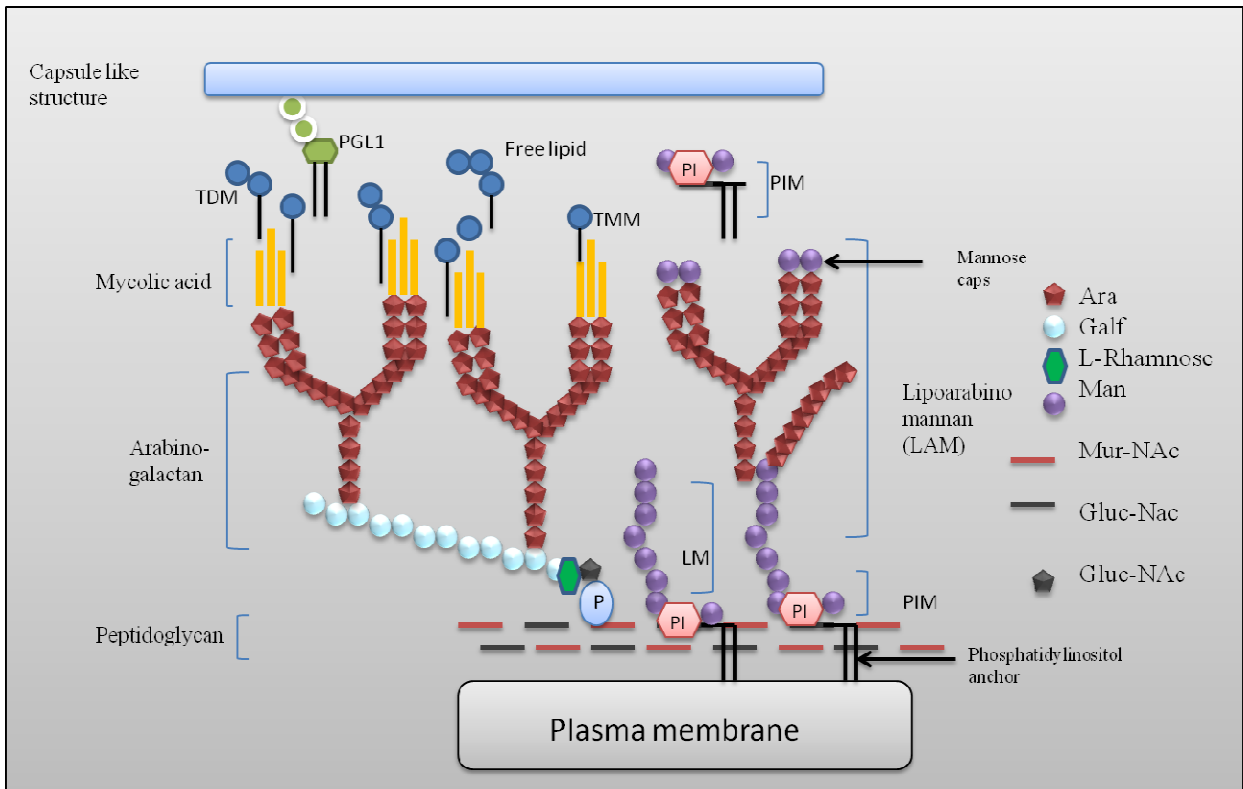
Figure 1.1: A model of *M. leprae* cell wall (Redrawn based on Brennan and Crick, 2007).

1.1.2 Significant roles of mycobacterial lipids

Mycobacterial lipids are important for the bacterial uptake by macrophages such as using the complement receptors (CRs) that recognize C3-opsonized mycobacteria and PIM via its lectin domain. Also, macrophage mannose-receptors (MR) can bind mannose and fucose-containing glycoconjugates on the bacterial surfaces. Mycobacterial lipids can also interact with toll-like receptors (TLRs) on macrophages that result in activation of signaling pathways through NF-κB, AP-1 and mitogen-activated proteins. For example, non-capped LAM, LM and PIM are activators of TLR2 leading to induction of host

immune response against the infection. Some mycobacterial lipids (ManLAM, trehalose 6,6-dimycolate (TDM)) can inhibit phagosomal maturation into phagolysosomes and blocks phagosomal acidification which are important for bacterial survival. PGL-1 in *M. leprae* is important for bacterial adhesion to Schwann cells **(Rambukkana A., 2001).** Moreover, LAM and PGL-1 can both suppress the production of pro-inflammatory mediators by phagocytic cells. Also, bacterial lipids can be processed by host enzymes such as mycobacterial cardiolipin by the macrophage phospholipase A2 and transport of the resulting lysocardiolipin out of the phagosomal compartment **(Guenin-Macé, L., 2009).** Cell wall components or lipids such as phosphatidylinositol mannosides (PIMs), peptidoglycan (PG), trehalose dimycolate (TDM), phenolic glycolipids (PGL), lipoarabinomannans (LAM) released by the bacterium can act either as antigen that stimulates the immune response or it can modulate the function of the host cell and suppress the inflammatory response **(Russell D., 2002).**

1.1.3 *M. leprae* pathways and *in vitro* trials

M. leprae is an uncultivable organism with slow growth rate with an approximate generation time of 12–14 days. Analysis of the genome sequence of *M. leprae* showed that only half of the small genome contains protein-coding genes, while the remainder consists of pseudogenes and non-coding regions. Therefore, there are gene deficiencies in many pathways. Genes for detoxification of reactive oxygen and nitrogen species are missing such as catalase-peroxidase (**Visca, P., 2002).** It lacks some genes needed in the enzymatic steps in glycolysis and the TCA cycle such as the enzyme that converts glucose-1P to glucose-6P and the enzyme that converts pyruvate to acetyl-CoA. *M. leprae* was also

found to have a deficiency in one of the trehalose biosynthesis pathways (TreY-TreZ pathway) and fatty acid biosynthesis (it cannot synthesize malonyl-CoA, lacks acetyl-CoA ligase and glutaryl-CoA dehydrogenase and lacks most of the lipase genes). In addition *M. leprae* is missing genes in pathways for thiamine (vitamin B1) and thiamine-PP biosynthesis. The genes for siderophore biosynthesis are also missing. *M. leprae* also lost anaerobic and microaerophilic electron transfer systems (making ATP from the oxidation of NADH). Like *M. tuberculosis*, *M. leprae* highly depends on lipid degradation and the glyoxylate shunt for energy **(Cole S., 2001).**

The first attempt to grow *M. leprae* was done by Shepard **(Charles B., 1960)** using footpad of athymic mice with Balb/C background. This mouse strain showed great susceptibility to *M. leprae* due to mutations in the main innate immune pathways (Nramp) and the absence of the T-cell mediated immunity **(Truman R., 2008).** Testing the viability of *M. leprae* derived from mouse foot pad or artificial media depends on the metabolic activity of the cells. This is done through measuring the metabolic activity with radiorespirometry (the oxidation of ^{14}C-labeled palmitic acid). Another method is by testing the cell wall integrity using a fluorescence viability staining assay **(Lahiri R., 2005).** Detection of *M. leprae* RNA such as 16SrRNA is a new molecular method for rapid assessment of bacterial viability **(Kurabachew M., 1998).**

1.2. LEPROSY

Leprosy is chronic, infectious disease. It is primarily a disease of the skin and peripheral nervous system. At the later stage of the disease the eyes, bone, lymph nodes and nasal structures can be involved. It is one of the unique diseases caused by an infectious agent and leads to non-traumatic nerve damage and blindness **(Hastings R. and Gillis T., 1988).**

1.2.1 Clinical features of leprosy

Patients commonly present with skin lesions (hypopigmented or erythematous), numbness or weakness caused by peripheral nerve involvement, or more rarely, a painless burn or ulcer in the hand or foot that results in deformities. Some patients may also develop a leprosy reaction during the chronic course of leprosy. Major nerves involved are the great auricular nerve, ulnar nerve, median nerve, radial-cutaneous nerve, posterior tibial nerve and lateral popliteal nerve associated with enlargement, with or without tenderness **(Croft R., 1999).**

1.2.2 Classification of leprosy

Leprosy is a spectral disease that can range from no disease, to localized disease, all the way to widespread and progressive disease. After exposure to *M. leprae*, the majority of the populations will develop adequate protective immunity to the infection and not develop clinically detectable symptoms. The minority of individuals that develop clinical leprosy can be classified into a five group spectrum based on their immune system **(Spierings E., 2000).** According to The Ridley–Jopling classification leprosy patients can be classified

8

into polar tuberculoid (TT), borderline tuberculoid (BT), borderline (BB), borderline lepromatous (BL), and polar lepromatous (LL) stages **(Ridley D., and Jopling W., 1966).** The TT form can be associated with rapid and severe nerve damage and is characterized by a strong Th 1 cytokine response (IFN-γ, IL-2, IL-7, IL-12, IL-15 and IL-18) with a single skin lesion or rarely two to three asymmetrical lesions with well-formed granulomas. It could also involve neural symptoms that include numbness, pain, tingling, muscle weakness. Histological section of TT skin usually shows few or no acid-fast bacilli (AFB), small tuberculoid granulomas, with Langhans giant cells and mostly CD4 positive cells. The LL form is associated with chronicity and long-term complications. It is dominated by a Th 2 response (IL-4, IL-5, IL-10) with lepromatous infiltrates that can be diffuse or nodular. The enlargement of the nodules in the advanced disease can destroy underlying structures such as the nasal cartilage causing a saddle nose deformity. Skin histology shows numerous AFB, diffuse foamy cells infiltration with few lymphocytes and plasma cells. The Bacterial Index (BI) used in this classification is based on quantification of average number of bacteria using Ridley's logarithmic scale that varies from 6+ to 1+ **(Gillis T., and Hastings R., 1992).**

Another type of leprosy classification is based on a WHO classification that depends on clinical signs used in the field. The patients are classified as paucibacillary if the slit skin smears are negative and the patient had five or fewer skin lesions, and multibacillary if the smears are positive for AFB and the patient had more than five skin lesions **(Worobec S., 2009). Figure 1.2** shows different type of leprosy classification.
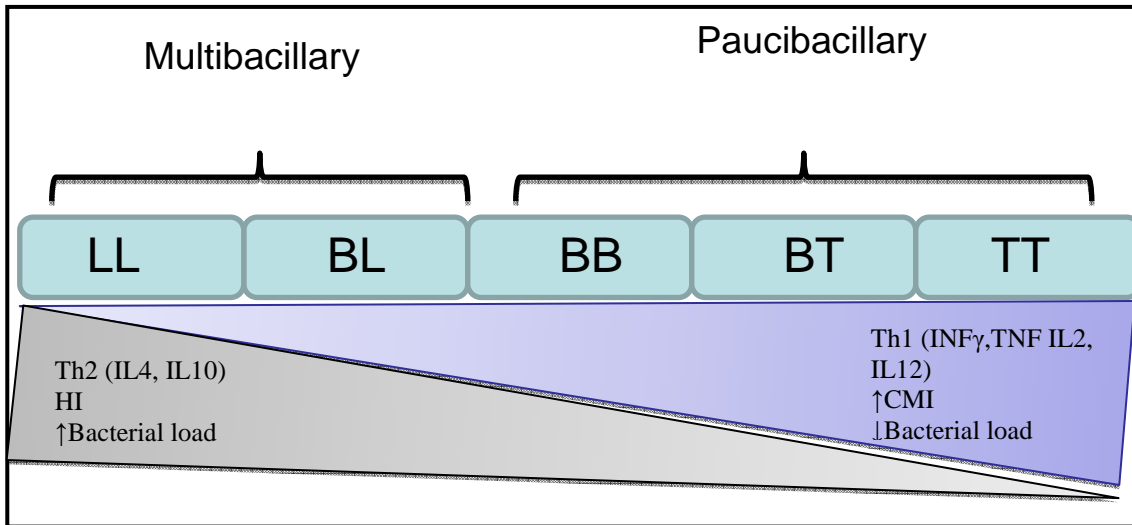
Figure 1.2: Leprosy classification: based on Ridley-Jopling (R-J) 5-group scheme (LL –

TT), and for clinical and treatment purposes leprosy also classified according to the WHO

to 2 group system (multibacillary-paucibacillary).

1.2.3 Leprosy reaction

Reactions in leprosy are sudden and can occur at any time (before, during or after treatment) in the skin, or nerves, or both and cause inflammation and irreversible damage. This is due to immune exacerbation against *M. leprae* and its component antigens. There are two major types of reactions in leprosy; i- Erythema nodosum leprosum (ENL) or type II reactions (which is mainly in the lepromatous form of the disease), and ii- Reversal reaction (RR) or type I reactions (which is particularly seen in the borderlines). The ENL reaction is an acute and urgent inflammation that occurs in one-half of leprosy patients (LL or BL). The patients will experience erythematous skin lesion, fever, malaise, myalgia, neuralgia, arthralgia and ophthalmic symptoms. These disease symptoms could result in peripheral motor and sensory nerve injury if not treated early. The initiation of the ENL reaction is thought to be due to a change in the immunological response in the patient with increase in immune complexes (IC) when the circulating antibodies are bound to the antigens in the skin **(Scollard D., 1992).** The ENL patients have massive infiltration of neutrophils in the lesions. There is also an increase in IFN-γ, TNF-α, IL-1β, IL-6, IL-8, IL-10**,** and IL-4. These cytokines promote antibody production and suppress T cell responses **(Yamamura M., 1992).** The ENL patients have also elevated levels of C-reactive protein, amyloid A protein and α-1 antitrypsin.

Type I reaction is characterized by edema, tenderness, erythema and neuritis that will resulted in sensory motor loss and nerve damage. The cause of the type I reaction is thought to be the stimulation of cell-mediated immunity (CMI) to *M. leprae* in the skin and nerve, resulting in inflammatory response with Th1 cytokines (IL-2, IFN-γ and TNF-α) and

irreversible tissue damage **(Yamamura, M., 1992).** In type I reaction there is an increase

in granuloma formation with predominant CD4^{+} T cells that produce Th1 cytokines and

also CD8^{+} that has a cytotoxic effect. Type-I T cells produce IFN- γ, TNF-α and TGF-β

that cause SC lysis **(Spierings E., 2000, WHO, 1998).**

1.2.4 Diagnosis of leprosy

Diagnosis of leprosy is based on clinical criteria, such as the presence of a skin patch or

patches with definite loss of sensation. Finding acid-fast bacilli in the skin or nerve

biopsies is another important aspect in the diagnosis. Another common procedure to

monitor the patients is the semi-quantitative enumeration of acid-fast organisms using the

slit-skin smear from infected patients before and after treatment. However, acid-fast

staining (AFS) method has low sensitivity that requires 10^3 bacilli per gram of tissue.

Therefore, using this method for diagnosis is difficult at the early stage of the disease or for

the tuberculoid form.

Molecules released by intracellular mycobacteria are either proteins or lipids that act as

antigens and are recognized by the immune system (cellular and humoral immune

response). Several immunological tests have been used for diagnosis. The lepromin skin

test is mainly used to test the ability to form granulomas after injection of a whole cell

suspension of killed *M. leprae.* Mainly the borderline tuberculoid (BT) and tuberculoid

(TT) will show positive reaction after 28 days compared to lepromatous (LL) patients, due

to the presence of antigen-presenting cells and CD4^{+} lymphocyte in TT and BT leprosy

patients that successfully eliminate the bacilli. However, the lepromin test is not commonly

used to diagnose leprosy, due to low specificity **(Brennan P., 2000).** A serological test, such as measuring the antibody (IgM) titer against PGL-1 by ELISA has been used since 1987. This test is mainly used to distinguish between different forms of leprosy **(Douglas J., 1987, Moudgil K., 1989).** The LL form usually has large amount of antibodies compared to the TT form. Testing for cell-mediated immune (T-cell) response is another diagnostic test that depends on the release of IFN-γ against *M. leprae* major antigens ESAT-6 (early secreted antigenic target-6 kD) and CFP-10 (culture filtrate protein-10) **(Aráoz R., 2006 and Pinheiro R., 2011).** These serological tests (detection of antibodies and cytokines) lack the specificity since they may reflect past infection.

Now with the availability of the *M. leprae* genome sequence since 2001, another approach is used for diagnosis based on molecular tests such as PCR assay to amplify genes encoding various *M. leprae* proteins such as the antigen 85 genes, 65 kD or the 16S rRNA from leprosy patient biopsy. These assays have been reported to be sensitive to 1-10 organisms and to be positive in 95-100% of BL/LL and 50-70% of TT, BT cases **(Kox L., 1997).**

1.2.5 Transmission of leprosy

The exact mode of *M. leprae* transmission is still unknown, but several studies pointed out that leprosy is transmitted from person to person through intact skin or penetration of wounds, or by inhalation of bacilli into nasal mucosa **(Hastings R., 1988).** The exposure to leprosy is believed to be through environmental sources such as armadillos or soil. Several studies reported the presence of viable *M. leprae* in soil or water samples in endemic areas

13

(Lavania M., 2008, Matsuoka M., 1999). *M. leprae* is known to remain viable for several days (up to 45 days) in droplets from the infected upper respiratory tract, in dried discharges from ulcers, or on fomites such as bedding or clothing **(Davey T., 1974, Job C., 1999).** Also it was found that *M. leprae* survives longer in moist and humid conditions. Multibacillary patients have been shown to excrete *M. leprae* from their nasal mucosa and skin, and repeated contact with these patients is also a source of transmission **(Job C., 2008).**

Recently, with the ability to conduct molecular strain typing based on polymorphisms either short tandem repeats (STRs) or variable numbers of tandem repeats (VNTR) **(Matsuoka M., 2000)** enables identifying the transmission patterns of leprosy. A new study in India reported the viability of *M. leprae* from patient discharge in to the environment (soil) using 16S rRNA as marker. In this study, author correlate the *M. leprae* strain found in the soil to that from patient in the same area. Both sources have the same strain (type 1) based on SNP analysis **(Turankar R., 2011).**

1.2.6 Prevalence of leprosy

Most individuals exposed to leprosy develop protective immunity (subclinical symptoms). Only a minority (5–10%) of individuals exposed to *M. leprae* will develop symptoms of leprosy, ranging from tuberculoid (localized lesions and low bacillary load) to lepromatous (generalized lesions and high bacillary load) **(Britton W., 1993).**

There are currently 192,246 leprosy cases registered for treatment worldwide with more than 228,474 new cases diagnosed during 2010 **(WHO).** Most of the leprosy cases are concentrated in India, Brazil, Indonesia, Bangladesh, Central African Republic, Democratic Republic of Congo, Madagascar, Mozambique, Nepal, and the United Republic of Tanzania. The new cases with multibacillary leprosy ranged from 32.70% in the Comoros in Africa to 95.04% in the Philippines. The new cases with grade 2 disabilities ranged from 1.45% in Liberia to 22.8% in China **(WHO Report 2010).** In 1991 the WHO declared the year of 2000 as a target for leprosy elimination (1 case per 10,000 population). Some highly endemic countries have now reached elimination at the national level. The WHO global strategy for leprosy 2006-2010 was to reduce global leprosy numbers, improved diagnosis, management leprosy services for general health care and develops adequate tools for disability management and rehabilitation.

1.2.7 Leprosy treatment

Sulfone (4-4´-diaminodiphenylsulfone, DDS) a compound was first synthesized in 1908 from *p*-nitrothiophenole by German scientists, Fromm and Whittmann, to treat streptococcal infection. In 1945 dapsone was used on leprosy patients and was reported to inhibit the progress of leprosy **(Zhu Y., 2001).** In the 1950s, dapsone was introduced as standard chemotherapy treatment for both multibacillary and paucibacillary leprosy **(Lowe J., 1950, 1951).** However, long-term mono-therapy with dapsone resulted in emergence of dapsone-resistant leprosy. Dapsone resistance resulted from misssense mutations in the *folP1* gene encoding dihydropteroate synthase. Other antimicrobial drugs such as rifampin and clofazimine were introduced for the treatment of leprosy. Drugs with anti-leprosy

activity, such as clofazimine proved to be only weakly bactericidal against *M. leprae.*

Other effective chemotherapeutic agents against *M. leprae* include ofloxacin (OFLX),

minocycline (MINO), levofloxacin (LVFX), sparfloxacin (SPFX), moxifloxacin (MFLX)

and clarithromycin (CAM). To overcome the problem of drug-resistance and to improve

treatment efficacy, the WHO recommended multidrug therapy (MDT) in 1982 for leprosy

(Scollard D., 2006). The MDT regime consists of three drugs: dapsone, rifampin, and

clofazimine. Dapsone and clofazimine are weakly bacteriocidal and rifampin is the most

effective bactericidal drug against *M. leprae*.

    Dapsone (4,4-diaminodiphenyl sulfone) is a synthetic sulfone. It targets

dihydropteroate synthase, an enzyme in the folate biosynthesis pathway, by acting as a

competitive inhibitor of *p*-aminobenzoic acid. **Rifampin** (3-{[(4-methyl-1-piperazinyl)-

imino]-methyl} is the bactericidal component of all recommended anti-leprosy drugs

treatment regimes. A single dose of 1,200 mg can reduce the number of viable bacilli in a

patient's skin to undetectable levels within a few days. The target for rifampin in

mycobacteria is the β-subunit of the RNA polymerase encoded by *rpoB* **(Scollard D.,

2006).**.**Clofazimine** [3-(*p*-chloroanilino)-10-(*p*-chlorophenyl)-2,10- dihydro-2-

(isopropylimino)phenazine] is a substituted iminophenazine. The mechanism of action is

not clear yet. It is highly lipophilic and binds preferentially to mycobacterial DNA at base

sequences containing guanine. Clofazimine has high intracellular levels in mononuclear

phagocytic cells. It acts on the immune cells, mainly altering the function of monocytes

and macrophages. It can inhibit the mobility of neutrophils and increase the number and

size of lysosomes and phagolysosomes of monocytes **(Gurfinkel P., 2009).**

Ofloxacin (4-fluoroquinolone) is a fluorinated carboxyquinolone. It has moderate anti-*M. leprae* activity. The mechanism of action of ofloxacin on *M. leprae* is unknown. In other bacteria it appears to inhibit DNA replication by inhibiting the DNA gyrase, containing two A-subunits (GyrA) and two B-subunits (GyrB) **(Scollard D., 2006).**

Leprosy treatment

Multibacillary (MB) leprosy (Adult)	Paucibacillary (PB) leprosy (Adult)
Rifampicin: 600 mg once a month	Rifampicin: 600 mg once a month
Dapsone: 100 mg daily	Dapsone: 100 mg daily
Clofazimine: 300 mg once a month and 50 mg daily Duration= 12 months.	Duration= six months

The WHO reported some rifampicin-resistant leprosy strains. These were mainly found when patients were given rifampicin monotherapy, or in combination with dapsone, to dapsone-resistant patients. [http://www.who.int/lep/en/].

1.2.8 Treatment during reaction

Mild ENL is treated with non-steroidal anti-inflammatory drugs (NSAIDs) such as aspirin. The treatment for severe ENL usually involves anti-inflammatory drugs such as corticosteroids that temporarily relieve the symptoms but do not reverse the damage. Another effective treatment for ENL is use of thalidomide, which inhibits recruitment and

cytokine production from polymorphonucleated cells (PMNs). Thalidomide drug has also been found to inhibit TNF-α and IgM responses. It also enhances IL-2 (Th1) production and promotes neutrophil apoptosis. Other anti-inflammatory drugs such as clofazimine and pentoxifylline have also been used **(Pinheiro R., 2011).** Clofazimine (CLF), which binds to mycobacterial DNA, inhibits mycobacterial growth and has slow bactericidal effects on *M. leprae.* It also has an anti-inflammatory property that makes it a useful drug to control erythema nodosum leprosum (ENL) reactions by mechanisms still poorly understood. It was proposed that it could decrease motility of neutrophils and lymphocytes transformation by disturbing antigen processing and presentation.

Other drugs that have been used to treat type 2 reactions, but with poor output, are cyclosporine, azathioprine, methotrexate, pentoxifylline and mycophenolate. From all these drugs that are used to treat a type 2 ENL reaction, it seems that the mechanisms of action are by inhibition of lymphocyte proliferation and antibody production. These drugs can also inhibit production of TNF-α, IL-2 and pro-inflammatory cytokines production **(Kahawita I., 2008).**

1.2.9 Immunoprophylaxis and chemoprophylaxis

Bacille Calmette Guerin (BCG) vaccine has been used in endemic countries to give some protection against leprosy. The first dose of BCG gave protection of between 14% and 80% against leprosy, while a second dose gave protection of between 0% and 50%. A single dose of rifampicin given to close contacts of newly diagnosed leprosy patients showed 57% efficacy in reducing new cases of leprosy **(Cross H., 2010).** Another study showed the protective effect of immune- and chemoprophylactic methods in controlling

leprosy. This was done through using BCG vaccination given in infancy, in combination with rifampicin given to leprosy contacts. However, the effect of this combination was more beneficial to contacts of PB form rather than with MB form **(Schuring R., 2009).**

1.2.10 Restoration of nerve function

Several approaches have been carried out to aid in nerve regeneration, such as using steroids or anti-inflammatory drugs, surgical intervention, neurotrophic factors (NTF) to stimulate SC-axon interaction, induction of SC proliferation and modulation of immune response. All these approaches had limited success **(Shetty V., 2000).**

1.3. OVERVIEW OF THE PERIPHERAL NERVOUS SYSTEM (PNS)

Schwann cells (SC) of the PNS are essential for the survival and function of the neurons; it wrap around the axons. These cells (SCs) were discovered by Theodore Schwann while investigating peripheral nerves. The function of the SC is to help myelinate the axons and direct the neurons. Myelination occurs only if the axonal diameter is greater than 0.7 μm and it requires direct contact between SCs and the axon. The SCs develop after birth from immature cells to become myelinating or non-myelinating SCs **(Figure 1.3)**. The immature cells first go through the myelination pathway at birth and then go through the non-myelin pathway later on in development **(Bhatheja K., 2006).** Both myelinating and non-myelinating SCs produce an extracellular matrix that forms a basal lamina containing collagen around the axon. The neuron is made up of axon-Schwann cell units and several neurons (fascicles) are surrounded by dense fibrous tissue

wrapping the perineurium. Further, these fascicles are also grouped and make a nerve trunk that is surrounded by another tissue called the epineurium.

Myelinating SCs form a fatty layer (myelin) that surrounds large axons to increase conductivity of the neuron. The unmyelinated SCs surround multiple small axons separated with cytoplasm. Myelin is formed by the differentiation of the plasma membrane of SC. Myelin is composed of multilayered membrane that wraps around selected axons in both central (CNS) and peripheral nervous system (PNS). It aids in increasing nerve impulse speed along the axon. Myelin contains 80% lipid and 20% protein that differ between PNS and CNS **(Greenfield S., 1973, Suresh S., 2010).** The major lipid classes found in other membranes are also found in the myelin such as neutral lipids, phosphoglycerides and sphingolipids. However, the PNS myelin has more sphingomyelin (10–35%), higher content of monogalactosylsphingolipids, with cerebrosides [Gal-C] (14–26%) and sulfatides [SGal-C] (2–7%) and less galactolipid and cholesterol compared to CNS myelin. The major fatty acid in the PNS myelin is oleic acid [C18:1(n-9)] (30%-40% of total fatty acid). Myelin is also characterized by its high content of very long-chain fatty acids (>18 carbon). The very long-chain fatty acids present in the sphingolipids are mostly saturated. The PNS myelin proteins are enriched in glycoproteins and basic proteins **(Garbay B., 2000, Gould R., 1992).**

The major PNS proteins are myelin protein-zero (myelin P0) 28 kD (50-60%) and 100 kD myelin-associated glycoprotein (MAG); these two proteins are expressed only by myelinated SCs to maintain tight structure of the myelin and axon-myelin integrity.

Peripheral myelin protein 22 (PMP-22 kD), myelin basic protein (MBP, 15%) and myelin P2 (10%), both MBP and myelin P2 are localized at the cytoplasmic side. Other high molecular mass glycoproteins such as periaxin 170 kD that are present in small amounts. Myelin P0, an immunoglobulin-like cell adhesion protein, is highly conserved among species, with a variety of post-translation modifications such as phosphorylation, acylation in the region of amino acids 110–119; glycosylation with a single, N-linked nine-sugar chain asparagine 93 **(Garbay B., 2000).** MBP in PNS has four polypeptide bands ranging between 14-21 kD. It has a variety of post-translation modifications such as phosphorylation and methylation and it is one of the major autoantigens in multiple sclerosis. Myelin P2 or fatty acid- binding protein-8, is a small protein (14 kD), with high positive charge and is concentrated mainly in thicker myelin sheaths. It is a member of a family of fatty acid-binding proteins, with a high affinity for oleic acid, retinoic acid and retinol. It functions in assembly and maintenance of myelin lipids. P2 is also an autoantigen in peripheral autoimmune neuropathy, Guillain Barre Syndrome (GBS). Its function is related to stabilizing the myelin membrane dynamics and lipid transport to and from the membrane **(Suresh S., 2010 and Gould R., 1992).**

Myelin is only produced if the cell comes into contact with certain types of axons. Axons send signals that are important for defining the SC lineage. Example of the axon signal is beta-neuregulin-1(NRG1) and glial growth factor (GGF), SCs can be activated to enter proliferation through NRG1 axonal signals that bind and activates the ErbB2/ErbB3 receptor complex on SCs to activate MAPK for cell proliferation. Factors that regulate SC myelination include Krox-20, Oct-6 and Sox-10 transcription factors; they also inhibit cell

death and proliferation. Myelin P0 protein is specific to SC myelin that decreases if the immature cells are not associated with the axon. If the SC loss its interaction with the axon, it can de-differentiate to immature SC. If cells associate with the axon again they become myelinating or non-myelinating depending on the signals. These mature SCs have the ability to block apoptosis through the effect of the insulin-like growth factors (IGFs), platelet derived growth factor-BB (PDGF-BB) and neurotrophin-3 (NT-3) in the autocrine circuit **(Bhatheja K., 2006).**

One of the pathogenesis events that associated with SCs is nerve injury and demyelination. This could be due to axonal damage and disruption of axonal-SC signals. Another cause is the immune stimulation (autoimmunity) that targets the myelin such as in multiple sclerosis and Guillain-Barre Syndrome (GBS). Like autoimmune disorders, *M. leprae* causes demyelination of the peripheral nerve that is started by damage to the myelin sheath and a decrease in the action-potential conduction velocity **(Rambukkana A., 2004).**

1.4. INTERACTION BETWEEN *M. LEPRAE* AND HOST CELLS

M. leprae has a unique tropism to the host cell. It especially infects and grows within Schwann cells (SCs) that surround the axons of the peripheral nerves. In fact *M. leprae* is the only bacterium known to infect the SC. Growth of the *M. leprae* in the SCs leads to the injury of the peripheral nerve (nerve damage), leaving the patient with disabilities and deformities **(Barker L., 2006).** The multi-drug therapy is effective in killing the bacteria,

but does not inhibit or reverse the nerve damage that has been started **(Rambukkana A., 1998).**

The exact molecular mechanism(s) of *M. leprae* interaction with the host cells (SCs) and causes of nerve damage are poorly understood. The availability of the live bacteria from the nine-banded armadillo tissues or the footpads of nude mice, allowed for some host- pathogen experiments to be done using mammalian SCs cultures.

SCs in the PNS are the ideal host for *M. leprae* survival and multiplication. This is due to the absence of lymphatics and the presence of blood-nerve and perineural barriers that provide protection from the immune cells and drugs. *M. leprae* binds to both myelinated and non-myelinated SCs. It has been found that non-myelinated SCs are more susceptible to *M. leprae* invasion *in vitro* and in leprosy biopsy (*in vivo*) with around 70-80% of the bacilli found in non-myelinated cells. However, in the advance stage of the disease where the non-myelinating SCs become limited, *M. leprae* induces SC demyelination and axonal damage. This will result in increase of number of non-myelinating SCs and increase bacterial invasion and survival **(Rambukkana A., 2001).**

In the late 1990's Rambukkana proposed a mechanism for *M. leprae* interaction with SCs. He showed that *M. leprae* targets the basal lamina that surrounds the SC-axon unit and binds to the G-domain of the laminin-α2 **(Rambukkana A., 1997).** Later the SCs receptor α-dystroglycan (α-DG) that interacts with laminin in the basal lamina was found to be the specific receptor for *M. leprae* to interact with SCs. He concluded that the G-

domain of the laminin- α2 has two binding sites, one for *M. leprae* and other for α-DG. In his experiment he also showed the importance of the carbohydrate moieties of α-DG for *M. leprae* interaction **(Rambukkana A., 1998).**

The bacterial factors that are involved in SCs invasion have been found to be unique molecules in *M. leprae* cell wall, such as the phenolic glycolipid-1 (PGL-1). The terminal tri-saccharide (dimethyl glucose, and two rhamnoses) of this molecule (PGL-1) binds to the laminin-α2 *in vitro* **(Ng V., 2000).** Another bacterial factor that interacts with SCs is laminin binding protein-21 (LBP21) that is coded by the ML1683 gene. Another protein is the 21 kD-histone-like protein (HLP) that was observed to bind *in vitro* to the SCs laminin-α2. Therefore, researchers postulate that there is more than one bacterial factor responsible for *M. leprae* adhesion to SCs and these factors could be targeted for leprosy treatment **(Barker L., 2006).** Also, experiments involving blocking of the SCs receptor α-DG, did not inhibit *M. leprae* invasion, which suggests the presence of other candidate receptors. These receptors that were found to bind to laminin-α2 were integrins and 25 kD phospho-protein **(Spierings E., 2000).** Other receptors that are used by the bacteria to enter the host cells are complement receptors (CR1, CR3 and CR4), and C-type lectin on DCs that recognize Man-LAM in the cell wall of mycobacteria.

After adhesion to the SCs, the bacilli are taken up by SCs through actin-mediated phagocytosis that depends on a series of host cell kinases (tyrosine kinase, calcium-dependent protein kinase and phosphatidylinositol 3-kinase). Inside SCs, live *M. leprae* survive in the endosomal compartment by avoiding fusion of the phagosome with

lysosomes, preventing O_2- radical production. As a result of this invasion, nerve and axonal damage and demyelination occur in the myelinated form of SCs. In the non-myelinated SCs, which are more susceptible to *M. leprae* invasion, axonal damage can occur leading to disease progression **(Barker L., 2006).**

Also, during SC infection, *M. leprae* can induce SC de-differentiation, leading to SC proliferation through controlling of the extracellular-signaling pathway such as Erk1 and Erk2 **(Tapinos N., 2005, 2006 and Rambukkana A., 2010).** Recently, *M. leprae* was found to induce expression of 9-O- acetyl GD3 ganglioside in SC membranes *in vitro* and *in vivo.* The 9-O- acetyl GD3 was concentrated on the internodal area of the infected nerves, which facilitated *M. leprae* attachment and invasion. It could also induce cell proliferation to increase the number of unmyelinated cells through signal transduction of ERK 1/2 pathway **(Ribeiro-R., 2010).** Once colonized inside SCs *M. leprae* down regulate the nerve communication machinery through controlling nerve-growth factor (NGF), neural glia cell adhesion molecule (NgCAM) and fibronectin, which will decrease SC regeneration and lead to axonal atrophy **(Birdi T., 2003). Figure 1.3** illustrates the interaction between *M. leprae* and SC in the peripheral nerves.

During *M. leprae* infection, it ensures SC survival to allow long-term survival of the bacteria. It does this through inhibition of apoptosis of the infected cells. Recently, a novel mechanism of preventing host cell apoptosis has been elucidated. It was found that *M. leprae* induces up-regulation of insulin growth factors (anti-apoptotic); IGF-I and IGF-II in

SC with a 2.7 and 1.6 fold increase, respectively, at 24 h post-infection **(Rodrigues L., 2010).**

Examining *M. leprae* infected SCs shows there are two types of demyelination in leprosy: i- segmental demyelination at localized areas with increase in inflammatory cells, ii- demyelination with reduction in axon caliber (axonal atrophy) **(Shetty V., 2000, Save M., 2004).** Several studies have used electron microscopy to look at the change in the nerve biopsies from leprosy patients. At the early stage of the infection no change in the nerve structure was found. However, at the later stage the nerve bundles were replaced by fibrous tissue with increased collagen. Some nerve fibers exhibited demyelination with cellular infiltration **(Job C., 1971, Jacobs J., 1987).** Also, in these nerve biopsies foamy cells were found in the endoneurium, perineurium, and epinurium. There is also an increase in inflammatory cells and lymphocyte infiltration around the nerve fibers **(Kajihara H., 2000).**
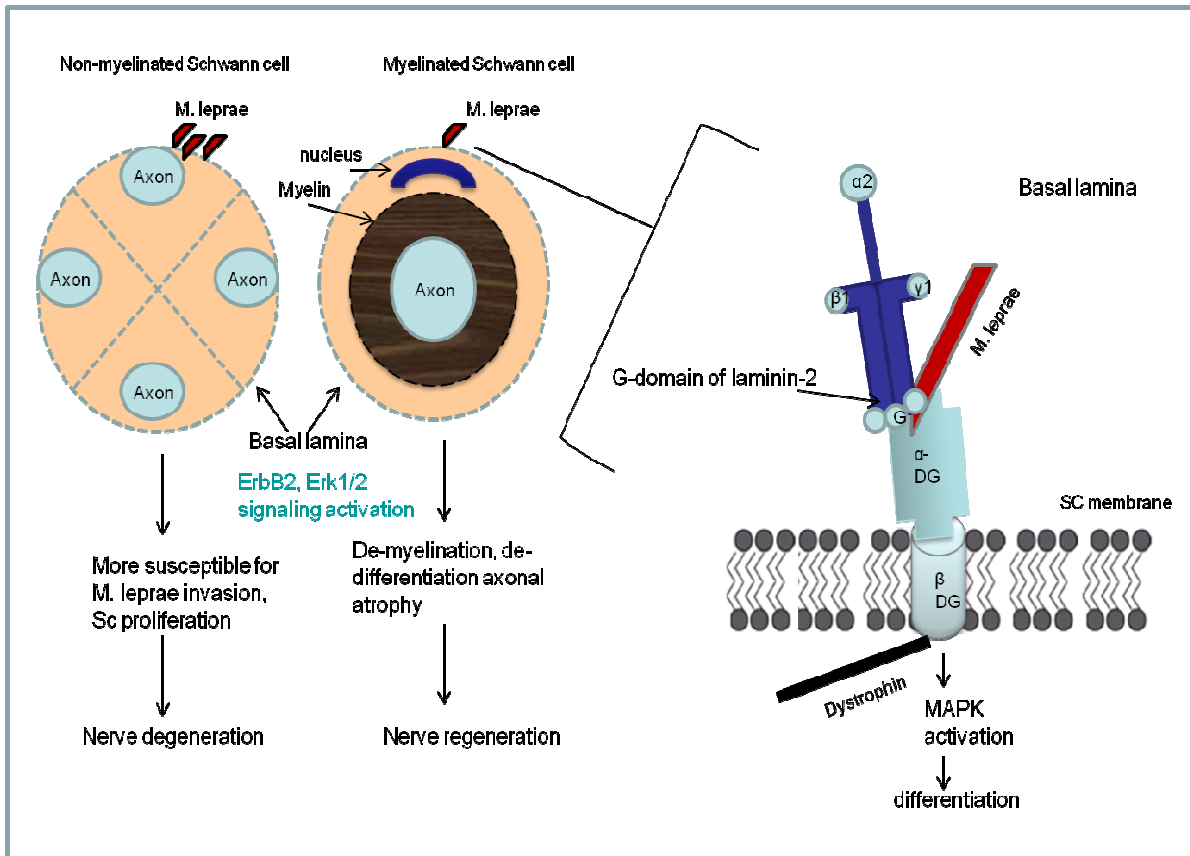
Figure 1.3: A model for the molecular basis of *M. leprae* interacting with peripheral nerves. It is believed that it interacts with α-dystroglycan receptors on Schwann cells via the G domain of laminin-2 (LNα2G), a component of the basal lamina. *M. leprae* interact with both myelinated and non-myelinated SCs. It induces de-myelination to infect more cells through activation of ErbB2, Erk1/2 signaling pathway. (Redrawn and modified based on Rambukkana A., 200, 2001, 2004).

1.4.1 Mechanisms of nerve damage in leprosy

It has been shown that throughout the disease spectrum leprosy patients can develop irreversible nerve damage that continues to develop during and even after antimicrobial therapy **(Rambukkana A., 2000).** The cause of nerve damage initiated by demyelination in leprosy is controversial with two different hypotheses being proposed in the literature. One refers to the role of *M. leprae* and bacterial proliferation as seen in the lepromatous form to induce demyelination and the other to immune-response to few bacteria or bacterial antigens as seen in the tuberculoid form.

I- The immunopathogenesis mechanism of nerve damage

A- Cellular immunity

SCs can take up, process, and present *M. leprae* specific antigens to T cells resulting in the production of Th1 immune modulators such as TNF-α and INF-γ **(Pereira R., 2005).** SCs have been shown to present mycobacterial antigen to MHC class I-restricted CD8$^+$ cytotoxic T cells and can also present mycobacterial antigens to MHC class II-restricted CD4$^+$ CTLs. SCs were also found to strongly express co-stimulatory and adhesion molecules for T cells. As a result of this stimulation, SCs will be killed by cytotoxic granules (granulysin, granzymes and perforins) produced by CTLs **(Spierings E., 2000, 2001).** SCs can express TLRs (TLR1 and 2) that can be activated by *M. leprae* LAM, lipoproteins such as 19 kD and 33 kD. Activation of SCs will lead to cytokine production (TNF-α, IL-12) and apoptosis **(Silva T., 2008).** Expression of TLR was found to be greater in TT patients compared to LL patients **(Krutzik S., 2003).** The large quantities of Th1

cytokines especially IL-12, IL-2 and TNF-α will lead to apoptosis of infected cells and decrease in bacterial load and increase granuloma formation as in TT lesions **(Hernandez M., 2003).**

Macrophages also play a role in immune stimulation in leprosy. *M. leprae* infected macrophages can present *M. leprae* antigens to T and B cells and release cytokines including TNF- α **(Barker L., 2006)**. Both SCs and macrophages can produce reactive oxygen intermediates (ROI) resulting in further nerve damage at the site of granulomas **(Birdi T., 2003).** *M. leprae* stimulate macrophages to produce TGF-β that is responsible for the decrease in nerve regeneration **(Birdi T., 2003).** Another antigen presenting cell, the dendritic cell was also found to effectively present *M. leprae* antigens and stimulate $CD4^+$ and $CD8^+$ (cytotoxic) T cells. Th1 cells are thought to be involved in CMI-DTH reactions and are important in responses against intracellular pathogens. In contrast, Th2 cytokines stimulate antibody production. C-type lectin DC-SIGN has been shown to bind to the ManLAM and trigger production of IL-10, TGF-β, while inhibiting IL-12 and TNF-α production **(Sieling P., 1999).**

It was proposed by Scollard, that *M. leprae* interacts with the blood vessel endothelial cells in the epineurium and perineurium before infecting SCs. This pointed to the possibility that *M. leprae* infects the peripheral nerve tissue through the bloodstream **(Scollard D., 2000).** These mechanisms may play an important role in the immunopathogenesis of SCs and nerve damage in leprosy.

B- Humoral immunity

High levels of antibodies (IgM and IgG) are usually found in lepromatous leprosy patients. The Th2 cytokines (IL-4, IL-5 and IL-10) found in LL patients down regulate TLR2 expression and stimulate B cell activation. Activated B cell can make neutralizing antibodies of IgM, IgA and IgG classes that are not effective in killing the intracellular bacteria. Therefore, *M. leprae* is able to survive and spread to cause nerve damage **(Yamamura M., 1992).** After chemotherapy, there is usually a decrease in antibody levels. There is a strong correlation between the bacterial load and the humoral immune response. Analysis of antibody responses has been proposed as a tool for leprosy classification **(Touw J., 1982).** Antibodies produced against *M. leprae*, play a role in the uptake of *M. leprae* by phagocyte cells and start the pathogenesis of the disease. For example, antibodies were found to bind complement, which then bind to PGL-I and fix C3 complement to *M. leprae.* This complement fixation will mediate the uptake of the bacilli through complement receptors on phagocytes **(Schlesinger L., 1994).** Also, secreted antibodies may form immune complexes with *M leprae* antigens or with cross-reactive host molecules. These complexes can then be recognized by antigen presenting cells through specific receptors and be presented to T cells. In LL patients there is excess antibody in the immune complexes. However, when taken up by antigen presenting cells (macrophages), it fails to activate T cells. Specific mature B cells markers (CD20, CD79, CD138) that produce antibody were found to be higher in skin lesions of BL/LL patients compared with the BT patients **(Iyer, A., 2007).** Moreover, comparing the gene expression of LL and TT leprosy skin lesions, showed upregulation of B cells specific genes. The

immunohistology of LL and TT skin lesions showed that IgM and IgA were more abundant in lesions from patients with lepromatous leprosy, which correlate with the Th2 immunity and increase in IL-5. LL is associated with elevated systemic humoral response **(Ochoa M., 2011).**

Another proposed mechanism that can lead to neuropathy in leprosy and is also related to the stimulation of the immune response during the infection is autoimmunity. The concept and general criteria of autoimmunity in leprosy has been around since 1969. It has been found that in leprosy there are increases in immune complexes (1gG-IgM, IgG-IgA and complement components) similar to other autoimmune diseases such as systemic lupus erythematosus (SLE), Guillain-Barre Syndrome (GBS) and in rheumatoid arthritis. The formation of antigen-antibody complex and stimulation of complement and recruitment of polymorphonucler leukocyte can cause tissue damage and injury to the vessel wall as seen in autoimmune diseases and leprosy **(Wager O., 1969).**

The T cells in leprosy lesions can be generated either to *M. leprae* specific antigens or to autoantigens such as HSP-66. This can lead to another mechanism of nerve damage caused by autoimmune-like destruction of the tissue (neuropathy) **(Spierings E., 2000).** In lepromatous leprosy patients there are decreased level of antigen-specific T cells against *M. leprae* 65 kD antigen, but at the same time there are elevated levels of anti-65 kD IgG antibodies **(Ilangumaran S., 1994).** The similarity between bacterial proteins and host components or the molecular mimicry is an important aspect for host-pathogen interaction. Using these mechanisms the pathogen can escape detection by the immune system or it can

31

lead to auto-immunity. Monoclonal antibodies raised against *M. leprae* antigens such as the 65 kD Ag, were found to react with host antigens like the peripheral axons found in the skin **(Naafs B., 1990).** Moreover, the protein sequence of the PNS myelin P0 was compared with the *M. leprae* protein sequence (leproma) and also to other genomic databases for protein sequence and structural similarities in other pathogens involved in neurodegeneration. This resulted in 11 hits with exact matches of six to seven residues of myelin P0 in *M. leprae* genome, but not in other genome of mycobacteria. Two of the matched in *M. leprae* are characterized proteins, ferrodoxin NADP reductase (62%) and a conserved membrane protein (36%) (ML2453, ML1504). Comparison to other pathogen databases showed that P0 had sequence similarities to human poliovirus receptor (23.4%) and the human herpes virus (4%). Also, by searching for the myelin P0 sequence against the entire genomic database revealed that it had sequence similarities to the immunoglobulin super family. This family plays a significant role in protein–protein and protein–ligand interactions. This similarity between the bacteria and the host could lead to autoimmunity and neurodegeneration (demyelination) as we see in leprosy infection. For example, anti-neural antibodies from leprosy sera were found to bind to the myelin P0 protein **(Vardhini D., 2004).**

Several auto-antibodies were found to be significant in leprosy patients from western India with 50% detected in LL, 44.4% in BL, 54.8% in BT patients. These auto-antibodies are anti-nuclear antibody (ANA), anti-double stranded DNA (dsDNA), and anti-single stranded DNA (ssDNA), anti-nuclear antigen (anti-ribonucleoprotein (nRNP), anti-Smith and anti-histone antigen (AHA).

Since leprosy is one of the differential diagnoses of rheumatic diseases, several auto-antibodies were examined in leprosy patient sera using ELISA techniques and correlated with joint involvement. For example, in Brazil most leprosy patients did not have active reaction. Therefore, the frequency of IgM- rheumatoid factor (RF), anti-cyclic citrullinated peptide antibodies (anti-CCP), antinuclear antibodies (ANA), antineutrophil cytoplasmic antibodies (ANCA) in leprosy patients were low. However, the prevalence of anticardiolipin antibodies (aCL) and anti-β2 glycoprotein I antibodies (β2GPI) was significantly higher in leprosy patients than in the control group **(Ribeiro S., 2009).**

Glycolipids and glycosphingolipid that are expressed as a surface determinant of myelin in the PNS are important for its function and stability. Inhibition of these molecules (glycolipids) by an auto-antibody can lead to demyelination and nerve damage as found in leprosy patients. Therefore, many scientists studied these auto-antibodies and their association with the nerve damage found in leprosy. An antibody to neuronal glycolipids or glycosphingolipid such as ceramide was studied in leprosy patients in India. Anti-ceramide IgM antibody titer was found to be significantly higher in MB leprosy patients in comparison to both controls and PB leprosy patients (96% of MB and 60% of PB patients) **(Singh K., 2010).** Groups in Brazil found increased levels of anti-cardiolipin (aCL) and anti-β2-glycoprotein I (anti- β2- GPI) in leprosy patients mainly in lepromatous patient with predominant IgM isotype. The percent of anti-phospholipids in leprosy could be due to the exposure of phospholipid antigens by tissue damage during the infection. Another explanation is the homology between the bacterial and host PLs that leads to the

production of antibodies against the cross-reactive hetrologous sequence **(Ribeiro S., 2011).**

Another anti-glycolipid antibody is anti-sulfatide (cerebroside) that also has been reported in various demyelinating peripheral polyneuropathies. Sulfatide, which is a glycolipid with a single sulfated saccharide, is associated with myelin membrane of the nerve cells. The antibody inhibits synthesis of sulfatide that is expressed on myelin as a surface determinant, which leads to demyelination. The IgM antibody subtype against sulfatide was found to be elevated in MB or lepromatous leprosy compared to PB and controls. The IgM anti-sulfatide was positively correlated to the patient's BI **(Wheeler P., 1994, Spierings E., 1999).** The similarity between mycobacterial sulfolipid with the sulfated trehalose and the host tissue (sulfatide) may stimulate an autoantibody against the host sulfatide with sulfated galactose **(Wheeler P., 1994).**

The variation in the amount of auto-antibodies found in leprosy patients, could be related to the genetic background of the study population, presence of associated infectious diseases and techniques used to detect auto-antibodies. The proposed hypothesis for the development of those antibodies during infection is due to adaptive immune response and polyclonal B cell activation. The bacterial or viral antigens, with a sequence homologous to host tissue, would be presented to T lymphocytes that stimulate B lymphocytes to produce antibodies against the heterologous sequence **(Paradhan V., 2004).**

In addition, auto-antibodies to antigenic epitopes of myelin proteins have been reported in many chronic demyelination diseases. For example, in chronic inflammatory polyradiculoneuropathy (CIDP), where both humoral and cellular immunity are involved, antibodies to myelin proteins are common. The major antigenic components of the myelin are; myelin P0, myelin P2 and peripheral myelin protein 22 (PMP22). These proteins are also associated with inducing experimental autoimmune neuritis (EAN) (**Rostami M., 1984, Sanvito L., 2009**). These auto-antibodies could be generated during tissue damage, and then continue to exacerbate further tissue damage during disease.

II- The non-immune mediated demyelination

Beside the inflammatory process the axonal-demyelination could be induced by the presence of *M. leprae* Rambukkana *et al*. have demonstrated a direct demyelinating effect of *M. leprae* on SC-neuron co-cultures (*in vitro*) and in Rag1$^{-/-}$ mice (*in vivo*), which lack mature T and B lymphocytes. In these models *M. leprae* was able to induce demyelination as early as 24 hours post infection without apoptosis or toxic effects on the cells. *M. leprae* components such as cell wall PGL-1 were also associated with SC demyelination in his models. Therefore, Rambukkana concluded that the viability of *M. leprae* is not required in induction of nerve demyelination *in vitro* and *in vivo* (**Rambukkana A, 2002**). Also, in his studies *M. leprae* was found to induce extracellular signal-regulated kinase Erk1/2 signaling through mitogen-activated protein kinase MEK-dependent pathway. This activation was due to a contact-dependence between *M. leprae* and primary SCs, without any apoptosis or cell death in SCs. In this scenario, *M. leprae* was found to bind and induce phosphorylation of ErbB2 receptors in SCs in addition to the

laminin receptor that is localized close to ErbB2. As a result of this signaling activation, *M. leprae* can successfully induce SCs proliferation and demyelination **(Tapinos N., 2005, 2006).** It has been stated by Rambukkana that the non-immune-mediated mechanisms of nerve injury plays a role in the early phases of the disease. However, it is the immune-mediated element that eventually induces nerve damage. When *M. leprae* antigens are presented by myelinated and non-myelinated SCs, both cells are subjected to immune attack by macrophages, T cells and the cytokines released from these inflammatory cells. The inflammatory responses will result in both SCs phenotypes and subsequent sensor-motor loss of the nerve **(Rambukkana A., 2002).**

Another proposed mechanism for nerve damage that can be grouped in the non-immune mediated form is the biochemical and metabolic changes in the nerve compartment. Example of this mechanism is the axonal atrophy due to hypophosphorylation of the myelin proteins and axonal neurofilaments. Many proteins in the PNS are phosphorylated such as myelin P0, MAP and neurofilament proteins. Studies that examined PNS protein phosphorylation in leprosy nerves compared to normal nerve found decreased levels of phosphorylation proteins around 25 kD protein in nerves of leprosy patients. The phosphorylated protein (25 kD) is thought to be the glycoprotein myelin P0 **(Suneetha L., 1996).** Later studies by the same group found that *M. leprae* could bind to this glycoprotein myelin P0 (25 kD) and inhibit its phosphorylation *in vitro*. This binding to the outer layer of the myelin may help *M. leprae* to reach the target SCs for invasion **(Suneetha L., 1997, 1998, 2003).**

Neurofilament proteins belong to intermediate filaments (IFs) found together with the microtubules and microfilaments in the cytoskeletal structures. Other proteins that make up the IF in the neurons are vimentin, peripherin, internexin and nestin. The NFs proteins in the axon are composed of triplet proteins; NF-H (high), NF-M (medium) and NF-L (low) molecular weight neurofilament proteins. Neurofilament proteins contain an amino-terminal head domain, a central α-helical domain, and a carboxyl-terminal tail domain of variable length. An increase in the total amount of the NF proteins in axons results in increased axonal diameter. Also, phosphorylations of the NF proteins are important for axonal caliber. The NF-M and NF-H are highly phosphorylated in the tail domain of the C-terminus at KSP repeats in the myelinated axons **(Chung-Liang Ho., 1996).** Several studies have shown that NF-H migrates more rapidly on SDS-PAGE after extensive dephosphorylation by alkaline phosphatases. Several studies have shown the important role of NFs in radial growth of myelinated axons using gene knockout of NFs proteins **(Lee M., 1996).**

In leprosy patients, decreases in axonal diameter were found to be associated with sensory and motor loss. Therefore, the relationship between neuropathy and the phosphorylation state of NF proteins was examined. Western-blot and immunohistochemistry techniques were used to examine the leprosy human nerve patients phosphorylated epitopes of NF (SMI 31). In addition Shetty *et al*. **(Save M., 2004)** found a decrease or loss of SMI31 staining in infected nerve fibers. NF protein bands migrated faster (lower) than expected and there was decreased level of NF protein content in the infected nerve. These results demonstrated hypophosphorylation of NF subunits during

leprosy infection, probably leading to enhanced susceptibility for proteolytic degradation of NFs **(Save M., 2004).** These results were in agreement with a previous study, in which phosphorylation was found to protect NFs against non-specific proteolysis by calpain **(Pant H., 1988).** Several studies by Shetty *et al.* found that lipoarabinomannan (LAM) from *M. leprae* can inhibit the enzyme protein kinase C (PKC) responsible for phosphorylation of neurofilament proteins. Recently, Save *et al* also validated the hypophosphorylation of the NF proteins by measuring the enzymatic activity of the kinase responsible for the phosphorylation of NFs in the nerves of infected mice. The authors showed that as the NFs lose their reactivity to the NF-phosphate specific antibody (SMI 31), there was a decrease in the KSPXK kinase activity of cyclin dependent kinases (CDKs) and mitogen activated protein kinases (MAPK) in the *M. leprae* infected nerves. This decrease in NF phosphorylation and subsequent NF degradation could result in a decrease in inter-filament distance that affects the axonal growth resulting in axonal atrophy **(Save M., 2009).**

Moreover, *M. leprae* was found to induce up-regulation of matrix metalloproteinases (MMP-2 and MMP-9) on SCs that causes demyelination and breakdown of the blood-nerve barrier **(Teles R., 2010).** The MMP protein family consists of proteolytic enzymes that participate in remodeling of the extracellular matrix and the regulation of leukocyte migration. MMP-2 degrades type I (gelatin) and MMP-9 degrades type IV collagen, a major component of the basement membrane. Increased secretion of MMP has been related to tissue damage and can be used as a biomarker in many inflammatory disorders. During mycobacterial infection there is up regulation of MMP-9 secretion that correlates

with TNF-α production. It was found that during tuberculoid leprosy and reaction type I (RR) lesions, the MMPs are increased in the central area of the granuloma, in which macrophages and epithelioid cells are predominant **(Teles R., 2010).**

Nerve damage in leprosy infection has been divided into two stages; i- The initial stage that occurs in the absence of inflammatory cells. This phase is initiated by *M. leprae* contact with SCs in the PNS and leads to nerve damage. This phase is common across the leprosy spectrum. It is characterized by sub-perineural edema, axonal atrophy and demyelination with loss of un-myelinated fibers. ii- The later phase is the inflammatory mediated phase with lymphatic cell in tuberculoid form and macrophages cells in lepromatous leprosy. In this stage the presence of auto-antibodies against nerve components was reported in leprosy as another mechanism of nerve damage. The presence of antigenic determinants that are common between *M. leprae*, skin and nerve such as heat-shock proteins, leads to auto-antibody production **(Birdi T., 2003).**

The presence of *M. leprae* in the nerves can also cause a pure neuritic leprosy. Neuritic leprosy accounts for about 10% of all leprosy cases. In this form there is no cutaneous manifestation found, but the nerve damage can be detected. The nerve damage could be due to the inflammatory infiltrate of macrophages full of bacilli that makes the foamy cells in the granuloma. This inflammatory process could be the cause of the stimulation of T cell cytotoxic activity, axonal degeneration following SC death, and demyelination. Using different SCs and axonal markers in immune-histochemical slides of neuritic leprosy nerve, a decrease in NF200 immuno-reactivity due to the loss of myelinated fibers was

found. Also, the S-100 protein staining of myelinated fibers was reduced due to fiber loss after demylination. The NGFr staining of neuritic nerves was also reduced in the SC and/or axons of small fibers. The decrease in the number of myelinated fibers resulted in decreased myelin basic protein (MBP) **(Antunes S., 2006).**

1.5. ANIMAL MODELS FOR LEPROSY

Different animal species were tested to find a susceptible host for leprosy other than humans. First, establishing an animal model for leprosy was done by Chapman Binford in 1956. He infected hamster ears and testes and found that *M. leprae* has a preference for low temperatures in the body **(Meyers W., 1992).** Another animal found to be susceptible is the nude mouse; inoculation of the mouse footpad (Carworth Farms white mice) supported the multiplication of *M. leprae* within 6-9 months **(Shepard C., 1960).** This model was mainly used as a source for live *M. leprae* used in research such as detection of drug-resistant strains of *M. leprae*. However, the slow development of nerve damage due to lack of immune response in this animal, makes it difficult to study the nerve damage associated with the disease.

In 1968 the armadillo (*Dasypus novemcinctus*) was first experimentally infected with *M. leprae* and found to have an increased amount of leprosy bacilli after two years. Highly susceptible armadillos were found to develop weak reactions to *M. leprae* without granuloma formation similar to the lepromatous leprosy form. This animal was selected because of its long life span and lower body temperature (30-35ºC) **(Kirchheimer and**

Storrs 1971, 1972). In 1975 leprosy was reported in wild armadillos in the southern United States, suggesting an association between natural leprosy disease in human and armadillos. In 1985 armadillos were first inoculated with *M. leprae* and examined by Truman to detect antibodies against the *M. leprae* major antigens. Serum or eluted whole blood was tested in an enzyme-linked immunosorbent assay (ELISA) for immunoglobulin M (IgM) antibodies to the species-specific phenolic glycolipid-I (PGL-1) antigen. However, these antibodies have no protective effect against *M. leprae* and usually associated with high false-positive rates within leprosy endemic regions **(Truman R., 1986).** A later study was conducted to find a new serological test for an early diagnosis of leprosy. Several *M. leprae* specific antigens when used in combination were found to be effective for early diagnosis of leprosy. The authors proposed that theses protein antigens could be used to both complement and supplement a PGL-I- based diagnosis **(Duthie M., 2011).** It was found that BCG vaccination gave effective protection to the armadillos against *M. leprae*. The armadillo is the only animal model that can demonstrate effective protection against *M. leprae* with BCG **(Scollard D., 2006)**

Examining tissue smears from armadillo lymph nodes, liver and spleen, resulted in finding un-cultivable acid-fast bacilli. This was supported by histopathological examination of the tissues showing *M. leprae* infection and nerve involvement **(Job C., 1985, Meyers M., 1986).** About 85 % of nine-banded armadillos get different types of leprosy (borderline to lepromatous type) with similar forms of nerve involvement to the human disease. The peripheral nerves (sciatic) of infected armadillo showed an increase in acid fast bacilli in the epineurial and increased cell proliferation. The bacilli inside

macrophages were also seen in epineurial lymphatic, small blood vessels and extra-cellular matrix. The nerves also showed increase in inflammatory infiltrates similar to lepromatous neuritis. Therefore, the armadillo appears to be a good experimental model for studying mechanisms of nerve injury in leprosy and for production of large quantities of *M. leprae* for research purposes **(Scollard D., 1996).** These big discoveries have led to increased use of the armadillo as a model for experimental leprosy. Since the armadillo is the only model for leprosy, a large armadillo colony was established in Carville, LA. The goal of this colony was to do more experimental studies on armadillos, providing leprosy bacilli to researchers.

Wild armadillos are usually screened using histopathological examination of ear biopsies to look for acid fast bacilli or to look for *M. leprae* specific antibodies in the serum. The *M. leprae* inoculum used to infect the armadillo is taken from lesions in the skin of leprosy patients or from nude mice. A homogeneous suspension is made and the bacilli are counted to arrive at an effective dose ranging from 10^3-10^8 AFB resulting in a 10,000-fold increases in the number of *M. leprae* over a period of 18 months. The *M. leprae* inoculation is usually delivered through the saphaneous vein and reticulo-endothelial tissues. The intravenous route is the most susceptible for the infection. After the bacilli are taken up, they can slowly proliferate and disseminate to other parts of the body (skin, bone mar- row, liver, spleen, lymph nodes, lungs and oesophagus). Another route for the infection is the footpad of the armadillo. Armadillos usually require between 18–24 months of incubation after the infection before they developing the disease. The infection is monitored through evaluation of antibody response to PGL-1. The antibody is

usually detected after 6 months of inoculation. The disease is characterized by the involvement of peripheral nerves with ulcerations and loss of sensitivity (**Vijayaraghavan R., 2009**). Histopathological sections of armadillo infected nerves showed the presence of the bacilli in SCs (intraneural), perineural and epineural sites of the nerve. It also shows macrophages harboring the bacilli in the epineural, blood vessel and extra cellular matrix. Most animals develop 10^{12} bacilli in their tissues (liver and spleen) within 14-24 months (**Job S., 1985, Truman R., 1986**).

It was hypothesized that leprosy in armadillo was due to armadillo escaping after experimental inoculations in 1968. However, a study by Truman *et al.* using serum samples taken from wild armadillos from 1960 to 1964, showed that the armadillos were infected before 1968**. (Truman R., 19986**). The distribution of these wild infected armadillos was found to match the pattern of human leprosy. In the southern United States more than 20% of armadillos are naturally infected with *M. leprae*. The author pointed that there are two possible hypotheses for this distribution; the ecologic (no infected armadillo found close to the area that exhibit substantial levels of infection) and the epidemic factors (both populations in eastern Mississippi/western Alabama contained at least one infected animal) (**Loughry W., 2009**).

Many studies pointed to the possible transmission of leprosy from armadillo to human (zoonotic transmission) (**Truman R., 1990**). Using genomic polymorphisms such as polymerase chain reaction restriction fragment length polymorphism (PCR-RFLP) and single nucleotide polymorphisms (SNPs), researchers were able to trace leprosy

43

transmission and determine whether the *M. leprae* strains found in humans were identical to those (*M. leprae*) found in wild infected armadillos **(Hamilton H., 2008).** Recently, wild armadillos infected in the southern United States were found to have the same *M. leprae* genotype as many leprosy patients living in the same area **(Truman R., 2011).** The armadillo (*Dasypus novemcinctus*) genome has been recently sequenced through the Human Genome Consortium genome. 75% of the total genome (2X coverage), is already completed and available at the NCBI database. This facilitated further research on leprosy using this animal model.

Although, it was believed that the nine-banded armadillos (*Dasypus novemcinctus*) are the only animal known to have naturally occurring infections of *M. leprae*, Donham detected leprosy in chimpanzees in 1976. Chimpanzees developed multibacilary leprosy and had high level of anti-PGL1 antibody. Recently, a few cases of leprosy in sooty mangabey monkey have been reported. Some of these monkeys were infected with SIV used as model for HIV and AIDS. It was found that *M. leprae* infection after HIV infection gave a protection role from progression of AIDS and death. This was explained by *M. leprae* lowering viral load, and preserving CD^{4+} and $CD^{4+}CD^{29+}$ T cell subsets **(Hamilton H., 2008).** Monkeys and chimpanzees develop disease similar to the human lepromatous form **(Meyers W., 1986).** However, the use of the monkey as a model is not ideal since the disease can take up to five years to develop and is complicated due to there are many constraints in dealing with these large animals.

Based on all the research done to find ideal animal models for leprosy, the armadillo

seems to be the best model to study the various aspects of leprosy. Many studies could be conducted to understand the mechanisms of nerve injury caused by *M. leprae* using armadillo model. This will help find anti-microbial methods to prevent neuritis.

1.6. HOST SUSCEPTIBILITY FACTORS

Leprosy is a complex disease, depending on several factors such as host genetic background, nutritional status, environmental, BCG vaccination and infection with other mycobacteria. The outcome of infection and clinical manifestation depend on the cellular immunity of the host that controls by genes. It is the host genetic factors that determine which exposed individuals develop disease, since the majority of exposed individuals do not become infected. Only about 0.1 – 1% of the infected population develops overt disease **(Moraes M., 2006).** The host genetic factors can be classified into three groups. The first group is the genetic risk factors that differentiate between being asymptomatic after exposure to *M. leprae* (the majority of people with protective immunity) and symptomatic people (susceptible). The second group is that associated with leprosy sub-types either paucibacillary or multibacillary. The third group of host genetic factors that is contributes to the development of leprosy reactions either type I (reversal reaction, RR) or type II (erythema nodosum leprosum, ENL) **(Moraes, M., 2006).**

Many studies have been done to show the relationship between host genetic factors and leprosy susceptibility. These include: family-based linkage and association studies, candidate gene association studies, and genome-wide association studies (GWASs).

45

I-Linkage studies (genome-wide linkage) look for evidence of the segregation of a genetic marker (microsatellites or SNPs) and a disease trait within families. Since it is un-biased to which chromosomal loci or genes might be associated to the disease it has been used to evaluate candidate genes or regions in leprosy **(Misch E., 2010).**

The first genome-wide scan was carried-out in India to identify regions associated with leprosy susceptibility. In that study the entire genome was covered using 388 microsatellite markers, resulting in finding 28 regions of interest. From a second screen one region on chromosome 10p (10p13) showed significant linkage with paucibacillary leprosy **(Misch E., 2010).** Another genome-wide linkage analysis performed by Mira *et al.* **(Mira M., 2004)** in Vietnamese families showed strong linkage with chromosome region 6q25-27 and equal proportions of PB and MB subtypes. In addition, this genome screen also confirmed the involvement of locus 10p13 in PB leprosy. Another study in India and Brazil suggested linkage for chromosome regions 20p13 for the lepromatous and borderline lepromatous families and 17q12 linked to the tuberculoid subtype and 17q21.33 regions were linked to leprosy **(Misch E., 2010).** Also, in these studies (Vietnam and Brazil) significant associations were found between leprosy and 17 markers located in a single linkage for gene PARK2 (PARKIN) and co-regulated gene PACRG. PARK2 codes for parkin, an E3 ubiquitin–protein ligase. It also has an anti-apoptotic effect through prevention of cytochrome-C release and participates in regulation of autophagy. Mutation was found to be associated with both neurological disease causing autosomal recessive early-onset Parkinson's and also to leprosy susceptibility **(Alcaïs A., 2005).** However, another study in India based on case-control, did not find a significant association between leprosy and SNPs in the PARK2 or PACRG co-regulatory region **(Misch E., 2010).** The genome-wide

scan performed with Vietnamese families also resulted in identification of eight SNPs in this gene region of lymphotoxin-α (LTA) of the HLA class III region on the chromosome 6p21. These SNPs LTA-293, rs3131628, rs2523500, LTA+80, LTA+368, rs2516479, rs2844484, and rs2256965 showed linkage to leprosy. The genome-wide linkage study of leprosy examined SNPs in exon 7 of the underlying mannose receptor C type 1 (MRC1) gene. These SNPs were found to be associated with the paucibacillary subtype in Vietnam and Brazil. Further study of these SNPs resulted in finding that G396S polymorphism was associated with protection against leprosy **(Alter A., 2011).** This mutation was found to inhibit *M. leprae* entry to the macrophages or subsequent signaling pathways after phagocytosis **(Cardoso C., 2011).**

II-Genetic association studies (GWAS) focus on the frequency of a particular genetic variant (hypothesis driven) between individuals with a disease compared to controls. The most common example is a case-control study that compares the frequencies of one or more polymorphisms or microsatellite markers between cases and controls. Case control studies were conducted in Vietnam and Brazil for two SNPs in the mannose receptor 1 gene (MRC1), located in the 10p13 region. These SNPs were found to be associated with protection against multibacillary leprosy and leprosy. Another gene associated study was done on chromosome 21 in Malawi for markers for the selected the chromosome region. This study resulted in finding that the 21q22 region locus affects susceptibility to a specific form of leprosy rather than leprosy overall. GWAS identified two polymorphisms in NOD2, rs9302752 and rs7194886 that were associated with susceptibility to leprosy in China and India. However, there were inconsistence in NOD2 and leprosy association

between populations and studies when repeated in India and Mali **(Misch E., 2010).** The NOD2 variant can affect autophagy and bacterial clearance **(Cardoso C., 2011).**

III-The candidate gene approach can be used to determine whether there is a biological mechanism relevant to disease pathogenesis. The similarity between leprosy and several inflammatory/autoimmune diseases, lead to studies of genetic variations of both infectious and inflammatory/autoimmune diseases. Many studies have been done in order to identify susceptibly genes related to multiple diseases and leprosy infection or subtypes. The most common candidate genes that were first studied are those involved in immunological pathways. For example, frame-shift mutation in NOD2, TNFSF15 and IL-12B have been associated with Crohn's disease. Strong association was found between human leukocyte antigen (HLA) and leprosy such as transporters associated with antigen processing TAP, MICA, and MICB, and two microsatellite markers of the tumor necrosis factor-alpha (TNF-α) gene located in the HLA region. Other non-HLA variants located in different genes and associated with leprosy genetic risk factors, such as the vitamin D receptor (VDR), the natural resistance-associated macrophage protein 1 (NRAMP1), the IL-10, and the PARK2/PACRG genes.

1.6.1 Candidate genes examined

    A- <u>HLA-gene complex</u>

The HLA gene complex located on chromosome 6p21, functions by processing and presentation of peptide antigens to T cells and production of IFN-γ. The haplotypes (many SNPs) associated with this gene were linked to development of different leprosy clinical forms. For example, the A11 allele in HLA class I was associated with susceptibility to leprosy in Korea, India and Brazil. The DRB1*04 that belong to HLA class II has a protective effect **(Cardoso C., 2011).**

    B- <u>Non-HLA: innate immune response</u>

SNPs found in NRAMP1 cause resistance in mice. NRAMP1 is an iron transporter that exports iron from the phagolysosome. It is also participate in autophagosome maturation. The association of this SNP and leprosy in different populations is not clear yet. The Vitamin D receptor (VDR) that acts as transcriptional factor for immuno-modulation genes is also implicated. Activation of vitamin D leads to autophagy and antimicrobial peptide production and bacterial control. Polymorphisms associated with VDR such as TaqI from different populations give conflicting results **(Cardoso C., 2011).**

<u>Non-HLA: pro-inflammatory</u>

Many studies were done on pro-inflammatory cytokine genes, such as TNF genes that are located on class III MHC region at 6p21·3. TNF cytokine is important in activation of macrophages and granuloma formation. However, different results were found regarding TNFα promoter region SNP G-308A. The first study in India found association between

TNFα SNPs and susceptibility to lepromatous leprosy (LL). In a Brazilian population the same SNP 308A was associated with paucibacillary disease. Finally, a later study reported opposite results where same allele was found to be protective against leprosy in Nepal. The TNF gene has not shown a consistent association with leprosy because its role in the pathogenesis and immunity of leprosy is still not well understood **(Moraes M., 2006, Misch E., 2010).** Individuals with TNF-308A, produce higher amount of TNF. In contrast the 308GG genotype, this shows less TNF and granulomas that facilitate progression of the disease **(Cardoso C., 2011).** Another pro-inflammatory cytokine that induces granuloma formation is IFN-γ which also regulates Th1 response. A case-control study in Brazil found that the SNP+874T was associated with leprosy resistance. The T allele individual was found to produce higher IFN-γ that explains the protective effect.

Another genetic study was done on Leukotriene A4 hydrolase (LTA4 H) that converts leukotriene A4 into the pro-inflammatory leukotriene B4. Inhibition of LTA4 changes the pathway toward an alternative product, the anti-inflammatory lipoxin A4 (LXA4). Leukotriene A4 (LTA4H) was associated with asthma and myocardial infarction but also found to be protective against multibacillary leprosy. Two SNPs in the LTA4 rs1978331, rs2660898 were associated with protection from multibacillary leprosy and found to give protection from tuberculosis **(Misch E., 2010).**

C- <u>Non-HLA:anti-inflammatory</u>

The IL-10 gene is located at 1q31-q32. The product IL-10 can suppress inflammatory mediators and antigen presentation. Polymorphism in the promoter 819T was associated with leprosy and with PB leprosy. Other haplotypes (3575T/22849G/22763C/

21082A/2819C/2592C) were associated with protection and allele 2819T was associated with leprosy susceptibility. Another group in India studied IL10 SNPs and haplotypes and found associations for 819TT genotypes with leprosy susceptibility and multibacillary (MB) leprosy. Also, individuals with the 592CC genotype were significantly protected from leprosy **(Moraes M., 2006**, **Misch E., 2010).**

D- Innate immune receptors: Polymorphisms in TLRs

Toll-like receptors (TLRs) are a family of trans-membrane proteins that play an important role in initiating the host immune response to mycobacterial infections. Therefore, mutations in TLRs influence susceptibility to a variety of infections. Susceptibility to leprosy involves successful invasion of *M. leprae* and overcoming the host mechanisms of bacterial killing. TLR1/2 is responsible for recognition of mycobacterial lipopeptides and activation of vitamin D and production of microbicidal peptides. TLR can also regulate autophagy through vitamin D to control the infection **(Cardoso C., 2011).**

Johnson *et al.*(**Johnson C., 2007**) found that the 602S allele or T1805G SNP that linked to a TLR1 trafficking defect and decreased IL-1, IL-6 and TNF production was associated with protection from leprosy in Turkey. Also in another study the G (602S) allele was found to be associated with protection against leprosy and RR reaction. Another TLR1 SNP, A743G (N248S), was associated with an increased risk of leprosy and the 248S allele was associated with increased risk of RR **(Wong S., 2010).**

Mutation in TLR2, which is important for recognition of *M. leprae* lipoproteins (19 kD and 33 kD) and establishment of the innate immune response, has also been linked to the

lepromatous form of leprosy. Kang and Chae **(Kang T., 2001)** detected an arginine to tryptophan substitution at position 677 of TLR2 (TLR2 Arg677→Trp) in ten out of 45 lepromatous leprosy patients, but did not find this polymorphism in tuberculoid leprosy patients or healthy controls **(Alcaïs A., 2005, Alter A., 2011).** The TLR2 gene microsatellite marker was also found to be associated with protection and susceptibility to leprosy reactions. For example, microsatellite (MS) 288-bp variant was found to be associated with an increased risk of RR reaction. On the other hand, SNP C597T was associated with protection from RR **(Misch E., 2010).** Abnormal signals through TLR1/2 can inhibit recognition of mycobacterial lipoproteins and microbicidal peptide production, which leads to more infection.

TLR4 polymorphisms (SNPs) G896A and C1196T were linked to an influence on human susceptibility to a number of infectious diseases. However, these SNPs were also associated with protection against leprosy or lepromatous leprosy in an Ethiopian cohort study **(Bochud P-Y., 2009).**

Vitamin D can control the adaptive immune response through enhancing of Th2 T cell responses and blocking Th1 responses. Stimulation of vitamin D receptor (VDR), resulted in activation of a microbicidal peptide that control mycobacterial infection. **(Cardoso C., 2011).** Several polymorphisms located near the 3' UTR of the vitamin D receptor gene (VDR) were studied. For example, TaqI C polymorphism (higher transcriptional levels of VDR) with genotype CC (tt) showed an increased risk of leprosy in Malawi. Another genotype TC (Tt) or CC (tt) combined were associated with protection from leprosy (lepromatous leprosy). Vitamin D receptor (VDR) located at 12-q14 region with T-C substitution at codon 352, resulted in susceptibility to leprosy **(Moraes M., 2006).**

All the genetic analysis and the risk factors indicated that genetic mutations in both innate and adaptive immunity are associated with lepromatous leprosy. Several genes could be associated with the outcome of the disease. The differences in the results (association or linkage) found between different alleles and leprosy susceptibility in different studies could be due to differences in ethnic background, variations in sample size and different types of leprosy. Also, changes in the experimental approaches, such as the reliance on *in vitro* assays of plasmid reporter gene expression versus *in vivo* assays with human cell lines, the use of specific cell lines, or variable stimulation conditions also many account for the differences.

1.7. BIOMARKER DISCOVERY

A biomarker is a molecule that reflects the biological state of the disease. This molecule could be a protein, lipid and/or metabolite. Studies of biomarkers require either tissue biopsy or biofluid (blood, urine) from patients and control groups. Identification of a disease specific biomarker is important for the diagnosis and the prognosis. Many clinics prefer using biofluid since it is easy to obtain with less sampling process compared to biopsy. For the research aspect, tissue biopsy is favorable to correlate the (omics) data to the gene expression **(Shen Hu., 2006).**

1.7.1 Omics approach to study host-pathogen interaction

The main tool used in Omics (proteomics, metabolomics, and lipidomics) studies is mass spectrometry. The first mass spectrometer was built and used by Thomson **(Thomson, J., 1899).** In the late 1980s the "soft" ionization technique such as electrospray ionization (ESI) was developed by John Fenn. This technique allows many molecules, including proteins, carbohydrates, and lipids, to be ionized in a liquid medium without the need for prior derivitization. Another type of mass spectrometer is the triple quadrupole mass spectrometer. This instrument can be used in single-scan (MS) mode to get information about molecular masses, or it can be run in a tandem-scan (MS/MS) mode to get additional information **(Harkewicz R., 2011).**

The "omics'' technologies can be divided into: I-Metabolomics is the systematic study of low-molecular-weight intermediates (the metabolome) contained in the cell. The metabolome represents many components that belong to different classes, such as amino acids, lipids, organic acids, nucleotides. The metabolome often correlates to actual phenotype of certain diseases. A variety of body fluids and tissues can be used to study metabolomes applied to different instruments such as nuclear magnetic resonance (NMR), GC-MS, HPLC-MS, UPLC-MS and quadrupole-TOF-MS. Using the TOF as mass analyzer provides accurate mass measurement with high-mass resolution. Metabolomics studies on plasma (or serum) are widely used since it is less invasive and it contains products of both anabolic and catabolic processes. There are two approaches used for metabolomic assays: metabolic profiling and metabolic fingerprinting. The metabolic profiling is quantitative and focuses on analysis of metabolites related to a specific

pathway or a class of compounds. Metabolic fingerprinting compares patterns or metabolites that change in response to disease. Metabolite fingerprints are described by *m/z* values, retention times (RT) and intensities of detected ions **(Dettmer K., 2007).** The first step in this method is metabolite extraction and protein precipitation. The extracts usually prepared in duplicate are ready to be analyzed by liquid chromatography (LC-MS) with multiple injections. LC-MS has many advantages, such as reduced ion suppression, which can separate isomers, and gives better detection limits with reduced background noise. The reversed phase liquid chromatography using C-18 narrow column has been widely used for metabolomic research **(Dettmer K., 2007).** For data analysis multivariate statistics and pattern recognition methods are applied to handle the data. Multivariate statistical analysis will show features, with difference in signal intensity between samples which can be a biomarker candidate. The next step is to identify the ion of interest by fragmentation using MS/MS on Q-TOF. A compound can be assigned from the fragmentation pattern, or by searching against a MS/MS library.

II- The proteomics field is based on identification and quantification of the gene products in the biofluid, cell or tissue. One method used for relative quantification (without using external reference) of proteins is LC-MS profiling (label-free methods). In this method the ratio of the proteins in two different samples are compared based on the number of proteolytic peptides in each of the two experiments. Use of ESI MS/MS will generate fragment ion spectra that will be compared to the theoretical spectra from protein sequence database. To overcome the proteome complexity, the protein sample is fractionated using ID or 2D gel system. The proteomics approach has been used widely for biomarker and

autoantigen discovery in many diseases such as cancer, heart disease and Alzheimer's disease (AD) **(Shen Hu., 2006).** Furthermore, these biomarkers can be further validated through western blot with specific antibody, immunoassays (ELISA), protein microarrays such as those developed for autoimmune disease **(Joos T., 2000).** These microarrays were also applied to infectious diseases such as leprosy to look at the host response in different groups **(Groathouse N., 2006).** The availability of soft ionization methods in the late 1980s and the introduction of ESI and MALDI, with the availability of genome sequences, facilitated analysis of peptides and small proteins. The peptide mass fingerprinting (PMF) technique starts by isolation of the protein from one or two-dimensional gel electrophoresis (2D-gel) spots, tryptic enzyme digestion, analysis by ESI- MS/MS and searching against a protein database. An example of the proteomic approach is called shotgun proteomics. This approach is based on 1D or 2D LC-MS/MS **(Griffiths W. J., 2009).** Another proteomics approach is label-free quantification**.** An example of this approach is the redundant peptide-counting method. This method is based on number of times specific peptides have been identified in a given LC-MS/MS run. The grater the number of the peptides identified, the greater the abundance of the protein in a given sample **(Griffiths W., 2009).**

III- Lipidomics is the study of lipid molecule subclasses and their quantification, structure and function (the lipidome) within the cells and tissues. Comparing the lipid profile during normal states versus diseased states can be helpful in finding biomarker(s) for the disease and understanding the role of these lipids in particular diseases. This comparson is also helpful in assessment of changes in lipid metabolism and lipid-mediated signaling

processes as a result of disease. The lipidome is a component of the metabolome that is

highly dependent on mass spectrometry (MS) technology. The main instrument used in

lipidomics analysis is the time-of-flight (TOF) mass spectrometer, which is useful in

determining the elemental composition of lipid molecules by providing mass accuracies of

5–20 ppm. It also offers the advantage that all fragment-ions are recorded in a single

MS/MS spectrum. The MS/MS fragmentation allows further identification of lipid species

or screening for individual lipid classes. The lipidomics assays using mass spectrometry

can be described as targeted when the lipid species to be monitored are known. This can be

done using LC-MS/MS and multiple reaction monitoring (MRM) or selected ion

monitoring (SIM) which excludes the observation of unexpected metabolites and their

conjugates. Another type of lipidomics assay is untargeted, which is qualitative of the

overall lipid profile. This is for the most abundant and easily ionisable compounds but not

for minor lipids or those which are difficult to ionise. This can be done using full-scan

mode to search for new mass-to-charge ratio peaks **(Harkewicz R., 2010).** An example of

the mass spectrometry approach used to study the lipidome is the shotgun lipidomics. This

technique is based on directly infusing the lipid extract into the mass spectrometer and then

subjecting it to chromatographic separation which analyzes the entire lipid sample. Other

untargeted lipidomics methods that focus on identifying lipids that change in abundance as

a consequence of treatment or infection. This method is done through adding an extra

dimension of separation (RT in addition to m/z) by incorporating LC prior to ESI. In the

mid 1990s, the ion-source polarity (ESI) switching was developed. This facilitated analysis

of the anionic lipids, neutral and weakly anionic lipids **(Griffiths W., 2009, 2011).** ESI in

the positive mode allows the detection of phosphatidylcholine, lysophosphatidylcholine,

phosphatidyl ethanolamine, and sphingomyelins. The negative mode ESI can detect free fatty acids, phosphatidic acid, phosphatidyl serine, phosphatidyl inositol, phosphatidyl glycerol, and phosphotidylethanolamine. Neutral lipids, such as triacylglycerols are not readily ionized by ESI, however they can be detected as ammonium, lithium, or sodium adducts with ESI in positive mode **(Dettmer K., 2007).**

1.7.2 Leprosy biomarkers

Early detection and treatment of leprosy can prevent the risk of deformities and disease transmission. Many researchers have tried to find a biomarker for the disease and use it for early diagnosis. For example, the antibodies produced against the bacterial common antigens (PGL-1 and Ag85) have been used as a marker of bacterial load. The anti-PGL-1 level is found to be higher in MB patients compared to PB. Moreover, the antibody levels decline with treatment making it a good indicator for monitoring treatment **(Moura R., 2008).** The availability of the *M. leprae* genome sequence facilitated the selection of specific candidate antigens with specific T cell binding motifs **(Geluk A., 2006).** Other biomarkers used to diagnose leprosy and differentiate between different leprosy groups are cytokines. IFN-γ and TNF-α were found to be elevated in TT as compared to LL sera where IL-10 and IL- 1β are elevated. During leprosy reaction, serum IL-1b was more comparable to non-reaction patients. Type I reaction patients showed elevated levels of IFN-γ, IL-2R and IL-1β, whereas in Type II reaction patients IL-10 levels were also elevated beside IFN-γ, IL-2R and IL-1β **(Moubasher D., 1998).** These cytokines were found to be decreased after treatment. Moreover, leprosy patients were found to have higher serum level of IL-6, TNF-α and the macrophage activation product neopterin

compared to healthy controls. Neopterin was shown to have higher levels in MB than in PB patients. Unlike other cytokines neopterin did not decline after MDT treatment **(Iyer A., 2007, Silva E., 2007).**

Another biomarker used in leprosy is chitotriosidase that serves as a crucial macrophage-derived biomarker to monitor disease onset. Chitotriosidase is an important component of the innate immune response that cleaves chitin. This enzyme has been used as a biomarker in many diseases, such as Gaucher disease, atherosclerotic lesions, malaria and sarcoidosis. It is elevated in diseases involving macrophage activation and lipid accumulation such as leprosy. It was found that leprosy MB patients have elevated level of serum chitotriosidase compared to PB and healthy controls (HC) The ENL patients have higher activity of chitotriosidase as compared to HC and RR patients. Like other cytokines chitotriosidase activity decreases in ENL patients on treatment with prednisolone **(Iyer A., 2009).** Acute phase proteins (APP), have been used in diagnosis, classification and monitoring of leprosy and reactions. Examples of these APPs that were tested in leprosy are serum amyloid A (SAA) and C-reactive protein (CRP). During type II reaction (ENL) patients were shown to have elevated levels of SAA and CRP as compared to non-reactional patients **(Scheinberg M., 1979, Silva E., 2007).** The limitation in these biomarkers is that they could change in any inflammatory, immune mediated conditions, thus lacking disease specificity. Therefore, a further search for better biomarkers for early detection of leprosy is needed.

1.8. RATIONAL AND OBJECTIVES

Many studies have been done to understand the host-*M. leprae* interaction at the molecular level using the *in vitro* model (SC-neurone co culture). Many of these studies have examined specific targets (host or bacterial) as a new biomarker of the disease that could leads to uncover the mechanisms of pathogenesis. It is clear now that *M. leprae* uses specific cell wall antigens to bind to specific receptors in SC. After this binding and colonization inside the SC, *M. leprae* induces nerve injury. Many proposed mechanisms for the nerve injury have been generated based on immunological and non-immunological factors. However, there is lack on global study to examine the molecular change(s) in the host biofluid or tissue after *M. leprae* infection.

We hypothesized that *M. leprae* can induces expression, alters modification patterns of host metabolism, lipids and nerve proteins. This will lead to: i- degradation of certain proteins that stimulate production of antibodies against modified degraded proteins, which may cause the nerve damage, ii- change overall metabolite and lipid profile in the infected tissue through controlling the host gene expression.

Recently, with the development of the new Omics technologies, the progress has been made to apply this technology in the discovery of diagnostic disease-specific biomarkers in the infectious disease. The main purpose of this research studies was to discover specific biomarkers for leprosy and to have a new view of the host-pathogen interaction in order to understand the mechanism of leprosy that will aid in finding new diagnostic tools. We adopted a mass spectrometry-based approach for analyzing the serum metabolites, protein

and lipid from control and infected tissue samples. The armadillo (a leprosy model) was used in these studies to understand the process of nerve damage in leprosy that will lead to identifying new diagnosis approach for the nerve damage at an early stage of the disease.

References

1. Meyers WM and Marty AM (1991) Hansen GHA: Bacillus leprae. Virchows Arch Pathol Anat Physiol Klin Med 1880, 79:32-42.

2. Lehmann KB and Neumann R (1896) Atlas und Grundriss der Bakteriologie und Lehrbuch der speziellen bakteriologischen Diagnostik. edn 1st. Munich: J.F. Lehmann

3. Shepard C (1960) The experimental disease that follows the injection of human leprosy bacilli into foot pads mice. J Exp Med 112:445-454.

4. Chehl S, Ruby J, Job CK, Hastings RC (1983) The growth of *Mycobacterium leprae* in nude mice. Lepr Rev 54:283-304.

5. Adams LB and Krahenbuhl JL (1996) Granulomas Induced by*Mycobacterium leprae.* Methods 9: 220-232.

6. Kirchheimer W, Stoors E (1971) Attempts to establish the armadillo as a model for the study of leprosy.I. Report of lepromatoid leprosy in an experimentally infected armadillo. Int J Lepr. 39:693-702.

7. Cole ST, Eiglmeier K, Parkhill J, James KD, Thomson NR, et al. (2001) Massive gene decay in the leprosy bacillus. Nature 409: 1007-1011.

8. Williams DL, Slayden R a, Amin A, Martinez AN, Pittman TL, et al. (2009) Implications of high level pseudogene transcription in *Mycobacterium leprae*. BMC genomics 10: 397.

9. Bhamidi S, Scherman MS, Jones V, Crick DC, Belisle JT, et al. (2011) Detailed structural and quantitative analysis reveals the spatial organization of the cell walls of in vivo grown *Mycobacterium leprae* and in vitro grown *Mycobacterium tuberculosis*. The Journal of biological chemistry 286: 23168-23177.

10. Daffe M and Draper P (1998) The envelope layers of mycobacteria with reference to their pathogenicity. Adv Microb physiol. 39:131-203.

11. Guenin-Macé L, Siméone R, Demangel C (2009) Lipids of pathogenic Mycobacteria: contributions to virulence and host immune suppression. Transboundary and emerging diseases 56: 255-68.

12. Brennan PJ, and Crick DC (2007) The cell-wall core of Mycobacterium tuberculosis in the context of drug discovery. Curr Top Med Chem 7:475-488.

13. Brennan PJ (1984) *Mycobacterium leprae*- The outer lipoidal surface. Journal of Biosciences 6: 685-689.

14. Russell DG, Mwandumba HC, Rhoades EE (2002) Mycobacterium and the coat of many lipids. The Journal of cell biology 158: 421-426.

15. Truman RW, Andrews PK, Robbins NY, Adams LB, Krahenbuhl JL, Gillis TP (2008) Enumeration of *Mycobacterium leprae* using real-time PCR. PLOS neglected tropical diseases 2: e328.

16. Lahiri R (2005) Application of a viability-staining method for *Mycobacterium leprae* derived from the athymic (nu/nu) mouse foot pad. Journal of Medical Microbiology 54: 235-242.

17. Kurabachew M, Wondimu a, Ryon JJ (1998) Reverse transcription-PCR detection of *Mycobacterium leprae* in clinical specimens. Journal of clinical microbiology 36: 1352-6.

18. Hastings RC, Gillis TP, Krahenbuhl JL, Franzblau SG (1988) Leprosy. Clinical microbiology reviews 1: 330-348.

19. Croft RP, Richardus JH, Nicholls PG, Smith WC (1999) Nerve function impairment in leprosy: design, methodology, and intake status of a prospective cohort study of 2664 new leprosy cases in Bangladesh (The Bangladesh AcuteNerve Damage Study). Lepr Rev 70: 140–159.

20. Brennan PJ (2000) Skin test development in leprosy: progress with first-generation skin test antigens, and an approach to the second generation. Lepr Rev. 71: S50-54.

21. Moudgil KD, Gupta SK, Naraynan PR, Srivastava LM, Mishra RS, et al. (1989) Antibody response to phenolic glycolipid I and Mycobacterium w antigens and its relation to bacterial load in *M. leprae*-infected mice and leprosy patients. Clinical and experimental immunology 78: 214-218.

22. Douglas JT, Celona RV, Abalos RM, Madarang MG, Fajardo T (1987) Serological reactivity and early detection of leprosy among contacts of lepromatous patients in Cebu, the Philippines. Int J Lepr Other Mycobact Dis 55:718-721.

23. Pinheiro RO, Souza Salles J de, Sarno EN, Sampaio EP (2011) *Mycobacterium leprae*-host-cell interactions and genetic determinants in leprosy: an overview. Future microbiology 6: 217-230.

24. Aráoz R, Honoré N, Banu S, Demangel C, Cissoko Y, et al. (2006) Towards an immunodiagnostic test for leprosy. Microbes and infection / Institut Pasteur 8: 2270-2276.

25. Kox LFF, Jansen HM, Kuijper S (1997) Multiplex PCR assay for immediate identification of the infecting species in patients with mycobacterial disease . Multiplex PCR Assay for Immediate Identification of the Infecting Species in Patients with Mycobacterial Disease. J Clin Microbiol. 35:1492-1498.

26. Hastings RC, Gillis TP, Krahenbuhl JL, Franzblau SG (1988) Leprosy. Clinical microbiology reviews 1: 330-348.

27. Matsuoka M, Izumi S, Budiawan T, Nakata N, Saeki K (1999) *Mycobacterium leprae* DNA in daily using water as a possible source of leprosy infection. Indian J Lepr71: 61-67.

28. Lavania M, Katoch K, Katoch VM, Gupta AK, Chauhan DS, Sharma R, etal. (2008) Detection of viable *Mycobacterium leprae* in soil samples: insights into possible sources of transmission of leprosy. Infect Genet Evol. 8:627-631.

29. Davey TF and Rees RJ (1974) The nasal discharge in leprosy: clinical and bacteriological aspects. Lepr. Rev 45:121–134.

30. Job CK, Jayakumar J, and Aschhoff M (1999) "Large numbers" of *Mycobacterium leprae* are discharged from the intact skin of lepromatous patients; a preliminary report. Int J Lepr Other Mycobact Dis 67:164-167.

31. Job CK, Jayakumar J, Kearney M, Gillis TP (2008) Transmission of leprosy: a study of skin and nasal secretions of household contacts of leprosy patients using PCR. Am J Trop Med Hyg 78:518–521.

32. Matsuoka M, Maeda S, Kai M, Nakata N, Chae GT, et al. (2000) Mycobacterium leprae typing by genomic diversity and global distribution of genotypes. Int J Lepr Other Mycobact Dis: official organ of the International Leprosy Association 68:121-128.

33. Turankar RP, Lavania M, Singh M, Siva Sai KSR, Jadhav RS (2011) Dynamics of Mycobacterium leprae transmission in environmental context: Deciphering the role of environment as a potential reservoir. Infection, genetics and evolution: Infect Genet Evol 12:121-126.

34. Britton WJ (1993) Immunology of leprosy. Trans. R. Soc. Trop. Med. Hyg. 87:508-514.

35. http://www.who.int/lep/en/

36. Spierings E, Boer T De, Zulianello L, Ottenhoff TH (2000) Novel mechanisms in the immunopathogenesis of leprosy nerve damage: the role of Schwann cells, T cells and *Mycobacterium leprae*. Immunol cell biol 78: 349-55.

37. WHO Expert Committee on Leprosy (1998) World Health Organ Tech Rep Ser 874: 1-43.

38. Ridley DS and Jopling WH (1966) Classification of leprosy according to immunity. A five-group system. Int J. Lepr other Mycobact Dis 34:255-723.

39. Worobec SM (2009) Treatment of leprosy / Hansen's disease in the early 21st century. Dermatologic Therapy 22:518-537.

40. Zhu YI, Stiller MJ (2001) Dapsone and sulfones in dermatology: overview and update J Am Acad Dermatol 45:420-434.

41. Lowe J (1950) Treatment of leprosy with diamino-diphenyl sulphone by mouth. Lancet 1:145-150.

42. Lowe J (1951) Diaminodiphenylsulphone in the treatment of leprosy. Lancet 1:18-21.

43. Scollard D, Adams L, Gillis T, Krahenbuhl J, Truman R, et al. (2006) The continuing challenges of leprosy Clin Microbiol Rev 19:338-381.

44. Gurfinkel P, Pina JC (2009) Use of Clofazimine in Dermatology. J. of drugs in dermatology 8: 846-851.

45. Cross H, Lockwood D, Saunderson P, Batty J (2010) Review of Leprosy Research Evidence (2002 – 2009) and Implications for Current Policy and Practice ILEP Technical Commission Contributors: Other contributors. Review Literature And Arts Of The Americas 81: 228- 275.

46. Schuring RP, Hendrik J, Pahan D, Oskam L (2009) Protective effect of the combination BCG vaccination and rifampicin prophylaxis in leprosy prevention. Expert Review of Vaccines 27: 7125-7128.

47. Scollard DM, Bhoopat L, Kestens L, Vanham G, Douglas JT, Moad J (1992) Immune complexes and antibody levels in blisters over human leprosy skin lesions with or without erythema nodosum leprosum. Clin Immunol Immunopathol. 63:230-236.

48. Yamamura M, Wang XH, Ohmen JD, Uyemura K, Rea TH, et al. (1992) Cytokine patterns of immunologically mediated tissue damage. J Immunol 149:1470-1475.

49. Kahawita IP, Lockwood DN (2008) Towards understanding the pathology of erythema nodosum leprosum. Trans R Soc Trop Med Hyg. 102:329-337.

50. Shetty VP, Mistry NF, Antia NH (2000) Current understanding of leprosy as a peripheral nerve disorder: significance of involvement of peripheral nerve in leprosy. Indian J Lepr 72: 339-350.

51. Bhatheja K, Field J (2006) Schwann cells: origins and role in axonal maintenance and regeneration. Int J Biochem Cell Biol 38:1995-1999.

52. Greenfield S, Brostoff S, Eylar EH, Morell P (1973) Protein composition of myelin of the peripheral nervous system. J Neurochem. 20:1207-1216.

53. Suresh S, Wang C, Nanekar R, Kursula P, Edwardson JM (2010) Myelin basic protein and myelin protein 2 act synergistically to cause stacking of lipid bilayers. Biochemistry 49: 3456-2463.

54. Garbay B, Heape a M, Sargueil F, Cassagne C (2000) Myelin synthesis in the peripheral nervous system. Progress in neurobiology 61: 267-304.

55. Gould RM, Jessen KR, Mirsky R and Tennekoon G (1992) The Schwann cell: an update. Chapter 3 of Myelin: Biology and Chemistry, CRC Press.

56. Rambukkana A (2004) *Mycobacterium leprae*-induced demyelination: a model for early nerve degeneration. Current opinion in immunology 16:511-518.

57. Barker LP (2006) *Mycobacterium leprae* interactions with the host cell: recent advances. Indian J Med Res 123:748-759.

58. Rambukkana a (1998) Role of -Dystroglycan as a Schwann Cell Receptor for *Mycobacterium leprae*. Science 282: 2076-2079.

59. Rambukkana a (2001) Molecular basis for the peripheral nerve predilection of *Mycobacterium leprae*. Current Opinion in Microbiology 4:21-27.

60. Rambukkana A, Zanazzi G, Tapinos N, Salzer JL (2002) Contact-dependent demyelination by *Mycobacterium leprae* in the absence of immune cells. Science. 296:927-931.

61. Rambukkana a, Salzer JL, Yurchenco PD, Tuomanen EI (1997) Neural targeting of *Mycobacterium leprae* mediated by the G domain of the laminin-alpha2 chain. Cell 88: 811-821.

62. Rambukkana A (2010) Usage of signaling in neurodegeneration and regeneration of peripheral nerves by leprosy bacteria. Progress in neurobiology 91:102-107.

63. Ng V, Zanazzi G, Timpl R, Talts JF, Salzer JL, Brennan PJ, Rambukkana A (2000) Role of the cell wall phenolic glycolipid-1 in the peripheral nerve predilection of *Mycobacterium leprae*. Cell 103:511-524.

64. Tapinos N, Rambukkana A (2005) Insights into regulation of human Schwann cell proliferation by Erk1/2 via a MEK-independent and p56Lck-dependent pathway from leprosy bacilli. Proceedings of the National Academy of Sciences of the United States of America 102:9188-9193.

65. Tapinos N, Ohnishi M, Rambukkana A (2006) ErbB2 receptor tyrosine kinase signaling mediates early demyelination induced by leprosy bacilli. Nature medicine 12:961-966.

66. Ribeiro-Resende VT, Ribeiro-Guimaraes ML, Lemes RMR, Nascimento IC, Alves L, et al. (2010) Involvement of 9-O-acetyl GD3 Ganglioside in *Mycobacterium Leprae* Infection of Schwann Cells. J Biol Chem 285: 34086-34096.

67. Birdi TJ, Antia NH (2003) Mechanisms involved in peripheral nerve damage in leprosy with special reference to insights obtained from in vitro studies and the experimental mouse model. Int J Lepr Other Mycobact Dis: official organ of the International Leprosy Association 71:345-354.

68. Rodrigues LS, Silva Maeda E da, Moreira MEC, Tempone AJ, Lobato LãS, et al. (2010) *Mycobacterium leprae* induces insulin-like growth factor and promotes survival of Schwann cells upon serum withdrawal. Cellular Microbiol 12:42-54.

69. Shetty VP, Mistry NF, Antia NH (2000) Current understanding of leprosy as a peripheral nerve disorder: significance of involvement of peripheral nerve in leprosy. Indian J Lepr 72:339-350.

70. Save MP, Shetty VP, Shetty KT, Antia NH (2004) Alterations in neurofilament protein(s) in human leprous nerves: morphology, immunohistochemistry and Western immunoblot correlative study. Neuropathology and applied neurobiology 30:635-650.

71. Job CK (1971) Pathology of peripheral nerve lesions in lepromatous leprosy--a light and electron microscopic study. International journal of leprosy and other mycobacterial diseases: official organ of the International Leprosy Association 39: 251-268.

72. Jacobs JM, Shetty VP, Antia NH (1987) Myelin changes in leprous neuropathy. Acta neuropathologica 74:75-80.

73. Kajihara H, Paturusi IA, Saleh RM, Rasyad C, Ikuta Y (2000) Light and electron microscopic study of peripheral nerve damage in patients with lepromatous leprosy (LL) and borderline lepromatous leprosy (BL). Hiroshima J Med Sci. 49:83-92.

74. Rambukkana A (2000) How does *Mycobacterium leprae* target the peripheral nervous system? Trends in Microbiology 8: 23-28.

75. Pereira RM, Calegari-Silva TC, Hernandez MO, Saliba AM, Redner P, Pessolani MC, Sarno EN, Sampaio EP, Lopes UG (2005) *Mycobacterium leprae* induces NF-kappaB-dependent transcription repression in human Schwann cells. Biochem Biophys Res Commun. 335: 20-26.

76. Spierings E, Boer T De, Zulianello L, Ottenhoff TH (2000) Novel mechanisms in the immunopathogenesis of leprosy nerve damage: the role of Schwann cells, T cells and *Mycobacterium leprae*. Immunology and cell biology 78: 349-355.

77. Silva TPD, Silva ACCD, Baruque MDGA, Oliveira RBD, Machado MP, et al. (2008) Morphological and functional characterizations of Schwann cells stimulated with *Mycobacterium leprae*. Memórias do Instituto Oswaldo Cruz 103: 363-369.

78. Krutzik SR, Ochoa MT, Sieling PA, Uematsu S, Ng YW, Legaspi A, Liu PT, et al. (2003) Activation and regulation of Toll-like receptors 2 and 1 in human leprosy. Nat Med. 9: 525-532.

79. Hernandez MO, Neves I, Sales JS, Carvalho DS, Sarno EN, Sampaio EPImmunology. (2003) Induction of apoptosis in monocytes by *Mycobacterium leprae* in vitro: a possible role for tumour necrosis factor-alpha. Immunology. 109:156-164.

80. Sieling P a, Jullien D, Dahlem M, Tedder TF, Rea TH, et al. (1999) CD1 expression by dendritic cells in human leprosy lesions: correlation with effective host immunity. J Immunol. 162:1851-1858.

81. Scollard DM. (2000) Association of *Mycobacterium leprae* with human endothelial cells in vitro. Lab Invest. 80:663-669.

82. Touw J, Langendijk EM, Stoner GL, Belehu A (1982) Humoral immunity in leprosy: immunoglobulin G and M antibody responses to *Mycobacterium leprae* in relation to various disease patterns. Infection and immunity 36:885-892.

83. Schlesinger LS, Horwitz M (1994) A role for natural antibody in the pathogenesis of leprosy: antibody in nonimmune serum mediates C3 fixation to the *Mycobacterium leprae* surface and hence phagocytosis by human mononuclear phagocytes. Infection and immunity 62:280-289.

84. Iyer AM, Mohanty KK, Van Egmond D, Katoch K, Faber WR, Das PK, Sengupta U. Hum P (2007) Leprosy-specific B-cells within cellular infiltrates in active leprosy lesions. 38:1065-1073.

85. Adams LB, Scollard DM, Ray N a, Cooper AM, Frank A a, et al. (2002) The study of *Mycobacterium leprae* infection in interferon-gamma gene--disrupted mice as a model to explore the immunopathologic spectrum of leprosy. J Infect Dis 185: S1-8.

86. Pradhan V, Badakere SS, Shankar Kumar U (2004) Increased incidence of cytoplasmic ANCA (cANCA) and other autoantibodies in leprosy patients from western India. Lepr Rev. 75:50-56.

87. Scollard DM, Lathrop GW, Truman RW (1996) Infection of distal peripheral nerves by *M. leprae* in infected armadillos; an experimental model of nerve involvement in leprosy. Int J Lepr Other Mycobact Dis: official organ of the International Leprosy Association 64:146-151.

88. Hu S, Loo JA, Wong DT (2006) Human body fluid proteome analysis. Proteomics 6: 6326–6353.

89. Ilangumaran S, Shanker Narayan NP, Ramu G, Muthukkaruppan VR (1994) Cellular and humoral immune responses to recombinant 65-kD antigen of *Mycobacterium leprae* in leprosy patients and healthy controls. Clin Exp Immunol 96:79-85.

90. Naafs B, Kolk AH, Chin A Lien RA, Faber WR, Dijk G Van, et al. (1990) Anti-*Mycobacterium leprae* monoclonal antibodies cross-react with human skin: an alternative explanation for the immune responses in leprosy. J Invest Dermatol 94: 685-8.

91. Vardhini D, Suneetha S, Ahmed N, Joshi DSM, Karuna S, et al. (2004) Comparative proteomics of the Mycobacterium leprae binding protein myelin P0: its implication in leprosy and other neurodegenerative diseases. Infection, genetics and evolution. Infect Genet Evol 2004 4: 21-28.

92. Ribeiro SL, Pereira HL, Silva NP, Souza AW, Sato EI (2009) Anti-β2-glycoprotein I antibodies are highly prevalent in a large number of Brazilian leprosy patients. Acta reumatológica portuguesa 36: 30-37.

93. Singh K, Singh B, Ray PC (2010) Original Article Anti-ceramide antibodies in leprosy: marker for nerve damage. J Infect Dev Ctries 30;4:378-381.

94. Wheeler PR, Raynes JG, McAdam KP (1994) Autoantibodies to cerebroside sulphate (sulphatide) in leprosy. Clin Exp Immunol 98:145-150.

95. Pradhan V, Badakere SS, Shankar K (2004) Increased incidence of cytoplasmic ANCA (cANCA) and other autoantibodies in leprosy patients from western India. Lep Rev 75:50-56.

96. Rostami M (1997) P2-reactive T cells in inflammatory demyelination of the peripheral nerve. J Infect Dis 176: S160-163.

97. Sanvito L, Makowska A, Mahdi-Rogers M, Hadden RDM, Peakman M, et al. (2009) Humoral and cellular immune responses to myelin protein peptides in chronic inflammatory demyelinating polyradiculoneuropathy. Journal of neurology, neurosurgery, and psychiatry 80:333-338.

98. Tapinos N, Rambukkana A (2005) Insights into regulation of human Schwann cell proliferation by Erk1/2 via a MEK-independent and p56Lck-dependent pathway from leprosy bacilli.Proc Natl Acad Sci USA 102:9188-9193.

99. Tapinos N, Ohnishi M, Rambukkana A (2006) ErbB2 receptor tyrosine kinase signaling mediates early demyelination induced by leprosy bacilli. Nature medicine 12: 961-966.

100. Suneetha LM, Satish PR, Suneetha S, Job CK, Balasubramanian AS (1997) *M. leprae* binds to a 28-30-kDa phosphorylated glycoprotein of rat peripheral nerve. Int J Lepr Other Mycobact Dis: official organ of the International Leprosy Association 65:352-356.

101. Suneetha LM, Satish PR, Korula RJ, Suneetha SK, Job CK, et al. (1998) *Mycobacterium leprae* binds to a 25-kDa phosphorylated glycoprotein of human peripheral nerve. Neurochemical research 23:907-911.

102. Suneetha LM, Singh SS, Vani M, Vardhini D, Scollard D, et al. (2003) *Mycobacterium leprae* binds to a major human peripheral nerve glycoprotein myelin P zero (P0). Neurochemical research 28:1393-1399.

103. Ho CL, Liem RK (1996) Intermediate filaments in the nervous system: implications in cancer. Cancer Metastasis Rev. 15:483-497.

104. Lee M K, and Cleveland DW (1996) Neuronal Intermediate Filaments. Annual Review of Neuroscience. 19:187-217.

105. Save MP, Shetty VP, Shetty KT, Antia NH (2004) Alterations in neurofilament protein(s) in human leprous nerves: morphology, immunohistochemistry and Western immunoblot correlative study. Neuropathology and applied neurobiology 30:635-650.

106. Pant HC (1988) Dephosphorylation of neurofilament proteins enhances their susceptibility to degradation by calpain. The Biochemical journal 256:665-668.

107. Save MP, Shetty VP, Shetty KT (2009) Hypophosphorylation of NF-H and NF-M subunits of neurofilaments and the associated decrease in KSPXK kinase activity in the sciatic nerves of swiss white mice inoculated in the foot pad with *mycobacterium leprae*. Lepr Rev 80:388-401.

108. Teles RMB, Teles RB, Amadeu TP, Moura DF, Mendonça-Lima L, et al. (2010) High matrix metalloproteinase production correlates with immune activation and leukocyte migration in leprosy reactional lesions. Infection and immunity 78:1012-1021.

109. Antunes SLG, Chimelli LM, Rabello ET, Valentim VC, Corte-Real S, et al. (2006) An immunohistochemical, clinical and electroneuromyographic correlative study of the neural markers in the neuritic form of leprosy. Braz J Med Biol Res 39:1071-1081.

110. Meyers WM, Gormus BJ, Walsh GP (1992) Nonhuman sources of leprosy. Int J Lepr Other Mycbact Dis 60:477-480.

111. Kirchheimer WF, Storrs EE (1972) Attempts to establish the armadillo (Dasypus novemcinctus Linn.) as a model for the study of leprosy. I. Report of lepromatoid leprosy in an experimentally infected armadillo. Int J Lepr Other Mycobact Dis: official organ of the International Leprosy Association 39: 693-702.

112. Truman RW, Morales MJ, Shannon EJ, Hastings RC. (1986) Evaluation of monitoring antibodies to PGL-I in armadillos experimentally infected with M. *leprae*. Int J Lepr Other Mycobact Dis. 54:556-559.

113.   Duthie MS, Truman RW, Goto W, O'Donnell J, Hay MN, et al. (2011) Insight toward early diagnosis of leprosy through analysis of the developing antibody responses of *Mycobacterium leprae*-infected armadillos. Clinical and vaccine immunology: CVI 18: 254-259.

114. Job CK, Sanchez RM, Hastings RC (1985) Manifestations Of Experimental The Armadillo Leprosy In. Tropical Medicine. Am J Trop Med Hyg 34:151-161.

115. Meyers M, Walsh P (1986) Naturally Acquired Banded Armadillo: I 975-i Leprosy in the Nine- A Decade of Experience. J Leuko Biol 656: 645-656.

116. Vijayaraghavan R (2009) Nine-banded Armadillo Dasypus novemcinctus Animal Model for Leprosy Indian J Lepr 36:167-176.

117. Loughry WJ, Truman RW, McDonough CM, Tilak M-K, Garnier S, et al. (2009) Is leprosy spreading among nine-banded armadillos in the southeastern United States? J Wildl Dis 45:144-152.

118. Truman RW, Job CK, Hastings RC (1990) Antibodies to the phenolic glycolipid-1 antigen for epidemiologic investigations of enzootic leprosy in armadillos (Dasypus novemcinctus). Lepr Rev 61:19-24.

119. Hamilton HK, Levis WR, Martiniuk F, Cabrera A, Wolf J (2008) The role of the armadillo and sooty mangabey monkey in human leprosy. Intern J Dermatol 47:545-550.

120. Truman RW, Singh P, Sharma R, Busso P, Rougemont J, et al. (2011) Probable zoonotic leprosy in the southern United States. New Engl J Med 364:1626-1633.

121. Moraes MO, Cardoso CC, Vanderborght PR, Pacheco AG (2006) Genetics of host response in leprosy. Lepr Rev 77:189-202.

122. Misch E, Berrington WR, Vary JC, Hawn TR (2010) Leprosy and the human genome. Microbiology and molecular biology reviews: MMBR 74:589-620.

123. Mira MT, Alcaïs A, Nguyen VT, Moraes MO, Flumeri C Di, et al. (2004) Susceptibility to leprosy is associated with PARK2 and PACRG. Nature 427: 636-640.

124. Kang TJ, Chae GT (2001) Detection of Toll-like receptor 2 (TLR2) mutation in the lepromatous leprosy patients. FEMS Immunol Med Microbiol 31: 53-58.

125. Alcaïs A, Mira M, Casanova J-L, Schurr E, Abel L (2005) Genetic dissection of immunity in leprosy. Current opinion in immunology 17: 44-48.

126. Alter A, Grant A, Abel L, Alcaïs A, Schurr E (2011) Leprosy as a genetic disease. Mammalian genome: official journal of the International Mammalian Genome Society 22: 19-31.

127. Cardoso CC, Pereira AC, Brito-de-Souza VN, Duraes SMB, Ribeiro-Alves M, et al. (2011) TNF -308G>A Single Nucleotide Polymorphism Is Associated With Leprosy Among Brazilians: A Genetic Epidemiology Assessment, Meta-Analysis, and Functional Study. J Infect Dis 204:1256-1263.

128. Johnson CM, Lyle EA, Omueti KO, Stepensky VA, Yegin O, et al. (2007) Cutting edge: A common polymorphism impairs cell surface trafficking and functional responses of TLR1 but protects against leprosy. J Immunol 178: 7520–7524.

129. Wong SH, Gochhait S, Malhotra D, Pettersson FH, Teo YY, et al. (2010) Leprosy and the adaptation of human toll-like receptor 1. PLoS pathogens 6: e1000979.

130. Hu S, Loo JA, Wong DT (2006) Human body fluid proteome analysis. Proteomics 6: 6326–6353.

131. Dettmer K, Aronov PA, Hammock BD (2007) Mass spectrometry-based metabolomics. Mass Spectrometry Reviews 26: 51.

132. Groathouse N a, Amin A, Marques MAM, Spencer JS, Gelber R, et al. (2006) Use of protein microarrays to define the humoral immune response in leprosy patients and identification of disease-state-specific antigenic profiles. Infect Immun 74: 6458-6466.

133. Griffiths WJ, Wang Y (2009) Mass spectrometry: from proteomics to metabolomics and lipidomics. Chemical Society reviews 38: 1882-1896.

134. Harkewicz R, Dennis E A (2010) Applications of Mass Spectrometry to Lipids and Membranes. Annu Rev of Biochem 80:1-25.

135. Thomson J. J. (1899) On the Masses of the Ions in Gases at Low Pressures Philosophical Magazine 48: 547-567.

136. Moura RSD, Calado KL, Oliveira MLW, Bührer-sékula S (2008) Leprosy serology using PGL-I: a systematic review Rev Soc Bras Med Trop 41:11-18.

137. Geluk A, Ottenhoff THM (2006) HLA and leprosy in the pre and postgenomic eras. Human immunology 67:439-445.

138. Moubasher a D, Kamel N a, Zedan H, Raheem DD (1998) Cytokines in leprosy, I. Serum cytokine profile in leprosy. International journal of dermatology 37:733-740.

139. Iyer A, Hatta M, Usman R, Luiten S, Oskam L, Faber W, Geluk A, Das P (2007) Serum levels of interferon-gamma, tumour necrosis factor-alpha, soluble interleukin-6R and soluble cell activation markers for monitoring response to treatment of leprosy reactions. Clin Exp Immunol. 150:210-216

140. Silva EA, Iyer A, Ura S, Lauris JR, Naafs B, Das PK, Vilani-Moreno F (2007) Utility of measuring serum levels of anti-PGL-I antibody, neopterin and C-reactive protein in monitoring leprosy patients during multi-drug treatment and reactions. Trop Med Int Health.12:1450-1458.

141. Iyer A, Eijk M van, Silva E, Hatta M, Faber W, et al. (2009) Increased chitotriosidase activity in serum of leprosy patients: association with bacillary leprosy. Clin Immunol 131: 501-509.

142. Scheinberg M , Masuda A, Benson MD, Mendes NF (1979) Serum amyloid protein SAA, C-reactive protein and lysozyme in leprosy. Int J Lepr Other Mycobact Dis: official organ of the International Leprosy Association 47:133-137.

CHAPTER 2

Serum Metabolomics Reveal Higher Levels of Polyunsaturated Fatty Acids in Lepromatous Leprosy: Potential Markers for Susceptibility and Pathogenesis

2.1 SUMMARY

2.1.1 Background

Leprosy is a disease of the skin and peripheral nervous system caused by the obligate intracellular bacterium *Mycobacterium leprae*. The clinical presentations of leprosy are spectral, with the severity of disease determined by the balance between the cellular and humoral immune response of the host. The exact mechanisms that facilitate disease susceptibility, onset and progression to certain clinical phenotypes are presently unclear. Various studies have examined lipid metabolism in leprosy, but there has been limited work using whole metabolite profiles to distinguish the clinical forms of leprosy.

2.1.2 Methodology & Principal Findings

In this study we adopted a metabolomics approach using high mass accuracy ultrahigh pressure liquid chromatography mass spectrometry (UPLC-MS) to investigate the circulatory biomarkers in newly diagnosed untreated leprosy patients. Sera from patients having bacterial indices (BI) below 1 or above 4 were selected, subjected to UPLC-MS, and then analyzed for biomarkers which distinguish the polar presentations of leprosy. We found significant increases in the abundance of certain polyunsaturated fatty acids (PUFAs) and phospholipids in the high-BI patients, when contrasted with the levels in the low-BI patients. In particular, the median values of arachidonic acid (2-fold increase), eicosapentaenoic acid (2.6-fold increase) and docosahexaenoic acid (1.6-fold increase) were found to be greater in the high-BI patients.

2.1.3 Significance

Eicosapentaenoic acid and docosahexaenoic acid are known to exert anti-inflammatory properties, while arachidonic acid has been reported to have both pro- and anti-inflammatory activities. The observed increase in the levels of several lipids in high-BI patients may provide novel clues regarding the biological pathways involved in the immunomodulation of leprosy. Furthermore, these results may lead to the discovery of biomarkers that can be used to investigate susceptibility to infection, facilitate early diagnosis and monitor the progression of disease.

2.2. AUTHOR SUMMARY

Leprosy is an infectious disease caused by the obligate intracellular bacterium *Mycobacterium leprae*. *M. leprae* infects the skin and nerves, leading to disfigurement and nerve damage, with the severity of the disease varying widely. We believe there are multiple factors (genetic, bacterial, nutritional and environmental), which may explain the differences in clinical manifestations of the disease. We studied the metabolites in the serum of infected patients to search for specific molecules that may contribute to variations in the severity of disease seen in leprosy. We found that there were variations in levels of certain lipids in the patients with different bacterial loads. In particular, we found that three polyunsaturated fatty acids (PUFAs) involved in the inhibition of inflammation were more abundant in the serum of patients with the higher bacterial loads. However, we do not know whether these PUFAs originated from the host or the bacteria. The variations in the metabolite profile that we observed provide a foundation for future research into the explanations of how leprosy causes disease.

2.3. INTRODUCTION

Leprosy is caused by *Mycobacterium leprae*, an obligate intracellular pathogen, which infects the skin and peripheral nerves. *M. leprae* invasion of Schwann cells leads to nerve damage, disability and deformity **[1-2].** However, not all infected patients have the same clinical course. The course of the disease may be punctuated by spontaneous and/or recurring episodes of immunological imbalances that need immediate medical attention and immune suppressive treatment. There are no routine laboratory tests for monitoring

clinical improvement, response to treatment or evolution of drug resistance, aside from monitoring the reduction of bacillary levels in skin smears. Even after several decades of multidrug therapy programs to reduce leprosy transmission, incidence is not declining at expected rates in some of the most endemic countries [3]. This persistent incidence in some regions is commonly believed to be due to undetected and undiagnosed subclinical cases [4].

Leprosy is conventionally described as a spectral disease using the well-established Ridley-Jopling scheme [5]. At one pole is the limiting form termed tuberculoid (TT) leprosy. In tuberculoid leprosy the bacterial load is low due to effective cell mediated immunity (CMI), and the infection is usually localized to either a skin patch or nerve trunk. At the site of infection, the immune response is dominated by Th1 associated pro-inflammatory cytokines (IFN-γ and IL-2) and granuloma formation. The opposite profile form is lepromatous (LL) leprosy, which shows a high bacterial load, poor CMI, and is characterized by Th2 associated anti-inflammatory cytokines (IL-4 and IL-10) and antibody production. Between the poles are borderline tuberculoid (BT), borderline (BB) and borderline lepromatous (BL).

There are multiple known and undefined factors that modulate the range of susceptibility to clinical outcomes, including metabolic and immune functions. The individual contributions of host and bacterium are not yet fully defined, although many human genetic loci and bacterial components have been implicated in the process of infection and perturbation of the immune response [6-10]. Host factors include single

77

nucleotide polymorphisms (SNPs) in genomic regions associated with a variety of products such as TNFα, IL-10, vitamin D receptor (VDR), parkin (PARK2) and parkin co-regulated gene protein (PACRG) **[11-12].** Nutritional and metabolic factors may also play a role in regulating the host immune response **[13-14].** The pathogen *M. leprae* is unique in that its genome has undergone massive decay, particularly in catabolic pathways and energy generating processes, and is therefore thought to be highly dependent on the host system for growth **[15].** Novel overlapping mechanisms have been described by which *M. leprae* modulates its environment for nutrition and immune evasion **[16].**

In this context, where leprosy is a product of complex host-pathogen relationships, there is a need for modern approaches to uncover underlying and/or novel biochemical signals that may be informative regarding those pathways that contribute to disease. Though leprosy is a disease of the skin and peripheral nerves, there may be biomarkers in the blood (circulatory biomarkers) which may indicate systemic factors. Several investigators have studied plasma and serum lipid composition in patients using traditional analytical methods such as thin layer chromatography (TLC) or gas chromatography (GC) **[17-18].** With the advent of sensitive ultrahigh pressure liquid chromatography (UPLC) quadrupole time-of-flight (Q-TOF) mass spectrometry (UPLC-MS), separation and detection of large numbers of small molecules (metabolites) in complex starting mixtures has become feasible. UPLC-MS provides rapid screening with accurate mass measurement, is of high resolution, has low-detection limits, permits ion fragmentation, and does not require a large amount of sample or a combination of different techniques to identify metabolites. This technology has made it possible to rapidly identify biomarkers

which distinguish normal states from various disease states using biological specimens such as urine, plasma and serum **[19-21].**

We sought to use this metabolomics approach to contrast the serum metabolome of patients with high and low bacterial indices (BI) using UPLC-MS. In the high-BI serum we discovered greater levels of the polyunsaturated fatty acids (PUFAs) eicosapentaenoic acid (EPA), arachidonic acid (AA) and docosahexaenoic acid (DHA). We discuss these findings in the context of emerging models regarding the interactions between lipid metabolism and immunity. The methods and findings have implications for discovery of novel biomarkers for diagnosis, identification of therapeutic targets and elucidation of pathogenic mechanisms.

2.4. MATERIALS AND METHODS

2.4.1 Ethical statement

Ethical approval for the use of these samples for research was obtained from the Institutional Review Board of Colorado State University and the Cebu Skin Clinic. Patient samples were collected as part of routine care following written informed consent.

2.4.2 Serum sample collection, preparation and selection

Sera were selected from a sample bank generated for ongoing research into the molecular epidemiology of leprosy involving newly diagnosed leprosy patients at the Cebu Skin Clinic in Cebu, Philippines [22]. Samples were taken prior to the initiation of multidrug therapy. Blood samples were drawn into a plain (no additive) evacuated tube (BD Vacutainer Serum) and centrifuged at 1,500 rpm for 10 min at 4 °C in a refrigerated centrifuge. The serum samples were aliquoted into multiple vials at 1 ml per vial and frozen at -20 °C until shipment. The sera were shipped on dry ice to Colorado State University and stored at -20°C until subsequent use in the laboratory.

Serum samples were selected from two groups of patients, those with BI<1 (n=10) and those with BI >4 (n=13) (**Table 2.1**). Sample selection was randomized and without consideration of clinical or demographic data aside from BI. Though factors such as age, gender, clinical presentation and medical history were not considered in the study design or analysis, such data were collected during patient intake and are presented in **Table 2.1**.

BI was measured at the Cebu Skin Clinic by microscopic examination of acid-fast stained slit-skin smears taken from six sites, including representative active lesions. BI was ranked on a log 10 scale from 0 to 6 **[23].**

Table 2.1. Patient demographic and clinical data.

Sample[a]	BI[b]	R-J Class[c]	PB/MB[d]	Sex	Age	Duration of Symptoms[e]	Medical History[f]
Low-BI							
L5	0.33	BT	MB	F	20	2Y	-
L32[g]	0.17	BT	MB	M	27	1Y	-
L40[g]	0.50	-	MB	M	38	-	-
L49	0.00	BT	PB	M	36	2Y	-
L74	0.33	BT	MB	M	62	5M	Hypertension
L76	0.50	BL	MB	M	64	5M	-
L77	0.00	BT	PB	M	36	10Y	-
L79	0.00	BT	PB	F	64	2Y	-
L85	0.17	BL	MB	F	42	5M	-
L90	0.00	BT	MB	F	24	2Y	-
High-BI							
L1	4.80	LL	MB	M	26	2Y	-
L9	4.70	LL	MB	M	25	5Y	-
L11	4.80	LL	MB	F	22	15Y	Congenital deformities
L15	5.00	LL	MB	M	25	2Y	-
L19	4.80	LL	MB	M	28	6Y	Appendicitis
L22	5.00	LL	MB	M	41	3Y	Peptic Ulcer
L29	4.80	LL	MB	M	18	3Y	-
L51	5.00	LL	MB	M	61	5Y	-
L53[h]	5.00	LL	MB	M	39	4Y	-
L58	5.00	LL	MB	M	37	2Y	-
L75	5.00	LL	MB	M	26	2Y	-

81

| L88 | 5.00 | LL | MB | M | 49 | 3Y | - |
| L89 | 5.00 | LL | MB | M | 30 | 1Y | - |

a. Sample names are as per Sakamuri et al, 2009 [22].
b. Ridley-Jopling classification of leprosy [5].
c. Bacterial index determined from slit-skin smear [23].
d. Clinical classification into either paucibacillary (PB) or multibacillary (MB) leprosy.
e. Self-reported duration of symptoms prior to treatment
f. Self-reported medical history; with the exception of patient L11, reported conditions do not reflect current illness at the time of diagnosis.
g. Patients who presented at the clinic in a type 1 reaction state.
h. Patients with deformities caused by leprosy.

A volume of 50 µl from each serum sample was prepared for analysis by UPLC-MS. Sera proteins were precipitated by the addition of 3 volumes (150 µl) of cold 100% methanol. The samples were vortexed, placed at -20 °C for two hours, then centrifuged for 10 minutes at 15,000 rpm to pellet the protein precipitate. The supernatants were carefully transferred to new Eppendorf tubes. From each supernatant, 1 µl was analyzed by UPLC-MS in both negative and positive modes with duplicate injections. To confirm the observations and mass spectrometry methods a subset of the selected sera were reanalyzed using new aliquots and triplicate injections. Five each from the low-BI (L32, L40, L76, L79, L85) and high-BI (L1, L11, L19, L58, L88) groups were pooled and retested; two low-BI (L40, L85) and two high-BI (L15, L88) samples were retested individually.

2.4.3 Instrumentation and UPLC-MS methods

The serum methanol extracts were separated on a Waters ACQUITY UPLC coupled with a Q-TOF under the control of MassLynx v4.1 [Waters. Millford, MA, USA]. 1 µl injections were performed on a Waters ACQUITY UPLC system. Separation was performed using a Waters ACQUITY UPLC C8 column (1.7 µM, 1.0 x 100 mm), using a gradient from solvent A (89% water, 5% acetonitrile, 5% isopropanol, 1% 500 mM ammonium acetate) to solvent B (49.5% acetonitrile, 49.5% isopropanol, 1% 500mM ammonium format). Injections were made in 100% A, which was held for 0.1 min. A 0.9 min linear gradient to 40% B was applied, followed by a 10 min gradient to 100% B which was held for 3 min, then returned to starting conditions over 0.1 min, and then allowed to re-equilibrate for 5.9 min. Flow rate was constant at140 µl/min for the duration of the run. The column was held at 50°C; samples were held at 5°C.

Mass data were collected between 50 and 1200 m/z at a rate of two scans per second. The voltage and temperature parameters were as follows: 3000 V capillary, 30 V sample cone, 2.0 V extraction cone, 350 °C desolvation temperature and 130 °C source temperature. Calibration was performed prior to sample analysis via infusion of sodium formate solution, with mass accuracy within 5 ppm. For MS/MS, the parent ion was selected by quadrupole and fragmented via collision-induced dissociation (CID) with argon at collision energy of 20 eV for fatty acids or 30 eV for phospholipids.

2.4.4 Data processing

UPLC-MS data were aligned, extracted and viewed using MarkerLynx v4.1 [Waters. Millford, MA, USA]. Chromatographic peaks were detected between 0 and 28 min with a retention time (RT) window of 0.1 min. Apex track peak detection parameters were used, with automatic detection of peak width and baseline noise. The spectrometric features were assigned by m/z and RT, while the relative intensity was based on the area of all features. Initial screening for compounds with significant differences in abundance between the low-BI and high-BI groups was performed by orthogonal projection onto latent structures (OPLS) with the software SIMCA-P+ v12.0 [Umetrics. Umeå, Västerbotten, Sweden], using a Po(corr) cut-off of 0.5. Further statistical analysis was performed using several R packages within R 2.12.1 [24]. Principal component analysis (PCA) was performed using stats::prcomp with both scaling and centering of the variables. Generation of receiver operating characteristic (ROC) curves for selected compounds was performed using the R package pROC v1.4.3 [25]; a 95% confidence interval was generated for sensitivity using

2,000 bootstrap replicates. For each selected compound, histogram bins were calculated using the Freedman-Diaconis rule and kernel density estimates were calculated using Gaussian smoothing. In order to compare the first (individual serum) and second (pooled sera) runs, data for each compound was standardized by subtracting the mean and dividing the result by the standard deviation (standard score) to account for shifts in instrument sensitivity over time; the data were then compared for statistically significant differences using the Mann-Whitney test.

2.4.5 Identification of compounds

Tentative compound class assignments (free fatty acid, glycerolipid, phospholipid, etc.) were made by querying the exact mass against the LIPID MAPS database [26] and the online web server MassTRIX: Mass Translator into Pathways [27]. The compounds that showed significant differences in intensity between the low-BI and high-BI groups, based on exact m/z and 0.05 min RT differences, were further fragmented by MS/MS in both positive and negative ion modes. Metabolite identities were manually examined for signature ions and verified by comparing the fragment spectra to those in LIPID MAPS and published data [28]. MassTRIX was also used to explore related pathways that may be associated with selected metabolites.

2.4.6 Standards

After preliminary assignments were made for some of the selected compounds, pure standards were obtained and analyzed by the previously described chromatographic methods. Pooled sera were rerun in the same experiment. Eicosapentaenoic acid (EPA,

20:5), arachidonic acid (AA, 20:4) and docosahexaenoic acid (DHA, 22:6) were purchased from Sigma-Aldrich [Saint Louis, MO, USA]; 1-palmitoyl-2-arachidonoyl-*sn*-glycero-3-phosphocholine (PAPC) was purchased from Avanti Polar Lipids [Alabaster, Alabama, USA]. All standards were dissolved in 75% methanol prior to UPLC-MS analysis.

2.5. RESULTS

2.5.1 Global characterization of mass spectrometry data

The UPLC-MS data was first characterized globally. Across both the low-BI (n=10) and high-BI (n=13) samples a total of 1668 features in the positive mode and 2489 features in negative mode were observed (**Supplement 2.S3**). A PCA, generated from abundance data of all positive and negative mode m/z-RT pairs (features), showed low-BI and high-BI patient sera clustering away from each other (**Figure 2.1**). The separation of patient groups indicates that there are m/z-RT pairs that are quantitatively distinct in the two groups. Close clustering of injection duplicates is also seen, which is the expected behavior.
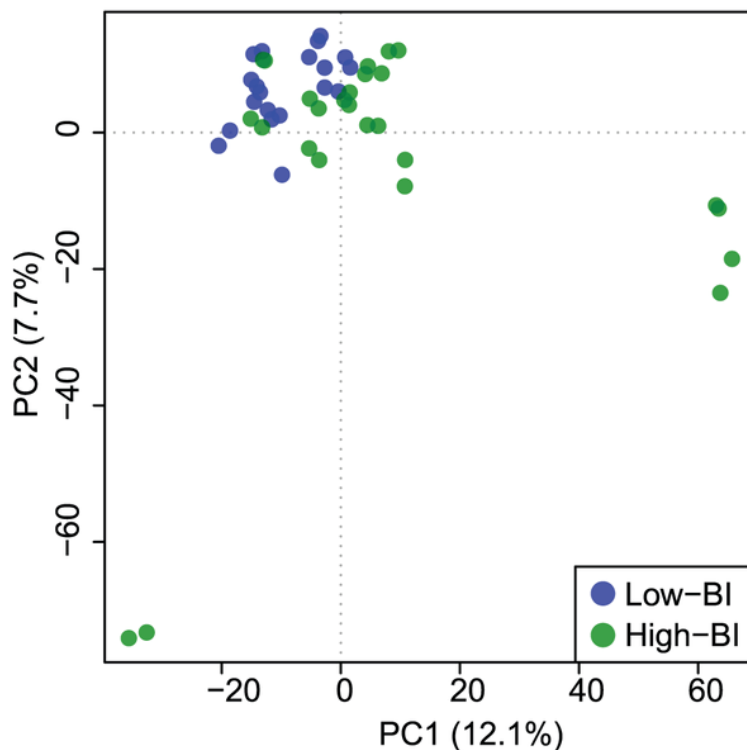
Figure 2.1: Principal component analysis of all positive and negative mode m/z values detected in serum of leprosy patients. A PCA score plot of all positive mode (n = 1668) and negative mode (n = 2489) m/z values collected from UPLC-MS analysis of 23 serum samples (10 low-BI, 13 high-BI). The first two components account for 20.4% of the variation in the data. Duplicate runs of each sample are visible as clustered pairs. A separation of samples is seen based on the BI of the patient.

2.5.2 Selection and validation of metabolite biomarkers

To identify the compounds that distinguished the low-BI from high-BI samples, the dataset was first pared down to features which exhibited the greatest difference in abundance between the two sample groups with OPLS (not shown). This yielded 48 features with masses up to approximately 1 kD - 19 from the positive mode and 29 from the negative mode. From these 48 features, 18 compounds were tentatively identified using the online databases LIPID MAPS and MassTRIX (**Table 2.2**). The data indicate an

increase in the level of several lipids in the high-BI sera compared to those in the low-BI sera. All of the 18 identified compounds were more abundant in the high-BI samples except for those with m/z 518.3245, 558.3196 and 566.3192, which were more abundant in the low-BI samples. A confirmatory second UPLC-MS analysis was performed using a pooled subset of samples. Though m/z and RT values shifted slightly, due to expected operational variability, we found the same 18 compounds again showed quantitative distinctions between low-BI and high-BI groups.

Table 2.2. Identities of significant features, observed values and measures of statistical support.

m/z[a]	RT[b]	Mode[c]	Name	Formula	Identified By[d]	LM ID[e]	Median Abundance[f]		AUC[g]
							Low-BI	High-BI	
Identified Compounds (1)[i]									
301.2174[h]	3.8001	-	Eicosapentaenoic Acid (EPA) (20:5)	$C_{20}H_{30}O_2$	Standard + LM MS/MS	LMFA01030759	56.5	151.6	86.2 ± 11.2
303.2324[h]	4.2763	-	Arachidonic Acid (AA) (20:4)	$C_{20}H_{32}O_2$	Standard + LM MS/MS	LMFA01030001	383.5	780.9	91.9 ± 15.3
327.2340[h]	4.1138	-	Docosahexaenoic Acid (DHA) (22:6)	$C_{22}H_{32}O_2$	Standard + LM MS/MS	LMFA01030185	238.2	474.3	82.7 ± 12.7
Putatively Annotated Compounds (2)[i]									
317.2114[h]	2.6914	-	5-oxo-eicosatetraenoic Acid (5-oxoETE)	$C_{20}H_{30}O_3$	LM MS/MS	LMFA03060011	22.0	46.9	71.5 ± 15.0
329.2465[h]	4.4796	-	Docosapentaenoic Acid (DPA) (22:5)	$C_{22}H_{34}O_2$	LM MS/MS	LMFA01030183	36.8	113.3	90.2 ± 9.4
335.2234[h]	4.0446	-	Leukotriene B4 (LTB4)	$C_{20}H_{32}O_4$	LM MS/MS	LMFA03020001	3.5	7.3	72.1 ± 15.5
516.3074[h]	3.7331	+	Lyso PC (18:4/0:0)	$C_{26}H_{46}NO_7P$	LM MS/MS	LMGP01050040	18.8	31.2	87.9 ± 10.0
Unconfirmed or Unknown Compounds (3,4)[i]									
279.2317	2.8074	+	γ-Linolenic Acid (18:3)	$C_{18}H_{30}O_2$	MassTRIX	LMFA01030141	2.2	5.5	74.8 ± 14.9
			or α-Linolenic Acid (18:3)	$C_{18}H_{30}O_2$	MassTRIX	LMFA01030152			
283.2423	4.1115	-	Stearic Acid (18:0)	$C_{18}H_{36}O_2$	MassTRIX	LMFA01010018	71.5	135.3	81.9 ± 13.0
305.2500	4.6343	-	Eicosatrienoic Acid (ETrE) (20:3)	$C_{20}H_{34}O_2$	LM Mass	LMFA01030157	73.0	151.5	87.7 ± 10.6
379.2847	5.4213	+	-	-	-	-	4.2	14.2	91.9 + 8.1
385.2387	4.2658	-	-	-	-	-	3.5	5.2	82.2 ± 12.2
395.2240	4.1131	-	Echitovenine	$C_{23}H_{28}N_2O_4$	MassTRIX	-	1.3	3.8	85.8 ± 11.0
509.3366	3.2629	+	Lyso PC (O-18:1/0:0)	C26H55NO6P	LM Mass	LMGP01070009	0.0	5.2	97.0 ± 5.7
			or Lyso PE (20:1/0:0)	$C_{25}H_{51}NO_7P$	Murphy	-			
518.3245	2.7152	+	Lyso PC (18:3/0:0)	$C_{26}H_{48}NO_7P$	LM Mass + Murphy	LMGP01050038	34.0	17.7	84.8 ± 12.3
558.3196[h]	2.7183	+	Lyso PC + unknown fatty acid	-	-	-	10.8	5.7	86.9 ± 12.4
566.3192	2.8304	+	Lyso PC (21:0/0:0)	$C_{29}H_{60}NO_7P$	LM Mass	LMGP01050051	4.1	0.0	75.4 ± 12.2
798.5707[h]	4.2907	-	PAPC-like	-	Standard + LM MS/MS	LMGP01010007 (PAPC)	11.0	23.2	79.8 ± 12.8

a. The observed mass to charge ratio.
b. The observed retention time.
c. Whether the m/z-RT pair was observed in position (+) or negative (-) ion mode.

d.   The basis for the identification of the compound. Standard: Comparison of MS/MS spectrum and RT to a commerical standard. LM MS/MS: Comparision of MS/MS spectrum to spectra published in LIPID MAPS. MassTRIX: Identified by MassTRIX based upon exact mass. LM Mass: Compound identity based upon exact mass matches in LIPID MAPS. Murphy: The compound was compared to mass data in Murphy, 2002 [29].

e.   The LIPID MAPS identification number for the compound.

f.   The median abundance value observed in the individual (non-pooled) samples.

g.   The area under the curve (AUC) of the receiver operating characteristic (ROC) curve with a 95% confidence interval denoted as a ± value.

h.   Compounds which fragmented in MS/MS. See Figures 2-4 and Figure S1 for MS/MS spectra of samples and commmerical standards. See Figure S2 for additional spectra.

i.   Confidence levels for compound identifications as per Sumner et al, 2007 [30]. Higher values indicate a more confident identification.

We also queried the complete list of m/z values against the MassTRIX annotation system, which performs a search for potential compound identities and associated pathways curated in KEGG: Kyoto Encyclopedia of Genes and Genomes [31]. MassTRIX assigned a total of 74 negative mode features to 143 compounds in 40 pathways, and 79 positive mode features to 89 compounds in 51 pathways. The predominant hits were pathways involved in AA metabolism (29 compounds) and synthesis of unsaturated fatty acids (13 compounds); not all compounds were unique.

2.5.3 Compound identification by tandem mass spectrometry

The 18 significant compounds that we tentatively identified were further characterized by MS/MS. From these 18 compounds, the compounds of the most interest to us - given their role in modulation of the inflammatory response - were the n-6 PUFA AA, the n-3 PUFAs EPA and DHA, and the compound with structural similarity to PAPC. Commercial standards of EPA, AA, DHA and PAPC were obtained and submitted to mass spectrometry in parallel with the serum samples. Not all of the 18 ions fragmented, but compound confirmation was achieved via MS/MS for 9 compounds by referencing the ion fragmentation pattern against published spectra and/or available standards (**Table 2.2**).

The chemical structures and fragmentation patterns of compounds listed in **Table 2.2** are shown in **Figures 2.(2-4)** and **Figures S1-S2**. In each of **Figures 2.(2-4)** and **Figure S1** the chemical structure of the compound is shown in **Panel A**, the fragmentation pattern of the commercial standard is shown in **Panel B**, and the fragmentation pattern of the

corresponding compound in the pooled serum sample is shown in **Panel C. Figure S2.2**

shows the fragmentation pattern in the pooled serum sample for the remaining compounds

putatively identified by MS/MS. The spectra illustrations have been adjusted from the

original MassLynx output files for clarity; the font of the axes and labels has been

changed, the line width of the spectra has been increased and extraneous text and borders

have been removed.
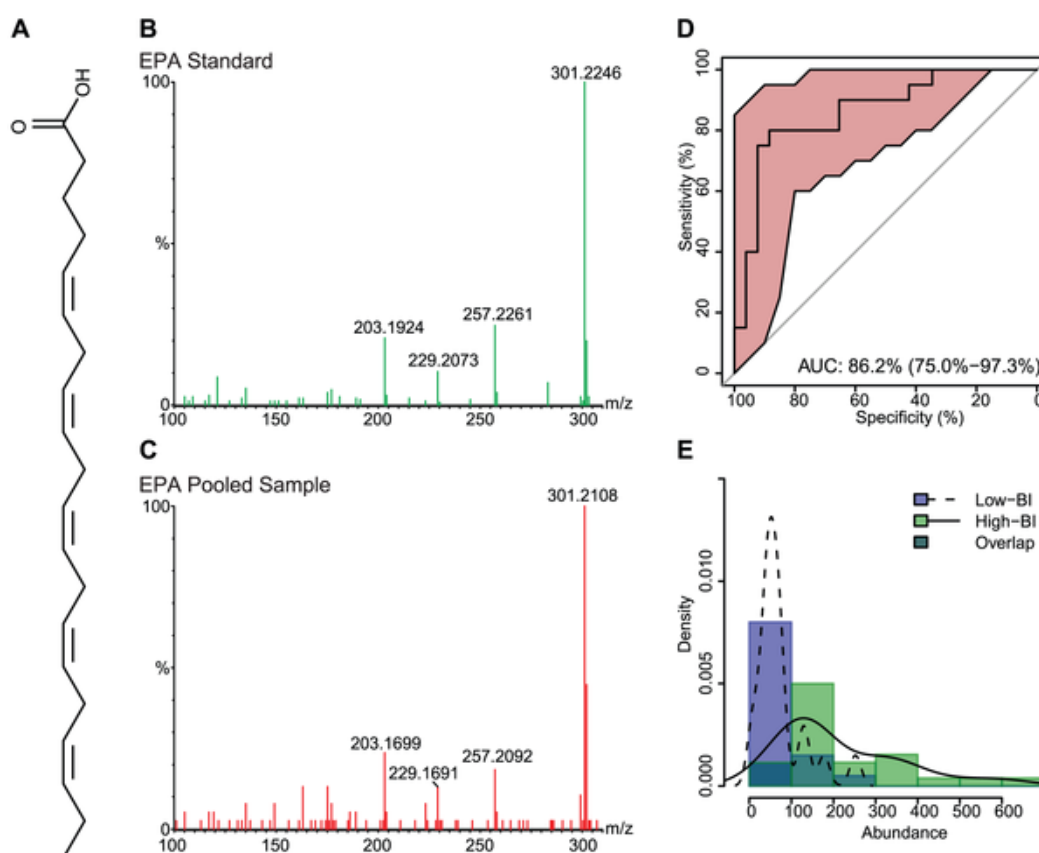
Figure 2.2: Eicosapentaenoic acid (EPA) chemical structure, MS/MS spectra, ROC curve and distribution across sample groups. (**A**) The chemical structure of EPA. (**B**) The MS/MS fragmentation pattern for the commercial standard. (**C**) The MS/MS fragmentation pattern of a representative pooled serum sample. (**D**) An ROC curve, showing the diagnostic accuracy of EPA in distinguishing low-BI from high-BI samples. The shaded (red) region surrounding the curve represents a 95% confidence interval for

sensitivity. The AUC is shown on the graph with a 95% confidence interval in parenthesis. (**E**) A histogram showing the distribution of EPA in the low-BI and high-BI groups. The overlaid curves show the kernel density estimates for each sample group.
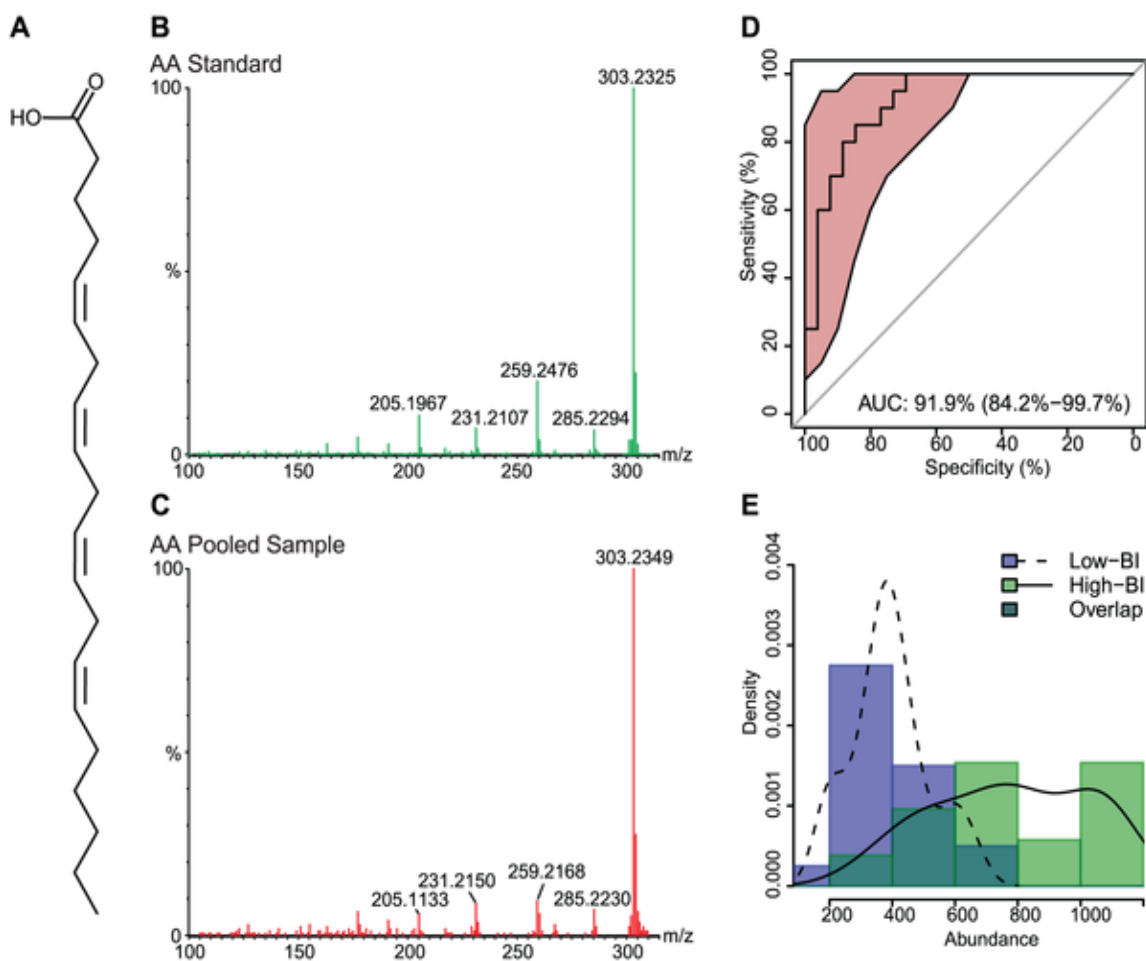
Figure 2.3: Arachidonic acid (AA) chemical structure, MS/MS spectra, ROC curve and distribution across sample groups. (**A**) The chemical structure of AA. (**B**) The MS/MS fragmentation pattern for the commercial standard. (**C**) The MS/MS fragmentation pattern of a representative pooled serum sample. (**D**) An ROC curve, showing the diagnostic accuracy of AA in distinguishing low-BI from high-BI samples. The shaded (red) region surrounding the curve represents a 95% confidence interval for sensitivity. The AUC is shown on the graph with a 95% confidence interval in parenthesis. (**E**) A histogram showing the distribution of AA in the low-BI and high-BI groups. The overlaid curves show the kernel density estimates for each sample group.

Figure 2.4: Docosahexaenoic acid (DHA) chemical structure, MS/MS spectra, ROC curve and distribution across sample groups. (**A**) The chemical structure of DHA. (**B**) The MS/MS fragmentation pattern for the commercial standard. (**C**) The MS/MS fragmentation pattern of a representative pooled serum sample. (**D**) An ROC curve, showing the diagnostic accuracy of DHA in distinguishing low-BI from high-BI samples. The shaded (red) region surrounding the curve represents a 95% confidence interval for sensitivity. The AUC is shown on the graph with a 95% confidence interval in parenthesis. (**E**) A histogram showing the distribution of DHA in the low-BI and high-BI groups. The overlaid curves show the kernel density estimates for each sample group.

The parent and daughter ions of EPA, AA and DHA appear as expected in both the standards and patient samples. However, we could not conclusively identify the feature we

observed in the serum samples with m/z of 798. The molecular weight of PAPC is 781, with an observed value of 766 under negative ionization due to loss of the methyl group from choline (**Figure S2.1B**). The feature with m/z of 798 produced several fragments consistent with the PAPC standard; specifically, ions with m/z 255, 303 and 480 (**Figure S2.1C**), which correspond to palmitic acid, arachidonic acid and lysophosphocholine (16:0/0:0), respectively. The RT for the PAPC standard was 8.5 min, while the RT for the feature with m/z 798 was 4.3 min. It is possible, but not confirmed, that the observed feature with an m/z of 798 is an oxidized form of PAPC [32]; additional investigation was performed, but did not yield satisfactory results.

2.5.4 Statistical support for biomarkers

The diagnostic accuracy of each feature, as measured by the extent to which each feature accurately distinguishes low-BI from high-BI samples, was determined using receiver operating characteristic (ROC) curves [33]. The ROC curve for the feature compares the distribution of abundance between low-BI and high-BI samples. The more the curve is pulled toward the upper-left corner - higher sensitivity, higher specificity and higher area under the curve (AUC) - the less overlap between the distributions in each group, and thus the more effective the feature is at discriminating low-BI from high-BI sera. The AUC for each significant feature, along with a 95% confidence interval indicated as a ± value, is shown in **Table 2.2**. ROC curves for features of interest are shown in **Panel D** of **Figures 2.(2-4)** and **Figure S2.1.**

The distribution of abundance values of the individual samples (first experiment) can be seen in **Panel E** of **Figures 2.(2-4)** and **Figure S2.1**, as both a histogram and kernel

density estimate. In addition to comparing the abundance values across patient groups, we also compared the first (individual sample) and second (pooled sample) experiments for statistically significant differences. Although the same qualitative differences were seen across patient groups in both experiments, the two experiments showed marked differences in mean abundance values, which we believe is due to variation in instrument sensitivity between runs. The distribution of abundance values between experiments was compared using the Mann-Whitney test following standardization to account for variation between runs. Between the two experiments, the distributions for EPA (low-BI p=0.15, high-BI p=0.07; **Figure 2.2E**), AA (low-BI p=0.65, high-BI p=0.34; **Figure 2.3E**), DHA (low-BI p=0.83, high-BI p=0.53; **Figure 2.4E**) and the PAPC-like compound (low-BI p=0.62, high-BI p=0.38; **Figure S2.1E**) were not found to differ significantly at 95% confidence.

We note that there is a sampling bias with regards to both age and sex in the selected patients (**Table 2.1**). Specifically, the median age is 37 in the low-BI and 28 in the high-BI, and the ratio of male to female is 6:4 in the low-BI and 12:1 in the high-BI. The parent study from which these patients were randomly selected (n=310) shows a concordant bias. In the parent study, the median age of a low-BI patient (n=63) is 37 and the median age of a high-BI patient (n=123) is 29. The odds of selecting a male patient from the low-BI group is 37:26 (1.42), and the odds of selecting a male patient from the high-BI group is 111:12 (9.25). Though patient age and sex were not considering in the study design or the analysis as a whole, we investigated the diagnostic accuracy of the features listed in **Table 2.2** when considering only the male patients. Though some shifts were seen in the AUC and median abundance in the two BI groups, the same set of features still showed

statistically significant differences between the low-BI and high-BI groups (data not shown).

2.6. DISCUSSION

The goal of our research was to explore the applicability of non-targeted metabolomics to the study of leprosy. Most research aimed at understanding variations in clinical presentations have been studies of gene expression profiles and immune response mechanisms using a variety of assays on whole blood, serum, plasma, peripheral blood mononuclear cells or skin biopsies **[17,34-36].** To date, metabolite profiles in leprosy have only been explored using target-based assays of blood samples **[37-38].** These techniques are limited in terms of sample throughput, the ability to resolve individual metabolites in complex specimens, the sensitivity of feature detection, and the accuracy of compound identification. By using a metabolomics approach based on mass spectrometry, we were able to discover several metabolites in serum with differential levels in low-BI and high-BI patient groups. In particular, we found that in the high-BI group there was a statistically significant increase in abundance of the n-3 PUFAs EPA and DHA, and the n-6 PUFA AA. The identification of differential levels of PUFAs in high-BI patients is intriguing, as lipid metabolism and lipid mediators have been implicated in many disease models, both infectious and non-infectious.

It has been widely thought that n-3 PUFAs (DHA and EPA) are beneficial to human health, because of their association with mitigation of the inflammatory response in

conditions such as autoimmune disorders, heart disease, arthritis and graft-versus-host disease **[13,39-40].** Conversely, the n-6 PUFAs (including AA) are generally considered deleterious in chronic diseases because they exert pro-inflammatory effects **[39] (Figure S2.3).** Ironically, it is this pro-inflammatory property that would provide the necessary anti-microbial activity to combat bacterial infections.

However, new research indicates that this is only a generalized model for the properties of the n-6 versus n-3 PUFAs. Consensus is absent on their strict pro- versus anti-inflammatory phenotypes, due to their interconnected metabolic pathways and the production of downstream products (eicosanoids). Recent studies have pointed to the benefits of AA and derived eicosanoids, finding that they had both pro- and anti-inflammatory roles. Deckelbaum and Calder clarified that prostaglandin E2 (PGE2) may inhibit the production of pro-inflammatory cytokines (TNF-α and IL-1) from monocytes and macrophages [41]. They also found that PGE2 inhibits production of leukotrienes (LTs), through control of 5-lipoxygenese, and induces production of lipoxins, through 15-lipooxygenase; leading to anti-inflammatory and pro-resolution activities by the action of lipoxins **[41].** Based on these results, AA n-3 PUFAs may control the inflammatory response by regulating both the pro- and anti-inflammatory cytokine networks. It has also been suggested that both n-3 and n-6 PUFAs play an anti-inflammatory role due to inactivation of reactive oxygen species by the unsaturated double bond. Furthermore, PUFAs may bind to peroxisome proliferator activated receptors, thus interfering with signaling molecules such as NF-κB, and repressing transcription of a variety of genes **[42].** Zeyda et al found that both n-3 and n-6 PUFAs inhibit cytokine production (TNF-α and IL-

12), T cell stimulation and dendritic cell differentiation at the gene level. PUFA treated dendritic cells were shown to be associated with altered membrane lipid composition, specifically an increase in unsaturated lipids, which implicates AA and EPA as anti-inflammatory mediators [14]. In the mycobacterial disease models, enrichment of n-3 PUFAs enhances susceptibility to *Mycobacterium tuberculosis* infection *in vitro* (infected macrophages) [43-44]. Anes et al showed that the pro-inflammatory effect of AA promotes increased bacteria killing inside macrophages by stimulating phagosomal actin assembly. In contrast, the same authors also showed that EPA and DHA promote bacterial survival and growth inside macrophages by lowering the levels of pro-inflammatory cytokines (IFN-γ, TNF-α, IL-1 and IL-6), weakening the oxidative response and hindering phagosome maturation [45].

In leprosy, Cruz et al postulated that the fatty acids and phospholipids which accumulate in lepromatous lesions are of host origin. They found a pronounced upregulation of host genes involved in lipid metabolism, such as phospholipases A2 (PLA2) and phospholipase C (PLC), for which functional counterparts are not encoded in the *M. leprae* genome [16]. An increase in phospholipase activity may contribute to the increased serum levels of AA we observed in our high-BI patients; PLA2 catalyzes the hydrolysis of phospholipids to release arachidonate in a single-step reaction, and PLC generates diacylglycerols, from which AA can be subsequently released by diacylglycerol- and monoacylglycerol-lipases.

Several other metabolites which modulate immunity either for or against mycobacterial survival have been described in the literature. These include cholesterol (HDL or LDL derived), triglycerides and vitamin D **[17-18, 46-47]**. We did not observe differential levels of these metabolites in our patient groups, though this does not imply variations were not present. The nature of the starting sample and the fractionation conditions may affect the metabolite pools; this study was based only on a simple one-step methanol extraction followed by C8 reverse phase UPLC-MS. Lysophosphatidylcholines (Lyso PCs) have been shown to have a potential role in immunomodulation, particularly pro-inflammatory functions **[48].** We tentatively assigned some significant features as Lyso PCs **-** three of which were more abundant in the low-BI sera **(Table 2.2)**. However, these identifications are preliminary and unconfirmed at his stage.

In this study we focused solely on identifying compounds with differential levels in patient sera based on the quantitative criterion of BI, rather than the more qualitative Ridley-Jopling and paucibacillary/multibacillary systems which are not always consistent across clinics **[49].** Though our results do not indicate that the serum signatures we found can be explained by the inherent sex bias in leprosy **[3]**, sex was not a controlled factor in our study. Further investigations which delve into whether there are specific metabolites that differentiate leprosy patients based upon other classification criteria, such clinical presentation, sex, age or genetics, would provide valuable insight into the intrinsic biological factors that contribute to bacterial growth in leprosy.

The metabolomic fingerprint we identified - higher levels of AA, DHA and EPA in the sera of high-BI leprosy patients - is consistent with diminished host innate immunity to infection [16]; reaffirming the role of altered host lipid metabolism in infection and immunity. The increased serum levels of n-3 and n-6 PUFAs we identified in high-BI patients may promote *M. leprae* survival through inhibition of both the innate and adaptive immune response of the host. These novel preliminary findings lend themselves to pathway specific genome expression analysis and further characterization of the AA derived lipid mediators. For instance, the leukotriene A4 hydrolase (*lta4h*) gene has been implicated as a susceptibility locus in leprosy and tuberculosis [50]. It is thought that the fine balance of lipoxin B4 and leukotriene B4 controls the propensity to infection or immunity. Of the 9 compounds we identified by MS/MS, those with m/z 317 and 335 are candidate AA derivatives suitable for further analysis. A longitudinal study that employs a metabolomics approach may shed light on the origins and dynamics of the lipid profile. By collecting and analyzing sera before multidrug therapy, during treatment, at the onset of reaction states and after the patient is released, we may discover fluctuations in the lipid profile over the course of the infection; enabling the ultimate aim of improving diagnostics, treatment options and creating a deeper understanding of the pathogenesis of leprosy.

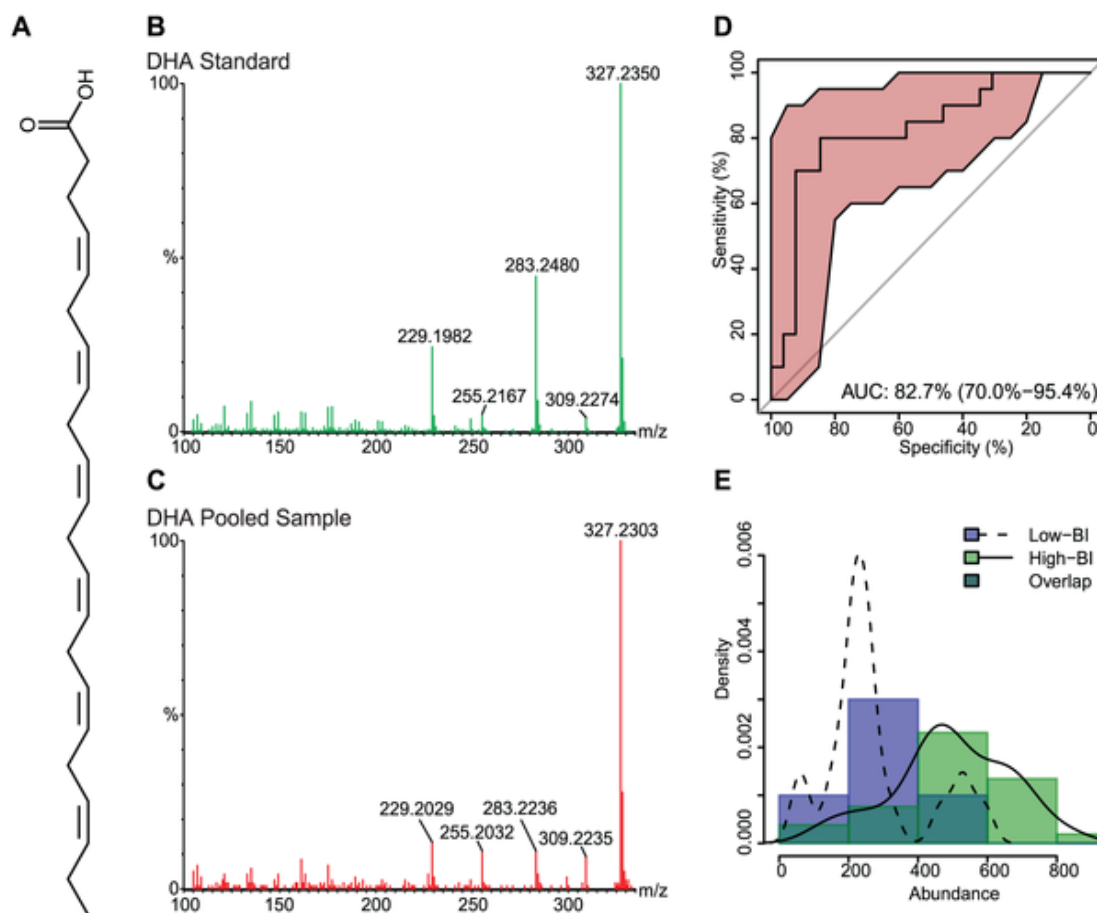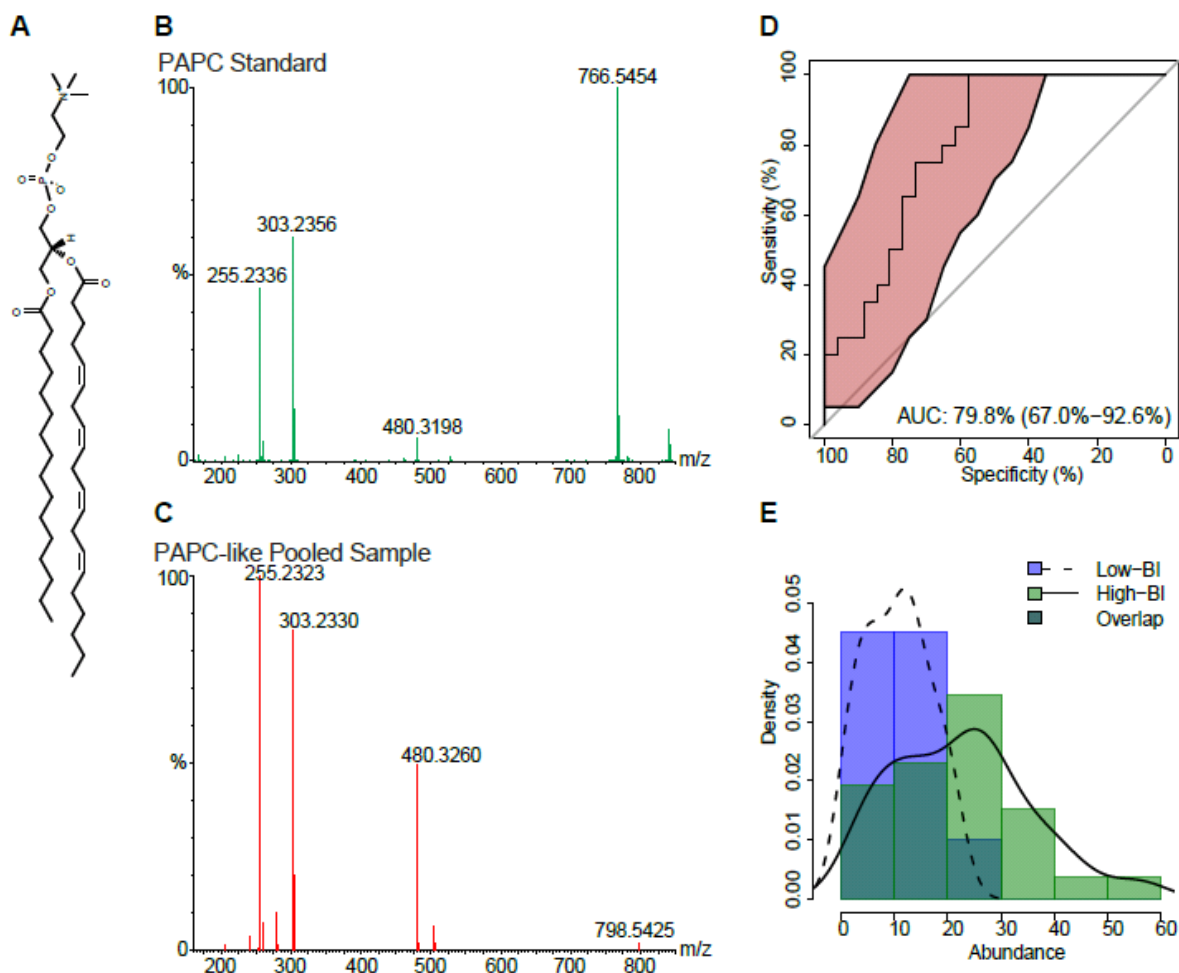**Figure S2.1: 1-palmitoyl-2-arachidonoyl-sn-phosphatidylcholine (PAPC) chemical structure, MS/MS spectra, ROC curve and distribution across sample groups.**

(A) The chemical structure of PAPC.

(B) The MS/MS fragmentation pattern for the PAPC commercial standard.

(C) The MS/MS fragmentation pattern for compound structurally similar to PAPC from a representative pooled serum sample.

(D) An ROC curve, showing the diagnostic accuracy of the PAPC-like compound in distinguishing low-BI from high-BI samples. The shaded (red) region surrounding the curve represents a 95% confidence interval for sensitivity. The AUC is shown on the graph with a 95% confidence interval in parenthesis.

(E) A histogram showing the distribution of the PAPC-like compound in the low-BI and high-BI groups. Curves are overlaid that show the kernel density estimates for each sample group.
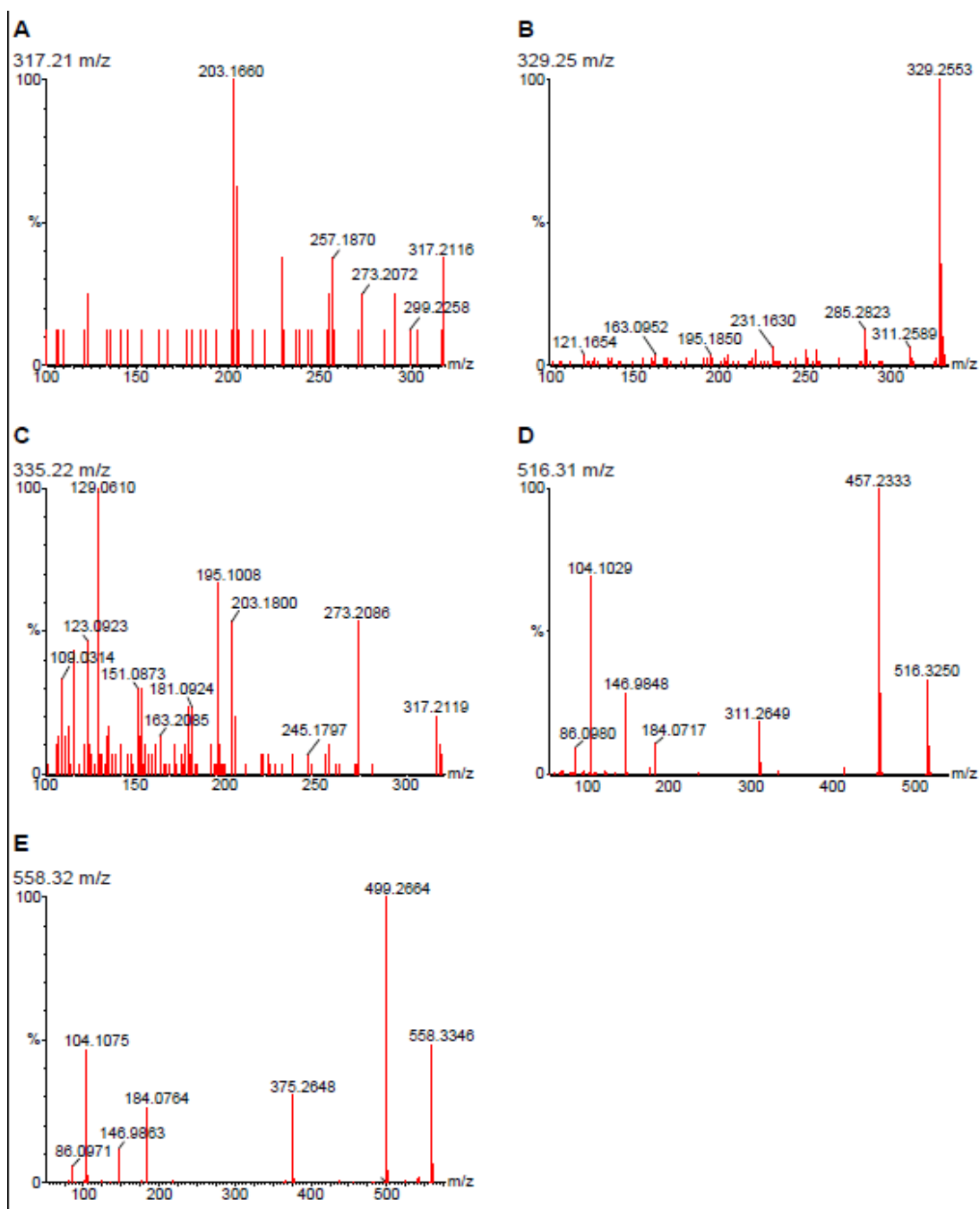
Figure S**2.2: Spectra for additional compounds identified by MS/MS.**
(A) The MS/MS fragmentation pattern for the compound with m/z 317.21.
(B) The MS/MS fragmentation pattern for the compound with m/z 329.25.
(C) The MS/MS fragmentation pattern for the compound with m/z 335.22.
(D) The MS/MS fragmentation pattern for the compound with m/z 516.31.
(E) The MS/MS fragmentation pattern for the compound with m/z 558.32.

103
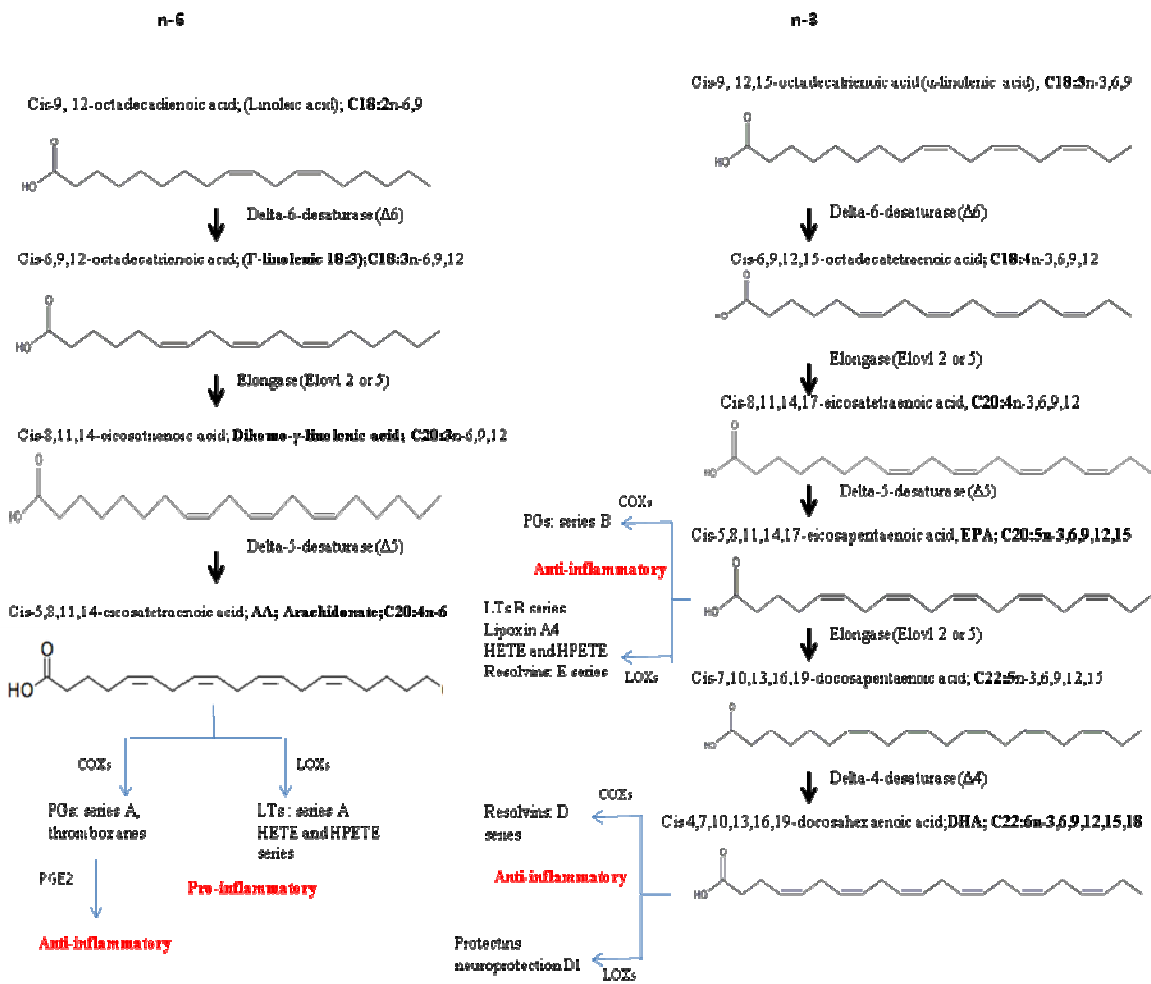
Figure S2.3: Biosynthesis of n-6 (AA) and n-3 (EPA, DHA).

104

References

1. Scollard DM, Adams LB, Gillis TP, Krahenbuhl JL, Truman RW, et al. (2006) The continuing challenges of leprosy. Clin Microbiol Rev 19: 338-381.

2. Scollard DM (2008) The biology of nerve injury in leprosy. Lepr Rev 79: 242-253.

3. World Health Organization (2010) Global leprosy situation, 2010. Wkly Epidemiol Rec 85: 337-348.

4. Moet FJ, Schuring RP, Pahan D, Oskam L, Richardus JH (2008) The prevalence of previously undiagnosed leprosy in the general population of northwest bangladesh. PLoS Negl Trop Dis 2: e198.

5. Ridley DS, Jopling WH (1966) Classification of leprosy according to immunity. A five-group system. Int J Lepr Other Mycobact Dis 34: 255-273.

6. Alter A, Grant A, Abel L, Alcaïs A, Schurr E (2011) Leprosy as a genetic disease. Mamm Genome 22: 19-31.

7. Alter A, Huong NT, Singh M, Orlova M, Van Thuc N, et al. (2011) Human leukocyte antigen class I region single-nucleotide polymorphisms are associated with leprosy susceptibility in Vietnam and India. J Infect Dis 203: 1274-1281.

8. Hashimoto K, Maeda Y, Kimura H, Suzuki K, Masuda A, et al. (2002) Mycobacterium leprae infection in monocyte-derived dendritic cells and its influence on antigen-presenting function. Infect Immun 70: 5167-5176.

9. Mattos KA, D'Avila H, Rodrigues LS, Oliveira VGC, Sarno EN, et al. (2010) Lipid droplet formation in leprosy: Toll-like receptor-regulated organelles involved in eicosanoid formation and Mycobacterium leprae pathogenesis. J Leukoc Biol 87: 371-384.

10. Misch EA, Berrington WR, Vary JC, Hawn TR (2010) Leprosy and the human genome. Microbiol Mol Biol Rev 74: 589-620.

11. Mira MT, Alcaïs A, Nguyen VT, Moraes MO, Di Flumeri C, et al. (2004) Susceptibility to leprosy is associated with PARK2 and PACRG. Nature 427: 636-640.

12. Moraes MO, Cardoso CC, Vanderborght PR, Pacheco AG (2006) Genetics of host response in leprosy. Lepr Rev 77: 189-202.

13. Harbige LS (2003) Fatty acids, the immune response, and autoimmunity: a question of n-6 essentiality and the balance between n-6 and n-3. Lipids 38: 323-341.

14. Zeyda M, Säemann MD, Stuhlmeier KM, Mascher DG, Nowotny PN, et al. (2005) Polyunsaturated fatty acids block dendritic cell activation and function independently of NF-kappa-B activation. J Biol Chem 280: 14293-14301.

15. Cole ST, Eiglmeier K, Parkhill J, James KD, Thomson NR, et al. (2001) Massive gene decay in the leprosy bacillus. Nature 409: 1007-1011.

16. Cruz D, Watson AD, Miller CS, Montoya D, Ochoa MT, et al. (2008) Host-derived oxidized phospholipids and HDL regulate innate immunity in human leprosy. J Clin Invest 118: 2917-2928.

17. Ahaley SK, Sardeshmukh AS, Suryakar AN, Samson PD (1992) Correlation of serum lipids and lipoproteins in leprosy. Indian J Lepr 64: 91-98.

18. Memon R, Kifayet A, Shahid F, Lateef A, Chiang T, et al. (1997) Low serum HDL-cholesterol is associate with raised tumor necrosis factor-alpha during ENL reactions. Int J Lepr Other Mycobact Dis 65: 1-11.

19. Chen X, Liu L, Palacios G, Gao J, Zhang N, et al. (2010) Plasma metabolomics reveals biomarkers of the atherosclerosis. J Sep Sci 33: 2776-2783.

20. Ramautar R, Mayboroda OA, Somsen GW, de Jong GJ (2011) CE-MS for metabolomics: Developments and applications in the period 2008-2010. Electrophoresis 32: 52-65.

21. Wang D-C, Sun C-H, Liu L-Y, Sun X-H, Jin X-W, et al. (2010) Serum fatty acid profiles using GC-MS and multivariate statistical analysis: potential biomarkers of Alzheimer's disease. Neurobiol Aging: in press.

22. Sakamuri RM, Kimura M, Li W, Kim H-C, Lee H, et al. (2009) Population-based molecular epidemiology of leprosy in Cebu, Philippines. J Clin Microbiol 47: 2844-2854.

23. Ridley DS (1964) Bacterial indices. In: Cochrane RG, Davey TF, editors. Leprosy in Theory and Practice. Baltimore, MD: The Williams & Wilkins Co. pp. 620-622.

24. R Development Core Team (2010) R: A Language and Environment for Statistical Computing. Vienna Austria R Foundation for Statistical Computing 1: ISBN 3-900051-07-0. Available: http://www.r-project.org.

25. Robin X, Turck N, Hainard A, Tiberti N, Lisacek F, et al. (2011) pROC: an open-source package for R and S+ to analyze and compare ROC curves. BMC Bioinformatics 12: 77.

26. Fahy E, Sud M, Cotter D, Subramaniam S (2007) LIPID MAPS online tools for lipid research. Nucleic Acids Res 35: W606-612.

27. Suhre K, Schmitt-Kopplin P (2008) MassTRIX: mass translator into pathways. Nucleic Acids Res 36: W481-484.

28. Kerwin JL, Wiens AM, Ericsson LH (1996) Identification of fatty acids by electrospray mass spectrometry and tandem mass spectrometry. J Mass Spectrom 31: 184-192.

29. Murphy RC (2002) Mass Spectrometry of Phospholipids: Tables of Molecular and Product Ions. Denver: Illuminati Press. 71 p.

30. Sumner LW, Amberg A, Barrett D, Beale MH, Beger R, et al. (2007) Proposed minimum reporting standards for chemical analysis. Metabolomics 3: 211-221.

31. Kanehisa M, Goto S, Furumichi M, Tanabe M, Hirakawa M (2010) KEGG for representation and analysis of molecular networks involving diseases and drugs. Nucleic Acids Res 38: D355-360.

32. Reis A, Domingues P, Ferrer-Correia AJV, Domingues MRM (2004) Tandem mass spectrometry of intact oxidation products of diacylphosphatidylcholines: evidence for the occurrence of the oxidation of the phosphocholine head and differentiation of isomers. J Mass Spectrom 39: 1513-1522.

33. Zweig MH, Campbell G (1993) Receiver-operating characteristic (ROC) plots: a fundamental evaluation tool in clinical medicine. Clin Chem 39: 561-577.

34. Bleharski JR, Li H, Meinken C, Graeber TG, Ochoa M-T, et al. (2003) Use of genetic profiling in leprosy to discriminate clinical forms of the disease. Science 301: 1527-1530.

35. Martins M (2008) Challenges in the post genomic era for the development of tests for leprosy diagnosis. Rev Soc Bras Med Trop 41: 89-94.

36. Wright S, Morse N, Manku MS (1991) Essential fatty acids in plasma of patients with leprosy. Int J Lepr Other Mycobact Dis 59: 271-277.

37. Blaho VA, Buczynski MW, Brown CR, Dennis EA (2009) Lipidomic analysis of dynamic eicosanoid responses during the induction and resolution of Lyme arthritis. J Biol Chem 284: 21599-21612.

38. Griffiths WJ, Koal T, Wang Y, Kohl M, Enot DP, et al. (2010) Targeted metabolomics for biomarker discovery. Angew Chem Int Ed Engl 49: 5426-5445.

39. Calder PC (2001) Polyunsaturated fatty acids, inflammation, and immunity. Lipids 36: 1007-1024.

40. Pischon T, Hankinson SE, Hotamisligil GS, Rifai N, Willett WC, et al. (2003) Habitual dietary intake of n-3 and n-6 fatty acids in relation to inflammatory markers among US men and women. Circulation 108: 155-160.

41. Deckelbaum RJ, Calder PC (2010) Dietary n-3 and n-6 fatty acids: are there "bad" polyunsaturated fatty acids? Curr Opin Clin Nutr Metab Care 13: 123-124.

42. Ferrucci L, Cherubini A, Bandinelli S, Bartali B, Corsi A, et al. (2006) Relationship of plasma polyunsaturated fatty acids to circulating inflammatory markers. J Clin Endocrinol Metab 91: 439-446.

43. Bonilla DL, Ly LH, Fan Y-Y, Chapkin RS, McMurray DN (2010) Incorporation of a dietary omega 3 fatty acid impairs murine macrophage responses to Mycobacterium tuberculosis. PLoS One 5: e10878.

44. Jordao L, Lengeling A, Bordat Y, Boudou F, Gicquel B, et al. (2008) Effects of omega-3 and -6 fatty acids on Mycobacterium tuberculosis in macrophages and in mice. Microbes Infect 10: 1379-1386.

45. Anes E, Kühnel MP, Bos E, Moniz-Pereira J, Habermann A, et al. (2003) Selected lipids activate phagosome actin assembly and maturation resulting in killing of pathogenic mycobacteria. Nat Cell Biol 5: 793-802.

46. Bansal SN, Jain VK, Dayal S, Nagpal RK (1997) Serum lipid profile in leprosy. Indian J Dermatol Venereol Leprol 63: 71-81.

47. Liu PT, Stenger S, Tang DH, Modlin RL (2007) Cutting edge: vitamin D-mediated human antimicrobial activity against Mycobacterium tuberculosis is dependent on the induction of cathelicidin. J Immunol 179: 2060-2063.

48. Sheikh AM, Ochi H, Manabe A, Masuda J (2005) Lysophosphatidylcholine posttranscriptionally inhibits interferon-gamma-induced IP-10, Mig and I-Tac expression in endothelial cells. Cardiovasc Res 65: 263-271.

49. Rao Pn, Pratap D, Ramana Reddy A, Sujai S (2006) Evaluation of leprosy patients with 1 to 5 skin lesions with relevance to their grouping into paucibacillary or multibacillary disease. Indian J Dermatol Venereol Leprol 72: 207-210.

50. Tobin DM, Vary JC, Ray JP, Walsh GS, Dunstan SJ, et al. (2010) The lta4h locus modulates susceptibility to mycobacterial infection in zebrafish and humans. Cell 140: 717-730.

CHAPTER 3

The Lipidome of *M. leprae* Infected Tissues: Accumulation of Unsaturated

Triacylglycerols in Leprosy

From a manuscript in preparation by: Reem Al- Mubarak[1], Jason Vander Heiden[1], Richard W. Truman[2], Patrick J. Brennan[1] and Varalakshmi Vissa[1]

[1]Department of Microbiology, Immunology and Pathology,

Colorado State University,

3.1. SUMMARY

Mycobacterium leprae, is an obligate intracellular pathogen with a restricted host range. Due to its extreme genome decay, *M. leprae* creates a survival niche, preferentially in the peripheral nervous system (Schwann cells) which results in nerve damage and deformity - the main manifestations of leprosy. However, the underlying processes of infection and nerve damage are poorly understood. In addition to mechanisms that implicate genes and products of bacterial origin, the modulation of the host biochemical environment, particularly of the lipidome, has been implicated in infection and escape from immunity.

The nine-banded armadillo (*Dasypus novemcintus*), a natural and experimental animal model of leprosy whose genome has recently been deciphered was utilized. In armadillos, besides the peripheral nerves, the liver and spleen are also infected. The lipid spectrum in

organic extracts of tissues from three each of uninfected and infected animals were compared following liquid chromatography (LC) electrospray ionization/mass spectrometry (ESI-MS) combined with quadrupole/time of flight (Q/TOF). Differentially abundant molecular features were identified and the expression levels of a panel of candidate regulated genes were assessed in mRNA prepared from the same tissue specimens.

The lipidomic analysis showed an increase of certain lipid groups, mainly neutral triacylglycerols (TAG) bearing acyl chains of specific lengths and unsaturation in all three types of infected tissues in comparison to naïve tissues. Gene expression studies related to TAG and fatty acid synthetic pathways in the liver, showed significant up-regulation of stearoyl-CoA desaturase 9 (SCD9) in infected tissues. Genes encoding elongase 5 (ELOVL5) and diacylglycerol acyltransferase (DGAT) were also slightly elevated. These comparative lipidome scanning results combined with quantitative gene expression analysis, correlate with the increased levels of TAGs with mono and di-unsaturated fatty acids in the lipid profiles of all three tissue types. This approach rapidly revealed biochemical markers of infection, modulated in part at the level of gene expression, which are functionally compatible with the generation of an anti-inflammatory, nutrient rich milieu for bacterial proliferation.

3.2. INTRODUCTION

M. leprae, the causative agent of leprosy, is an obligate intracellular pathogen with a tropism for peripheral nerves and skin. As a result, neuropathy occurs if the disease is not treated early enough. Study of the pathogenesis of leprosy is impeded by the slow doubling time (~ 2 weeks) of *M. leprae*, the prolonged incubation period spanning many years, and the lack of common laboratory animal models that mimic the full range of human clinical leprosy. Reductive evolution of the *M. leprae* genome has contributed to the restriction of the natural host range and a failure to propagate in axenic media **[1].** During leprosy infection, especially in lepromatous lesions, whole transcriptome profiling has shown that there is up-regulation of host lipid metabolism genes such as those encoding lipases, phospholipase, α-methylacyl-CoA racemase (AMACR) and scavenger receptors **[2]**. These findings led to a disease model in which *M. leprae* actively modulates host gene expression to generate host-derived lipids for use as energy sources while certain classes (e.g., oxidized phospholipids) serve as anti-inflammatory virulence factors. The role of lipids corroborates with historical histological findings of lipid laden Virchow cells at sites of infection. Subsequently, the composition of lipid droplets (LDs) characteristic of lipid laden cells, were defined as triacylglycerols among other host-derived lipids in the cases of a number of infectious disease settings, notably tuberculosis **[3, 4]**. However, there is inadequate description of the metabolomic composition of the infected tissues, particularly in leprosy, due to the practical limitations described.

In this context, a modern 'omics' approach was considered to address the lipidome of *M. leprae* infected tissue as a prelude for human studies. The nine-banded armadillo

(*Dasypus novemcinctus*) is one of the rare natural hosts for *M. leprae*. It has been

successfully infected with human lesion derived *M. leprae* and shown to develop

generalized lepromatous leprosy with bacterial dissemination in the skin, peripheral nerves,

bone marrow, liver, spleen, lymph nodes and lungs **[5].** The involvement of neuropathy in

ulcerations and loss of sensitivity in the extremities are similar to those observed in human

patients; 85% of nine-banded armadillos get extensive type of leprosy. Therefore,

armadillos have been a means for *in vivo* propagation of *M. leprae* **[6].**

Studying host-pathogen interactions in terms of lipid homeostasis in the normal and

infected state is important when identifying biomarkers and understanding the mechanism

of the disease. Therefore, in this study, lipids from tissues (nerve, liver and spleen),

harvested from three independent uninfected and infected armadillos were extracted and

analyzed by mass spectrometry. The shot-gun lipid profiles were compared between

infected and non-infected tissues and tissue types to reveal underlying metabolic pathways

that are modulated for successful multibacillary infection. The findings are presented in the

context of comparable disease models and have implications for identification of pathways

that can be interrupted to prevent pathogen survival and peripheral nerve damage.

3.3. MATERIALS AND METHODS

3.3.1 Armadillo tissues

Nine-banded armadillos were captured from the wild, screened for pre-existing

infections and conditioned for *in vivo* propagation of *M. leprae* at the laboratories of the

National Hansen's Disease Program (Baton Rouge, LA). Those selected for experimental

studies were inoculated intravenously with $1x10^9$ highly viable *M. leprae* and allowed to progress through their experimentally induced infections as previously described **[7]**. The animals are closely monitored for a variety of physiological indicators and humanely sacrificed when they exhibit signs of fully disseminated leprosy. Naïve animals are obtained and conditioned similarly; but may be sacrificed for control purposes without experimental inoculation of bacilli. All procedures for obtaining armadillos, their husbandry, maintenance and experimental use were conducted according to a previously approved protocol under an existing animal assurance (A3032-01) **[8]**. Six animals were used in this study: two were experimentally infected (549 and 774 days in animal colony), one was naturally infected (3 days in animal colony) and three were uninfected animals (0, 4 and 52 days in animal colony). The uninfected and infected animals will henceforth be coded as AU and AI, and numbered as AU-1, AU-2, AU-3, AI-1, AI-2 and AI-3. All the infected animals had disseminated lepromatous leprosy with high burdens of *M. leprae* at the time of sacrifice. Upon humane sacrifice the harvested nerves and organs were immediately flash frozen, and stored at -70 ^{o}C till used. Small portions of frozen liver and spleen (~ 1g) and 3-5 cm segments of peripheral nerves from each of the six animals were shipped on dry ice packing to Colorado State University (CSU) when available. At first, only nerve samples were processed and analyzed by LC-MS. Subsequently, stored liver and spleen samples harvested from the same animals were processed together.

3.3.2 Tissue handling and lipid extraction

The samples were opened and handled in a laminar flow hood following BL2 procedures. From each animal (uninfected and infected) tissue type, three small fragments

(50-100 mg of liver and spleen, and 1 cm of nerve) were excised with a disposable punch

biopsy or cut with a sterile scalpel. Sterile petri plates were used during these steps. All

contaminated lab-ware were autoclaved. Unused tissue was returned to -70 $^{\circ}$C for other

uses.

For each animal, three independent nerve, liver and spleen extracts were prepared. The

tissues were kept on dry ice during the procedures. The fragments were placed in separate

wells of a pre-chilled sterile Multi-well BioPulverizer device (BioSpec Products, Inc, OK,

USA) and crushed with the pestles provided. The pulverized tissue materials were

carefully transferred to 13 x 100 mm screw capped glass tubes. Lipid was extracted from

each of the frozen tissues and kept separate during the procedures. Solvent, 6 ml of

chloroform:methanol:water (10:10:3 v/v/v) was added and the samples were rocked in the

extraction solvent for 2 hours at room temperature, and centrifuged for 3,000 x g for 10

min. The supernatants were collected and transferred to fresh 13 x 100 mm glass tubes and

the extraction was repeated. The combined supernatants were dried under a gentle stream

of nitrogen, and stored at -20 °C until used. The samples were reconstituted with the same

extraction solvent for a final concentration of 100 μg/100 μl, transferred to an auto-sampler

vial, and 1 μl was analyzed by LC-MS.

3.3.3 *M. leprae* lipid extraction

M. leprae (3mg dry weight, ~6x10^9 cells) obtained from the NIH-NIAID Leprosy

Research Support Contract at CSU was extracted with 6 ml of chloroform:methanol:water

solvent as described above for the tissue lipid extraction. The lipid extract was dried and

resuspended in the same solvent for a final concentration of 1mg/ml. For LC-MS analysis of lipid extract (5 µl, ~10^7 cells) was injected for LC-MS.

3.3.4 Liquid chromatography-mass spectrometry (LC-MS)

The nerve extracts were analyzed in two LC-MS systems. Initial nerve experiments were performed using an Agilent 1200 HPLC at the Central Instrument Facilities, Department of Chemistry, CSU. Subsequent nerve experiments, all liver and spleen extracts were analyzed with a Waters Acquity UPLC system at the Proteomics and Metabolomics Facilities, CSU. The chromatography and mass spectrometry procedures for each instrumentation system are described below.

LC-MS using Agilent 1200 HPLC **-** Agilent 6220 TOF with ESI/APCI Agilent 1200 HPLC (Agilent Technologies, CA) was used with a 2.1 (i.d.) x 150 mm, 3.5 µm XBridge C18 column (Waters, MA) heated to 45 ºC with a binary solvent system and flow rate of 320 µl/min. Another 2.1 (i.d.) x 10 mm, 3.5 µm XBridge C18 guard column (Waters) was placed in series in front of the analytic column. The columns were equilibrated with 100% solvent A [5mM ammonium acetate in methanol/water (99:1 v/v)] for 2 min, and the sample components were separated over 30 min with a linear gradient reaching 100% solvent B [5mM ammonium acetate in n-propanol/hexane/water [(79:20:1 v/v/v)]. Solvent B was maintained for an additional 3 min. All solvents and chemicals were HPLC grade.

The LC eluent was analyzed by an Agilent 6220 TOF with ESI/APCI multimode source for positive (+) and negative (-) ion data as described **[9].** The mass spectrometer

operated at the following settings: capillary voltage, 2000V; nebulizer, 45 psig; drying gas, 8L/min at temperature of 300 ºC; charging, 2000V and skimmer, 60V. The mass spectra were generated in 4 GHz high resolution mode at a rate of 1.02 spectra/s and 9700 transients/spectrum. The profiled spectra were collected as a mass range of 250 to 3200 Da. The data were collected with the Agilent MassHunter WorkStation Data Acquisition, software version B.02.00.

LC-MS using Waters Acquity UPLC-Waters Q-TOF Micro MS Waters Acquity UPLC system was used with a UPLC 1.0 (i.d) x 100 mm) 1.7 µM C8 column, using a gradient from solvent C (89% water, 5% acetonitrile, 5% isopropanol, 1% 500 mM ammonium acetate) to solvent D (49.5% acetonitrile, 49.5% isopropanol, 1% 500 mM ammonium format). Sample injections (1 µl) were held in 100% solvent C at a flow rate of 140 µl/min for 0.1 min. A 0.9 min linear gradient to 40 % D was applied, followed by a 6 min gradient to 100% D which was held for 0.5 min. Then, the flow rate was increased to 0.24 ml/min for 7.5 min to wash the column, then returned to starting conditions over 0.1 min, and allowed to re-equilibrate over 5.9 min. The column was held at 50 °C, and samples were held at 5 °C. The column eluent was infused into a Waters Q-TOF Micro MS, fitted with an electrospray source. Data were collected in positive ion mode, scanning from 50-1200 Da at a rate of 0.9 sec/ scan with 0.1 sec inter-scan delay. Calibration was performed prior to sample analysis via infusion of sodium formate solution, with mass accuracy within 5 ppm. The capillary voltage was held at 2200V, the source temperature at 130 °C, and the desolvation temperature at 300 °C at a nitrogen desolvation gas flow rate of 400 l/hr. The quadrupole was held at 7V collision energy.

For MS/MS, the ion was isolated with a quadrupole and then fragmented using low-energy impact with a collision gas, producing a characteristic fragmentation pattern. The collision energy was held at 20 eV for fatty acids and 30 eV for phospholipids.

3.3.5 Data processing and statistical analyses

For the data acquired from the Agilent 1200 HPLC, the Agilent MassHunter WorkStation Data Acquisition software version B.02.00 (Agilent Technologies, Santa Clara, CA) was used for analysis. Molecular features (MFs) were extracted from the raw data as described previously [9]. A feature is defined by its m/z and retention time (RT). The lists of features were exported as an 'analysis report' in Microsoft Excel format for further comparisons based on feature abundance.

The data from Waters UPLC Q-TOF were viewed using MarkerLynx v4.1 (Waters, Millford, MA, USA). Chromatographic peaks were detected with a RT window of 0.1 min. Apex track peak detection with automatic estimation of peak width and baseline noise parameters were used. The spectrometric features were assigned by m/z and RT, while the relative intensity was based on the area of all features. Initial screening for compounds with significant differences in abundance between the infected and uninfected tissues was performed by orthogonal projection onto latent structures (OPLS) with the software SIMCA-P+ v12.0 (Umetrics. Umeå, Västerbotten, Sweden) using a Po (corr) cut-off of 0.8 as previously used [10]. The statistical significance of the mean difference between the infected and uninfected samples was determined using a two-sided Student's t-test, with the

p-values adjusting using the false discovery rate (FDR) approach, yielding a q-value (adjusted p-value) for each feature. Tests of significance where performed in R 12.14.0 using the stats package **[11]**.

3.3.6 Identification of compounds by MS/MS

The compounds that showed significant differences in intensity between infected and uninfected tissues, based on exact m/z and RT differences of 0.05 min (these features are henceforth defined as 'significant features') were further fragmented by MS/MS in both positive and negative ion modes and manually examined for signature ions and compared to several existing free databases **[12,13].**

3.3.7 Tissue DNA and RNA extraction and purification

The uninfected and infected liver samples (3 animals for each group with two biopsies from each), were used to extract DNA and RNA using Allprep DNA/RNA/Protein Mini Kit (Qiagen, USA) spin columns and buffers therein. Briefly, the biopsies (~50 mg) were transferred to a 2 ml vial containing 500 µl Lysing Matrix B (0.1-mm silica spheres) and one ceramic bead (1/4" (6.35 mm) diameter ceramic grinding sphere) (MP Biomedicals, USA). Lysis buffer, RLT (600 µl) containing freshly added beta mercaptoethanol was added to each vial. The tissues were disrupted at a speed setting of 6 using a Fast Prep-24 (MP biomedical) equipment for 40 sec. The lysates were transferred to Allprep DNA spin columns and centrifuged for 30 sec at 8000 x g (10,000 rpm) rpm in a microfuge. The columns were placed in new collection tubes and stored at 4 ˚C for later DNA purification. For the RNA extraction, one volume of 70% ethanol was added to the flow-through from

the DNA column and the sample was mixed immediately. Then, the materials were transferred into RNeasy spin columns and centrifuged for 15 sec at 8000 x *g*. DNase solution (80 µl) (Qiagen, US) was added to the RNeasy columns to degrade DNA. The columns were washed twice with RPE buffer plus ethanol, spun dry and the RNA was eluted with 50 µl RNase-free water. For the DNA samples, the columns were washed with AW1 and AW2 buffer, and then the DNA was eluted with 100 µl of elution buffer EB.

3.3.8 Reverse transcription

The QuantiTect Rev. Transcription Kit (Qiagen, USA) was used to prepare cDNA from tissue RNA. Briefly, the RNA templates (~1µg) (20 µl of a 50 µl total/per biopsy) were first treated with gDNA Wipeout Buffer in a total volume of 28 µl for 5 min at 42 °C. The sample was split into two reactions, reverse transcriptase plus and minus (RT+ and RT-).Both reactions (final volume of 20 µl) contained Quantiscript RT Buffer, RT Primer Mix (Qiagen). Quantiscript Reverse Transcriptase (1 µl) was added only in the RT+ reaction. Both reactions were incubated for 30 min at 42 °C. The reactions were stopped by incubation at 95 °C for 3 min.

3.3.9 Reverse transcription-quantitative PCR (RT-qPCR)

The expression levels of the armadillo genes involved in fatty acid and acylglycerol synthesis listed in **Table 3.1** were examined by quantitative real-time PCR on the cDNA generated from uninfected and infected liver RNA samples (3 tissues for each group, duplicate biopsies per tissue, and duplicate PCR replicates per cDNA). The gene sequences were taken from armadillo database (Ensembl genome databases

[http://www.ensembl.org/index.html]). The specific primer pairs for each gene were designed using the Real Time PCR Assay Design Tool [Integrated DNA Technologies (IDT) (http://www.idtdna.com/Scitools/Applications/RealTimePCR/Default.aspx)]. Each target was pre-amplified in 10 cycles of PCR containing 0.2 µM of each primer pair. The PCR products were diluted 1:5 and used for qRT-PCR. Each reaction (20 µl) contained 2 µl of diluted template, 0.4 µM for each primer and iQ SYBR Green Supermix kit (Bio Rad, US) to generate fluorescently labeled PCR products. Product formation was monitored by real time PCR performed with the following cycling conditions: 95 °C for 3 min, 40 cycles of 95 °C for 15 sec, 55 °C for 30 sec and 72 °C for 30 sec. The reverse transcriptase minus (RT-) control samples were also analyzed by PCR, to account for any residual genomic DNA contamination (data not shown).

The relative level of each transcript was obtained by the $2^{-\Delta\Delta Ct}$ method using GAPDH as a reference gene **[14].**

Table 3.1: Genes and primers used for quantitative reverse transcriptase-polymerase chain reaction.

Gene	Accession number	Primer sequence	cDNA size bp
Elongase-5(ELOVL5)	*ENSDNOT00000011356*	F- AGACAGCCATTCTCTTGCC R-ATTTGCCTTCCCATACTCCTG	115
Stearoyl-CoA desaturase (SCD-9 or Δ9-desaturase)	*ENSDNOG00000004507*	F- AGCTGCCAGATCTACACTTG R- GCAATGACTAGGAAGACCCG	147
Stearoyl-CoA desaturase (SCD-5)	ENSDNOG00000013484	F- GGCAGAACATCGTTTGGAGG R- GAGGAAGCAGAAGTAAGCCCAG	125
Fatty acid desaturase (FADS1or Δ5d)	ENSDNOG00000016115	F-GATCACCTTCTACGCCCG R-AAGAAAAGACCCAGGAAGCC	75
Di-acylglycerol acyltransferase	ENSDNOG00000019644	F- GCTCAGTAGGTCCAAGGTG R- ACCTTTCTTGGGCGTGTCC	187

120

(DGAT2)			
Mono-acylglycerol acyltransferase (MOGAT1)	ENSDNOG00000002515	F- TGGTTTTACTTCGACTGCCG R- TCCTTAAAGTACCTCCAAACCG	89
Glyceraldehyde 3-phosphate dehydrogenase (GAPDH)	DQ403048.1	F- GCATCCCATCACTATCTTCCA R- CACGCCCATCACAAACATG	193

[1] http://uswest.ensembl.org/Dasypus_novemcinctus/Info/Index

3.4. RESULTS

3.4.1 The lipidome of armadillo peripheral nerves as profiled by LC-MS: Changes detected in *M. leprae* infected nerves

Two different instruments and chromatography systems were used to resolve and detect molecular features in the chloroform:methanol:water, 10:10:3 organic extracts from three independent nerve specimens from each of the animals groups; uninfected and infected. Since each nerve was cut into three pieces, extracted and injected separately, a total of nine data sets were obtained for each group.

The infected nerve extracts should, in principle, comprise both armadillo and *M. leprae* components. The Agilent C18 LC-MS methods that were in development to display mycobacterial (*M. tuberculosis*, *M. tb*) lipids were explored so as to identify *M. leprae* specific components over the host lipidome background **[9]**. Using the same methods, a sample of *M. leprae* lipid extract was analyzed. We could tentatively identify typical mycobacterial lipids such as pthiocerol dimycocerosates (DIMA and DIMB), trehalose conjugated mycolic acids (trehalose monomycolate (TMM), phosphatidyl inositol

mannosides (PIMs) and their acylated versions (AcPIMs) in the positive mode (**Figure S3.1 and Table 3.S1, 3.S2**). The *M. leprae* spectrum also had features matching penta acylated trehalose (PAT), and glucose monomycolate (GMM), but a match for PGL-I was not detected in the positive mode. Trehalose dimycolate and diacylated trehalose (DAT) appeared at early retention times. For the tissue extracts in the negative mode, the MassHunter software detected 90 features in the infected (average of 9 data sets) and 127 features in the uninfected nerves (average of 9 data sets). In the positive mode, 159 features were detected in the infected nerves and 150 features in the uninfected nerves. The ions of the detected masses ranged from 200-1000 m/z. Ions in both modes were compared based on the features represented by mass/charge/retention time (m/z/RT) in a scatter plot.

The molecular masses were compared to the published *Mtb* lipid database and other online accessible lipid databases such as LIPID MAPS; several were found in multiple databases, indicating that they could be of armadillo or *M. leprae* origin [9]. These include common lipids belonging to groups such as triacylglycerols (TAGs), diacylglycerols (DAGs) and glycerophospholipids [phosphatidyl ethanolamine (PE) and phosphatidyl choline (PC)]**.** However, we could not identify typical mycobacterial lipids as described above. The amount of sample injected may have limited the sensitivity of detection of *M. leprae* specific features contained in the total tissue extract; an equivalent of least 10^5 bacteria may be required to detect such components **[9]**.

In **Figure 3.1**, a scatter plot shows all the features detected in positive mode from the uninfected animals (**panel A**) and the infected animals (**panel B**). A series of features that were found in infected but not in uninfected tissue extracts was readily discerned.
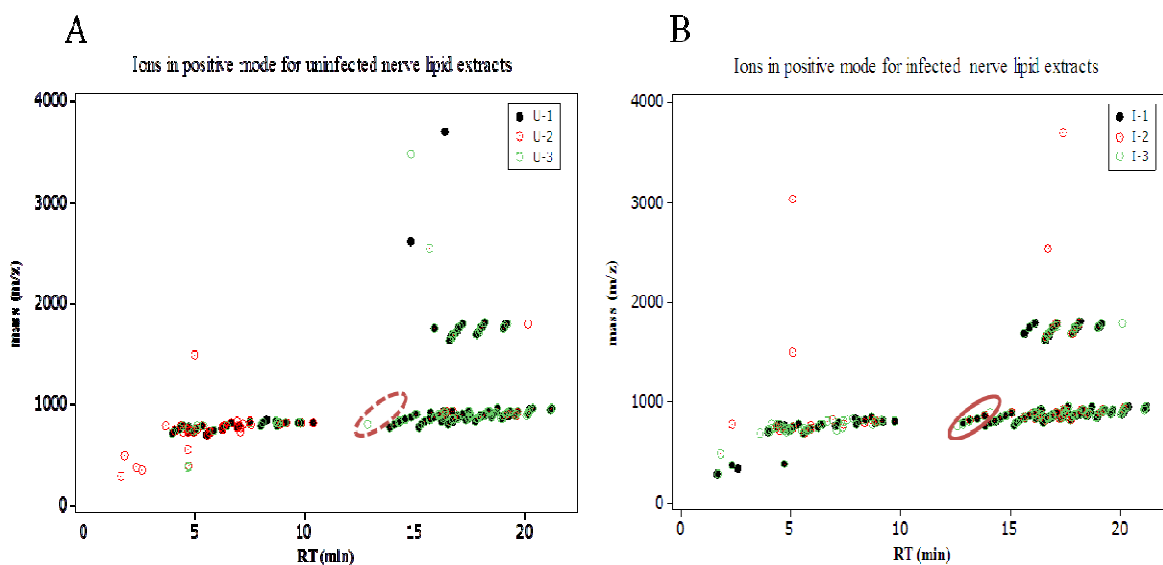
Figure 3.1: Scatter plots of positive ion C18 LC-MS (Agilent) features in nerve lipid extracts of uninfected (A) and infected animals (B). Each feature is represented by m/z and RT. The infected nerves show an extra series of features (circled) compared to the uninfected nerves.

The lipid extracts from all six nerves (AU-1, 2 and 3 and AI-1, 2 and 3) were re-analyzed using UPLC- Q-TOF (Waters) for further quantification, selection and identification of significant features, since the Agilent 1200 HPLC lacks MS/MS fragmentation capability. The run times were shorter and the mass capacity ranged from m/z of 50-1000. The numbers of features detected are listed in **Table 3**.**2**. Feature selection was performed by orthogonal projection onto latent structures (OPLS), and with a

123

cut off of 0.8 that compared data sets obtained per LC-MS run (from multiple extracts

from one uninfected and one infected animal) as described in the methods sections. The

majority of these 'significant features' belonged to the infected nerve group, particularly

those detected in the positive mode (**Table S3.3**). The significant features (positive mode)

from all six animals that were first detected by the Agilent system and also detected in the

Waters system were selected for further characterization by tandem mass spectrometry

(MS/MS). The chemical identities of these features were deciphered on the basis of the

exact masses to be neutral lipids triacylglycerols (TAG) containing acyl-chains of different

chain lengths and saturation (**Table 3.3 and Figure S3.2**). The TAGs in the positive mode

were found as $[M+NH4]^+$ adducts. These compounds form a series of TAGs, with mono-

and di-unsaturated fatty acids being the predominant significant compounds in the infected

nerve (**Figure 3.2 and 3.3**).

Table 3.2: Number of features detected by UPLC (C8)-Q-TOF LC-MS in tissues of

infected and uninfected armadillos

Tissue	Animals	Mode	Number of features
Nerve	AU-1 + AI-2	positive	1143
	AU-2 + AI-2	positive	345
	AU-3 + AI-3	positive	779
Liver and spleen	AU-1 + AI-2	positive	2584 (2520 Liver only, 2370 Spleen only)
	AU-2 + AI-2	positive	461 (453 Liver only, 442 Spleen only)
	AU-3 + AI-3	positive	1325 (1267 Liver only, 1210 Spleen only)
Liver and spleen	AU-1 + AI-2	Negative	813 (760 Liver only, 775 Spleen only)
	AU-2 + AI-2	Negative	347 (340 Liver only, 320 Spleen only)
	AU-3 + AI-3	Negative	665 (622 Liver only, 619 Spleen only)

Table 3.3: Significant features present in all infected armadillo tissue types (nerve, liver and spleen)

Ions abundant in *M. leprae* infected tissues			
Nerves			Liver and Spleen
m/z	Compound ID based on MS/MS	P value (abundance)	m/z
822.7541	TAG(14:0/16:0/18:1)	0.011881	822.7544
844.7426	TAG(14:0/18:2/18:2)	0.000257	844.7377
846.7574	TAG(14:0/18:1/18:2)	0.007596	846.7582
870.7551	TAG(16:1/18:2/18:2)	0.0000031	870.7572
872.7701	TAG(16:1/18:1/18:2)	0.005953	872.7703
878.8209	TAG(16:0/18:0/18:1)	0.006517	878.741
898.7861	TAG(18:1/18:2/18:2)	0.003642	898.7858
848.7694	-	0.031802	848.7711
874.7816	-	0.0261099	874.7879
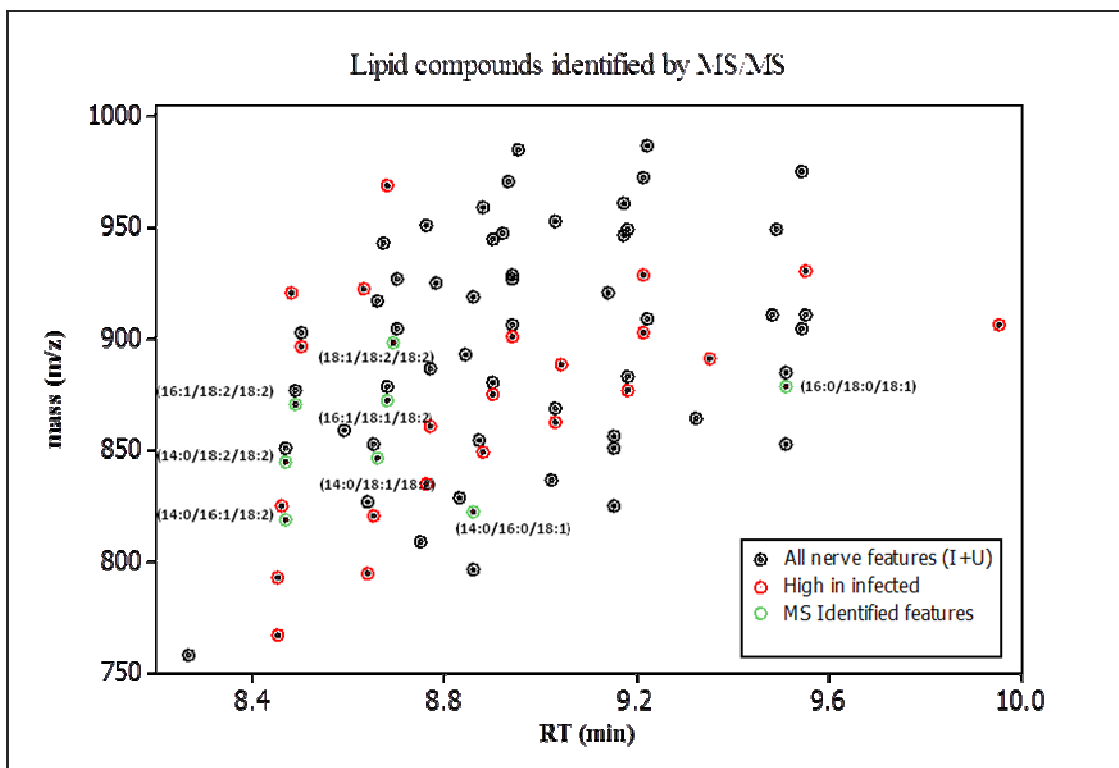
Figure 3.2: Significant features in infected nerves and chemical identification by LC-MS/MS. Each ion (feature) is represented by m/z and RT. The features indicated within red circles are 'significant features' elevated in the infected tissue. The chemical formulae of the features indicated within green circles could be assigned by MS/MS. Infected nerves have elevated levels of neutral lipids triacylglycerol (TAG) with unsaturated FAs (mono- and di-saturated fatty acids).
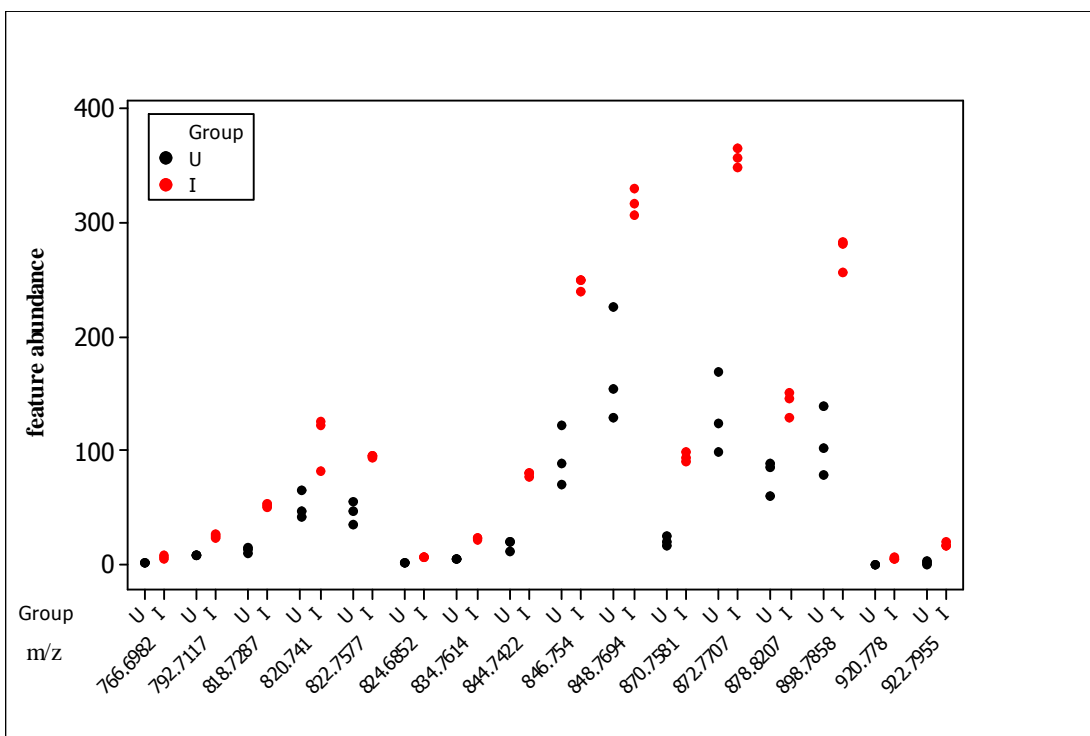
Figure 3.3: Comparison of the abundances of selected significant features in the infected nerves. All of the selected features were more abundance in the infected samples (red dots).

3.4.2 The lipidome of armadillo liver and spleen as profiled by LC-MS: Changes detected in *M. leprae* infected tissues

The crude lipid extracts from armadillo livers and spleens from infected and uninfected animals were analyzed as described for the peripheral nerve extracts using the UPLC Q-TOF system (Waters). On each LC-MS run, extracts from only one uninfected and one infected animal were injected. The spleen and liver extracts were injected in the same run. Therefore, their features could be combined and compared (**Table 3.2**). The liver and spleen samples are more complex than the nerve samples **(Figure S3.3).** Interestingly, as seen with nerves, the number of features in animals AU-2 and AI-2 were fewer than in the other animals (1 and 3).

It was expected that there will be features that distinguish each of the tissue types (data not shown). However, the objective of this study was to identify metabolic components that separate infected from corresponding uninfected tissue types. The significant features from these analyses are listed in **Table S3.3**. Tentative chemical identifications were feasible by querying the m/z values against MassTrix and Mtb databases. The majority of them were uniquely identified as TAGs, DAGs and glycerophospholipids of the nitrogen containing metabolically related PC, PE and phosphatidyl serine (PS). Also ceramides and related sphingomyelin were significant features in some comparisons (**Table S3.3).** Interestingly, Vitamin D3 appeared as a significant feature in two infected tissues. Retention times were not directly comparable from nerve to the liver and spleen LC-MS data sets, as the solvent system or elution time changed. However, of these, a further subset of m/z values common to all three infected tissue types was distilled, as shown in **Table 3.3**. These were all triacylglycerols.

3.4.3 Transcriptional regulation of the lipidome in *M. leprae* infected tissues

To investigate if there are underlying molecular mechanisms that contribute to the increase in certain TAG species, the expression levels of candidate genes involved in fatty acid and triacylglycerol synthesis were measured in the infected and uninfected liver samples (**Figure 3.4**). Primer design for qRT-PCR was feasible due to the recent availability of the 2X coverage complete armadillo genome sequence from the Broad Institute [http://uswest.ensembl.org/Dasypus_novemcinctus/Info/Index]. The qRT-PCR

products for seven genes amplified from cDNA were examined by agarose gel for specificity before performing the qRT-PCR (**Figure 3.5**).
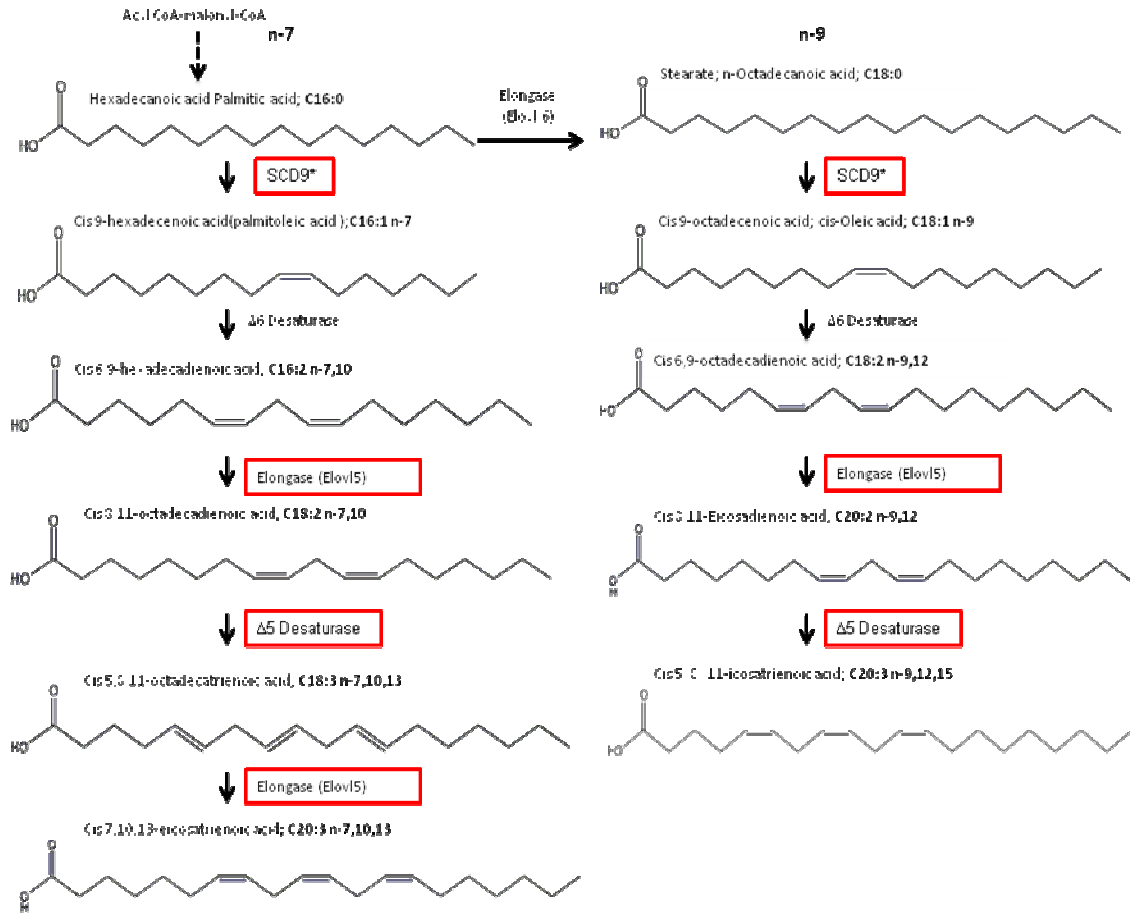
Figure 3.4: Fatty acid elongation and desaturation pathways in mammals. Transcript levels of genes encoding enzymes shown within red boxes were measured by quantitative reverse transcriptase-PCR.
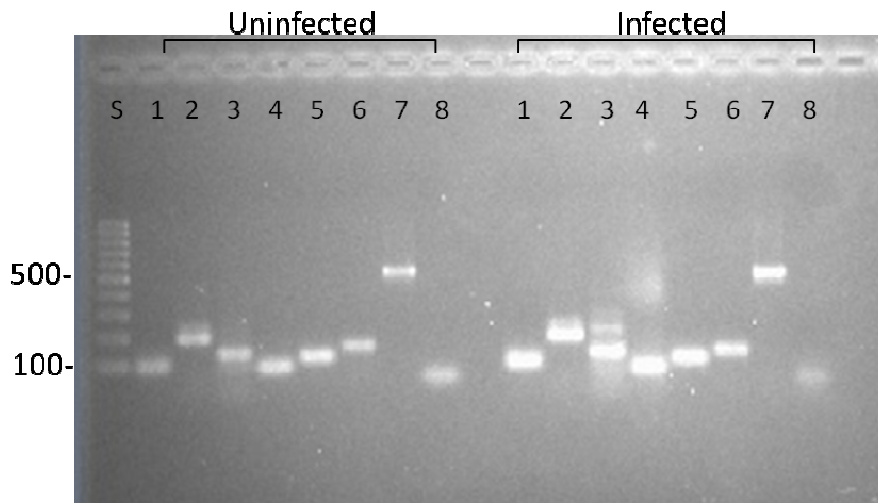
Figure 3.5: Detection of transcripts of fatty acid and TAG synthesis genes in the armadillo liver by reverse transcriptase PCR. The products were detected by agarose gel electrophoresis: lanes: 1- MOGAT; 2- DGAT; 3- ScD-5; 4- Δ5D; 5- ELOVL-5; 6- SCD-9; 7- GAPDH. The cDNAs from an uninfected (AU-2) and an infected (AI-2) liver specimens were used as templates.

After standardization of the reaction conditions and verification of the gene products by gel, quantitative qRT-PCR was performed using iQ SYBR Green Supermix for each gene. The melt curve for each gene tested showed single peals with distinct melting temperatures indicating the specificity of the primers **(Figure S3.4).**The Ct values were obtained for the tested genes in uninfected and infected liver samples (three animals per group, three biopsies per animal, duplicate PCRs for each cDNA template preparation) . The qRT-PCR experiment was repeated using the same cDNA stock preparations. The Ct values from the two experiments were normalized against the corresponding Ct values obtained for the reference gene GAPDH (ΔCt= Ct of target gene - Ct of GAPDH).

The ΔCt (Ct of target gene - Ct of GAPDH) comparisons between all uninfected and infected tissues (for the genes tested) are shown in **Figure 3.6A.** The fold change in gene expression calculated using $2^{-\Delta\Delta Ct}$ method, showed that expression of SCD9 was highly up-regulated in the infected tissue (~20 fold increase) (**Figure 3.6B**). Other genes that showed detectable but smaller increases in expression in the infected tissues are Δ5D, ELOVL5 and DGAT. However, these increments are not statistically significant.
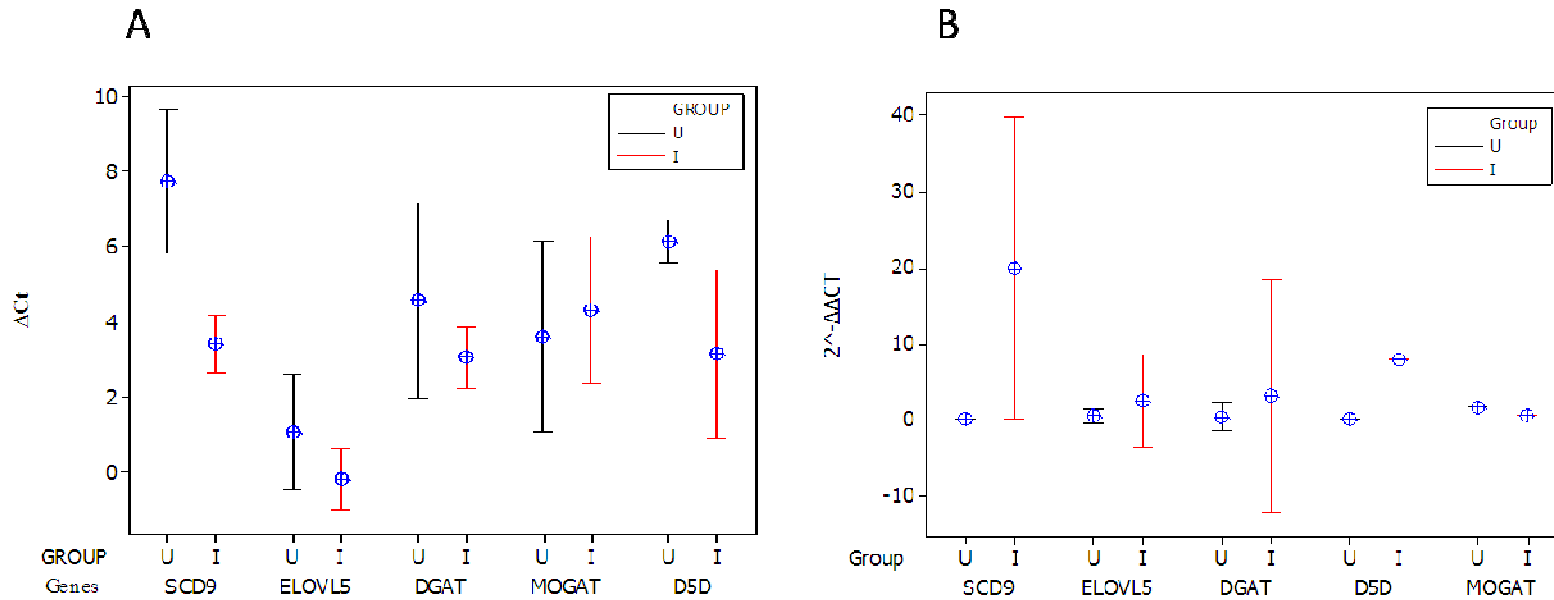
Figure 3.6: Relative gene expression of a panel of fatty acid elongases, desaturases and acyltransferases in uninfected and infected liver. A: The Ct value for each gene was normalized to GAPDH Ct value (ΔCt). The differences (ΔCt) between uninfected and infected are significant for SCD9 (p= <0.005) and Δ5D (p= 0.02). **B**: Fold change in mRNA abundance for each gene tested using $2^{-\Delta\Delta Ct}$ method. The gene expression of SCD9 was significantly increased in the infected samples (Student's *t*-test, p=0.006). Δ5D expression was increased but not significantly (p=0.15).

132

3.5. DISCUSSION

Pathogens take advantage of host metabolites at various stages of infection and survival. This is particularly important for obligate intracellular pathogens such as *M. leprae* that modulate host metabolism for their own survival. *M. leprae* is believed to access host nutrients that it cannot manufacture due to its gene loss **[1]**. Host lipids are especially important as a carbon source, but also play roles in complex and dynamic processes, such as membrane signaling and manipulation of the immune system **[2].** To gain insight into these processes, a comparative study of the metabolome with an emphasis on the lipidome in infected and uninfected states is a useful approach. Biomarker discovery is a step towards identifying underlying biological pathways involved in host-pathogen interactions.

Mycobacterial diseases have long been associated with foamy, lipid laden 'Virchow or Lepra cells' in sites of infection. In 1970 different histochemical staining techniques were applied to show that fatty acids, neutral lipids, cholesterol, glycolipids and phospholipids accumulate in lepromatous leprosy skin biopsies **[15]**. It was believed that the lipids inside the fatty cells were from dead bacilli which accumulate in the host **[16].** Such techniques lacked the sensitivity to identify and quantify the lipid species. Our study revisits host-pathogen metabolism in leprosy using current 'omics' technologies based on LC-MS. We attempted to develop and compare fingerprints of small molecules extracted from uninfected and infected tissues of the nine banded armadillo, the only well established animal model for leprosy. While the peripheral nerve is the niche for *M. leprae* infection and the biological basis for the characteristic manifestations of sensory loss and disability,

in the armadillo model of lepromatous infection, the liver and spleen are also highly

bacilliferous; such infected organs have served as the primary source of large amounts for

M. leprae for research purposes. Therefore all three tissue types: peripheral nerves, liver

and spleen were investigated.

The comparative mass spectrometry based ion profiles of simple chloroform/methanol

tissue extracts identified a series of ions in greater abundance in the infected nerve that

corresponded to triacylglycerols. MS/MS was achieved for some of these ions, confirming

that they were TAGs. TAGs composed of 14:0/16:1/18:2; 16:0/14:0/18:1; 14:0/18:2/18:2;

14:0/18:1/18:2; 16:1/18:2/18:2; 16:1/18:1/18:2; 16:0/18:0/18:1, 18:1/18:2/18:2 were found

in the infected specimens. The two notable properties in these TAGs are the lengths and

the unsaturation of the acyl chains. The accumulation of TAGs during infection correlate

with our knowledge of the biochemical changes compatible with mycobacterial disease

while the details about the composition of TAGs advances our understanding of the

specific molecules that may contribute to the survival of *M. leprae in vivo*.

TAG elevation has been associated with HIV besides TB and leprosy **[17].** During

bacterial or viral infections there is an increase in serum TAG levels (hypertriglyceridemia)

by the action of cytokines TNF(α and β), IL-1, IL-2, IL-6, leukemia inhibitory factor,

ciliary neurotropic factor (CNTF), nerve growth factor (NGF), keratinocyte growth factor

(KGF), platelet activating factor (PAF), and parathyroid hormone-related protein (PTHrP)

[18]. Based on the sensitivity level of the mass-spectrometry in our study and the nature of

the fatty acids (all animal cell rather than bacterial in nature), the TAGs are probably of

host and not bacterial origin. It has been shown that an injected sample equivalent of $>10^5$ mycobacteria are required for detection of the bacterial lipid components by the mass spectrometry conditions applied to this study **[9]**. The 1μl injection of extract would correspond to fewer than ~10^5 *M. leprae*. *M. leprae* genome lacks the genes desaturases: Δ 5, 6 and 12 needed to synthesize long-unsaturated types of fatty acids. These specific TAGs were found in higher abundance in the infected livers and spleens when compared to the uninfected tissues.

To account for the synthesis of unsaturated fatty acids and TAGs composed of these lipids in the infected tissues, we considered the common pathways as summarized in **Figure 3.4**. In general, fatty acid synthesis, from acyl CoA precursor units is accomplished by fatty acid synthases which generate products of 14-16 Carbon unit length, which are extended by a variety of elongases that have chain length specificities. Likewise, desaturases produce the double bonds at specific locations. Depending on the position of the double bond inserted by the desaturases, n-3, n-6, n-7 and n-9 families of unsaturated fatty acids are generated. The fatty acids are transferred to glycerol-3 phosphate backbone to produce diacylglycerol and the TAGs. These are monoacyl glycerol transferase (MOGAT, diacylglycerol transferase (DGAT). It has been shown that these enzymes can be regulated at the transcriptional level through transcription factors. To investigate if altered gene expression levels contributed to the observed TAGs, a set of genes encoding the elongases, desaturases and transferases were identified in the ENSEMBL database which now includes the genome sequence of the *Dasypus novemcinctus*.

SCD9 expression was increased in infected armadillo tissues, which correlates nicely with the increase in 18:1n-9 and 16:1 n-7 MUFAs in TAG. We also found a definite increase in the gene expression of ELOVL5, the enzyme that can convert the 16:2, n-7 to 18:2, n-7. Although the location of the desaturation has not been defined, the infected tissues comprise TAGs with 18:2 (n-7 or n-9). The DGAT was also slightly up-regulated (2 fold) in the infected tissues. Based on these results, it is surmised that the specific TAGs found in the infected tissues are primarily a consequence of the infection. In the current study, the diet and housing conditions of the infected versus the uninfected animals were not equivalent and could not be experimentally controlled. Yet, we found that one of the three infected animals (AI-3) was captured as such from the wild (natural sylvan infection), was in the colony for only 3 days, but had the mass features in the LC-MS profiles as detected in the experimentally infected animals which were housed for many months. The uninfected animals were sacrificed soon after capture from the wild.

The mass spectrometry results are compatible with a number of studies in the literature. In different infectious and non-infectious disease conditions, the foamy appearance of macrophages has been attributed to the accumulation of lipid droplets (LDs). In recent years, details are emerging regarding the composition, location and the origin of the LDs, and how the lipids from these are mobilized /utilized by pathogens. LDs are made of an outer monolayer of phospholipids and an internal core rich in neutral lipids such as triacylglycerol, cholesterol esters, retinol ester and diacylglycerols. Tanigawa *et al* showed that *M. leprae* increased LD formation through regulation of host adipose differentiation related protein (ADRP) and perilipin expression in *in vivo* settings such as in skin lesions

of lepromatous leprosy and in *in vitro* after infection of human promonocytic cell line THP-1 cells with live *M. leprae* [19]. Mattos *et al* showed that *M. leprae* induces foamy cell formation *in vivo* in a pleurisy mouse model and *in vitro* in human peripheral monocytes and mouse macrophages. Furthermore, they demonstrated that LD induction occurs in the infected and even in neighboring uninfected human macrophages via TLR2 and TLR6 dependent mechanisms. TLR2 signaling stimulates production of IL-1β and PGE2, anti-inflammatory mediators that suppress innate immunity and the Th1 response [4]. However, when tested in Schwann cells (SCs) the induction of LDs by *M. leprae* was dependent on the ER, Golgi apparatus, motor proteins and microtubules *via* a TLR6 and not TLR2 pathway. After *M. leprae* recognition, SCs send a signal for phagocytosis, LD formation, cytokine and PGE2 production which promote bacterial survival [20, 21]. The interaction between LDs and the phagosomes was also found in *M. tuberculosis* and also used for acquisition of host cellular iron [22].

During tuberculosis foamy cells with LDs are present in the outermost layer of the granuloma [23]. It has been suggested that inside the granuloma, mycolic acids or trehalose-6,6′-dimycolate (TDM) of mycobacterial origin, trigger the formation of foamy cells in a TLR2-dependent pathway. Within the granuloma, the bacilli are also filled with intracellular lipophilic inclusions (ILIs). Analysis of the lipid constituents of the pulmonary TB granuloma showed enrichment of the lipids of LD origin in foamy cells, such as cholesterol, and cholesteryl esters, TAG and lactosylceramide [3]. Gene expression analysis of TB granuloma showed up-regulation of gene encoding ADRP, which resulted in increased uptake and synthesis of long-chain fatty acids (LCFAs) and TAGs composed

of saturated (palmitic acid, 16:0), mono-unsaturated (oleic acid, C18:1), or polyunsaturated fatty acids. Also, up-regulation of acyl Co-A synthase long chain family member 1 (ACSL1) leads to synthesis of LCFAs, that incorporate into TAG and lipid droplet formation. Mass spectrometry showed increase in CE and another compound with *m/z* 876.8 corresponding to a TAG with two unsaturated bonds in the fatty acyl chains (52:2) **[24, 25].** This TAG species was also found to be significantly increased in the armadillo infected tissues.

M. tuberculosis and *M. leprae* dysregulate the host lipid metabolism for long term bacterial survival. There are many ways by which the bacteria perturb the host lipidome such as by controlling the host lipases, expression of fatty acid synthesis genes, lipid signaling, and accumulation of lipid in vacuoles or LDs. Several studies have shown that the same list of lipid metabolism genes were up-regulated during both tuberculosis and lepromatous leprosy infection **[2, 24].** While *M. tuberculosis* bacilli produce their own TAGs, by increased expression of triacylglycerol synthase (*tgs*) under stress conditions such as oxygen depletion and/or elevated ratio of carbon:nitrogen, it is also thought that they obtain lipids released from the host LDs **[22].** It has been shown that the lipids within bacterial ILIs are of cellular origin because the TAG fatty acids are similar to those of host TAGs in LDs with the majority being C16:0, 18:0 and 18:1 fatty acids **[23, 26, 24, 27].** However, it is not yet clear how the bacilli translocate cellular LD lipids to their own cytoplasm. Regardless of the source, the TAGs in ILIs are the major source of energy during latency and as precursors for building the complex mycobacterial cell wall for future growth.

In terms of the biological significance, our findings are also consistent with the phenotype of multibacillary leprosy. It is known that fatty acids composition (chain length and saturation) of TAG and membrane phospholipids impact the host immune system *via* physical changes in permeability and fluidity. Medium-chain triglycerol (MCT, C8-C18) treatment of neutrophils result in inhibition of the phagocytic and bacteriocidal activities and reduction in hydrogen peroxide production compared to long-chain triglycerol (C14-22) [28]. It was found that MUFA 16:1, n-7 can increase the insulin sensitivity of peripheral tissues in cystic fibrosis. The 18:1, n-9 has been shown to be involved in inflammation [29]. The deficiency in SCD9 was found to promote tissue inflammation and reduce plasma triglycerides [30]. In another study, the decrease of SCD9 expression and consequent changes in levels of 16:1 and 18:1 lipid species (using liquid chromatography-mass spectrometry (LC-MS)-based metabolomic approach) was correlated with elevated expression of pro-inflammatory cytokines [31]. In our armadillo leprosy study, SCD9 is increased in infection; concordant with the anti-inflammatory phenotype.

When together, our approach of global lipidomics followed by targeted genomics have revealed that certain TAGs composed of unsaturated fatty acids are biomarkers of lepromatous tissues. In terms of establishment of infection, the TAGs contribute towards the establishment of survival niche for *M. leprae* by providing an anti-inflammatory environment and nutrients. Biological targets for therapeutics and/or vaccines may be found within this multifaceted virulence process.

3.6. CONCLUSIONS

Lipid has been known as major carbon source for nutrition during growth of *Mycobacterium* spp, such as *M. leprae*. In order for *M. leprae* to survive in the macrophage or SCs phagosomes, it creates a lipid rich environment. This lipid environment is formed by the accumulation of host derived lipids inside macrophages or SCs vacuoles (lipid bodies) (**Figure 3.7**).

Lipidomics is a new useful approach that depends on using liquid chromatography and mass spectrometry to study host-bacterial interaction. This approach allows detection, characterization and quantification of many different classes of lipids from tissue samples. As a result of this characterization, biomarkers can be identified. These biomarkers help in understanding the pathogenesis of the disease, which facilitate new diagnostic approaches and therapy.

The lipidomics approach was applied to study changes during *M. leprae* infection of armadillos (leprosy model tissues). Comparing the lipid profile of uninfected armadillo with the infected tissues resulted in finding significant features in both groups. Out of these significant features, different species of triacylglycerol (TAG) were chemically identified in the infected nerves. These TAG were found to contain mono- and di-unsaturated fatty acids. The source for these TAGs was examined through testing the gene expression of several genes involved in TAG and unsaturated fatty acids. The gene that encodes SCD9 was significantly increased in the infected tissues. This enzyme convert saturated FAs (16

18) to mono-unsaturated FS (16:1, n-7, 18:1, n-9). These fatty acids are mostly esterified into triacylglycerols (TAGs). These monounsaturated fatty acids were the main fatty acids found in the elevated levels of TAGs in infected tissues and they could participate in the immunological phenomena of the disease. Moreover, to determine the source of these up-regulated TAGs in the infection and test the assumption that they could be derived from LDs of foamy cells, the foamy cell lipid should be further studied. Many researchers have looked at the foamy cell lipid and found that it is rich in TAG, but the exact TAG species had not been identified. The role of the SCD9 and others in TAG synthesis can be addressed by suitable *in vitro* assays and manipulation of gene expression levels and use of enzyme inhibitors.
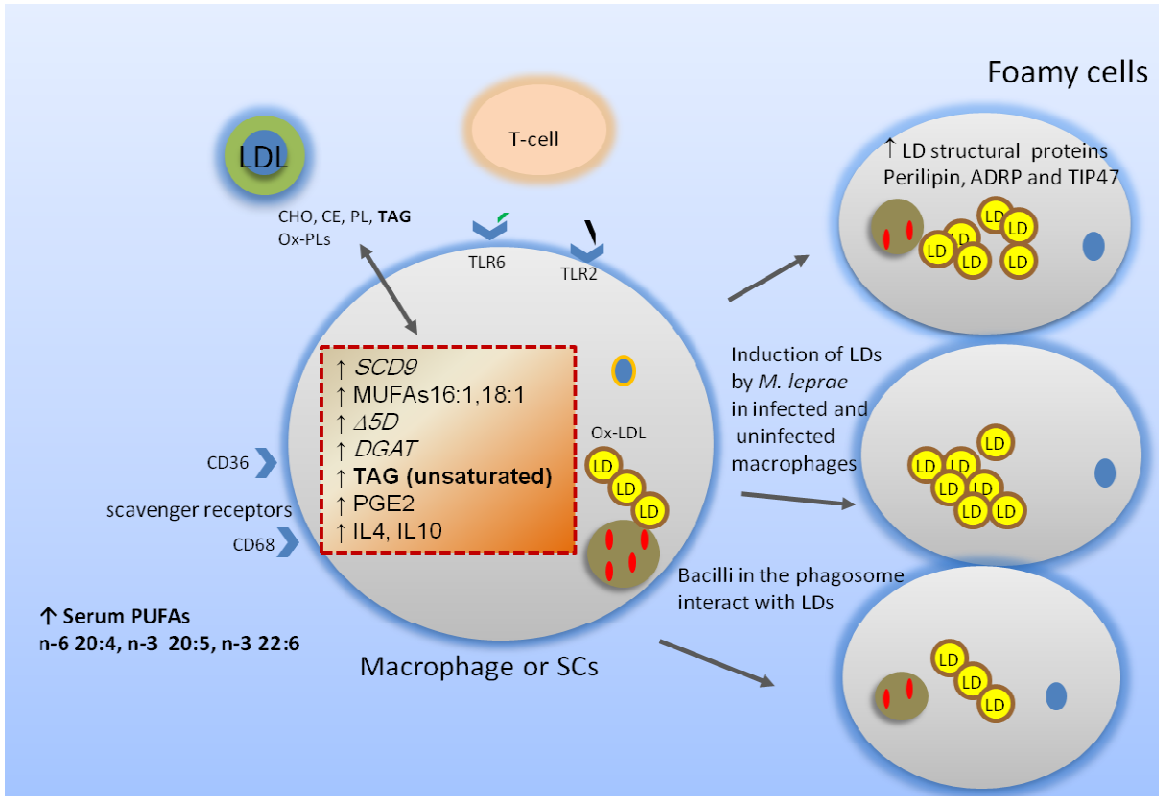
Figure 3.7: A model of *M. leprae* induction of certain species of TAGs inside macrophages or SCs by upregulation of upstream SCD9 and DGAT genes. These specific TAGs would be incorporated into LDs and harnessed by *M. leprae* as a source of energy for intracellular survival.

3.7. FUTURE DIRECTIONS

The lipidome study of armadillo tissues during and prior to *M. leprae* infection resulted in identification of different forms of TAGs that are increased during infection. In this study we did not account for the dietary differences between uninfected and infected armadillos. Almost all the uninfected animals were captured from the wild and spent few days at the in-house colony and they were tested for leprosy. The infected animals (2 animals) were also captured from the wild and infected with *M. leprae* and stayed in the colony (>18months) until they develop the late stages of the disease. One of the infected animals was naturally infected with *M. leprae* (wild infected). More control experiment should be done in the future using more wild infected armadillo or have the uninfected armadillos stay for a long time in the in-house colony. Using these sorts of control animals we can define the dietary intake for both infected and uninfected animals. Other things that could be controlled in designing this experiment are the age and the sex of these animals. In our experiment the selected armadillos were all mature with an average age of 2-4 years.

Another follow up experiment that should also be done to validate the use of these TAGs as biomarker is through monitoring the change in the abundance of TAG at different stages of the disease; also, follow up the changes before and after leprosy treatment. The lipid profile of armadillo serum can be examined and correlated to the tissue lipid profile.

Further new experiment that also will help validation of this biomarker is through testing the lipidome profile from several leprosy patients. The lipid profile of skin biopsy from

different forms of leprosy (low versus high BI) should be studied while monitoring the changes in TAG species. These experiments will not only confirm and validate the use of these TAG species as biomarker but also confirm that the change is due to the disease not to other factors.

Another area in this research topic that could be expanded is to identify the exact mechanism(s) that led to up-regulation of different forms of TAG during infection. To answer this question we tested the gene expression profile for synthesis of TAG and different FAs and compared infected versus uninfected tissues. Moreover, to determine the source of these up-regulated TAG in the infection and test the assumption that they could be derived from LDs of foamy cells, the lipid in the foamy cell should be studied. Many researchers have looked at the foamy cell lipids and found that it is rich in TAG, but the exact TAG species (fatty acid composition) have not been identified.

Moreover, gene expression of SCD9 and DGAT was found to be up-regulated in the infected tissue compared to uninfected liver sample. As a result of this up-regulation, TAGs with monounsaturated fatty acids were increased in these tissue samples. Further study after inhibition or silencing of these genes (SCD9 and DGAT) would be useful, to validate the relationship between *M. leprae* infection, increase in SCD9 and DGAT and elevated TAGs with monounsaturated fatty acids. This approach could be done by using an in vitro system (macrophages infected with *M. leprae*) after inhibition of SCD9 and DGAT. The lipids would be extracted to determine any changes in TAG species compared to the normal state macrophages (infected and uninfected).

Additional data files

Table S3.1- *M. leprae* ions detected in positive mode and tentative compound identification based on querying the *Mtb* Lipid database [9].

RT	Mass	Compounds (Abbreviation)	Formula	Ion
0.237	921.00304	TG(55:1)	C58H114NO6	[M+NH4]+
0.557	921.00293			
0.875	921.00306			
1.251	6179.45349			
1.265	2857.62558	TDM(C185)	C185H356O15K	[M+K]+
1.27	1252.78435	Ac1PIM1(50:2)	C65H123NO19P	[M+NH4]+
1.275	1695.00899	Ac2PIM2(69:2)	C90H169NO25P	[M+NH4]+
1.276	1783.05822	Ac1PIM4(53:1)	C86H161NO34P	[M+NH4]+
1.279	1457.85396	Ac1PIM2(53:4)	C74H131O24PNa	[M+Na]+
1.281	3033.80628	TDM(C198)	C198H383O17	[M+H]+
1.282	1413.82857	Ac1PIM2(50:5)	C71H123O24PNa	[M+Na]+
1.283	1325.7759	PIM3(C34)	C61H114O28P	[M+H]+
1.283	3203.90616			
1.285	1563.93745	Ac1PIM3(C50)	C77H144O29P	[M+H]+
1.288	1369.80191	Ac1PIM2(48:2)	C69H126O24P	[M+H]+
1.293	737.94326			
1.294	1342.80357	PIM3(C34)	C61H117NO28P	[M+NH4]+
1.295	1650.98701	Ac1PIM3(C55)	C82H157NO29P	[M+NH4]+
1.296	252.12152			
1.296	1484.85393	Ac1PIM2(55:2)	C76H143NO24P	[M+NH4]+
1.298	445.25196	Mycolipenic acid(C28)	C28H54O2Na	[M+Na]+
1.298	357.20101	MG(18:1)	C21H41O4	[M+H]+
1.298	401.22711	MG(C21)	C24H49O4	[M+H]+
1.306	1462.81199	PIM4(C31)	C64H121NO33P	[M+NH4]+
1.306	296.14758			
1.307	1418.78454	Ac1PIM2(C50)	C71H137NO24P	[M+NH4]+
1.309	1374.75937	Ac1PIM2(47:1)	C68H129NO24P	[M+NH4]+
1.309	822.49221	PG(38:1)	C44H89NO10P	[M+NH4]+
1.31	1330.73179			
1.311	1286.7069	PIM3(C30)	C57H109NO28P	[M+NH4]+
1.32	1735.01424	Ac1PIM4(50:4)	C83H149NO34P	[M+NH4]+
1.321	1748.95828	Ac1PIM4(51:4)	C84H151NO34P	[M+NH4]+

1.321	1204.72594	PIM2(36:2)	C57H107NO23P	[M+NH4]+
1.331	1660.89826	PIM5(34:3)	C73H131NO38P	[M+NH4]+
1.332	2882.92049	TDM(C188)	C188H370NO15	[M+NH4]+
1.333	779.45282	PG(C36)	C42H84O10P	[M+H]+
1.333	1386.82978	Ac1PIM2(48:2)	C69H129NO24P	[M+NH4]+
1.333	1466.90334	Ac1PIM2(54:4)	C75H137NO24P	[M+NH4]+
1.334	916.49109			
1.335	1943.15033	Ac2PIM4(64:5)	C97H173NO35P	[M+NH4]+
1.337	1837.02607	Ac1PIM4(57:2)	C90H167NO34P	[M+NH4]+
1.338	872.4646	Mbt -Fe(C20)	C80H	[M+H]+
1.338	1572.84995	Ac1PIM3(50:4)	C77H139NO29P	[M+NH4]+
1.343	1298.77825	CL(59:1)	C68H134NO17P	[M+NH4]+
1.344	828.43905			
1.347	784.41241	PE(C37)	C42H84NO8PNa	[M+Na]+
1.35	744.413	PE(36:2)	C41H79NO8P	[M+H]+
1.35	2431.36613			
1.351	740.38532	PE(34:1)	C39H76NO8PNa	[M+Na]+
1.354	260.12484			
1.354	700.38665	PE(C31)	C36H72NO8PNa	[M+Na]+
1.355	696.35921	PG(29:1)	C35H71NO10P	[M+NH4]+
1.355	2607.47887	TDM(C168)	C168H326O15Na	[M+Na]+
1.356	2216.33172	Ac2PIM5(71:1)	C110H201O40PNa	[M+Na]+
1.358	652.33133			
1.359	656.3602			
1.36	2072.21389	Ac2PIM4(73:6)	C106H185O35PNa	[M+Na]+
1.362	2587.53146	TDM(C167)	C167H325O16	[M+H]+
1.362	1210.72381	Ac1PIM1(47:2)	C62H117NO19P	[M+NH4]+
1.363	608.30367			
1.364	612.33411			
1.366	469.28917	Lyso-PE(16:1)	C21H46N2O7P	[M+NH4]+
1.367	320.18395	MG(C14)	C17H38NO4	[M+NH4]+
1.367	559.32101			
1.367	425.26263	MG(C20)	C23H46O4K	[M+K]+
1.368	366.19071			
1.368	568.3075	DG(31:2)	C34H66NO5	[M+NH4]+
1.37	348.17688	MG(C16)	C19H42NO4	[M+NH4]+
1.37	381.23682	MG(C18)	C21H42O4Na	[M+Na]+
1.37	524.28156			
1.371	410.21626			
1.372	515.29475			
1.373	563.35225	Lyso-PG(C20)	C26H53O9PNa	[M+Na]+

1.373	519.32601	Lyso-PG(17:1)	C23H45O9PNa	[M+Na]+
1.373	454.24225	Lyso-PE(C16)	C21H45NO7P	[M+H]+
1.373	475.29975	Mycocerosic acid(C30)	C30H60O2Na	[M+Na]+
1.374	370.22098			
1.374	414.24703	Mycosanoic or Mycocersoci acid(C26)	C26H56NO2	[M+NH4]+
1.374	480.25523	Lyso-PE(18:1)	C23H47NO7P	[M+H]+
1.376	326.19493			
1.377	293.18451			
1.378	282.16852			
1.38	255.16875			
1.381	783.48319	PI(C30)	C39H76O13P	[M+H]+
1.383	804.4158			
1.384	760.38819	PE(37:1)	C42H83NO8P	[M+H]+
1.386	716.36076	PE(34:2)	C39H75NO8P	[M+H]+
1.387	628.30778	Lyso-PI(19:2)	C28H55NO12P	[M+NH4]+
1.387	672.33432			
1.387	584.28122			
1.389	540.2551			
1.39	496.22929	Lyso-PE(C19)	C24H51NO7P	[M+H]+
1.446	345.24587	MG(C17)	C20H41O4	[M+H]+
1.456	314.24863			
1.461	329.25722	MG(16:1)	C19H37O4	[M+H]+
1.464	360.28647	MG(17:1)	C20H42NO4	[M+NH4]+
1.468	312.23202			
1.476	404.31418	MG(C20)	C23H50NO4	[M+NH4]+
1.476	282.22186			
1.485	1711.09589	Ac2PIM2(70:1)	C91H173NO25P	[M+NH4]+
1.487	296.23568			
1.498	278.22471			
1.508	315.27777	MG(15:1)	C18H35O4	[M+H]+
1.513	294.21969			
1.523	292.20295			
1.547	1760.14079	Ac2PIM3(C63)	C90H168O30P	[M+H]+
1.567	322.25064			
1.584	1032.68005	PIM1(C35)	C50H99NO18P	[M+NH4]+
1.591	318.28002			
1.591	1945.27137	Ac2PIM4(64:4)	C97H175NO35P	[M+NH4]+
1.592	1759.1364	Ac2PIM3(62:2)	C89H165NO30P	[M+NH4]+
1.592	1939.24127	Ac2PIM4(C63)	C96H181NO35P	[M+NH4]+
1.594	929.62468	PG(C44)	C50H99O10PK	[M+K]+
1.599	753.52037			

1.601	988.65712	PIM1(32:1)	C47H91NO18P	[M+NH4]+
1.602	885.59936	PI(36:2)	C45H83O13PNa	[M+Na]+
1.603	1059.68865	PIM1(37:3)	C52H93O18PNa	[M+Na]+
1.606	841.57236	PG(39:1)	C45H87O10PNa	[M+Na]+
1.607	1847.18676	Ac2PIM3(C68)	C95H181NO30P	[M+NH4]+
1.607	1019.69026	PIM1(34:2)	C49H89O18PNa	[M+Na]+
1.608	1015.66282	PIM1(C35)	C50H96O18P	[M+H]+
1.612	384.28759			
1.615	797.54673	PG(36:2)	C42H79O10PNa	[M+Na]+
1.616	975.66591	DAT2(C54)	C54H103O14	[M+H]+
1.619	934.58544	Mycocerosic or Phthioceranic acid(C31)	C31H62O2Na	[M+Na]+
1.622	489.36644			
1.623	445.33989	Mycolipenic acid(C28)	C28H54O2Na	[M+Na]+
1.623	533.39223	Hydroxyphthioceranic acid(C33)	C33H66O3Na	[M+Na]+
1.637	665.46895	DG(39:1)	C42H81O5	[M+H]+
1.651	892.57412	PI(37:3)	C46H87NO13P	[M+NH4]+
1.654	278.15236			
1.654	621.44302	DG(36:2)	C39H73O5	[M+H]+
1.655	848.54702	PI(34:4)	C43H79NO13P	[M+NH4]+
1.656	755.5364	PG(33:2)	C39H73O10PNa	[M+Na]+
1.659	577.41793	DG(C31)	C34H66O5Na	[M+Na]+
1.662	711.51066			
1.69	535.40755	DG(C28)	C31H60O5Na	[M+Na]+
1.706	324.26681			
1.707	491.38181	Lyso-PG(15:1)	C21H41O9PNa	[M+Na]+
1.722	386.30389	Mycosanoic or Mycocerosic acid(C24)	C24H52NO2	[M+NH4]+
1.728	447.35577	Mycocerosic acid(C28)	C28H56O2Na	[M+Na]+
1.731	342.27699			
1.753	1977.27023	Ac2PIM4(66:2)	C99H183NO35P	[M+NH4]+
1.762	1713.11036	Ac2PIM2(C70)	C91H175NO25P	[M+NH4]+
1.767	901.59408	PI(37:1)	C46H87O13PNa	[M+Na]+
1.769	1625.05786	Ac2PIM2(64:2)	C85H159NO25P	[M+NH4]+
1.774	945.6208	PIM1(C30)	C45H86O18P	[M+H]+
1.789	949.65121	TG(57:3)	C60H110O6Na	[M+Na]+
1.797	861.5997	PI(36:3)	C45H82O13P	[M+H]+
1.811	817.57446	PG(C36)	C42H83O10PK	[M+K]+
1.818	773.54876	PG(C34)	C40H79O10PNa	[M+Na]+
1.83	729.52161	PG(31:1)	C37H71O10PNa	[M+Na]+
1.848	641.47133			
1.86	597.44471	DG(C34)	C37H73O5	[M+H]+

1.869	553.41827	DG(31:1)	C34H65O5	[M+H]+
1.886	509.3924	MG(C26)	C29H58O4K	[M+K]+
1.899	421.3406	Mycosanoic or Mycocerosic acid(C25)	C25H50O2K	[M+K]+
1.905	377.31429			
1.918	316.26192			
1.937	481.35169	Mycocerosic acid(C32)	C32H65O2	[M+H]+
1.938	507.37139	MG(C27)	C30H60O4Na	[M+Na]+
1.951	541.87553			
1.96	1061.70692	PIM1(37:2)	C52H95O18PNa	[M+Na]+
1.966	497.84937			
1.974	973.65421	PIM1(37:2)	C52H95O18PNa	[M+Na]+
1.975	2045.35589	Ac2PIM4(71:3)	C104H191NO35P	[M+NH4]+
1.984	2934.02606	TDM(C193)	C193H375O15	[M+H]+
1.985	1859.25699	Ac2PIM3(69:1)	C96H181NO30P	[M+NH4]+
1.988	933.65775			
1.993	1087.72252			
2.002	1789.17745	Ac2PIM3(64:1)	C91H171NO30P	[M+NH4]+
2.003	1851.22975	Ac2PIM3(69:5)	C96H173NO30P	[M+NH4]+
2.006	885.60146	PG(C42)	C48H95O10PNa	[M+Na]+
2.007	889.63337	PG(C42)	C48H95O10PNa	[M+Na]+
2.008	1959.2729	Ac2PIM4(65:4)	C98H177NO35P	[M+NH4]+
2.009	510.85723			
2.013	1003.69687	DAT2(C56)	C56H107O14	[M+H]+
2.016	841.57553	PG(39:1)	C45H87O10PNa	[M+Na]+
2.022	845.60714	PI(35:4)	C44H78O13P	[M+H]+
2.023	850.56223	PI(34:3)	C43H81NO13P	[M+NH4]+
2.025	797.5486	PG(36:2)	C42H79O10PNa	[M+Na]+
2.028	959.67168	DAT1(C54)	C54H103O13	[M+H]+
2.032	955.64258	TG(56:1)	C59H112O6K	[M+K]+
2.034	1929.26054	Ac2PIM3(74:1)	C101H191NO30P	[M+NH4]+
2.034	801.58112	PG(C36)	C42H83O10PNa	[M+Na]+
2.047	2747.97682			
2.05	806.53712	PG(37:2)	C43H85NO10P	[M+NH4]+
2.051	920.60481	PG(45:1)	C51H103NO10P	[M+NH4]+
2.053	757.55419	PG(33:1)	C39H75O10PNa	[M+Na]+
2.056	1821.18644	Ac2PIM3(67:6)	C94H167NO30P	[M+NH4]+
2.057	871.62096	PI(35:2)	C44H81O13PNa	[M+Na]+
2.059	867.59018	PI(C36)	C45H88O13P	[M+H]+
2.062	713.52878	DG(41:2)	C44H82O5Na	[M+Na]+
2.074	827.59519	PG(38:1)	C44H85O10PNa	[M+Na]+
2.077	716.47479	PE(34:2)	C39H75NO8P	[M+H]+

2.082	672.44411			
2.085	669.50219			
2.085	832.55206	TG(49:3)	C52H98NO6	[M+NH4]+
2.087	783.56922	PG(35:2)	C41H77O10PNa	[M+Na]+
2.095	625.47641	DG(C36)	C39H77O5	[M+H]+
2.101	581.45009	DG(33:1)	C36H69O5	[M+H]+
2.101	788.52604	PE(39:1)	C44H87NO8P	[M+H]+
2.105	630.43141	Lyso-PI(19:1)	C28H57NO12P	[M+NH4]+
2.105	739.54365			
2.119	537.42413	Phthioceranic acid(C36)	C36H73O2	[M+H]+
2.119	744.4995	PE(36:2)	C41H79NO8P	[M+H]+
2.12	695.51718	PE(C31)	C36H76N2O8P	[M+NH4]+
2.122	586.4062	DG(C32)	C35H72NO5	[M+NH4]+
2.13	493.39781	MG(C26)	C29H58O4Na	[M+Na]+
2.134	651.49085	MG(C26)	C29H58O4Na	[M+Na]+
2.136	700.47288	PE(C31)	C36H72NO8PNa	[M+Na]+
2.149	449.37195	Mycolipanolic acid(C27)	C27H54O3Na	[M+Na]+
2.152	607.46479	DG(35:2)	C38H71O5	[M+H]+
2.152	656.44611	DG(C37)	C40H82NO5	[M+NH4]+
2.159	405.34558	Mycosanoic or Mycocerosic acid(C25)	C25H50O2Na	[M+Na]+
2.163	612.42087	Mycosanoic or Mycocerosic acid(C25)	C25H50O2Na	[M+Na]+
2.164	344.29313			
2.167	563.43895	DG(C30)	C33H64O5Na	[M+Na]+
2.179	519.41291	Lyso-PG(17:1)	C23H45O9PNa	[M+Na]+
2.202	414.33477	Mycosanoic or Mycocersoci acid(C26)	C26H56NO2	[M+NH4]+
2.25	1001.68388	PIM1(C34)	C49H94O18P	[M+H]+
2.25	463.38737	Mycocerosic acid(C28)	C28H56O2K	[M+K]+
2.258	283.28806			
2.261	402.33499	Mycocerosic acid(C28)	C28H56O2K	[M+K]+
2.27	957.65693	PG(C46)	C52H103O10PK	[M+K]+
2.284	913.6306	PG(C44)	C50H99O10PNa	[M+Na]+
2.285	949.61955			
2.301	370.30862			
2.304	873.63493	PG(C40)	C46H91O10PK	[M+K]+
2.306	390.27711	MG(C19)	C22H48NO4	[M+NH4]+
2.319	1843.24116	Ac2PIM3(68:2)	C95H177NO30P	[M+NH4]+
2.323	829.60997	PG(C38)	C44H87O10PNa	[M+Na]+
2.323	458.36033	Mycolipanolic acid(C28)	C28H60NO3	[M+NH4]+
2.331	1669.13342	Ac2PIM2(67:1)	C88H167NO25P	[M+NH4]+
2.345	785.58464	PG(35:1)	C41H79O10PNa	[M+Na]+

150

2.363	741.55871	PG(32:2)	C38H71O10PNa	[M+Na]+
2.366	746.51466	PE(36:1)	C41H81NO8P	[M+H]+
2.381	702.48911	PE(33:2)	C38H73NO8P	[M+H]+
2.386	695.51234	PE(C31)	C36H76N2O8P	[M+NH4]+
2.4	653.50743	DG(C38)	C41H81O5	[M+H]+
2.421	656.45178	DG(C37)	C40H82NO5	[M+NH4]+
2.426	609.48134	DG(35:1)	C38H73O5	[M+H]+
2.433	614.43689	Lyso-PI(18:2)	C27H53NO12P	[M+NH4]+
2.449	563.43359	DG(C30)	C33H64O5Na	[M+Na]+
2.454	570.41044	DG(31:1)	C34H68NO5	[M+NH4]+
2.469	521.42896	Lyso-PG(C17)	C23H47O9PNa	[M+Na]+
2.5	433.37676	Mycocerosic acid(C27)	C27H54O2Na	[M+Na]+
2.608	902.53069	PI 18:0/18:1		
2.623	337.33473	MG(15:1)	C18H34O4Na	[M+Na]+
2.802	365.36589	MG(17:1)	C20H38O4Na	[M+Na]+
3.08	493.55877	MG(C26)	C29H58O4Na	[M+Na]+
3.162	563.42187	DG(C30)	C33H64O5Na	[M+Na]+
3.199	530.4008	Lyso-PG(C18)	C24H53NO9P	[M+NH4]+
3.273	674.53518			
3.403	576.51163			
3.72	521.58985	Hydroxyphthioceranic acid(C31)	C31H62O3K	[M+K]+
3.749	2091.42534	Ac2PIM4(74:1)	C107H201NO35P	[M+NH4]+
3.766	781.56169			
3.787	2047.39974	Ac2PIM4(71:2)	C104H193NO35P	[M+NH4]+
3.825	2003.37257	Ac2PIM4(68:3)	C101H185NO35P	[M+NH4]+
3.869	1959.34684	Ac2PIM4(65:4)	C98H177NO35P	[M+NH4]+
3.924	1915.31972	Ac2PIM3(73:1)	C100H189NO30P	[M+NH4]+
4.039	702.56801	PE(33:2)	C38H73NO8P	[M+H]+
4.135	731.54669	MPM(C32)	C38H77O9PNa	[M+Na]+
4.139	662.44645	PE(30:1)	C35H69NO8P	[M+H]+
4.142	720.49994	PE(C34)	C39H79NO8P	[M+H]+
4.268	519.50131	Mycocerosic acid(C32)	C32H64O2K	[M+K]+
4.273	537.51217	Phthioceranic acid(C36)	C36H73O2	[M+H]+
4.28	852.57348	PI(34:2)	C43H83NO13P	[M+NH4]+
4.292	757.56228	PG(33:1)	C39H75O10PNa	[M+Na]+
4.299	592.54329			
4.304	559.49351	Phthioceranic acid(C36)	C36H72O2Na	[M+Na]+
4.331	384.33951			
4.364	757.21418	Lyso-PIM1(C16)	C31H59O17PNa	[M+Na]+
4.375	627.57932	DG(35:0)		
4.41	704.58283	PE(33:1)	C38H75NO8P	[M+H]+

151

4.425	783.57766	PG(35:2)	C41H77O10PNa	[M+Na]+
4.507	805.5594	PG(38:1)	C44H86O10P	[M+H]+
4.598	722.61649	DG(42:2)	C45H88NO5	[M+NH4]+
4.642	549.62149	DG(C29)	C32H62O5Na	[M+Na]+
4.65	368.34442			
4.732	382.32367			
4.76	380.30827			
4.854	750.54574	PG(33:2)	C39H77NO10P	[M+NH4]+
4.899	793.59737	PG(C37)	C43H86O10P	[M+H]+
4.963	743.57793	DG(43:1)	C46H88O5Na	[M+Na]+
5.007	733.56248	PE(34:2)	C39H78N2O8P	[M+NH4]+
5.025	717.53288	PG(C30)	C36H71O10PNa	[M+Na]+
5.061	730.59866	PE(35:2)	C40H77NO8P	[M+H]+
5.079	769.59502	PG(34:2)	C40H75O10PNa	[M+Na]+
5.107	759.57817	PG(C33)	C39H77O10PNa	[M+Na]+
5.123	767.54848			
5.124	1329.98632	Ac1PIM1(57:4)	C72H130O19P	[M+H]+
5.167	834.23252			
5.172	831.23314			
5.197	809.59202	TG(47:3)	C50H90O6Na	[M+Na]+
5.244	1307.94142	Ac1PIM1(55:1)	C70H132O19P	[M+H]+
5.314	743.54901	PG(32:1)	C38H73O10PNa	[M+Na]+
5.349	1268.93158	Ac1PIM1(51:1)	C66H127NO19P	[M+NH4]+
5.354	682.62156	DG(39:1)	C42H84NO5	[M+NH4]+
5.372	1263.9149	Ac1PIM1(52:2)	C67H124O19P	[M+H]+
5.397	785.59386	PG(35:1)	C41H79O10PNa	[M+Na]+
5.437	708.63766	DG(41:2)	C44H86NO5	[M+NH4]+
5.467	1223.91931	Ac1PIM1(49:1)	C64H120O19P	[M+H]+
5.568	732.61296	PE(35:1)	C40H79NO8P	[M+H]+
5.64	678.42353	PE(31)	C36H73NO8P	[M+H]+
5.678	811.60875	PG(37:2)	C43H81O10PNa	[M+Na]+
5.786	719.58297	PE(33:2)	C38H76N2O8P	[M+NH4]+
5.909	745.59854	TG(C42)	C45H86O6Na	[M+Na]+
6.295	761.59385	PE(36:2)	C41H82N2O8P	[M+NH4]+
6.318	758.62978	PE(37:2)	C42H81NO8P	[M+H]+
6.422	787.60897	TG(44:1)	C47H88O6K	[M+K]+
6.575	733.56327	PE(34:2)	C39H78N2O8P	[M+NH4]+
6.702	810.65883	PG(C37)	C43H89NO10P	[M+NH4]+
7.395	747.61368	PE(35:2)	C40H80N2O8P	[M+NH4]+
7.524	646.45057			
8.024	786.66123	PE(C36)	C41H82NO8PK	[M+K]+

8.11	812.67645	PE(C39)	C44H88NO8PNa	[M+Na]+
8.507	621.6055	Phthioceranic acid(C42)	C42H85O2	[M+H]+
8.581	647.62075	Hydroxyphthioceranic acid(C40)	C40H80O3K	[M+K]+
9.667	814.69133	PI(C31)	C40H81NO13P	[M+NH4]+
9.928	621.58211	DG(36:2)	C39H73O5	[M+H]+
11.106	1252.8548	Ac1PIM1(50:2)	C65H123NO19P	[M+NH4]+
11.108	592.5431			
11.109	1414.90748	Ac1PIM2(50:2)	C71H133NO24P	[M+NH4]+
11.109	2895.76306	TDM(C188)	C188H365O17	[M+H]+
11.26	759.85554			
11.524	840.61858			
12.953	794.63994	PG(36:1)	C42H85NO10P	[M+NH4]+
13.449	846.67146	TG(50:3)	C53H100NO6	[M+NH4]+
13.562	770.64013	PE(C36)	C41H82NO8PNa	[M+Na]+
13.776	796.65597	PG(C36)	C42H87NO10P	[M+NH4]+
13.9	872.68786			
14.01	822.67136	PG(38:1)	C44H89NO10P	[M+NH4]+
14.138	898.70801	PI(C37)	C46H93NO13P	[M+NH4]+
14.288	896.74442	PI(37:1)	C46H91NO13P	[M+NH4]+
14.303	924.72366			
14.307	848.68699	TG(50:2)	C53H102NO6	[M+NH4]+
14.431	852.7195	PG(C40)	C46H95NO10P	[M+NH4]+
14.553	1405.00308	Ac1PIM2(C49)	C70H135NO24P	[M+NH4]+
14.56	576.51205			
14.561	1448.96882	PG(34:2)		
14.562	594.5225			
14.679	862.68511	TG(51:2)	C54H104NO6	[M+NH4]+
14.682	900.71816			
14.794	848.68707	TG(50:2)	C53H102NO6	[M+NH4]+
14.842	793.71586	TG(C47)	C50H97O6	[M+H]+
14.847	798.67161	PE(C38)	C43H86NO8PNa	[M+Na]+
14.884	950.73621	TG(C57)	C60H120NO6	[M+NH4]+
14.9	874.70307	TG(52:3)	C55H104NO6	[M+NH4]+
15.019	824.68722	PG(C38)	C44H91NO10P	[M+NH4]+
15.024	819.73098	TG(49:1)	C52H99O6	[M+H]+
15.109	900.7189			
15.22	850.70285	TG(50:1)	C53H104NO6	[M+NH4]+
15.228	926.73488			
15.23	845.74701	TG(51:2)	C54H101O6	[M+H]+
15.235	921.77897	TG(55:3)	C58H106O6Na	[M+Na]+
15.298	864.70048	PG(41:1)	C47H95NO10P	[M+NH4]+

15.388	871.76298	TG(C51)	C54H104O6Na	[M+Na]+
15.396	876.7188	TG(52:2)	C55H106NO6	[M+NH4]+
15.512	897.77764	TG(53:1)	C56H106O6Na	[M+Na]+
15.533	902.73433	TG(54:3)	C57H108NO6	[M+NH4]+
15.667	926.73726			
15.756	952.75244			
15.814	928.74971	TG(56:3)		
15.96	876.71774	TG(52:2)	C55H106NO6	[M+NH4]+
16.032	826.70297	PE(C40)	C45H90NO8PNa	[M+Na]+
16.037	902.7343	TG(54:3)	C57H108NO6	[M+NH4]+
16.041	821.74731	TG(C49)	C52H101O6	[M+H]+
16.123	786.63211	PE(C36)	C41H82NO8PK	[M+K]+
16.155	954.76641			
16.159	923.79396	TG(55:2)	C58H108O6Na	[M+Na]+
16.161	928.74986			
16.192	852.71894	TG(55:2)	C58H108O6Na	[M+Na]+
16.201	847.763	TG(51:1)	C54H103O6	[M+H]+
16.324	873.77917	TG(53:2)	C56H105O6	[M+H]+
16.325	894.70833	PG(C43)	C49H101NO10P	[M+NH4]+
16.325	878.735	TG(52:1)	C55H108NO6	[M+NH4]+
16.434	899.7951	TG(C53)	C56H108O6Na	[M+Na]+
16.452	904.75063	TG(54:2)	C57H110NO6	[M+NH4]+
16.467	920.72436	TG(55:1)	C58H114NO6	[M+NH4]+
16.752	930.76491	TG(56:3)	C59H112NO6	[M+NH4]+
16.981	956.7811			
17.058	904.74899	TG(54:2)	C57H110NO6	[M+NH4]+
17.08	828.71813	TG(48)		
17.131	930.76487	TG(56:3)	C59H112NO6	[M+NH4]+
17.142	854.73436	PI(34:1)	C43H85NO13P	[M+NH4]+
17.153	849.77846	TG(C51)	C54H105O6	[M+H]+
17.24	858.76803			
17.244	880.75049	TG(C52)	C55H110NO6	[M+NH4]+
17.336	901.81051	TG(55:2)	C58H109O6	[M+H]+
17.355	906.76623	TG(54:1)	C57H112NO6	[M+NH4]+
17.565	932.78102			
17.584	838.73988	TG(C49)	C52H104NO6	[M+NH4]+
17.639	864.7568	TG(51:1)	C54H106NO6	[M+NH4]+
17.857	956.78453			
17.998	840.79061			
18.12	856.75042	PI(C34)	C43H87NO13P	[M+NH4]+
18.175	882.76579	PI(36:1)	C45H89NO13P	[M+NH4]+

18.182	877.81015	TG(C53)	C56H109O6	[M+H]+
18.252	903.82612	TG(55:1)	C58H111O6	[M+H]+
18.259	908.78175	TG(C54)	C57H114NO6	[M+NH4]+
18.376	929.84095	TG(57:2)	C60H113O6	[M+H]+
18.384	934.79709	TG(56:1)	C59H116NO6	[M+NH4]+
18.411	814.74003	PI(C31)	C40H81NO13P	[M+NH4]+
18.439	818.77326	TG(48:3)	C51H96NO6	[M+NH4]+
18.444	840.75523	PI(33:1)	C42H83NO13P	[M+NH4]+
18.537	866.77076	TG(C51)	C54H108NO6	[M+NH4]+
18.579	960.8116	TG(58:2)	C61H118NO6	[M+NH4]+
18.618	892.7912	TG(53:1)	C56H110NO6	[M+NH4]+
18.85	806.80813	TG(47:2)	C50H96NO6	[M+NH4]+
18.872	854.80486			
19.093	884.78197	PI(C36)	C45H91NO13P	[M+NH4]+
19.133	910.79729			
19.138	905.84124	TG(C55)	C58H113O6	[M+H]+
19.208	931.85697	TG(57:1)	C60H115O6	[M+H]+
19.211	936.81299	TG(C56)	C59H118NO6	[M+NH4]+
19.318	957.8727	TG(59:2)	C62H117O6	[M+H]+
19.326	962.82909	TG(58:1)	C61H120NO6	[M+NH4]+
19.387	842.7711	PI(C33)	C42H85NO13P	[M+NH4]+
19.406	868.78684	PI(35:1)	C44H87NO13P	[M+NH4]+
19.448	988.84389	TG(60:2)	C63H122NO6	[M+NH4]+
19.463	894.80356	TG(C53)	C56H112NO6	[M+NH4]+
19.869	874.87046	TG(52:3)	C55H104NO6	[M+NH4]+
20.025	938.8288			
20.029	933.873	TG(C57)	C60H117O6	[M+H]+
20.07	959.88897	TG(59:1)	C62H119O6	[M+H]+
20.074	964.8446	TG(C58)	C61H122NO6	[M+NH4]+
20.162	990.85992	TG(60:1)	C63H124NO6	[M+NH4]+
20.29	896.81773	PI(37:1)	C46H91NO13P	[M+NH4]+
20.852	966.86073			
20.893	992.87574	TG(C60)	C63H126NO6	[M+NH4]+
21.114	924.84943			
21.616	960.98098	TG(58:2)	C61H118NO6	[M+NH4]+
21.619	994.89206			
22.044	874.70335			
22.047	890.67725			
22.065	950.73568			
22.108	840.66182			
22.109	819.73152			

22.109	824.68722			
22.174	916.69308			
22.182	900.71847			
22.233	866.67779			
22.241	845.74766			
22.244	850.70333			
22.262	942.70906			
22.274	926.73491			
22.282	921.77767			
22.302	902.68702			
22.313	989.01223	TG(60:2)	C63H122NO6	[M+NH4]+
22.319	864.70088			
22.345	871.76215			
22.352	892.69276			
22.354	876.71914			
22.425	897.77748			
22.439	918.70847			
22.44	902.73462			
22.44	924.77774			
22.509	926.73765			
22.538	952.75195			
22.542	942.71348			
22.643	800.68714			
22.652	876.71837			
22.678	842.67763			
22.682	826.70357			
22.688	821.74764			
22.724	786.633			
22.734	944.72529			
22.741	928.75016			
22.758	868.69315			
22.764	852.71945			
22.765	923.79292			
22.771	847.76312			
22.795	954.76671			
22.833	918.70952			
22.835	894.70941			
22.836	878.7355			
22.836	873.77913			
22.841	897.77864			
22.842	902.73477			

22.895	900.79791			
22.905	905.75445			
22.913	921.72825			
23.006	866.73396			
23.064	892.74972			
23.067	946.73981			
23.073	930.76517			
23.139	972.7558			
23.151	956.781			
23.186	828.71777			
23.213	870.70853			
23.217	854.73448			
23.227	849.77897			
23.266	896.72444			
23.268	880.7509			
23.269	875.79494			
23.314	901.81059			
23.324	906.76646			
23.325	922.74039			
23.33	888.75591			
23.394	812.73373			
23.396	927.82504			
23.429	932.78084			
23.429	838.73944			
23.431	948.75622			
23.459	864.75654			
23.471	894.76564			
23.506	920.78076			
23.541	890.77379			
23.548	804.78751			
23.549	958.7967			
23.589	818.80761			
23.683	898.73986			
23.686	882.76596			
23.688	856.74746			
23.692	877.81024			
23.723	903.82633			
23.724	908.78186			
23.724	924.75622			
23.774	929.84166			
23.785	950.77124			

23.787	934.79693			
23.811	814.74076			
23.821	818.77226			
23.827	840.75512			
23.86	896.7817			
23.866	960.81258			
23.872	866.77111			
23.897	922.7961			
23.897	892.79085			
23.971	806.80856			
23.976	854.80524			
24.054	419.96343			
24.112	926.772			
24.113	1991.63957			
24.114	910.79767			
24.117	905.84193			
24.137	884.77843			
24.147	952.78764			
24.148	936.81333			
24.149	931.85713			
24.187	957.87307			
24.194	962.8286			
24.197	978.80243			
24.249	988.84313			
24.259	842.77054			
24.261	868.78651			
24.283	894.8032			
24.332	950.82787			
24.376	1014.85933	PIM1 19:0/16:0	C50H95O18P1	[M+H]+
24.525	954.80342			
24.526	938.82865			
24.528	912.8113			
24.529	933.87314			
24.544	964.84468			
24.545	959.8883			
24.546	980.81845			
24.566	2019.67123	TG 2C18:1/1C26	C65H122O6	[2M+Na]+
24.58	990.85935			
24.67	896.81821			
24.671	870.80145			
24.684	922.83345			

24.7	2033.6843			
24.797	921.00291			
24.911	982.83543			
24.913	959.85938			
24.921	966.85968			
24.928	954.92075			
24.934	1008.85166			
24.961	1018.8903			
24.999	2042.74505			
25.002	2047.70389	PAT(C128)	C128H240NO16	[M+NH4]+
25.073	924.84927			
25.085	898.83304			
25.138	2061.71666			
25.268	982.96236			
25.301	994.89097			
25.311	1020.90649			
25.42	2070.77648			
25.42	2075.73543	PAT(C130)[1]	C130H244NO16	[M+NH4]+
25.503	2089.74832	PAT(C131)	C131H246NO16	[M+NH4]+
25.606	1137.06058			
25.825	2098.80642	PAT(C130)	C130H242O17Na	[M+Na]+
25.827	2103.76612	PAT(C132)	C132H248NO16	[M+NH4]+
25.87	2117.78024	PAT(C133)	C133H250NO16	[M+NH4]+
26.206	2131.79499	PAT(C134)	C134H252NO16	[M+NH4]+
26.497	1459.42074	GMM(Alpha-MA(monoenoic or monocyclopropanoic)(C88)	C94H188NO8	[M+NH4]+
26.667	2019.67047			
26.926	1487.45158	GMM(Alpha-MA(monoenoic or monocyclopropanoic)(C90)	C96H192NO8	[M+NH4]+
27.003	1431.39183	GMM(Alpha-MA(monoenoic or monocyclopropanoic)(C86)	C92H184NO8	[M+NH4]+
27.037	2061.71499			
27.073	1345.31914	GMM(Alpha-MA)(C80)	C86H170NO8	[M+NH4]+
27.356	1359.33392	GMM(Alpha-MA)(C81)	C87H172NO8	[M+NH4]+
27.374	1403.39275	GMM(Alpha-MA(monoenoic or monocyclopropanoic)(C84)	C90H180NO8	[M+NH4]+
27.423	1459.4225	GMM(Alpha-MA(monoenoic or monocyclopropanoic)(C88)	C94H188NO8	[M+NH4]+
27.425	1400.37991	GMM(Alpha-MA(monoenoic or monocyclopropanoic)(C85)	C91H179O8	[M+H]+

159

27.438	1397.39832	DIMB(C93)	C93H186NO5	[M+NH4]+
27.512	1373.35112	GMM(Alpha-MA)(C82)	C88H174NO8	[M+NH4]+
27.53	1368.39012	DIMA(C92)	C92H183O5	[M+H]+
27.638	1387.36604	GMM(Alpha-MA)(C83)	C89H176NO8	[M+NH4]+
27.672	1359.33484	GMM(Alpha-MA)(C81)	C87H172NO8	[M+NH4]+
27.704	1432.42219	DIMA(C95)	C95H188O5Na	[M+Na]+
27.765	1333.31881	GMM(Alpha-MA(monoenoic or monocyclopropanoic)(C79)	C85H170NO8	[M+NH4]+
27.784	1459.42385	GMM(Alpha-MA(monoenoic or monocyclopropanoic)(C88)	C94H188NO8	[M+NH4]+
27.826	1433.41275	Lyso-PIM5(C18)	C57H103O37PNa	[M+Na]+
27.859	1427.40594	DIMA(C95)	C95H192NO5	[M+NH4]+
27.938	1401.38309	GMM(Alpha-MA)(C84)	C90H178NO8	[M+NH4]+
27.945	1396.42606	DIMA(C94)	C94H187O5	[M+H]+
27.949	1437.45287	TMM(Alpha-MA)(C75)	C87H170NO13	[M+NH4]+
28.049	1415.39785	GMM(Alpha-MA)(C85)	C91H180NO8	[M+NH4]+
28.096	1387.36686	GMM(Alpha-MA)(C83)	C89H176NO8	[M+NH4]+
28.11	1410.44075	DIMA(C95)	C95H189O5	[M+H]+
28.114	1382.41097	DIMA(C93)	C93H185O5	[M+H]+
28.186	1397.4245	DIMB(C93)	C93H186NO5	[M+NH4]+
28.198	1361.35149	GMM(keto-MA)(C80)	C86H170NO9	[M+NH4]+
28.203	886.90888			
28.205	1356.3948	GMM(Alpha-MA)(C82)	C88H171O8	[M+H]+
28.346	1424.45796	DIMA(C96)	C96H191O5	[M+H]+
28.347	1429.41431	GMM(Alpha-MA)(C86)	C92H182NO8	[M+NH4]+
28.36	1465.48473	TMM(Alpha-MA)(C77)	C89H174NO13	[M+NH4]+
28.422	1443.42978	GMM(Alpha-MA)(C87)	C93H184NO8	[M+NH4]+
28.429	1438.47234	DIMA(C97)	C97H193O5	[M+H]+
28.434	1375.36618	GMM(Alpha-MA(monoenoic or monocyclopropanoic)(C82)	C88H176NO8	[M+NH4]+
28.509	1415.39905	GMM(Alpha-MA)(C85)	C91H180NO8	[M+NH4]+
28.527	1410.44154	DIMA(C95)	C95H189O5	[M+H]+
28.593	1425.45598	DIMB(C95)	C95H190NO5	[M+NH4]+
28.613	1389.38368	GMM(keto-MA)(C82)	C88H174NO9	[M+NH4]+
28.617	914.94053			
28.619	1384.42754	Alpha-MA(C)	C94H184O3Na	[M+Na]+
28.724	1398.44245	GMM(Alpha-MA)(C85)	C91H177O8	[M+H]+
28.732	1403.39859	GMM(Alpha-MA(monoenoic or monocyclopropanoic)(C84)	C90H180NO8	[M+NH4]+
28.749	1457.44685	GMM(Alpha-MA)(C88)	C94H186NO8	[M+NH4]+

28.75	1493.5156	TMM(Alpha-MA)(C79)	C91H178NO13	[M+NH4]+
28.752	1452.48949	DIMA(C98)	C98H195O5	[M+H]+
28.81	1471.46147	GMM(Alpha-MA)(C89)	C95H188NO8	[M+NH4]+
28.814	1466.50395	DIMA(C99)	C99H197O5	[M+H]+
28.876	1485.47607	GMM(Alpha-MA)(C90)	C96H190NO8	[M+NH4]+
28.901	1443.43034	GMM(Alpha-MA)(C87)	C93H184NO8	[M+NH4]+
28.917	1438.47278	DIMA(C97)	C97H193O5	[M+H]+
28.997	1453.48693	DIMB(C97)	C97H194NO5	[M+NH4]+
29.013	914.94039			
29.019	1417.41514	GMM(Alpha-MA(monoenoic or monocyclopropanoic)(C85)	C91H182NO8	[M+NH4]+
29.019	942.97139			
29.023	1412.45927	GMM(Alpha-MA)(C86)	C92H179O8	[M+H]+
29.03	886.90827			
29.125	1426.47393	GMM(Alpha-MA)(C87)	C93H181O8	[M+H]+
29.128	1480.51933	DIMA(C100)	C100H199O5	[M+H]+
29.131	1485.47771	GMM(Alpha-MA)(C90)	C96H190NO8	[M+NH4]+
29.159	1431.4299	GMM(Alpha-MA(monoenoic or monocyclopropanoic)(C86)	C92H184NO8	[M+NH4]+
29.192	1499.49218	GMM(Alpha-MA)(C91)	C97H192NO8	[M+NH4]+
29.195	1494.53418	DIMA(C101)	C101H201O5	[M+H]+
29.283	1471.46202	GMM(Alpha-MA)(C89)	C95H188NO8	[M+NH4]+
29.29	1466.50307	DIMA(C99)	C99H197O5	[M+H]+
29.391	1481.51773	DIMB(C99)	C99H198NO5	[M+NH4]+
29.403	1445.44649	GMM(Alpha-MA(monoenoic or monocyclopropanoic)(C87)	C93H186NO8	[M+NH4]+
29.407	1440.49072	GMM(Alpha-MA)(C88)	C94H183O8	[M+H]+
29.412	914.94024			
29.419	942.97126			
29.487	1454.50506	GMM(Alpha-MA)(C89)	C95H185O8	[M+H]+
29.52	1459.46126	GMM(Alpha-MA(monoenoic or monocyclopropanoic)(C88)	C94H188NO8	[M+NH4]+
29.562	1527.52106	GMM(Alpha-MA)(C93)	C99H196NO8	[M+NH4]+
29.778	1473.47747	GMM(Alpha-MA(monoenoic or monocyclopropanoic)(C89)	C95H190NO8	[M+NH4]+
29.778	1509.54779	DIMB(C101)	C101H202NO5	[M+NH4]+
29.78	1468.52114	GMM(Alpha-MA)(C90)	C96H187O8	[M+H]+
29.785	942.97122			
29.844	1482.53662	GMM(Alpha-MA)(C91)	C97H189O8	[M+H]+
29.887	1487.49273	GMM(Alpha-MA(monoenoic or	C96H192NO8	[M+NH4]+

161

		monocyclopropanoic)(C90)		
30.127	1501.50813	GMM(Alpha-MA(monoenoic or monocyclopropanoic)(C91)	C97H194NO8	[M+NH4]+
30.131	1496.5524	GMM(Alpha-MA)(C92)	C98H191O8	[M+H]+
30.132	1537.57768	DIMB(C103)	C103H206NO5	[M+NH4]+
30.138	971.00209			
30.179	1510.56698	GMM(Alpha-MA)(C93)	C99H193O8	[M+H]+
30.215	1515.52378	GMM(Alpha-MA(monoenoic or monocyclopropanoic)(C92)	C98H196NO8	[M+NH4]+
30.407	1529.53832	GMM(Alpha-MA(monoenoic or monocyclopropanoic)(C93)	C99H198NO8	[M+NH4]+
30.526	1543.55379	GMM(Alpha-MA(monoenoic or monocyclopropanoic)(C94)	C100H200NO8	[M+NH4]+
30.578	1557.56824	GMM(keto-MA)(C94)	C100H198NO9	[M+NH4]+
30.889	1468.52095			
30.891	1473.47679			
30.892	942.97099			
30.901	1509.54642			
30.94	1482.53546			
30.971	1487.49156			
31.169	971.00168			
31.169	1496.55093			
31.174	1501.50725			
31.175	1537.57678			
31.203	1510.56562			
31.241	1515.5217			
31.4	1529.5319			
31.488	1543.55044			
31.527	1557.56635			

The genes for PAT synthesis as described for *M. tuberculosis* appear to be present in *M. leprae* except that *pks3* and *pks4* are combined in one gene (*pks4*)

Table S3.2- *M. leprae* ions detected in negative mode and tentative compound identification based on querying the *Mtb* Lipid database [9].

RT	Mass	Compound	Formula	Ion
12.616	1414.90696	AcPIM2 16:0/16:0/19:0		
25.573	1209.23188	Keto mycolic acid 82		
25.907	1251.27736	Keto mycolic acid 85		
25.99	2029.67811	Ac1PIM6(49:2)	C94H166O44P	[M-H]-
26.228	2057.70858	Ac1PIM6(51:2)	C96H170O44P	[M-H]-
26.468	2085.74086	Ac1PIM6(53:2)	C98H174O44P	[M-H]-
26.699	2113.77117	Ac1PIM6(55:2)	C100H178O44P	[M-H]-
26.932	2141.80296	Ac1PIM6(57:2)	C102H182O44P	[M-H]-
22.497	622.0093	DG(36:1)	C39H73O5	[M-H]-
22.849	622.0087	DG(36:1)	C39H73O5	[M-H]-
26.475	622.00896	DG(36:1)	C39H73O5	[M-H]-
26.718	622.00954	DG(36:1)	C39H73O5	[M-H]-
29.525	622.00871	DG(36:1)	C39H73O5	[M-H]-
29.801	622.00938	DG(36:1)	C39H73O5	[M-H]-
6.959	705.62627	DG(42:1)	C45H85O5	[M-H]-
6.697	679.61064	DG(C40)	C43H83O5	[M-H]-
10.35	693.66234	DG(C41)	C44H85O5	[M-H]-
8.481	707.6423	DG(C42)	C45H87O5	[M-H]-
26.042	1081.11154	Dicyclopropanoyl-a-mycolic acid 74		
26.133	1095.12614	Dicyclopropanoyl-a-mycolic acid 75		
26.378	1109.14238	Dicyclopropanoyl-a-mycolic acid 76		
26.7	1137.17456	Dicyclopropanoyl-a-mycolic acid 78		
27.02	1165.20541	Dicyclopropanoyl-a-mycolic acid 80		
27.275	1193.23635	Dicyclopropanoyl-a-mycolic acid 82		
22.521	697.99604	DP(C)	C50H81O	[M-H]-
22.795	697.99612	DP(C)	C50H81O	[M-H]-
23.113	697.9958	DP(C)	C50H81O	[M-H]-
6.856	480.48963	fatty acid mycoceranic acid		
20.298	552.03989	Hydroxyphthioceranic acid(C36)	C36H71O3	[M-H]-
21.284	552.0404	Hydroxyphthioceranic acid(C36)	C36H71O3	[M-H]-
21.919	552.0398	Hydroxyphthioceranic acid(C36)	C36H71O3	[M-H]-
25.653	1223.24827	Keto mycolic acid 83		

25.831	1237.26022	Keto mycolic acid 84		
22.114	632.64771	Keto mycolic acid 86		
21.214	464.01993	Lyso-PE(17:1)	C22H43NO7P	[M-H]-
21.971	464.01984	Lyso-PE(17:1)	C22H43NO7P	[M-H]-
26.462	464.01996	Lyso-PE(17:1)	C22H43NO7P	[M-H]-
26.701	464.01981	Lyso-PE(17:1)	C22H43NO7P	[M-H]-
26.934	464.0198	Lyso-PE(17:1)	C22H43NO7P	[M-H]-
29.56	464.0198	Lyso-PE(17:1)	C22H43NO7P	[M-H]-
8.768	508.52138	Lyso-PE(C20)	C25H51NO7P	[M-H]-
22.506	371.01357	MG(C19)	C22H43O4	[M-H]-
8.385	735.59817	MPM(C34)	C40H80O9P	[M-H]-
9.21	686.6175	PE(32:2)	C37H69NO8P	[M-H]-
23.021	686.69476	PE(32:2)	C37H69NO8P	[M-H]-
23.254	700.71066	PE(33:2)	C38H71NO8P	[M-H]-
23.698	728.74234	PE(35:2)	C40H75NO8P	[M-H]-
22.522	742.66327	PE(36:2)	C41H77NO8P	[M-H]-
23.864	742.75854	PE(36:2)	C41H77NO8P	[M-H]-
24.024	742.75781	PE(36:2)	C41H77NO8P	[M-H]-
17.381	786.63158	PE(39:1)	C44H85NO8P	[M-H]-
9.82	802.62564	PE(C40)	C45H89NO8P	[M-H]-
6.956	759.59757	PG(35:2)	C41H76O10P	[M-H]-
7.168	819.63439	PG(C39)	C45H88O10P	[M-H]-
20.534	634.04305	Phthioceranic acid(C43)	C43H85O2	[M-H]-
21.931	634.0425	Phthioceranic acid(C43)	C43H85O2	[M-H]-
29.262	704.01265	Phthioceranic acid(C48)	C48H95O2	[M-H]-
29.548	704.01228	Phthioceranic acid(C48)	C48H95O2	[M-H]-
29.802	704.01244	Phthioceranic acid(C48)	C48H95O2	[M-H]-
23.461	834.76958	TG		
23.72	848.78557	TG		
23.835	862.80122	TG		
24.153	876.81536	TG		
24.247	890.83092	TG		
24.531	904.84687	TG		
24.702	918.86377	TG		
24.89	932.87919	TG		
25.056	946.89479	TG		
25.227	960.91047	TG		
8.487	761.61389	TG(45:1)	C48H89O6	[M-H]-
22.519	787.63872	TG(47:2)	C50H91O6	[M-H]-
7.181	843.67873	TG(51:2)	C54H99O6	[M-H]-
22.549	855.98577	TG(52:3)	C55H99O6	[M-H]-

27.019	1549.32998	TMM a dicyclopropanoic 81		
25.724	1607.37364	TMM ketomycolyl 84		
23.256	820.75308	Triacylglycerol 2C16/1C18		
6.62	707.56648			
6.625	653.59506			
6.626	629.55049			
6.681	655.57014			
6.899	638.59543			
6.958	681.58217			
6.958	684.58316			
6.962	708.60259			
7.22	655.61038			
7.248	869.69365			
7.447	643.56644			
7.451	667.61133			
7.504	693.62676			
7.576	683.59835			
7.582	707.64017			
7.776	655.58662			
7.777	628.5667			
7.78	652.6114			
7.792	706.58252			
7.888	846.68443			
8.388	657.58213			
8.388	681.62656			
8.472	683.60082			
8.491	710.61961			
8.762	590.52456			
9.102	871.70914			
9.157	737.6141			
9.166	659.59759			
9.178	683.64206			
9.255	709.65782			
9.466	671.59754			
9.467	695.64194			
9.478	698.61862			
10.038	818.61982			
10.25	643.60265			
10.27	667.64734			
10.328	697.65636			
10.687	709.65818			

10.688	685.61315			
10.689	688.61427			
10.694	763.62904			
10.703	712.63406			
10.775	818.62059			
11.464	306.03003			
11.491	388.03319			
12.061	688.67231			
13.544	214.06296			
13.571	818.62079			
13.751	702.6887			
14.333	870.6879			
15.255	816.64141			
15.466	716.70428			
15.99	588.58437			
17.41	730.72011			
17.576	816.64205			
18.316	602.60017			
20	470.03603			
20.068	306.03048			
20.08	224.02732			
20.183	388.03368			
20.216	470.03685			
20.229	634.04239			
20.315	616.61595			
20.506	306.03057			
20.519	470.03673			
20.59	552.03953			
20.59	388.03378			
20.877	546.02296			
20.885	784.61631			
20.889	716.04518			
20.89	322.00468			
20.991	224.02753			
20.995	552.04023			
21.014	388.03386			
21.024	792.03166			
21.147	634.04299			
21.147	470.03692			
21.176	736.65899			
21.199	716.0462			

21.2	628.02628			
21.203	710.02929			
21.205	322.00512			
21.231	546.02308			
21.234	404.00779			
21.261	382.01704			
21.284	224.02758			
21.295	486.01179			
21.296	792.03222			
21.314	388.03406			
21.359	306.03085			
21.533	1590.99075			
21.534	1508.98745			
21.536	1405.00479			
21.54	1426.98652			
21.574	863.69157			
21.588	284.03633			
21.611	1453.0017			
21.611	1432.02327			
21.625	630.63227			
21.626	712.63531			
21.71	714.63228			
21.722	738.673			
21.75	382.01677			
21.786	772.76771			
21.806	750.67415			
21.835	726.6411			
21.862	854.69596			
21.898	716.04433			
21.927	874.03391			
21.937	470.0366			
21.939	628.02606			
21.944	792.03189			
21.947	738.67228			
21.951	710.02908			
21.954	388.03369			
21.96	382.01657			
21.961	224.02738			
21.974	546.02282			
21.975	306.03054			
21.982	658.66297			

22.07	865.70552			
22.095	726.65316			
22.096	714.64936			
22.097	644.64784			
22.23	530.04528			
22.234	906.82461			
22.242	764.69062			
22.256	382.01697			
22.258	448.04261			
22.265	740.64734			
22.268	743.64779			
22.285	786.01392			
22.307	366.03959			
22.335	668.03605			
22.344	688.03395			
22.365	606.03159			
22.369	508.05134			
22.387	426.04789			
22.407	524.02912			
22.414	284.03654			
22.419	852.68013			
22.419	846.02371			
22.426	202.03329			
22.444	344.0453			
22.462	764.02157			
22.465	442.02595			
22.469	682.01838			
22.469	658.6637			
22.497	862.00135			
22.511	360.0227			
22.514	600.01463			
22.515	216.04936			
22.521	518.01088			
22.524	937.98794			
22.531	766.70576			
22.536	300.01401			
22.54	754.66306			
22.541	668.03597			
22.542	778.7065			
22.632	218.01083			
22.632	458.00356			

22.655	540.00673			
22.689	615.99312			
22.699	376.00036			
22.73	672.67933			
22.751	533.98984			
22.766	855.98603			
22.768	937.98815			
22.781	754.69569			
22.803	773.98229			
22.804	792.72162			
22.809	768.67745			
22.81	814.81351			
22.811	436.10914			
22.811	771.67908			
22.825	862.00161			
22.843	779.99844			
22.847	300.014			
22.894	682.01735			
22.902	660.67872			
22.93	204.03152			
22.961	458.0034			
22.972	218.05517			
23	219.01421			
23.012	782.69315			
23.017	284.03644			
23.029	648.67901			
23.034	948.87399			
23.043	806.73668			
23.044	828.8305			
23.078	533.98972			
23.081	376.00037			
23.091	346.04191			
23.092	442.02603			
23.12	224.02775			
23.149	779.99818			
23.186	794.73639			
23.191	770.69412			
23.215	360.0223			
23.257	962.88937			
23.262	796.70905			
23.267	842.84624			

23.433	952.8636			
23.435	976.90645			
23.438	688.7112			
23.446	810.72578			
23.461	856.86269			
23.465	615.99362			
23.54	714.72686			
23.551	202.03344			
23.553	300.01413			
23.585	284.03654			
23.615	990.92181			
23.651	870.87799			
23.689	822.76955			
23.72	825.74573			
23.731	540.00995			
23.777	980.89547			
23.785	1004.94026			
23.814	836.78548			
23.827	884.89431			
23.996	284.03656			
24	898.91151			
24.029	824.75962			
24.156	852.77167			
24.158	879.79814			
24.159	855.77311			
24.173	756.77342			
24.223	864.8151			
24.229	867.78937			
24.264	770.78875			
24.363	284.03647			
24.4	1012.95483			
24.401	1036.99618			
24.431	852.79196			
24.438	770.78942			
24.533	880.8031			
24.535	883.80358			
24.536	907.82803			
24.633	784.80562			
24.674	892.84585			
24.698	895.82203			
24.827	798.82017			

24.89	908.83353			
24.891	935.86019			
25.016	812.83548			
25.017	855.98772			
25.051	922.84937			
25.198	826.85051			
25.203	934.89437			
25.302	1181.19959			
25.372	840.86686			
25.393	1195.21613			
25.468	1579.34518			
25.848	1067.09608			
25.979	300.01378			
26.006	366.03974			
26.228	284.0359			
26.316	2071.72257			
26.386	1191.14423			
26.46	366.03922			
26.465	540.00621			
26.466	628.02594			
26.469	300.01368			
26.472	388.03377			
26.485	546.02288			
26.556	284.03613			
26.556	2099.75405			
26.7	1219.17709			
26.72	1519.29091			
26.72	300.01359			
26.729	388.0333			
26.736	1522.3042			
26.768	2127.7858			
26.801	382.01664			
26.934	284.03611			
26.939	546.02277			
26.94	202.03285			
26.946	306.03041			
26.959	195.99591			
27.009	1247.20786			
27.153	2169.83091			
27.221	1571.51035			
28.763	464.02026			

28.773	540.00637			
29.013	470.03686			
29.015	382.01662			
29.04	546.02305			
29.262	710.0287			
29.264	628.02659			
29.266	470.03696			
29.269	540.00646			
29.272	786.01576			
29.273	464.02016			
29.275	300.01381			
29.276	868.0184			
29.277	552.03996			
29.279	382.01702			
29.28	388.03398			
29.535	306.03057			
29.545	786.01494			
29.546	540.00583			
29.552	382.0166			
29.554	300.01353			
29.562	552.03925			
29.73	224.02739			
29.799	546.0229			
29.801	786.01522			
29.801	540.00586			
29.804	552.03985			
29.805	284.03605			
29.807	306.03056			
30.034	300.01372			
30.043	382.01682			
30.059	306.03073			

Comments on *M. leprae* lipid profile (Table S1, S2)

Mass spectrometry (m/z) comparison of *M. leprae* lipid extract to the published *M. tuberculosis* lipidome (*M.tb* database) resulted in tentative identification of 426 compounds out of 693 total positive ions and 77 compounds out of 391 negative ions.

In the positive and negative mode several ions matched with common lipid such as phospholipids with predominant PG (46 in positive and 2 in negative mode), PE (33 in positive and 9 in negative mode), PI (24 in positive mode) TG (70 in positive and 14 in negative mode), DG (27 in positive and 10 in negative mode) and MG (19 in positive mode).

We also identified some mycobacterial specific lipids such as; PIMs (16 in positive mode), Ac1PIMs (25 in positive and 5 in negative mode) and Ac2PIMs (27 in positive mode). Other *M. tuberculosis* lipids identified in *M. leprae* and have been confirmed to be present in *M. leprae*; TMM (3 in positive and 2 in negative mode) and TDM (7 in positive mode). DAT (3 were found in positive mode), which also has been shown in *M. leprae*. PAT (7 in positive mode), the genes for PAT synthesis (polyketide synthase gene ***pks3/4 and the acyltransferase papA3***) are available in *M. leprae*. GMM with Alpha and keto-MA (52 in positive mode) was also identified. Mycocerosic acid (14 in positive mode) was found with different chain length (24, 25, 26, 27, 28, 30 and 32) and Phthioceranic acid (4 in positive and 5 in negative); majority with C36, For the Hydroxyphthioceranic acid (3 in positive and negative mode). DIMA (15 in positive mode) majority (23%) have C95 and C99 (17%) **(Figure S1),** DIMB (7 were found in positive mode).

Table S3.3: Significant features selected from each LC-MS dataset by comparison of feature abundance in uninfected versus infected tissues using OPLS (≥0.8 cut off)

Tissue Pairs, Detection mode	Selected features	Mass	q- value (abundance)	Mean	Mean	Chemical identification [1,2,3]	Formula	Comment
	RT	Mass		U	I			
	13.04	390.279	0.034744	0.89845	5.501327	Fatty acid tetracosanoic acid [1]	C24H48O2	[M+Na]+
	6.57	522.356	0.018412	0.315295	1.09104	Lyso-PC (18:1/0:0)[2]	C26H52NO7P	[M+H]+
	12.79	610.189	0.033502	0.123293	0.445438	Lyso-PI (16:0)[1]	C25H49O12P1	[M+K]+
	13.77	645.551	0.0152	0.114925	1.2194	Ceramides (d18:0/22:0); N-docosanoyl-sphinganine [2]	C40H81NO3	[M+H]+
	13.01	585.528	0.030392	0.438156	2.712333	Diacylglycerol (16:0/16:0)[1]	C35H68O5	[M+NH4]+
	13.25	702.533	0.046898	29.44333	57.40863	Diacylglycerol [1]	C43H84O5	[M+Na]+
	12.41	712.529	0.001921	0.111919	0.676758	Diacylglycerol 1C19/1C22	C44H86O5	[M+NH4]+
	13.04	**718.566**	0.083608	5.538323	51.11997	Diacylglycerol [1]	C43H84O5	[M+K]+
	12.88	724.531	0.021297	0	8.97492	Diacylglycerol [1]	C43H84O5)	[M-H+2Na]+
	11.97	725.551	0.002871	17.3305	35.40627	Diacylglycerol [1]	C45H88O5	[M+NH4]+
	13.85	730.57	0.102921	10.56704	24.79333	Diacylglycerol [1]	C45H88O5	[M+Na]+
	13.45	746.578	0.033384	0.20654	12.29675	Diacylglycerol [1]	C45H88O5	[M+K]+
Nerves AU-1+AI-1, positive mode	13.93	787.66	0.056648	30.98883	59.83573	Diacylglycerol [2]	C49H96O5	[M+Na]+
	13.09	676.527	0.033176	0.694032	1.916353	PE [2] (with saturated FA; 14:0 or 16:0 or 18:0)	C37H74NO7P	[M+H]+
	11.91	722.563	0.007603	0.082124	0.526311	PE 1	C38H76N1O8P1	[M+NH4]+
	13.01	**726.54**	0.068877	7.427327	24.18847	PE 19 compounds (with saturated FA in 4 compounds, mono- or di-saturated FA in 5 comp) [2]	C39H78NO7P, C41H76NO7P	[M+H]+
	12.75	**731.592**	0.051063	11.42571	71.1118	PE (19:0/16:1) [1]	C40H78N1O8P1	[M+H]+
	12.81	**744.585**	0.023009	3.984467	41.0452	PE (22 compounds, 12 with mono-unsaturated FA), PC (4 compounds, all with 18:2 FA)[2]	C41H78NO8P	[M+H]+
	13.04	750.54	0.034247	0	18.80477	PE or PC (8 compounds with 18:1) [2]	C42H82NO8P or C41H78NO7P	[M+H]+
	12.72	753.584	0.002559	9.649477	23.0393	PE (18:1/16:1)[1]	C39H74N1O8P1	[M+K]+

174

	12.91	757.616	0.081671	2.400657	20.24849	PE (18:1/16:2)[1]	C39H72N1O8P1	[M-H+2Na]+
	13.69	**782.646**	0.091802	1.405853	19.67456	PC (51 compounds, all with di (18:2)-or poly-unsaturated FA (20:4)[2]	C44H80NO8P	[M+H]+
	12.6	**784.579**	0.050709	18.22827	37.0709	PC (30 compounds, 8 compounds with (18:1) and 7 with (18:2) FA)[2]	C44H82NO8P	[M+H]+
	13.14	**794.605**	0.046639	13.922	26.35233	PC (29 compounds, 18 with (18:1) FA and the rest 11 with polyunsaturated FA)[2]	C46H84NO7P	[M+H]+
	13.68	788.662	0.03075	0.17246	2.945083	PS, 9 compounds(mainly with 18:1 in 4 compounds or 18:2 in 5 compounds)[2]	C42H78NO10P	[M+H]+
	12.43	788.542	0.069128	2.121587	16.47482	PS (mainly with 18:1 or 18:2)[1]	C42H78NO10P	[M+H]+
	13.11	810.594	0.015517	0	16.91317	PI (16:0/16:0)[1]	C41H79O13P1	[M+H]+
	14.14	820.6577	0.00498	5.338347	11.70697			
	14.11	832.664	0.001171	0	3.47222	TAG[1]	C53H100O6	[M+H]+
	11.24	779.52	0.026231	0.02542	0.790124	TAG[1]	C49H95O6	[M+H]+
	17.21	938.799	0.008049	0.19656	0.889529	TAG[1]	C59H112O6	[M+Na]+
	13.81	848.655	0.006918	1.658957	0.193085			
	17.54	89.2304	0.00481	0.42902	3.787883			
	10.57	215.178	0.016045	0.093574	0.411369			
	13.51	392.294	0.026492	0.781117	4.282183			
	13.28	462.3	0.027878	0	2.327457			
	6.57	544.336	0.019213	0.687947	1.893243			
	17.92	577.523	0.11599	50.77907	22.6476			
	12.88	583.509	0.011208	0.19862	0.785352			
	13.04	609.529	0.004686	0.287987	1.480047			
	12.02	625.512	0.011283	0.087244	0.572102			
	13.9	630.615	0.020991	0.425641	1.358786			
	11.46	701.565	0.019932	0.122021	0.996733			
	13.04	720.579	0.047881	18.65297	55.53253			
	13.43	728.548	0.074856	26.9147	55.41103			
	13.08	745.607	0.053312	3.29308	70.17203			
	13.13	754.612	0.041045	0	18.17923			
Nerves AU-2+AI-2, positive mode	7.62	**726.545**	0.058871	31.3486	60.3517	PE 19 compounds (with saturated FA in 4 compounds, mono- or di-saturated FA in 5 compounds)[2]	C39H78NO7P, C41H76NO7P	[M+H]+

175

7.81	750.553	0.028146	19.18083	37.91043	PE (11 compounds, 7 compounds mainly with 18:1)[2]	C42H82NO8P or C41H78NO7P	[M+H]+
8.64	**794.725**	0.053319	13.6549	26.6049	PC (29 compounds, 18 with (18:1) FA and the other 11 with polyunsaturated FA)[2]	C46H84NO7P	[M+H]+
8.47	**818.729**	0.00014	13.028	51.5419	TAG(14:0/16:1/18:2)[3]	C51H92O6	[M+NH4]+
8.86	**822.758**	0.011881	45.62383	94.4225	TAG(14:0/16:0/18:1)[3]	C51H96O6	[M+NH4]+
8.76	834.761	6.10E-05	5.075867	23.13253	TAG [1]	C53H102O6	[M+NH4]+
8.47	**844.742**	0.000257	17.75163	79.16367	TAG(14:0/18:2/18:2)[3]	C53H94O6	[M+NH4]+
8.66	**846.755**	0.007596	93.59373	246.1773	TAG(14:0/18:1/18:2)[3]	C53H96O6	[M+NH4]+
8.88	848.769	0.031802	170.0857	317.4373	TAG[1]	C53H98O6	[M+H]+
8.77	860.775	0.016005	8.09209	35.1649	TAG[1]	C55H104O6	[M+NH4]+
9.03	862.79	0.018589	17.59097	44.08147	TAG (16:0/16:0/18:1)[1]	C52H98O6	[M-H+2Na]+
8.49	**870.758**	3.11E-05	20.2798	94.22427	TAG(16:1/18:2/18:2)[3]	C55H96O6	[M+NH4]+
8.68	**872.771**	0.005953	130.3475	356.826	TAG(16:1/18:1/18:2)[3]	C55H98O6	[M+NH4]+
8.9	874.782	0.02611	294.5963	572.684	TAG[1]	C55H100O6	[M+H]+
9.51	**878.821**	0.006517	77.9148	141.2987	TAG(16:0/18:0/18:1)[3]	C55H104O6	
9.04	888.809	0.021929	6.024033	34.3555	TAG[1]	C57H108O6	[M+H]+
9.35	890.827	0.016333	11.79788	28.2623	TAG[1]	C57H110O6	[M+H]+
8.5	896.775	0.036905	19.8138	77.4851	TAG[1]	C56H106O6	[M+Na]+
8.69	898.786	0.003642	106.7541	273.6047	TAG(18:1/18:2/18:2)[3]	C57H100O6	[M+NH4]+
8.94	**900.8**	0.035588	222.773	424.7397	TAG[1]	C58H108O6	[M+H]+
9.21	**902.818**	0.027508	223.492	431.7783	TAG[1]	C58H110O6	[M+H]+
9.95	906.861	0.000642	2.717668	19.52793	TAG (18:1/18:1/18:1)[1]	C57H104O6	[M+Na]+
9.21	928.836	0.017283	8.561677	21.26357	TAG[1]	C57H110O6	[M+K]+
9.55	930.857	0.033857	5.819067	24.88107	TAG[1]	C60H114O6	[M+H]+

176

	11.96	184.074	0.010725	0	2.74508			
	13.3	364.263	0.056551	4.632067	17.86157			
	11.47	723.536	0.016647	0.698253	2.32961			
	12.21	751.57	0.034082	0.342317	2.269977			
	13.42	759.612	0.022657	25.25257	111.9716			
	8.45	766.698	0.019137	1.696523	6.5834			
	13.71	773.646	0.036766	4.474177	40.0763			
	13.48	**785.639**	0.030077	24.45147	80.4728			
	13.05	786.584	0.023697	41.3235	84.02277			
	8.45	792.712	0.001482	8.45821	24.77223			
	13.74	799.661	0.044706	8.865883	36.46307			
	14.24	801.677	0.022523	4.221287	23.36797			
	13.59	811.661	0.025965	6.31217	22.52227			
	8.65	820.741	0.030293	51.05043	109.8788			
	8.46	**824.685**	7.05E-05	1.64099	6.505767			
	8.48	920.779	0.001015	0.526646	5.754607			
	8.63	922.796	0.001339	1.79086	17.57647			
Nerves AU-3+ AI-3, positive mode	6.99	385.35	0.00061	4.180286	20.10779	Vitamin D3, Cholestenone[2]	C27H44O	[M+H]+
	7.49	717.592	0.056357	55.054	79.24301	PE (18:1/16:0)[1]	C39H76N1O8P1	[M+H]+
	7.6	**731.604**	0.013716	88.13277	146.6541	PE (19:0/16:1)[1]	C40H78N1O8P1	[M+H]+
	7.68	745.614	9.65E-05	70.50234	130.8534	PE (18:0/18:1)[1]	C41H80N1O8P1	[M+H]+
	7.83	773.651	0.007706	121.6362	216.9201	PE (19:1/16:1)[1]	C40H76N1O8P1	[M-H+2Na]+
	8.55	780.713	0.000534	0.031074	6.821107	PC (63 compounds, 15 with unsaturated FA, and 7 PE compounds with 5 18:1)[2]	C42H80NO8P or C44H78NO8P	[M+H]+
	8.66	**794.726**	0.002611	0.355237	8.682869	PC (29 compounds, 18 with (18:1) FA and the rest 11 with polyunsaturated FA)[2]	C46H84NO7P	[M+H]+
	8.38	778.693	0.055121	33.43627	21.41061	Diacylglycerol (19:0/28:0)[1]	C50H98O5	[M+H]+
	7.86	795.649	0.004017	1.577394	6.939494	Diacylglycerol (19/28)[1]	C50H98O5	[M+NH4]+
	8.77	808.745	9.13E-05	0.213053	12.45367	Diacylglycerol (20:0/28:0)[1]	C51H100O5	[M+NH4]+
	9.04	836.776	0.064718	1.177744	7.045903	Diacylglycerol[1]	C51H100O5	[M-H+2Na]+
	8.55	**806.731**	0.000338	0.052696	8.702424	TAG (16:0/16:0/16:0)[1]	C51H98O6	[M+H]+
	8.49	**818.728**	9.75E-06	0.738544	14.94609	TAG(14:0/16:1/18:2)[3]	C51H92O6	[M+NH4]+

177

8.68	820.745	0.001654	2.653076	18.1128	TAG[1]	C51H94O6	[M+H]+
8.9	822.76	0.001674	2.963793	16.89739	TAG(16:0/14:0/18:1)[3]	C51H96O6	[M+NH4]+
8.58	832.744	1.14E-07	0.255237	14.37651	TAG[1]	C53H100O6	[M+H]+
8.79	834.76	1.08E-07	0.527124	23.62411	TAG [1]	C53H102O6	[M+H]+
8.37	842.727	0.00376	0.029058	7.391886	TAG[1]	C52H100O6	[M+Na]+
8.51	**844.742**	0.000218	0.956903	18.01319	TAG(14:0/18:2/18:2)[3]	C53H94O6	[M+NH4]+
8.7	**846.756**	0.007712	5.888688	26.60468	TAG(14:0/18:1/18:2)[3]	C53H96O6	[M+NH4]+
8.91	848.773	0.009758	4.681883	3.056316	TAG[1]	C53H98O6	[M+H]+
9.2	850.791	0.004118	5.186392	27.32547	TAG (C16:0/16:0/16:0) [1]	C51H98O6	[M-H+2Na]+
8.61	858.759	0.000109	0.089002	15.8411	TAG (C18:1/18:1/16:0)1	C55H102O6	[M+H]+
8.81	860.775	3.55E-05	0.487701	25.79742	TAG[1]	C55H104O6	[M+H]+
9.07	862.791	0.004165	0.960169	31.03903	TAG(C16:0/16:0/C18:1)[1]	C52H98O6	[M+H]+
9.37	864.809	0.007211	0.271362	24.78572	TAG(C16:0/16:0//18:0)1	C52H100O6	[M-H+2Na]+
8.83	886.793	0.004066	0.114533	19.62911	TAG (18:1/18:1/18:0)[1]	C57H106O6)	[M+H]+
8.52	870.76	6.87E-05	1.140052	24.42882	TAG(16:1/18:2/18:2)[3]	C55H96O6	[M+NH4]+
8.71	**872.774**	0.006555	8.654872	33.33799	TAG(16:1/18:1/18:2)[3]	C55H98O6	[M+NH4]+
8.93	**874.789**	0.024763	13.62311	40.45812	TAG[1]	C55H100O6	[M+H]+
9.22	876.806	0.013295	12.84172	48.62461	TAG[1]	C55H102O6	[M+H]+
9.57	878.821	0.00213	2.607335	29.37228	TAG(16:0/18:0/18:1)[3]	C55H104O6	
9.1	888.809	0.004379	0.4457	29.27861	TAG	C57H108O6	[M+H]+
9.4	890.822	0.009589	0.263724	34.35786	TAG[1]	C57H110O6	[M+H]+
8.63	896.776	0.002954	0	11.93639	TAG[1]	C56H106O6	[M+Na]+
8.53	896.779	0.028429	1.516109	24.50735	TAG[1]	C56H106O6	[M+Na]+
8.73	**898.791**	0.003906	6.815158	25.32937	TAG(18:2/18:2/18:2)[3]	C57H100O6	[M+NH4]+
8.95	**900.806**	0.012502	11.67834	39.22213	TAG[1]	C58H108O6	[M+H]+
9.26	**902.823**	0.010348	11.15124	44.87723	TAG[1]	C58H110O6	[M+H]+
9.61	**904.841**	0.005502	4.069172	31.62973	TAG[1]	C58H112O6	[M+H]+
10.03	906.857	3.06E-05	0.124996	12.36393	TAG(18:1/18:1/18:1)[1]	(C57H104O6)	[M+Na]+
9.14	914.823	4.18E-05	0.042756	16.89617	TAG[1]	C56H108O6	[M+K]+
8.48	920.778	0.003412	0.020853	10.1357	TAG[1]	C56H108O6	[M-H+2Na]+
9.3	928.841	3.22E-05	0.398395	18.55493	TAG[1]	C57H110O6	[M+K]+
8.54	754.692	0.000979	0.005626	2.31648			

	8.63	768.713	0.077522	5.795067	12.11567			
	9.54	852.8	0.001671	0.232078	6.969934			
Liver and spleen AU1 + AI-1, positive mode	12.54	603.536	9.68E-05	22.41065	40.60523	1-(14-methyl-pentadecanoyl)[2]	C39H70O4	[M+H]+
	9.39	385.346	0.03307	0.011936	6.451763	Vitamin D3, Cholestenone[2]	C27H44O	[M+H]+
	12.03	742.537	0.003259	29.07993	51.44833	PC (21 compounds mainly with saturated FA), PE (33 compounds, 5 with 18:1, 4 with 18:2 and the rest with saturated FA)[2]	C39H78NO8P, C41H76NO8P	[M+H]+
	12.54	**744.554**	0.004073	49.03525	121.3732	PE, PC (26 compounds, 12 compounds mainly with 18:1)[2]	C41H78NO8P	[M+H]+
	12.49	**770.604**	0.013408	8.619788	59.06096	PC (19 compounds, 8 with 18:1 and the rest with 18:0)[2]	C42H86NO7P, C44H84NO7P	[M+H]+
	11.88	**782.551**	0.000131	273.4368	200.6386	PC (51 compounds, all with di (18:2)-or poly-unsaturated FA (20:4)[2]	C44H80NO8P	[M+H]+
	11.81	716.524	0.000355	13.0077	26.33846	Diacylglycerol[1]	C44H86O5	[M+Na]+
	13.39	**806.65**	0.002553	1.604973	5.408773	TAG(C16:0/16:0/16:0)1	C51H98O6	[M+H]+
	12.98	**785.65**	0.00393	7.788051	20.70911			
	11.81	575.505	0.000145	8.999187	17.69625			
	12.03	601.52	0.013612	14.21396	23.50035			
	11.64	603.534	0.002295	12.78614	28.66438			
	12.99	605.551	0.001	7.231091	13.9125			
	12.71	746.593	0.00607	63.67597	207.0068			
	12.74	**796.62**	0.003393	1.804867	21.41726			
	17.8	**824.772**	0.00049	13.95003	7.639616			
Liver and spleen AU-1+AI-1, negative mode	8.91	339.326	0.000884	3.306268	8.719055	Oxo-heneicosanoic acid [2]	C21H40O3	[M-H]-
	13.84	646.612	0.005063	76.1426	111.9418	Ceramide [2]	C42H81NO3	[M-H]-
	13.39	842.672	0.001458	6.756669	17.74878	Sphingomyelin[2]	C49H100N2O6P	[M+H]+
	11.81	714.507	0.000147	1.966465	0.768293	PE (11 compounds, 6 with mainly mono- and 5 with di-saturatedFA) [2]	C39H74NO8P	[M-H]-
	12.1	775.55	0.000567	11.26934	21.4179	PG (18:0/18:1)[2]	C42H81O10P	[M-H]-
	11.61	861.548	0.005219	36.70501	105.437	PI (8 compounds, 5 with 18:1, and 2 with 18:2 FA)[2]	C45H83O13P	[M-H]-
	12.15	913.582	0.000655	12.44985	19.13585	PI (12 compounds, all with poly-unsaturated FA) [2]	C49H87O13P	[M-H]-

179

14.4	762.625	0.001693	10.7404	7.595149			
13.1	652.586	0.000948	3.605	0			
12.26	698.515	0.000209	5.820293	2.359072			
12.54	742.535	0.06075	10.71407	17.1516			
12.04	851.567	0.013828	0.059207	91.38065			
11.34	871.53	0.007624	10.16552	3.801933			
11.68	885.543	0.002308	368.4731	273.2143			
Liver and spleen AU-2+AI-2, positive mode	8.3566	732.555	0.001968	6.27235	51.75061	PC (16 compounds) or PE (6 compounds) (20 with mono-unsaturated FA)[2]	C40H80NO8P	[M+H]+
	8.6571	**_742.534_**	0.039359	0.120456	4.388728	PC (21 compounds mainly with saturated FA), PE (33 compounds, 5 with 18:1, 4 with 18:2 and the rest with saturated FA)[2]	C41H78NO8P	[M+H]+
	8.4494	758.57	0.012692	268.451	620.5982	PC (with mono-unsaturated FA)[1]		[M+NH4]+
	8.7991	760.586	0.03294	282.2038	645.0357	PC (28 compounds, 18 with 18:1 FA)[2]	C42H82NO8P	[M+H]+
	8.4505	780.553	0.036077	20.35434	46.15447	PC (63 compounds, 15 with unsaturated FA, and 7 PE compounds, 5 with 18:1)[2]	C42H80NO8P	[M+H]+
	8.5445	**_784.587_**	0.007726	87.89816	274.6576	PC (30 compounds, 8 compounds with (18:1), and 7 with (18:2) FA)2	C44H82NO8P	[M+H]+
	8.4399	754.567	0.103411	14.80464	0.117667	TAG [1]	C53H100O6	[M+Na]+
	11.2725	**_874.788_**	0.079861	3.200672	68.46109	TAG [1]	C56H106O6	[M+H]+
	11.4536	882.766	0.071056	0.725061	5.3001	TAG [1]	C55H104O6	[M+H]+
	8.6653	**_796.591_**	0.149226	31.1877	0.604794			
Liver and spleen AU-2+AI-2, negative mode	9.9861	646.615	0.00384	4.125539	14.32343	Ceramide[2]	C42H81NO3	[M+H]-
	8.5303	842.591	0.000229	64.5595	191.3729	Sphingomyelin[2]	C49H100N2O6P	[M-H]-
	8.8786	844.609	0.009489	135.0091	242.8838	Sphingomyelin[2]	C49H102N2O6P	[M-H]-
	8.5101	714.508	0.005198	0.990828	38.42561	PE (11 compounds, 6 with mainly mono- and 5 with di-saturated FA)2	C39H74NO8P	[M-H]-
	8.5028	738.507	0.014758	33.09288	123.5674	PE (27 compounds, 18 mainly with poly-unsaturated and 6 with 18:2 FA)[2]	C41H74NO8P	[M-H]-
	8.6223	740.528	0.001354	2.50455	63.86743	PE or PC (21 compounds, with 13 poly-unsaturated FA)[2]	C41H76NO8P	[M-H]-

8.4127	742.538	0.001855	17.94376	116.3698	PC, PE (27 compounds,with 11 (18:1)[2]	C39H78NO8P,	[M-H]-
						C41H76NO8P	
8.8004	760.532	0.070894	14.54144	0.307167	PC or PE (34 compounds, all with saturated FA)[2]	C42H84NO8P	[M-H]-
8.5308	770.574	0.09155	0.0079	11.16337	PC (with 18:0 or 18:1 or 18:2)[2]	C42H86NO7P, C44H84NO7P)	[M-H]-
8.7142	789.602	0.006121	0	12.95783	PE (18:1/18:1)[1]	C41H78N1O8P1	[M-H]-
7.5388	771.52	0.002469	0.769572	9.663144	PG [2]	C42H77O10P	[M-H]-
8.7649	804.576	0.003268	6.078272	83.50931	PS (18:0/19:0)[1]	C43H84NO10P	[M-H]-
8.7464	818.594	0.005329	167.2042	358.5437	PS(18:0/20:0) [2]	C44H86NO10P	
8.4169	816.577	0.000828	183.0132	382.7328			
6.2296	579.382	0.086749	0	7.312044			
9.9725	692.624	0.010935	5.859456	22.15938			
9.9814	709.604	0.000942	4.387167	15.94434			
8.8732	716.524	0.058191	0.49975	36.83187			
8.9448	742.541	0.000674	6.530978	30.67298			
8.4216	802.561	0.000439	21.11072	79.14308			
8.4182	826.559	0.000821	6.902494	25.38259			
8.5254	828.579	0.000149	0.540583	36.97608			
9.1973	832.605	0.05935	0	54.39824			
9.8102	859.691	0.01607	53.31586	3.320661			
9.595	871.696	0.034795	23.32086	50.96536			
7.9898	339.29	4.81E-05	6.021261	31.14227	Docosenoic acid[2]	C22H42O2	[M+H]+
8.6556	601.525	0.001026	5.03115	23.87169	1-(14-methyl-pentadecanoyl)[2]	C39H70O4	[M+H]+
9.6111	813.684	0.003544	66.12987	154.9185	Sphingomyelin (d18:0/24:1) [2]	C47H93N2O6P	[M+H]+
7.9753	730.545	0.000655	6.232306	18.72518	PE (18:1/16:2)[1]	C39H72N1O8P1	[M+NH4]+
8.1764	<u>782.57</u>	0.000302	18.46017	197.0989	PC (51 compounds, all with di (18:2)-or poly-unsaturatedFA (20:4)[2]	C44H80NO8P	[M+H]+
8.9328	<u>718.549</u>	0.000612	1.866544	8.439456	Diacylglycerol[1]	C43H84O5	[M+K]+
9.0044	774.613	0.0034	81.90647	13.16766	Diacylglycerol[1]	C47H92O5	[M+K]+
9.4836	800.669	0.000593	0.935822	6.439094	Diacylglycerol[1]	C50H98O5	[M+Na]+
11.3044	**<u>900.807</u>**	0.000181	13.15451	60.70834	TAG[1]	C55H106O6	[M+K]+
11.4906	**<u>902.816</u>**	0.000139	25.28832	79.17214	TAG[1]	C58H110O6	[M+H]+

Liver and spleen AU-3+AI-3, positive mode

181

	11.1218	**904.757**	0.000534	0.251844	1.514467	TAG[1]	C58H112O6	[M+H]+
	8.17	627.536	0.000182	119.2645	64.79762			
	7.9556	551.513	0.000885	0.249694	1.490406			
	8.5503	575.517	0.001173	4.928922	23.37566			
	7.9732	613.529	0.010895	2.772822	0.507478			
	9.1234	629.56	0.000492	3.018894	13.69499			
	9.9638	630.622	3.92E-05	7.026811	29.96439			
	8.6557	**742.546**	0.000143	10.89141	50.61101			
	8.111	756.558	0.00133	12.88752	63.98964			
	9.1307	**770.574**	0.000498	3.307633	39.30843			
	8.6627	**796.596**	0.004029	47.70854	6.569078			
Liver and spleen AU-3+AI-3, negative mode	6.3332	309.281	0.001006	2.705572	9.502661	Eicosenoic acid[2]	C20H38O2)	[M-H]-
	7.7248	365.344	0.000427	3.192428	9.877117	Nervonic acid[2]	C24H46O2	[M-H]-
	4.9548	279.231	0.001149	60.15215	140.6801	Octadecatrienoic acid (18:3) [2]	C18H30O2	[M-H]-
	9.9824	**646.617**	0.002073	21.43141	56.10984	Ceramide[2]	C42H81NO3	[M-H]-
	8.8983	**844.607**	0.000301	118.9633	209.3746	Sphingomyelin [2]	C49H102N2O6P	[M-H]-
	8.5347	714.51	0.00015	15.53687	80.48356	PE (11 compounds, 6 with mainly mono- and 5 with di-saturated FA)[2]	(C39H74NO8P	[M-H]-
	8.9026	716.526	8.99E-05	15.67844	80.14642	PC or PE (24 compounds, all with mono-unsaturated FA)[2]	C39H76NO8P	[M-H]-
	9.0056	742.54	0.000485	91.29389	321.5574	PC, PE (27 compounds,with 11 (18:1)) 2	C39H78NO8P, C41H76NO8P	[M-H]-
	9.3183	744.557	0.000318	65.55831	147.3598	PE, PC (31 compounds, mainly with 20 18:1)[2]	C41H78NO8P	[M-H]-
	7.7424	833.52	0.000533	12.47504	42.5005	PI (8 compounds, 4 with 18:1)[2]	C43H79O13P	[M-H]-
	7.7035	771.52	0.002143	22.06222	85.79083	PG [2]	C42H77O10P	[M-H]-
	9.9767	692.622	0.000783	21.73727	60.90678			
	5.0786	329.246	0.007693	12.57793	3.877217			
	7.0776	337.313	0.000565	1.037794	4.238639			
	7.9944	403.361	2.49E-05	0.465144	4.969922			
	9.5001	702.547	0.001306	0.355283	2.998744			
	9.9815	706.638	0.003159	12.72283	37.93326			
	8.7825	728.53	0.00357	5.451756	11.61117			
	8.9782	736.532	0.068997	76.02555	10.06047			
	8.6438	740.526	0.001144	30.65109	125.4777			
	9.0861	815.625	0.000217	8.463494	0.070783			

9.3267	826.581	0.000533	0.53095	2.63075
8.899	830.595	0.000492	11.85245	54.19976
9.2061	832.603	0.000525	5.629856	30.35067
9.8135	859.69	0.009498	14.45394	70.80578
7.9846	871.538	0.002909	40.80832	4.3531

[1]Compounds identified in *Mtb* Lipid database **[9].**
[2]Compounds identified in MasssTrix database [**12, 13**].
[3]Compounds identified by MS/MS fragmentation.
The features (mass) that were found in more than one tissue are underlined and in bold.
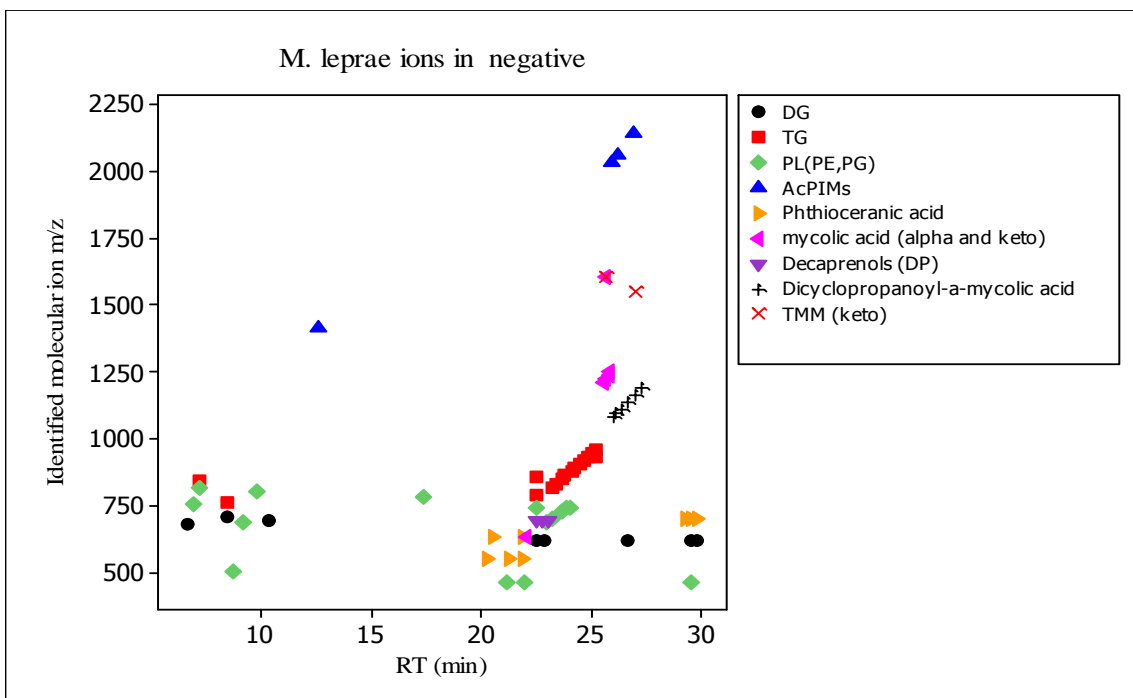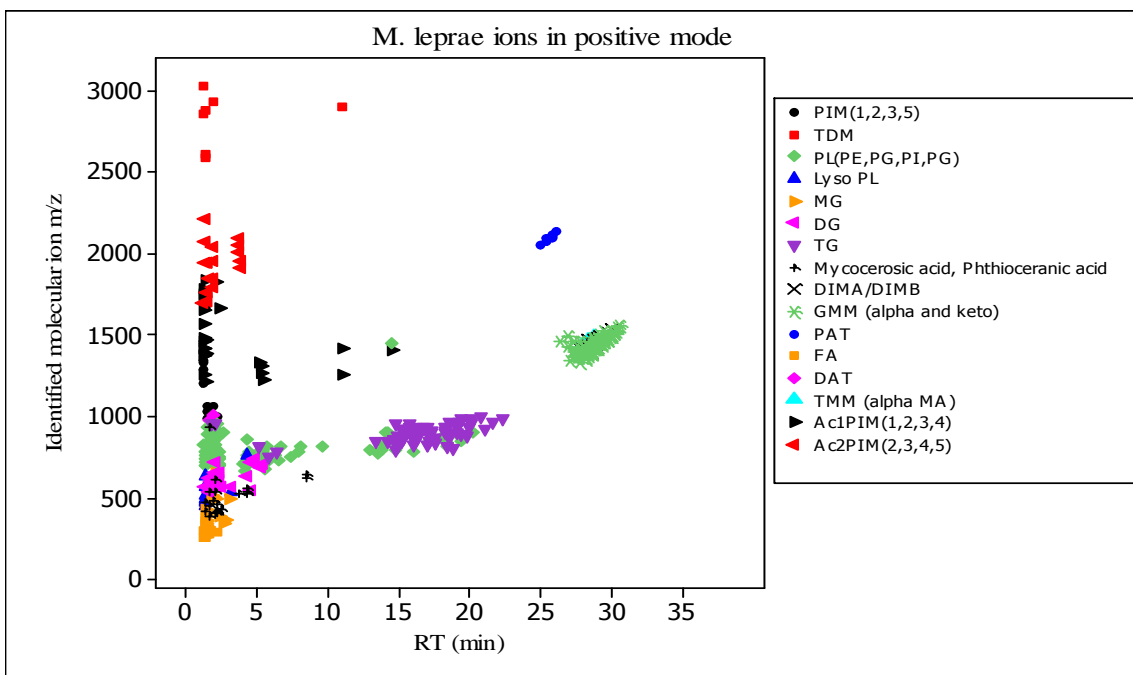
Figure S3.1: *M. leprae* molecular features identified from positive and negative ions LC/MS analyses of a lipid extract by comparison against the *Mtb* LipidDB.
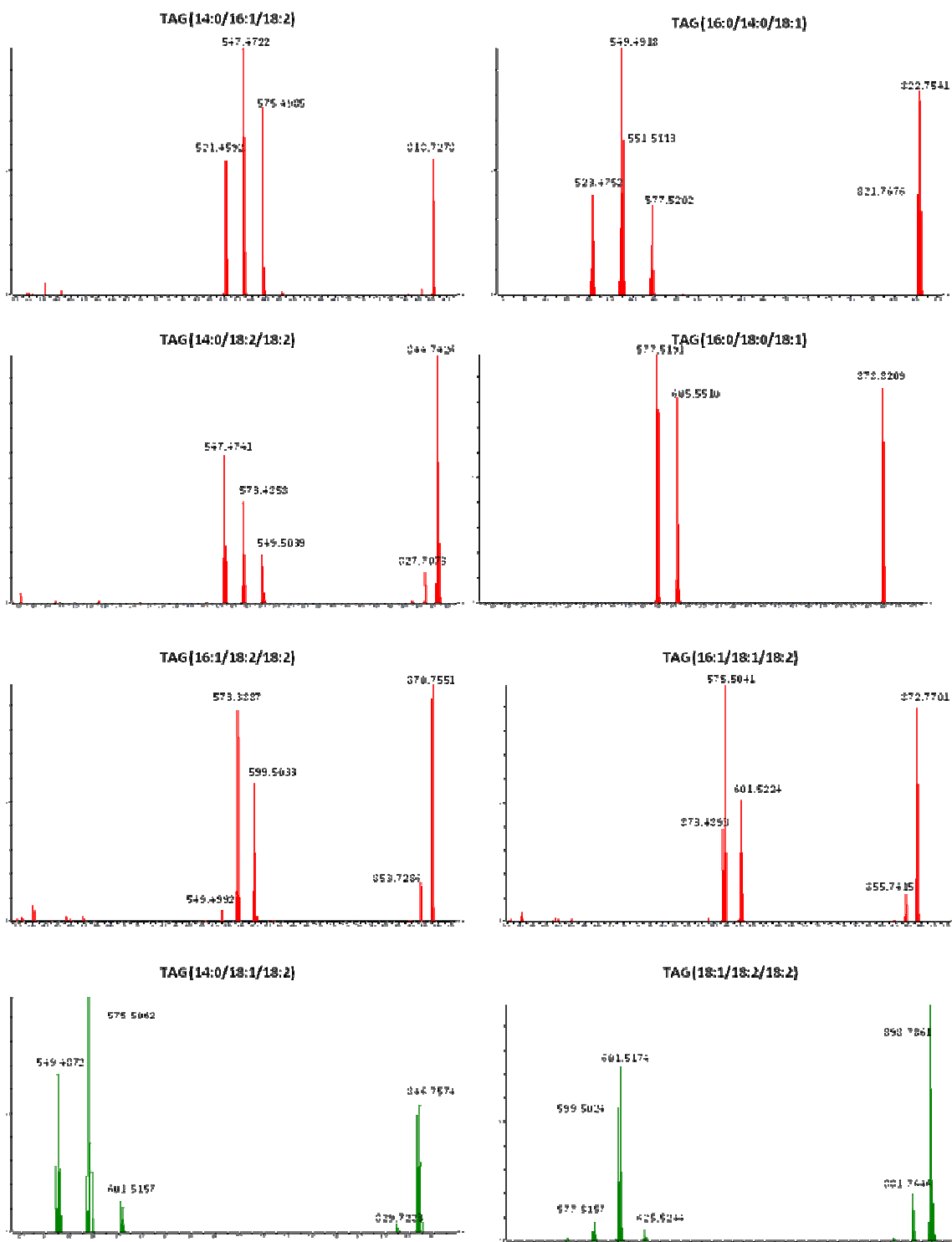
Figure S3.2: **MS/MS fragmentation of selected significant features (positive mode) from infected nerve**. The compounds identities were assigned based on the fragmentation pattern (loss of fatty acids). All the selected compounds are triacylglycerols (TAGs) esterified with fatty acids of different saturation and chain length as indicated on the top of each panel.
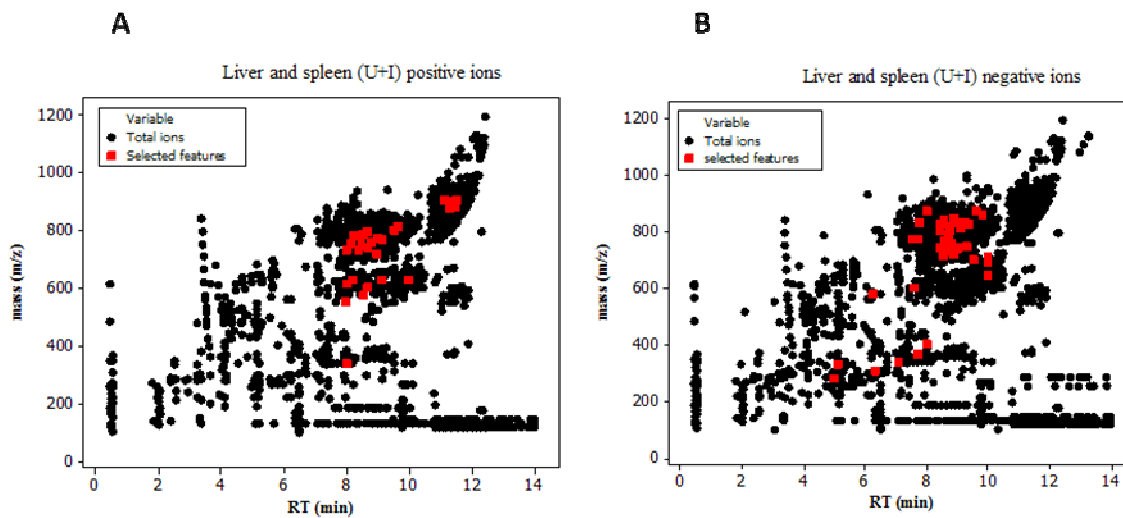
Figure S3.3: **Representative scatter plots of LC/MS UPLC-QTOF (Waters) features in liver and spleen lipid extracts from uninfected (AU-3) and infected (AI-3) armadillos**. Each feature is represented by m/z and RT. A: positive mode, B: negative mode. The features shown in red are the OPLS selected significant features that are elevated in the infected tissues.
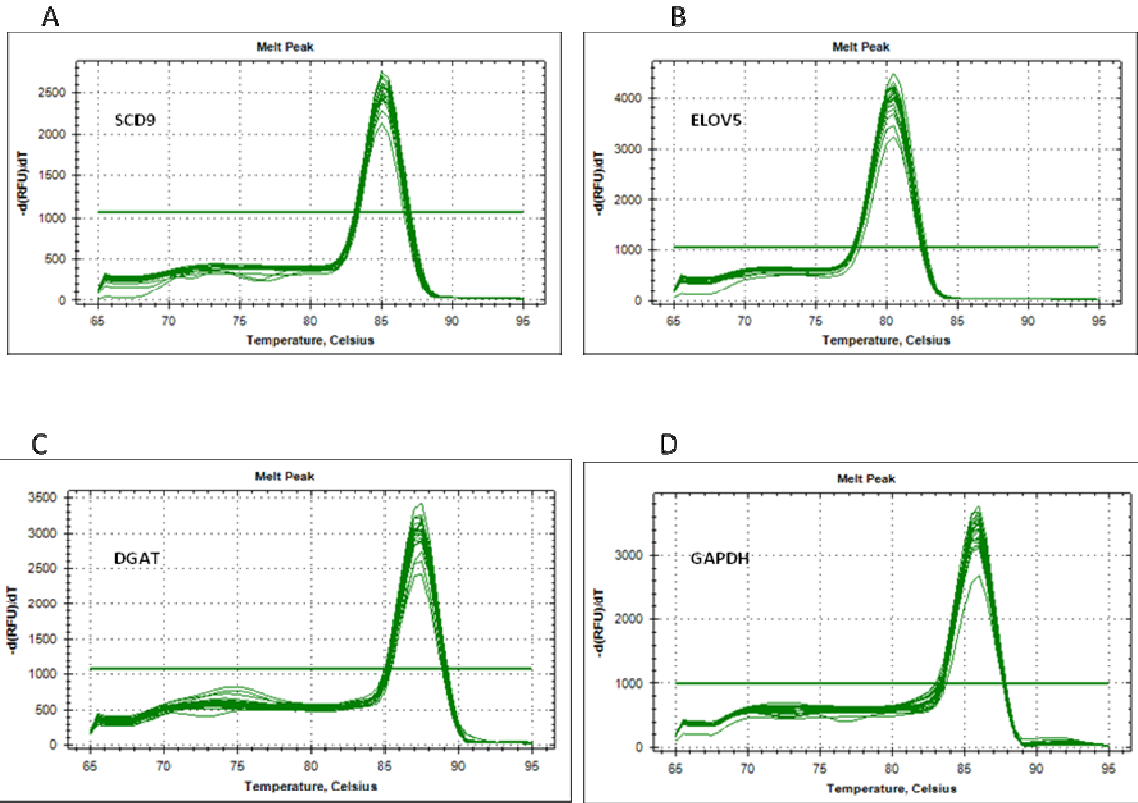
Figure S3.4: **Reverse transcriptase real time-PCR of armadillo genes**. Melt curves of transcripts of SCD9, ELOV5, DGAT and GAPDH amplified from cDNA prepared from uninfected and infected liver tissues are shown in panels A-D.

References

1. Cole ST, Eiglmeier K, Parkhill J, James KD, Thomson NR, et al. (2001) Massive gene decay in the leprosy bacillus. Nature 409: 1007-1011.

2. Cruz D, Watson AD, Miller CS, Montoya D, Ochoa MT et al. (2008) Host-derived oxidized phospholipids and HDL regulate innate immunity in human leprosy. J Clin Invest 118: 2917-2928.

3. Russell DG, Cardona P-joan, Kim M-jeong, Allain S (2009) Foamy macrophages and the progression of the human TB granuloma. Nat Immunol 10: 943-948.

4. Mattos KA, D'Avila H, Rodrigues LS, Oliveira VG, Sarno EN (2010) Lipid droplet formation in leprosy: Toll-like receptor-regulated organelles involved in eicosanoid formation and *Mycobacterium leprae* pathogenesis. J Leukoc Biol 87: 371-384.

5. Kirchheimer WF, Storrs EE, Binford CH (1972) Attempts to establish the Armadillo (Dasypus novemcinctus linn.) as a model for the study of leprosy. II. Histopathologic and bacteriologic post-mortem findings in lepromatoid leprosy in the Armadillo. Int J Lepr Other Mycobact Dis 40: 229-242.

6. Job CK (2003) Nine-banded armadillo and leprosy research. Indian J Pathol Microbiol 46: 541-550.

7. Truman R W and Krahenbuhl J L (2001) Viable *M. leprae* as a research reagent. Int J Lepr Other Mycobact Dis 69: 1-12.

8. Truman R W and Sanchez R M (1993) Armadillos: Models for leprosy. Lab Animal 22: 28-32.

9. Sartain MJ, Dick DL, Rithner CD, Crick DC, Belisle JT (2010) Lipidomic analyses of Mycobacterium tuberculosis based on accurate mass measurements and the novel "Mtb LipidDB." J Lipid Res 52: 861-872.

10. Al-Mubarak R, Vander Heiden J, Broeckling CD, Balagon M, Brennan PJ, Vissa VD (2011) Serum Metabolomics Reveals Higher Levels of Polyunsaturated Fatty Acids in Lepromatous Leprosy: Potential Markers for Susceptibility and Pathogenesis. PLoS Negl Trop Dis 5: e1303.

11. R Development Core Team. R: A Language and Environment for Statistical Computing. Vienna Austria R Foundation for Statistical Computing 2010, 1(09/18/2009): ISBN 3-900051-07-0.

12. Suhre K, Schmitt-Kopplin P (2008) MassTRIX: mass translator into pathways. Nucleic Acids Res 36: W481–484.

13. Fahy E, Sud M, Cotter D, Subramaniam S (2007) LIPID MAPS online tools for lipid research. Nucleic Acids Res 35: W606–612.

14. Livak KJ, Schmittgen TD (2001) Analysis of relative gene expression data using real-time quantitative PCR and the 2(-Delta Delta C(t)) Method. Methods 25: 402-408.

15. Sakurai I, Skinsnes OK (1970) Lipids in leprosy. 2. Histochemistry of lipids in human leprosy. Int J Lepr Other Mycobact Dis 38: 389-403.

16. Verma KC, Chugh TD, Chaudhary SD (1977) Tissue lipids in leprosy. Lepr India 49: 510-515.

17. Worm SW, Kamara DA, Reiss P, Kirk O, El-Sadr W, et al. (2011) Elevated triglycerides and risk of myocardial infarction in HIV-positive persons. AIDS 25: 1497-1504.

18. Khovidhunkit W, Kim MS, Memon RA, Shigenaga JK, Moser AH, et al (2004) Effects of infection and inflammation on lipid and lipoprotein metabolism: mechanisms and consequences to the host. J Lipid Res 45: 1169-1196.

19. Tanigawa K, Suzuki K, Nakamura K, Akama T, Kawashima A, Wu H, et al. (2008) Expression of adipose differentiation-related protein (ADRP) and perilipin in macrophages infected with Mycobacterium leprae. FEMS Microbiol Lett 289: 72-79.

20. Mattos KA, Lara FA, Oliveira VG, Rodrigues LS, D'Avila H, (2011) Pessolani MC: Modulation of lipid droplets by *Mycobacterium leprae* in Schwann cells: a putative mechanism for host lipid acquisition and bacterial survival in phagosomes. Cell Microbiol 13: 259-273.

21. Mattos K a, Oliveira VGC, D'Avila H, Rodrigues LS, Pinheiro RO (2011) TLR6-Driven Lipid Droplets in *Mycobacterium leprae*-Infected Schwann Cells: Immunoinflammatory Platforms Associated with Bacterial Persistence. J Immunol 187: 2548-2558.

22. Van der Meer-Janssen YPM, Galen J van, Batenburg JJ, Helms JB (2010) Lipids in host-pathogen interactions: pathogens exploit the complexity of the host cell lipidome. Prog Lipid Res 49: 1-26.

23. Peyron P, Vaubourgeix J, Poquet Y, Levillain F, Botanch C (2008) Foamy macrophages from tuberculous patients' granulomas constitute a nutrient-rich reservoir for M. tuberculosis persistence. PLoS Pathog 4: e1000204.

24. Kim MJ, Wainwright HC, Locketz M, Bekker LG, Walther GB, et al. (2011) Caseation of human tuberculosis granulomas correlates with elevated host lipid metabolism. EMBO Mol Med 2: 258-274.

25. Gao J, Serrero G (1999) Adipose differentiation related protein (ADRP) expressed in transfected COS-7 cells selectively stimulates long chain fatty acid uptake. J Biol Chem 274: 16825-16830.

26. Cáceres N, Tapia G, Ojanguren I, Altare F, Gil O, Pinto S, Vilaplana C, Cardona PJ (2009) Evolution of foamy macrophages in the pulmonary granulomas of experimental tuberculosis models. Tuberculosis 89: 175-182.

27. Daniel J, Maamar H, Deb C, Sirakova TD, Kolattukudy PE (2011) Mycobacterium tuberculosis Uses Host Triacylglycerol to Accumulate Lipid Droplets and Acquires a Dormancy-Like Phenotype in Lipid-Loaded Macrophages. PLoS Pathog 7: e1002093.

28. Bellinati-Pires R, Waitzberg DL, Salgado MM, Carneiro-Sampaio MM (1993) Functional alterations of human neutrophils by medium-chain triglyceride emulsions: evaluation of phagocytosis, bacterial killing, and oxidative activity. J Leukoc Biol 53: 404-410.

29. Thomsen KF, Laposata M, Njoroge SW, Umunakwe OC, Katrangi W, Seegmiller AC (2011) Increased elongase 6 and Δ9-desaturase activity are associated with n-7 and n-9 fatty acid changes in cystic fibrosis. Lipids 46: 669-677.

30. MacDonald MLE, Eck M van, Hildebrand RB, Wong BWC, Bissada N (2009) Despite antiatherogenic metabolic characteristics, SCD1-deficient mice have increased inflammation and atherosclerosis. Arterioscler Thromb Vasc Biol 29: 341-347.

31. Chen C, Shah YM, Morimura K, Krausz KW, Miyazaki M, (2008) Metabolomics reveals that hepatic stearoyl-CoA desaturase 1 downregulation exacerbates inflammation and acute colitis. Cell Metab 7: 135-147.

CHAPTER 4

Approaches to the Identification of Biochemical Markers of Infection and Nerve Damage in Leprosy; Proteomics and Humoral Immune Response of *M. leprae* Infected Tissue

4.1. SUMMARY

Nerve damage and deformity are the main manifestation of leprosy. However, the mechanisms of nerve damage in leprosy are poorly understood. Studies have been done to understand the interaction between *Mycobacterium leprae* and Schwann cells *in vitro,* and many mechanisms have been proposed for the Schwann cells demyelination in leprosy, such as hypophosphorylation of the axonal proteins, autoimmune against host's own antigens.

In this study we attempted to use the nine-banded armadillo (*Dasypus novemcintus*) as a model to understand the host-bacteria (*M. leprae*) interaction at the molecular level. Using mass spectrometry approach we analyzed changes in the protein expression profile and modification of the nerve fractions separated by one or two-dimensional gel electrophoresis (2DE) and compared infected nerves to the naïve animal nerves.

The protein profile showed decreased amount of proteins (bands/spots) in the infected nerve. There was increase in the amount of immunoglobulins IgG and IgM in the infected nerve. Also, antibodies against nerve components (myelin P2) were detected in the leprosy

patient's sera. This new approach will help in finding marker (s) for the infection and nerve damage in leprosy.

4.2. INTRODUCTION

Infection of peripheral nerves is a unique property of *Mycobacterium leprae*, which leads to injury, paralysis and deformity, characteristic of leprosy. However, the exact mechanism(s) underlying nerve injury in leprosy is very poorly understood. Neuropathy in leprosy arises not only from infection of peripheral nerves by *M. leprae*, but also from the inflammatory and immunologic responses to the pathogen. The nerve damage occurs during and after treatment completion **(Harboe M., 2005).** Therefore, *M. leprae*-nerve interaction needs to be investigated in depth to find new strategies for the prevention and treatment of disabilities.

After *M. leprae* invades Schwann cells (SCs), it can survive in the endosome by avoiding fusion of the phagosome with lysosomes. As a result of this invasion, nerve axonal damage and demyelination occurs. In the non-myelinated SCs, which are more susceptible to *M. leprae* invasion, proliferation and axonal damage can occur. In the myelinated form of SCs the invasion can lead to demyelination, which then leads to propagation of the cycle and invasion of more *M. leprae* cells, axonal damage and disease progression **(Barker L., 2006, Rambukkana A., 2000).**

Studies have been conducted to understand the interaction between *M. leprae* and SCs *in vitro*, and many mechanisms have been proposed for SCs demyelination in leprosy. The nerve damage in leprosy has been divided into two stages. i- The initial stage that occurs in the absence of inflammatory cells. This stage is initiated by direct contact between *M. leprae* and SCs in the PNS that leads to nerve damage. This is common across the leprosy spectrum. It is characterized by sub-perineural edema, axonal atrophy and demyelination along with loss of un-myelinated fibers. Another proposed mechanism, in the non-immune mediated form, is biochemical and metabolic changes in the nerve compartment. Example of this mechanism is the axonal atrophy due to hypophosphorylation of the myelin proteins and axonal neurofilaments. For example decrease in phosphorylation of the glycoprotein myelin P0 (**Suneetha L., 1997**) and hypophosphorylation of neurofilament (NF subunits) during leprosy infection. These NFs become more susceptible to proteolytic degradation (**Save M., 2004**). Phosphorylation was found to protect NFs against non-specific proteolysis by calpain (proteolytic enzymes) (**Pant H., 1988**). ii- The later stage is mediated by inflammation with lymphatic cells in tuberculoid form and macrophage cells in lepromatous leprosy. In this stage the presence of auto-antibodies against nerve components was reported in leprosy as another mechanism of nerve damage. The presence of antigenic determinants common to *M. leprae*, skin and nerve such as heat-shock proteins lead to auto-antibody production **(Birdi T., 2003).** Leprosy patients have increased levels of antibodies against myelin glycolipid components (**Spierings E., 1999, Singh., 2010, Ribeiro., S., 2011 and Raju, R., 2011**).

The availability of the nine-banded armadillo (*Dasypus novemcintus*) model for leprosy allows investigation of biochemical and molecular changes in tissues (nerves) due to *M. leprae* infection. The genome sequence of the armadillo with 6 x coverage is anticipated while 2 x is being annotated and available through Ensembl database **(Adams L., 2005).** The armadillo thus can be a valuable model to study the neurological aspects of leprosy and to understand the host-*M. leprae* interactions at the molecular level**.**

The goal of this study was to examine the proteome profile of uninfected and *M. leprae* infected peripheral nerve from armadillos. Using mass spectrometry we identified the protein profile of the nerve lysate and fractions separated by one or two-dimensional gel electrophoresis (2DE). This new approach will help in finding marker (s) for infection and nerve damage in leprosy.

4.3. MATERIALS AND METHODS

4.3.1 Chemicals and reagents

Tris-HCl, EDTA, EGTA, NaCl, phosphate buffer, phenyl methyl sulphonyl fluoride, CHAPS, iodoacetamide (IAA) were obtained from Sigma (Sigma, US). Dithiothreitol (DTT) was obtained from Invitrogen (Invitrogen, US). IPG-strips immobilized pH gradient, sodium dodecyl sulfate (SDS), acrylamide/bisacrylamide solution was obtained from Bio Rad (Bio Rad, US). The carrier ampholytes 3-10 was obtained from GE Healthcare (GE Healthcare, US). Methanol and chloroform were from Fisher (Fisher, US). Anti-human polyvalent immunoglobulins (IgG, IgM and IgA), anti-human IgG, anti-

194

human IgM, anti-rabbit IgG and anti-mouse IgG antibody all conjugated with alkaline

phosphatase were obtained from Sigma (Sigma, US). Anti human recombinant myelin P2

(Santa Cruz Biotechnology, US), anti-neurofilament (heavy H and medium M),

(Invitrogen, US) were conjugated with alkaline phosphatase.

4.3.2 Armadillo tissue

Naïve (5 animals were captured from the wild) and infected (5 animals were inoculated

intravenously with 1×10^9 highly viable *M. leprae*) **(Table 4.1)** armadillos were provided

by Dr. Truman (the National Hansen's Disease Program at Louisiana State University

(Baton Rouge, LA) **(Truman R., 1993).** We obtained armadillo tissues sets (nerve, spleen

and liver) from the same animal. The armadillo nerves were harvested prior to sacrifice,

surgically, with the animal under anesthesia. The nerves were immediately snap frozen and

then stored at -70°C for shipment. Following surgery the animals were sacrificed.

Table 4.1: Armadillo used for the protein study

Uninfected armadillo #	Origin	Date sacrifice	Infected armadillo #	Origin	Date sacrifice
8-55,	Baton Rouge, LA	2008	5M13	Atchafalaya levee, LA	2008
8-52	Pointe Coupee, LA	2008	5J24	St. Francisville, LA	2008
10-23	Pointe Coupee, LA	2010	7Q04	St. Helena, LA	2008
10-32	Arkansas	2010	8U74	Baton Rouge, LA	2010
10-19	-	2010	8V94	St. Helena, LA	2010

4.3.3 Peripheral nerves protein preparation, processing and intermediate filaments (IF) and enrichment from PNS

Protein extracts was prepared from at least three armadillo peripheral nerves from each group (infected and naïve). Briefly, the nerve tissues were stripped out of the bundles of nerve fibers, homogenized using a Fast Prep-24 instrument (MP Biomedical, USA) in a lysis buffer containing 40 mM Tris-HCl pH 8.8, 0.5% tritonix, 10% glycerol, 5 mM EDTA, 65 mM DTT. For intermediate filament and myelin enrichment different buffer was used (25 mM phosphate (pH 6.8), 100 mM NaCl, 1 mM EDTA, 1 mM EGTA, 0.5% Triton-X-100, 3.5 ng/ml of phenyl methyl sulphonyl fluoride (PMSF) and protease inhibitor, Pefabloc SC (Roche, US)). Total protein concentrations of lysates were measured by bicinchoninic acid (BCA) protein assay reagent. Aliquots were made in 1.5 ml tubes with 200-300 µg each and lyophilized.

The protein samples were separated by 1 and 2-dimensional SDS-gel electrophoresis (IPG 3-10; 7 cm or large size 18 x 16 cm) (Bio Rad). The proteins were visualized by either silver stain, Coomassie blue, SyproRuby stains (Invitrogen, USA) for total proteins; or for post-translation modification such as Periodic acid-Schiff (PAS) for glycoproteins and phosphate florescence staining (Pro Q Diamond) (Invitrogen, USA). At the same time the protein samples were analyzed using ConA lectin specific for glycoproteins in a Western blot.

For the IF enrichment; frozen nerve biopsies 1.5 cm were homogenized (1:20 w/v) in extraction buffer containing 25 mM phosphate pH 6.8, 100 mM NaCl, 1 mM EDTA and

EGTA and 0.5% tritonX-100 with protease inhibitors, phenyl methyl sulphonyl fluoride (PMSF) 1 mM, benzamidine 3.5 ng/ml). The samples were centrifuged at 20,000g for 30 min at 10°C, the #1 supernatants were stored. The pellets were re-homogenized in the same extraction buffer with 1 M sucrose. The suspensions were centrifuge at 20,000 x g for 30 min and the #2 supernatants were stored (myelin rich fraction). The homogenization and the centrifugation steps were repeated until floating myelin was absent and #3 supernatants were stored. The neurofilaments (NF) rich pellets were re-suspended in the extraction buffer without Triton-X -100 and centrifuged as above and the detergent-free pellet was collected **(Save M.P., 2004).**

4.3.4 Two- dimensional gel electrophoresis (2DE gels), immobilized pH gradient (IPG) first dimension and SDS-PAGE second dimension

Preparation of the protein samples for 2DE; the protein powders were de-lipidated with chloroform: methanol: water (10:10:3 v/v/v) by shaking at 4ºC for 1 hour; the samples were centrifuged (3000 rpm x10 min), the supernatants were collected and the lipid extraction was repeated again. The extra salts in the de-lipidated protein samples were removed by the ReadyPrep 2-D Clean Up Kit (Bio Rad, US). Briefly, the protein samples were suspended in 100 µl water, precipitated with 300µl of precipitation Agent 1 and incubated on ice for 15 min. After 15 min, 300 µl of precipitation Agent 2 was added, vortexed and centrifuged at 14.000 rpm for 5 min. All the supernatant were discarded and 40 µl of wash reagent 1 was added and vortexed and centrifuged at 14.000 rpm for 5 min. The supernatant were discarded. 25 µl of mili-Q water was added and vortexed. The samples were washed with 1 ml of wash solution with 5 µl additive added, vortexed and

197

incubated at -20ºC for 30 min. Finally, the samples were centrifuged at 14.000 rpm for 5 min and the supernatant were discarded. The samples were dried for 3 min and stored at -20ºC until processed.

For the first dimension; the dry aliquots of 200-300µg nerve proteins were re-suspended in 140 µl of rehydration buffer (8 M urea, 2% CHAPS and a few drops of bromophenol blue stock, 0.3% DTT) and 1% IPG buffer ampholytes was added; the samples were vortexed and sonicated to dissolve the protein. The rehydrated samples were loaded into a IPG strip holder and the IPG strip (3-10 nL, Bio Rad) was placed on top after removing the plastic and aligning the + and - ends. The strip was allowed to rehydrate at least for 10-20 min, covered with mineral oil. The samples in the IPG strips were incubated overnight (14 hours) to rehydrate in Amersham Pharmacia Botech GE system at 20°C. After the rehydration step the isoelectric focusing was started for 6 hours total using IPGphor isoelectric focusing system 3-10 non-linear gradient (NL); 200V for 1 hour, 500V for 1 hour, 500-8000V for 2 hours and 8000V for another 2 hours.

For the second dimension; after the focusing step, the strips were incubated in equilibration buffer 1 for 15 min (6M urea, 30% glycerol, 2% SDS and 0.5M tris pH6.8) plus 0.2g/10 ml DTT). After the first equilibration buffer the strips were placed in equilibration buffer 2 for 10 min (has the same components as buffer 1, but with 0.25g/10 ml of iodoacetamide (IAA) instead of DTT). The strips were removed after equilibration and placed on 15% SDS-PAGE. The strip in the gel was covered with 0.25% agarose gel

made in the same running buffer to remove any bubbles; the tank was filled with SDS-electrophoresis buffer and run at 130V until the dye reached the end.

4.3.5 Staining the gel: Silver nitrate and Periodic acid Schiff (PAS)

The gel was placed in first fix (methanol, acetic acid and water) for 45 min to overnight. $NaIO_4$ 0.7g/100 ml was added for 7 min (for PAS stain only). The second fix was added for 5 min. 2.5% gluteraldehyde was added for 5 min, washed with water 4 times, 10 min each. 2.5 mg of DTT in 100 ml water was added for 6 min and then the gel is rinsed with water. The gel was stained with 100 mg $AgNO_3$ in 100 ml water for 10 min. The reaction was developed with 6 g Na_2CO_3 in 200 ml water and 6 drops of 37% formaldehyde. The reaction was stopped by added 50% citric acid, and then the gel was washed and stored in water until dry. For gel drying the gel was incubated in (10% ethanol and 10% glycerol) for 30 min then dried.

The spots of interest were excised from the gel using a new razor blade and cut into 1 mm pieces, saved in water at -20ºC until processed. The spots were de-stained with special de-staining solution for silver nitrate to make it compatible for mass spectrometry analysis. The silver stained gel pieces were first rinsed with water and then a fresh solution of potassium ferricyanide (10 mg/ml) and sodium thiosulfate (16 mg/ml) was added in 1:1 ratio to cover the gel and incubated for 10 min at room temp. After incubation the supernatant was discarded and the de-staining step was repeated until the silver-brown color was removed. After the destaining the gel pieces were washed in 100 mM ammonium bicarbonate (NH_4HCO_3) for 20 min and kept ready for enzyme (trypsin) digestion.

199

4.3.6 In-gel digestion using Protease MAX surfactant and mass spectrometry analysis

The spots were destained for 5 min in 200 µl of acetonitrile (ACN)/50 mM ammonium bicarbonate (1:1 v/v), centrifuged, the supernatants were discarded, and the destaining was repeated. The gel pieces were dehydrated with 200 µl of 100 % ACN, vortexed for 5 min and the supernatants were discarded. The samples were dried for 5 min at room temperature. The gel pieces were rehydrated in 200 µl of 25 mM DTT in 50 mM ammonium bicarbonate and incubated 20-30 min at 60ºC. The supernatants were removed and 200 µl of 55 mM IAA in 50 mM ammonium bicarbonate was added and incubated 20 min at room temperature in the dark. The gel pieces were washed with water two times. The samples were dehydrated for 5 min in 200 µl of ACN/50mM ammonium bicarbonate (1:1 v/v). 200 µl of 100 % ACN was added, vortex for 5 min. The samples were dried at room temperature for 5 min. The samples were rehydrated in 20 µl of 2 ng/µl trypsin (Roche Applied Science, US) in 0.01% Protease Max surfactant for 10 min. More 0.01% of Protease Max (10µ) was added, and incubated for 3 hours at 37ºC. The samples were centrifuged (12,000 x g for 5 min) and the supernatants were collected. 2.5% TFA was added to the samples and vortexed for 15 min. All the sample extracts were combined and dried in a speed vacuum centrifuge. The dry samples were re-suspended in 10 µl of 0.1% TFA and 3% ACN and analyzed by LC-MS/MS for protein identification.

Peptides were purified and concentrated using an on-line enrichment column (Agilent Zorbax C18, 5ìm, 5 x 0.3 mm). Subsequent chromatographic separation was performed on a reverse phase nanospray column (Agilent 1100 nano HPLC, Zorbax C18, 5 µm, 75 µm

ID x 150 mm column) using a 42 min linear gradient from 25%-55% buffer B (90% ACN, 0.1% formic acid) at a flow rate of 300 nanoliters/min. Peptides were eluted directly into the mass spectrometer (Thermo Scientific LTQ Linear Ion Trap). Mass spectra were collected over a m/z range of 200–2000 using a dynamic exclusion limit of 2 MS/MS spectra of a given mass for 30 sec (exclusion duration of 90 sec).

Compound lists of the resulting spectra were generated using Bioworks 3.0 software (Thermo Scientific) with an intensity threshold of 5,000 and 1 scan/group. MS/MS spectra were searched against the appropriate protein database using the Mascot database search engine (version 2.3). Mascot, Sequest and X Tandem (Version 2007.01.01.1) were set up to search a database Mammalia (mammals) NCBInr 20081107 (7294643 sequences; 2525198067 residues) and armadillo 20090414 (4024 sequences; 1984269 residues). Mascot and Sequest searches allowed for 1 and 5 missed cleavages, respectively. Oxidation of methionine (+16) and the iodoacetamide derivative of cysteine (+57) were specified as variable modifications. The results were posted as Scaffold (Proteome Software, Portland, OR), which is a proteomics software program.

Peptide identifications were accepted if they could be established at greater than 90% probability as specified by the Peptide Prophet algorithm. Protein identification contains at least two identified peptides. Proteins identified by two peptides were subject to manual validation for final confirmation.

4.3.7 Purification of immunoglobulin (IgG) from armadillo tissue lysates (nerve and spleen) and lepromatous leprosy patient serum pool

The tissue lysates were diluted in 1X PBS buffer and passed through a protein A/G spin column (Pierce, USA). The flowthrough was collected for further protein analysis. The immunoglobulin was eluted by adding acidic elution buffer (0.1M glycine-HCl, pH 2.8). The eluates were tested for the purity of the immunoglobulin by Coomassie blue stain and Western blot using anti-IgG antibody. The sera from five different lepromatous leprosy patients were pooled. The IgG immunoglobulin was purified by protein A/G spin column (Pierce, USA). The purified IgG was tested using anti-human IgG antibody in a western blot.

4.3.8 Western blot

The protein samples resolved by SDS-PAGE gels were electro-blotted to nitrocellulose membranes. The membranes were blocked with 3% BSA in Tris-buffer saline with 0.05% Tween 80 (TBS-T) for at least 2 hours. The primary antibody was added and incubated for at least 2 hours, washed with TBS-T. The blot was probed with alkaline-phosphatase-conjugated antibody for 1 hour, and washed extensively. The result of Ag-Ab complexes were visualized by color development with 5-bromo-4-chloro-indoyl-phosphatase-nitroblue tetrazolium substrate (BCIP-NBT) (Sigma, US).

4.4. RESULTS

4.4.1 Protein profiles of uninfected and infected armadillo nerves from 1D gel

The 1D and 2D profiles of infected and naïve armadillo nerve lysates were examined. As armadillo is a new model, a reference map of PNS protein has been initiated. As a pilot approach to systematically identify the nerve proteins in the total lysate samples; 1D SDS-PAGE gel stained with Coomassie blue was used for both infected and uninfected nerve proteins (20 µg each). Bands were excised from the gel as highlighted in **Figure 4.1**, subjected to tryptic in-gel digestion. The proteins were identified based on peptide mass and sequence information obtained by mass spectrometry. Four bands were analyzed from each sample around 75, 50, 25 and 15 kD. The protein identified was based on armadillo [http://uswest.ensembl.org/Dasypus_novemcinctus/Info/Index]**)** and mammalian databases (**NCBInr 20081107**) using a cut off of 95% with two peptides minimum for each protein. Totally, 15 unique PNS nerve proteins were identified in both infected and uninfected samples. **Tables 4.2 and 4.3** summarize the results of protein identification.
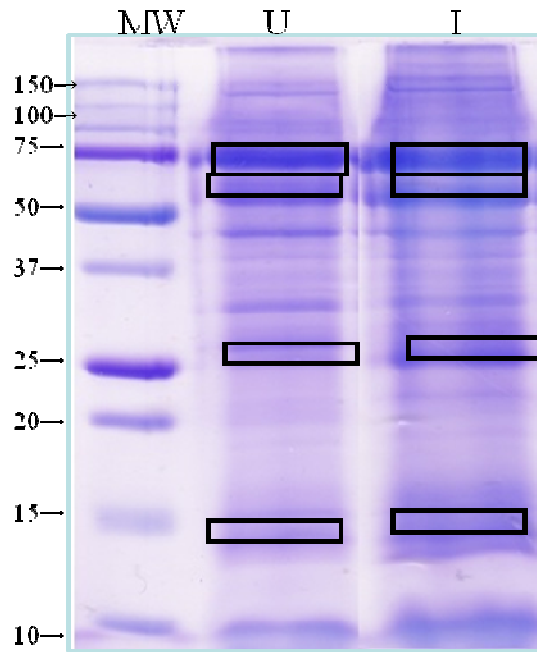
Figure 4.1: Protein reference map for armadillo using 1D SDS-PAGE of the nerve lysates from uninfected (U) and infected (I) nerves. Proteins were visualized by Coomassie blue staining. Coomassie-stained bands were subjected to mass spectrometric protein identification (ESI-MS/MS) after tryptic digestion. Data were analyzed by searching the peptides against mammalian and armadillo database (Table 4.2 and 4.3).

Table 4.2: Armadillo nerve protein mapping from 1D gel bands and searched against mammal database NCBInr 20081107

(7294643 sequences; 2525198067 residues)

Bands #	Protein ID, size	Accession number	Uninfected nerve # of unique spectra	Uninfected nerve Percentage of coverage (%)	Infected nerve # of unique spectra	Infected nerve Percentage of coverage (%)
75kD	Myelin P0, 42 kD	GI:126311340	3.7	3.7	8.3	8.3
	Neurofilament3 (150kD medium),103kD	GI:109085914	-	12	4	13
	Neurofilament, light polypeptide, 62 kD	GI:105990539	2	7.6	5	12
	Serum albumin, 69 kD	GI:1351907	5	19	12	13
	Vimentin, 54 kD	GI:158962631	19	14	13	19
	Tubulin beta chain, 50 kD	GI:135490	14	2.7	19	2.7
	Similar to Periaxin, 132 kD	GI:194215457	2.7	20	2.7	19
	Dihydropyrimidinase-like 2, 62 kD	GI:115496400	20	10	19	2.7
	Peripherin, 54 kD	GI:166063971	2	7.2	1	3.7
	ATP synthase, H+ transporting, 56 kD	GI:194037554	7.2	14	3.7	5.5
	Muscle creatine kinase isoform 2, 43 kD	GI:194018722	14	9.4	5.5	9.4
	Similar to pyruvate kinase 3 isoform 3, 58 kD	GI:109518934	9.4	8.7	9.4	16
	Gamma actin-like protein, 44 kD	GI:6425087	8.7	17	16	17
	Immunoglobulin heavy chain variable region, 50 kD	GI:118405955	17	28	17	30
	Chain A, Tubulin-Colchicine: Stathmin-Like Domain, 50 kD	GI:47169120	28	4.3	30	5.3
	Heat shock 70 kDa protein, 71 kD	GI:74191381	4.3	12	5.3	19
	Intermediate filament protein, 54 kD	GI:74139645	12	11	19	11

50kD	Neurofilament 3 medium, 103 kD	GI:109085914	7	20	6	17
	Neurofilament, light polypeptide, 62 kD	GI:105990539	6	18	5	11
	Vimentin, 54 kD	GI:57114172	5	28	3	12
	Chain A, Tubulin-Colchicine, 50 kD	GI: 47169120	28	53	12	29
	Chain B, Tubulin-Colchicine, 50 kD	GI: 67463742	53	5.8	29	2.8
	Peripherin, 54 kD	GI: 156139125	5.8	21	2.8	-
	Tubulin B3, 50 kD	GI:145966774	7	14	-	13
	Similar to ATP synthase subunit beta, 56 kD	GI: 194037554	4	9.4	-	17
25kD	Ubiquitin carboxyl-terminal esterase L1, 28 kD	GI:114051423	14	12	13	12
	Peroxiredoxin 6, 25 kD	GI:118597400	9.4		17	13
	Similar to Myelin P0 protein, 42 kD	GI:127722	8	16	7	19
	Similar to Myelin P0 protein, 42 kD	GI:127722	-	-	4	37
20kD	Hemoglobin subunit beta, 16 kD	GI:78099778	-	-	5	-
15kD	Similar to Peripheral myelin protein 2,15 kD	GI:149721294	2	-	1	-
	Histone cluster 1,14 kD	GI:10645195	-	-	2	-

Table 4.3: Armadillo nerve protein mapping from ID gel bands and searched against armadillo database (Ensembl 20090414 (4024 sequences); 1984269 residues)

Bands #	Protein ID, size	Accession number (ENSDNO)	Uninfected nerve # of unique spectra	Uninfected nerve Percentage of coverage (%)	Infected nerve # of unique spectra	Infected nerve Percentage of coverage (%)
75kD	Medium polypeptide (NF-M)(Neurofilament triplet M protein), 81 kD	G00000003384	7	14	9	16
	Precursor (Transferrin)(Siderophilin)(Beta-1-metal-binding globulin), 63 kD	G00000004595		-	7	19
	Beta-2B chain tubulin, 43 kD	G00000001779	3	14	5	22
	Myotubularin-related protein 14, 60 kD	G00000002738	2	9.1	2	9.1
	Protein 1 (DRP-1)(Collapsin response mediator protein 1)(CRMP-1), 48 kD	G00000005068	-	-	3	16
	Protein 1 subunit gamma, 55 kD	G00000000057			2	6.9
	Zinc finger CCCH domain-containing protein 10, 25 kD	G00000000333		-	2	19
	Fibrinogen, 56 kD	G00000002377	3	10	3	10
	Ubiquitin-protein ligase RNF19A, 91 kD	G00000004532	2	7.5	2	8.7
	Zinc finger CCHC domain-containing protein 14, 81 kD	G00000010289	-	-	2	8.8
	Light polypeptide (NF-L)(Neurofilament triplet L protein), 32 kD	G00000003389	3	29	2	16
	Protein 14, 60 kD	G00000002738	2	9.1	9.1	2
50kD	Type II cytoskeletal 3 (Cytokeratin-3), 53 kD	G00000002471		-	2	9.4
	Leucine- rich repeat-containing protein 50, 42 kD	G00000005156	2	17	2	21
	Type II cytoskeletal 3 (Cytokeratin-3), 53 kD	G00000002471		-		18
	Tubulin, alpha, 50 kD	G00000004121	7	22	6	22
	3'-phosphodiesterase, 43 kD	G00000004854	2	13		
25kD	Zinc finger CCCH domain-containing protein 10, 25 kD	G00000000333		-	2	21
	D2 phospholipase (PLD 2)(hPLD2), 89 kD	G00000002986		-	2	6.9
	Nuclease HARBI1	G00000002083		-	2	11

	DNA-binding- protein A (Cold shock domain-containing protein A), 34 kD	G00000000480			2	16
	Affinity copper uptake protein 1 (Copper transporter 1)(hCTR1), 21 kD	G00000001328		-	2	20
	Melanoma associated antigen B18 (MAGE-B18 antigen), 33 kD	G00000001649	2	26		-
15kD	Acetyltransferase, 40 kD	G00000001955	2	17		
	P2 protein, 13 kD	G00000002174	3	44	4	34
	Histone (H2A) type 2-B, 13.9 kD	G00000002427		-	2	29

4.4.2 Protein profiles of uninfected and infected armadillo nerves from 2DE gel

The uninfected and infected armadillo nerve lysates (300 µg each) were visualized in a

2DE gel stained with SyproRuby. The protein patterns look slightly different with more

intense protein spots found in uninfected compared to infected nerves as showed in **Figure**

4.2.
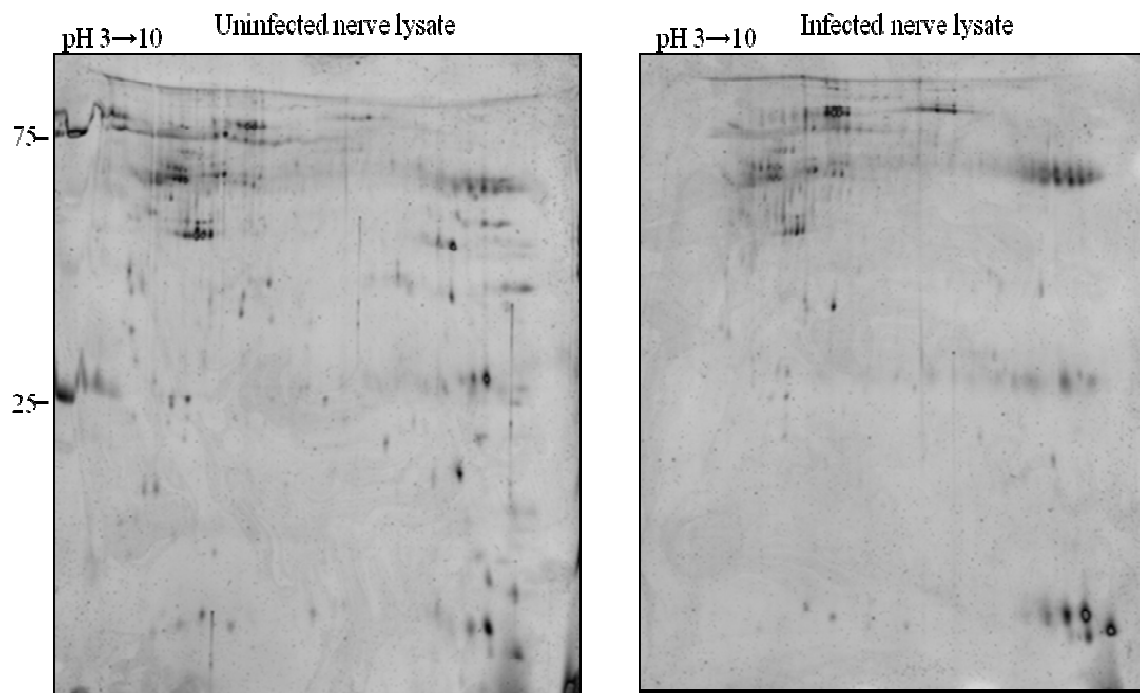
Figure 4.2: 2D-SDS gel of nerve proteins, Sypro-Ruby stained. The uninfected nerve

gel has more intense proteins spots**;** however, the overall pattern appears to be similar.

4.4.3 Fractionation of the nerve; enrichment for the myelin and intermediate filament (IF) proteins

During leprosy infection some nerve components may experience changes on their post-translation modification that leads to degradation of the protein, which affect the nerve function. For example, neurofilament proteins are highly phosphorylated, which is important for axonal caliber. Looking at the differences between uninfected and infected at the nerve main components such as the myelin and the intermediate filament proteins, these components were enriched from the nerve total lysate using established procedures. The supernatant is myelin rich and the final pellet consist of the IF proteins. The PNS IF is composed of the three subunits of the neurofilament (heavy, medium and light), peripherin and vimentin, which were assigned in the gel based on their molecular weight, **Figure 4.3**. The NF proteins (M and H) were also confirmed in a western blot and using anti-NF-M and H, **Figure 4.4 A.** The same material was also analyzed on SDS gels and staining with fluorescence stain (Sypro Ruby and ProQ) for phosphorylated protein **(Figure 4.4 B).** Based on these gel results, there were no obvious differences between uninfected and infected nerve.
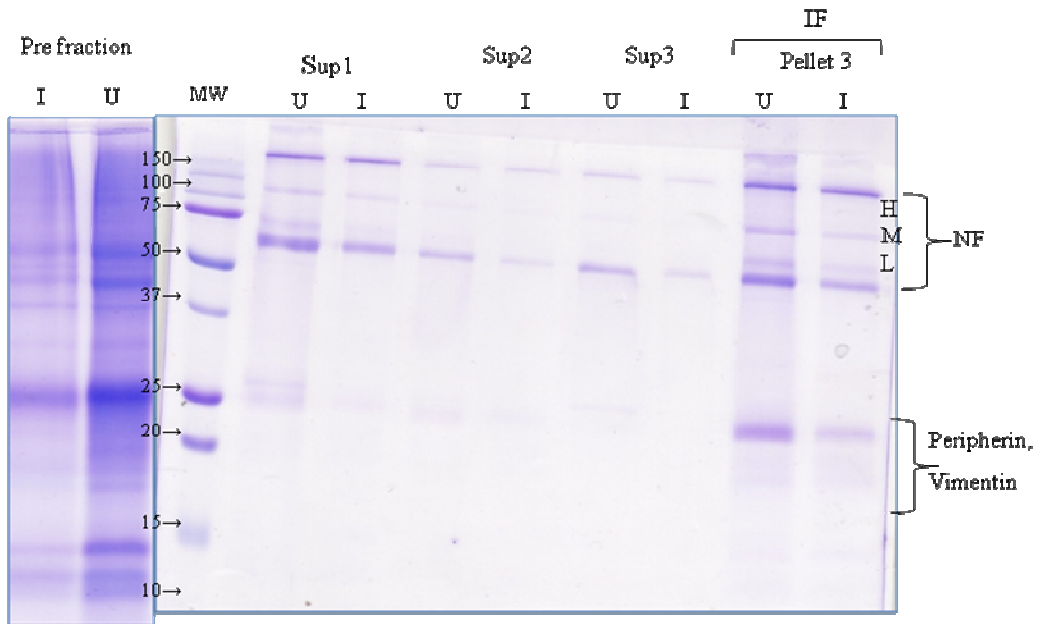
Figure 4.3: **Separation of nerve fractions from uninfected (U) and infected (I) animals.** SDS-PAGE of the pre-fraction, supernatant (Sup) 1, 2, 3 stained with Coomassie blue. The intermediate filament (IF) proteins enriched in the final pellet after ultracentrifugation of supernatants 1 and 3. The IF consists of neurofilaments (high H, medium M and low L).
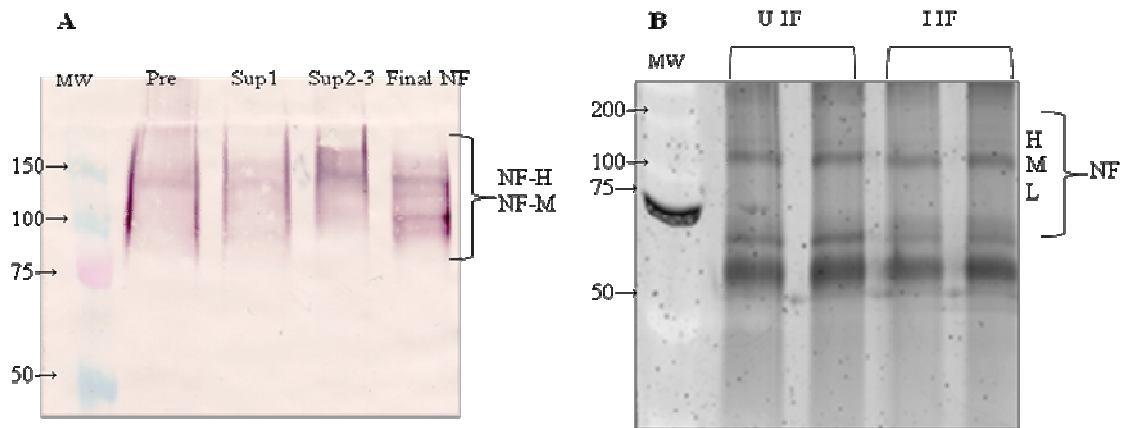
Figure 4.4: **Detection of neurofilament in the IFs fraction (the pre fraction, supernatant 1, 2, 3 and the final pellet)** using; **A-** Western bloting with anti-neurofilament (H and M) antibody as primary antibody and anti-mouse IgG as secondary antibody. **B-** Phosphate staining of the intermediate filament (IF) fractions from uninfected (U) and infected (I) nerves (30μg) by ProQ stain (Molecular Probes). The major phosphorylated IF proteins are stained, i.e. Neurofilaments H, M and L. No difference was found between the uninfected and infected neurofilaments based on the staining.

4.4.4 Protein post-translation modification

Since many nerve proteins are associated with different kinds of post-translational modifications (phosphorylation, glycosylation,..etc), we decided to look at changes in these modification patterns. Periodic acid-Schiff (PAS) stain was used to look for glycosylated proteins. The protein samples from the myelin and NF enrichment methods (buffer B) were used to look at the differences. The uninfected nerve lysate showed an extra dark band below 15 kD stained by PAS or silver nitrate (red arrow) that was not detectable in the infected lysate (**Figure 4.5 A).** The gel electrophoresis was repeated for the same nerve sample, the membrane was probed with lectin ConA to detect the glycoproteins as shown in **Figure 4.5 (B).** The same dark band in the uninfected nerve sample strongly reacted to ConA. There are other proteins that reacted differently in the infected nerve as indicated with black arrows.
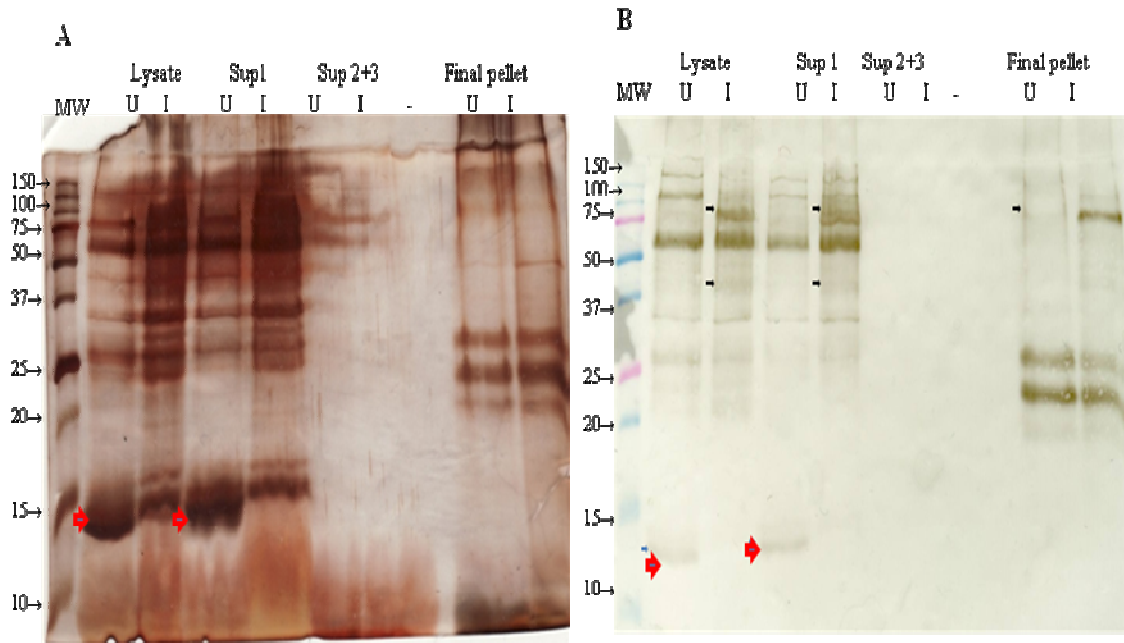
Figure 4.5: Detection of glycosylated components in armadillo uninfected and infected nerves. Total and partially fractionated nerves (lysates, supernatants and final IF pellet) were resolved by SDS-PAGE and **A**: stained with PAS and **B**: probed after transfer to nitrocellulose with ConA lectin. The darker bands in the uninfected nerve (below 15 kD) also reacted to ConA (red arrow). Other proteins that reacted differently to ConA in the infected nerve are indicated with black arrows.

4.4.5 Infected and uninfected two-dimensional electrophoresis (2DE) comparison and protein mapping

To improve separation and proteome coverage, and to provide reference maps, 2DE protein separation techniques were applied. The nerve samples homogenized in buffer (B) were used to detect the glycosylation changes in a 2D gel stained with PAS in **Figure 4.6**. The 2D gel profile was reproduced for nerves more than 5 times using different nerve lysate. Some protein spots around 15 kD did not have corresponding spots in the infected sample. The abundant spots in the uninfected nerve sample in **Figure 4.6** were characterized using LTQ LC-MS. We were able to characterize 45 proteins from searching the armadillo database and 44 proteins by searching mammal databases from 12 spots as summarized in **Table 4.4.** Some proteins were found in more than one spots and each spot has many protein hits. Some protein spots did not yield protein identification, due to the incomplete sequence annotation of the available armadillo genome, or the lack of homology between the armadillo and other mammalian genomes. Also, some proteins that based on their size, charge, posttranslational modifications, and hydrophobicity are not efficiently resolved by 2D analysis, such as some myelin proteins (myelin basic protein and myelin associated glycoprotein) **(Tayler C., 2004).**
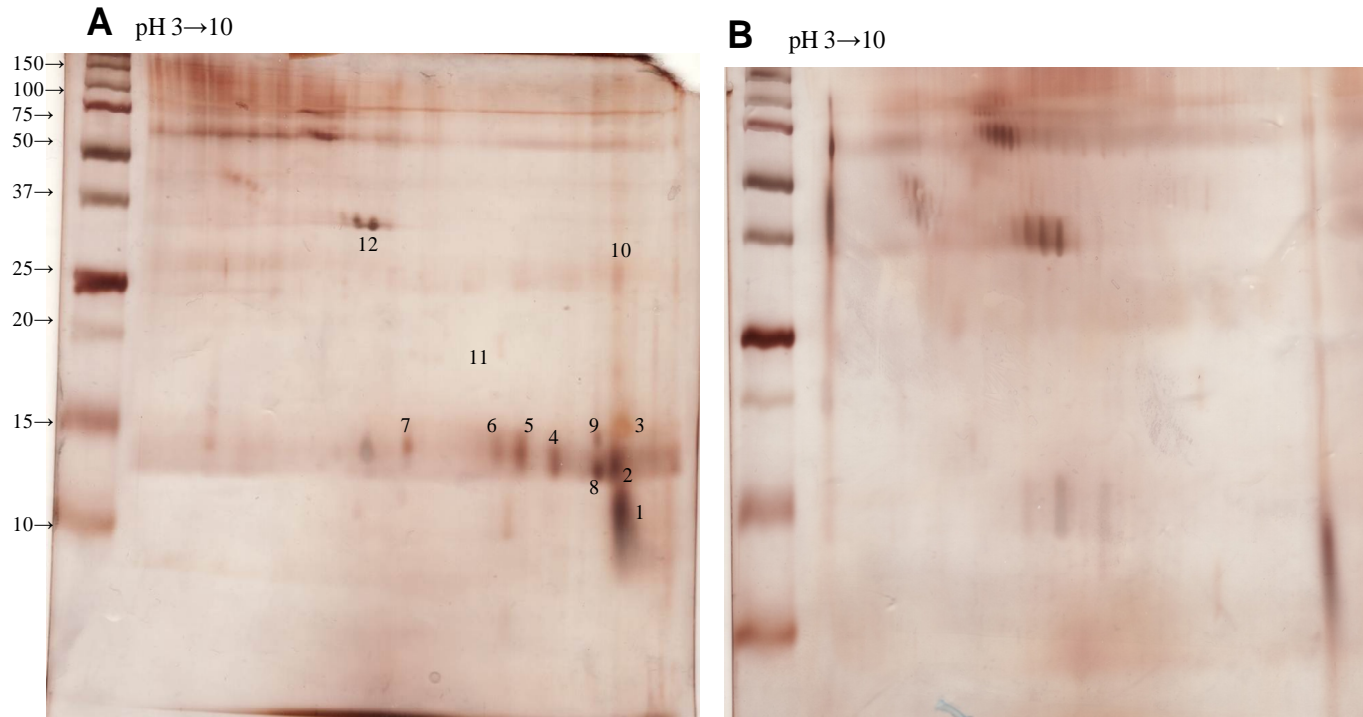
Figure 4.6: 2D gel of uninfected (A) and infected (B) nerve lysate, PAS stained. Tryptic peptides from uninfected protein

spots (1-12) were analyzed by ESI-MS/MS and searched against mammalian and armadillo databases (Table 4.4).

216

Table 4.4: Armadillo nerve protein mapping from 2D spots, searched against armadillo database (Ensembl 20090414 (4024 sequences); 1984269 residues) and mammal database (NCBInr 20081107 (7294643 sequences; 2525198067 residues)

	Armadillo database				Mammal database			
Spot #	Protein ID, size	Number of unique spectra	Percentage of coverage (%)	Accession number (ENSDNO)	Protein ID, size	Number of unique spectra	Percentage of coverage (%)	Accession number
Un-1	Type II cytoskeletal 1, 30kD	2	4.1	G00000003234	Hemoglobin subunit alpha, 15 kD	3	22	GI:122393
	Kelch-like ECH-associated protein 1 (chain precursor), 67	2	4.4	G00000004816	Serum albumin, 69 kD	3	3.5	GI:76363596
	Myelin P2, 13 kD	3		G00000002174	Hemoglobin subunit beta, 16 kD	2	21	GI:226875232
	Alpha1 chain precursor (collagen)	2		G00000001489	RNA polymerase II transcription subunit 1, 14 kD	2		GI: 272476910
					mRNA-associated protein41, 36 kD	2		GI: 226507080
Un-2*	Hemoglobin Beta, 15kD	8		G00000023773	Hemoglobin subunit alpha chain, 15 kD*	7, 6	43, 37	GI:122393
					Hemoglobin Beta, 16 kD*	8, 5	63, 45	GI:226875232
	Metavinculin, 94 kD	2	3.7	G00000002969	Serum albumin, 69kD*	9, 6	16, 12	GI:76363596, GI:1351907
	Protein 2,stomatin like protein, 39 kD	2	10	G00000001030	Similar to Fibrinogen gamma chain, 52 kD	3	13	GI:194208381
	Phosphodiesterase, 50kD	2	10	G00000000095	Chain A (FK506 binding protein,	2	25	GI:6682

					Isomerase, 12 kD			
	Globin like,12 kD	4	64	G00000023773				
	Profilin 1, 10 kD	2	20	G00000011649				
Un-3*	Con A family protein, 14 kD	2	14	G00000010626	Hemoglobin subunit alpha chain, 15 kD	2	22	GI:122393
	Myelin P2, 13 kD*	9, 4	58, 28	G00000002174	Myelin P2, 15 kD*	8, 9	45, 52	GI:126723169, GI:115497670
					Hemoglobin Beta, 16kD	6	44	GI:226875232
	Hemoglobin subunit beta, 12 kD	3	37	G00000023773	Serum albumin, 69 kD*	15, 3	28, 6.4	GI:1351907
	Hemoglobin subunit beta, 15 kD	8		G00000023773	Hemoglobin subunit alpha, 15kD*	7, 3	57, 22	GI:122393
Un-4	Type II cytoskeletal 1, 30 kD	3	14	G00000003234	Hemoglobin Beta, 16kD	8	61	GI:226875232
	B-cell lymphoma 9 protein. 127 kD	4	9.2	G00000002638	Similar to Fibrinogen gamma chain, 52 kD	4	13	GI:194208381
	Ligase domain, 50 kD	2	8.4	G00000002259	Serum albumin, 69 kD *	8, 18	12, 36	GI:76363596
	Myelin P2, 13 kD	2	15	G00000002174	Immunoglobulin kappa light chain, 11kD	3	15	GI:14625929
	Globin like,12 kD	3	28	G00000023773	Immunoglobulin lambda light chain variable region, 11 kD	2	30	GI:21310430

	Protein			Accession	Protein			Accession
	Peroxiredoxin, 19 kD	2	13	G00000018488				
	Hemoglobin subunit beta, 15 kD	8		G00000023773	Hemoglobin subunit alpha, 15 kD	7	57	GI:122393
Un-5	Alpha crystalline, 15 kD	14	79	G00000006781	Alpha-crystallin B chain, 20 kD	6	27	GI:126722693
	Domain contain protein80, 73 kD	2	4.2	G00000002178	Serum albumin-69 kD *	7, 14	10, 29	GI:76363596
	Muscle type (phosphohexokinase) 77 kD	2	5.5	G00000004291	Hemoglobin Beta, 16kD	8	58	GI:226875232
	C3 and PZP like-macroglobulin, 123 kD	2	2.4	G00000004709	Fibrinogen A-alpha chain, 50 kD	3	16	GI:3789960
	Dynein heavy chain12	2		G00000000327				
	S100-A11, 8 kD	2	38	G00000005442				
	Hemoglobin subunit beta, 12 kD	8	81	G00000023773	Hemoglobin subunit alpha chain, 15 kD	8	57	GI:122393
Un-6	Con A family protein, 14 kD	2	19	G00000010626	Hemoglobin Beta, 16kD	9	69	GI:226875232
	Myelin protein 2,13 kD	2	17	G00000002174	Serum albumin, 69 kD	4	7.9	GI:1351907
	Lectin, galactoside-binding, 14 kD	3	32	G00000024830				
	alpha-fetoprotein, 69 kD	2	3.6	G00000011444				
	Hemoglobin subunit beta, 12 kD	9	81	G00000023773	Hemoglobin subunit alpha chain, 15 kD	2	19	GI:122393
Un-7*	Myelin protein 2, 13 kD	7	52	G00000002174	Hemoglobin Beta,	8, 5	60, 39	GI:226875232

				16 kD*			
	Lectin, galactoside-binding, 14 kD	4	32	G00000024830	Myelin protein 2, 15 kD	6	36	GI:126723169
	Con A family, 14 kD	7	21	G00000010626	Fatty acid binding protein 4, adipocyte, 15 kD	2	33	GI:109086789
	Haptoglobin, 39 kD	6	13	G00000006694	Similar to epidermal fatty acid-binding protein, 15 kD	2	22	GI:149721423
	Globin like, 12 kD	6	68	G00000023773	Similar to SH3 domain-binding glutamic acid-rich-like protein, 15 kD	2	21	GI:109131389
	Acid binding protein 4, adipocyte, 15 kD [2]	2	25					
	Acid binding protein 5 (psoriasis-associated), 15 kD	4	49					
	Hemoglobin alpha, 15 kD	8		G00000023773	Hemoglobin subunit alpha, 15 kD	7	37	GI:122393
	Myelin P2, 13 kD	2		G00000002174	Hemoglobin Beta, 16 kD	9	56	GI:226875232
Un 8	Alpha-1 chain Precursor (collagen), 89 kD	2	6	G00000001489	Serum albumin, 69 kD	6	10	GI:76363596
	mRNA-associated protein 41, 37 kD	2	17	G00000003627	Peripheral myelin P2, 15 kD	2	14	GI: 109086785
	Ribonucleoside-diphosphate (reductase	2	16	G00000000042				

	subunit M2), 35 kD						
	Hemoglobin subunit beta, 12 kD	5	52	G00000023773	Hemoglobin Beta, 16 kD	4	41	GI:226875232
					Myelin protein P0, 28 kD	3	11	GI:127722
Un-10*					Immunoglobulin kappa light chain variable region, 11 kD	3	15	GI:14625929
					Immunoglobulin lambda light chain variable region, 10 kD	2	30	GI:21310430
					Serum albumin, 69 kD	15	29	GI:1351907
					Neurofilament 3 (medium), 103 kD	3	4.1	GI:109085914
Un-11	Albumin, 70 kD	7	12		Serum albumin, 69 kD	2	21	GI:1351907
Un-12	Neurofilament, medium polypeptide, 83 kD	3	5.1		F-actin capping protein alpha-1 subunit, 33 kD	3	15	GI:109013601
					Haptoglobin, 48 kD	4	6.6	GI:283467275

* Identified from two gels.

Based on the 2DE profile and the mass spectrometry data, several spots contained more than one protein. For example, there are several different proteins that correspond to the darker bands around 15 kD found in the 1D gels. Examples of these proteins that were identified by mass spectrometry and have a molecular weight around 15 kD; hemoglobin (15 kD), myelin P2 protein (15 kD), fatty acid binding protein 4 and 5 (15 kD), crystallin, alpha B (15 kD) and ConA family (14 kD). Almost all of them have certain kind of post-translation modifications as listed in **Table 4.5**, which may explain the different staining and reactivity seen in PAS stained 1D gel between uninfected and infected nerves.

Table 4.5: Major characteristic features of some nerve proteins

Protein	comment
Hemoglobin subunit alpha, 15 kD	Glycosylation of hemoglobin at the N-terminus of the beta chain as well as at the N-terminus of the alpha chain and at certain lysine residues[1].
Myelin P2 protein, 15 kD	Autoantigen, induce experimental autoimmune neuritis (EAN), bind to fatty acids (oleic acid, retinoic acid and retinol)[2,3]
Fatty acid binding protein 4, adipocyte, 15 kD	FABP4 regulate efflux and influx of fatty acids in the adipocyte in response to anabolic and catabolic conditions[4].
Acid binding protein 5 (psoriasis-associated), 15 kD	These proteins are thought to facilitate the transfer of fatty acids between extra- and intracellular membranes[4].
Myelin protein P0; Myelin protein zero; (MPZ); 28 kD	Autoantigen, it can be phosphorylated, acylation in the region (amino acids 110–119), glycosylation with single, nine-sugar chain through *N*-glycosidically linked to asparagine[3,5].
Crystallin, alpha B, 15 kD	Autoantigen, has N-terminal acetylation of αA-crystallin. Phosphorylation of α-B-crystallin at Ser 45, Ser 19, and Ser 59 [6].
Con A family, 14 kD	The galectins are a family of beta-galactoside-binding proteins implicated in modulating cell-cell and cell-matrix interactions, immune response associated with natural killer (NK) and lymphokine-activated killer (LAK).

1-(Woodi, Murali., 2009), 2- (Rostami, A., 1984), 3- (Inglis, H R., 2007)
4- (Chmurzyńska A, 2006), 5- (Suneetha, L M., 1998)
6- (Bahk, Song-chul, 2007)

4.4.6 Humoral immune responses in *M. leprae* infected tissue

The infected armadillo tissues were used to detect and purify IgG antibody. The

unbound immunoglobulins (flow through) were collected for identifying IgM. The flow

through and eluates were tested by Western blot analyses using human polyvalent Ig

antibodies (anti-IgM and anti IgG). Infected armadillo tissues (nerve and spleen) were

found to have increased level of the putative immunoglobulins (IgG/ IgM) compared to uninfected tissue based on Western blot of the tissue lysate shows in **Figure 4.7 A.** The IgG was purified from both infected and uninfected tissue samples and analyzed by Western blot with anti-IgG antibody. The gel of the infected nerve tissue shows that the IgG molecule was purified **(Figure 4.7 B)** compared to IgG from uninfected which was undetectable.
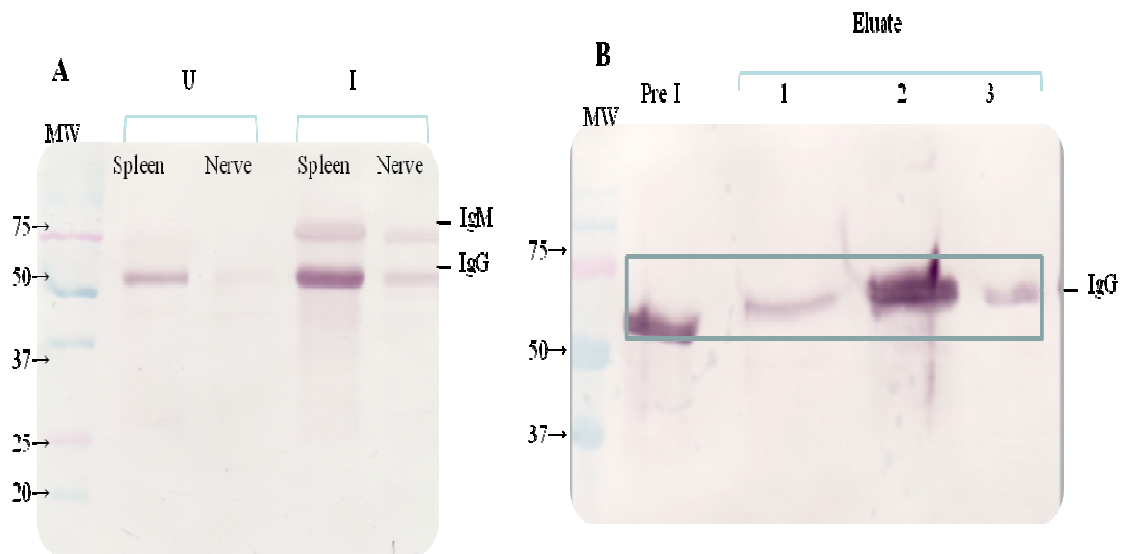
Figure 4.7: Detection of immunoglobulins in the infected tissues before and after column purification. (A) Western blot of nerve and spleen from uninfected (U) and infected (I) lysate probed only with secondary Ab anti-human polyvalentimmunoglobulins. **(B)** The Infected nerve lysate (pre-fraction) and Ig fractions (eluate 1, 2 and 3) after protein A/G spin column purification probed with anti-IgG**. The immunoglobulin (IgG) was successfully isolated from the infected tissues (nerve and spleen).

In order to further confirm the purity and identity of the immunoglobulin(s), the eluate fraction from the protein A/G affinity chromatography column and the flowthrough from the column were resolved by 1D SDS-PAGE, and stained with Coomassie blue. The identified bands were excised and subjected to in-gel trypsin digestion and analyzed by ESI-LC/MS. Querying the mammalian database for peptides derived from both 50 and 25 kD bands, resulted in matches to the immunoglobulin gamma heavy and light chain, respectively. Also, from searching the peptides from 25 and 50 kD bands against a mycobacteria database (Mycobacterium NCBInr 20081107 (7294643 sequences; 2525198067 residues), the 65 kD antigen (gi|149924, gi|15827082) (Heat shock protein 65 or GroEL-2) was identified in both protein bands (25 and 50 kD). The 75 kD bands (flowthrough) matched with albumin based on mammal database search, and cytochrome P450 (gi|145224060), 65 kD antigen (gi|149924), hypothetical protein Rv1025 (gi|15608165) and hypothetical protein Rv0756c (gi|15607896) based on mycobacteria database search as shown in **Figure 4.8.** All the proteins identified were above the cut off score >39 with significant threshold ($p<0.05$).
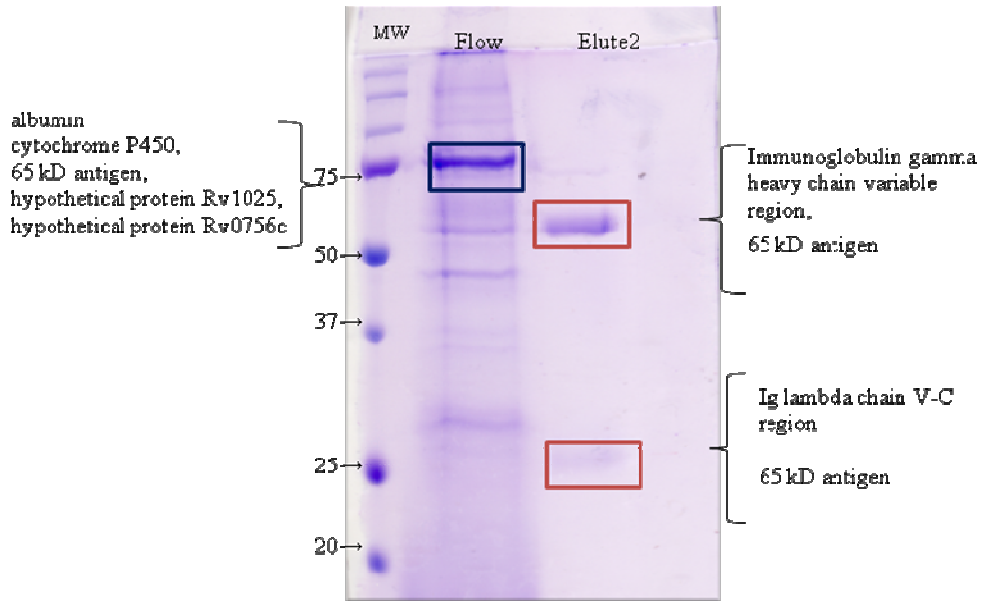
Figure 4.8: Analyzing the proteins after immunoglobulin purification from Protein A/G affinity chromatography using Coomassie blue stained SDS-PAGE gel. The flowthrough band (75 kD) and eluate fraction from the column (elute2) bands (50, 25 kD) were subjected to protein identification by peptide mass fingerprinting. It confirmed the identity of the immunoglobulin purified (IgG) and the tentative mycobacterium targets.

4.4.7 Searching for antibodies against nerve components

Similarity between the host and pathogen proteins can stimulate immune cells, resulting in auto-antibodies against lesion and nerve components such as myelin proteins which have similarity to *M. leprae* proteins. Many nerve proteins are antigenic and in leprosy patients, especially the LL form can develop auto-antibodies against proteins in the nerve. In order to test this theory, the nerve components prepared from both infected and uninfected nerves were probed with IgG antibody prepared from pooled serum of LL patients as a primary antibody and anti-IgG as a secondary antibody. The result depicted in **Figure 4.9,** shows that the same extra bands (of the same size) that were stained with PAS and reacted to ConA in the uninfected nerve (**Figure 4.5**) were also recognized by the leprosy patients IgG. Taken together all these findings, suggest that the protein(s) that is more abundant in the uninfected nerve and decreased during infection could be glycosylated and antigenic.
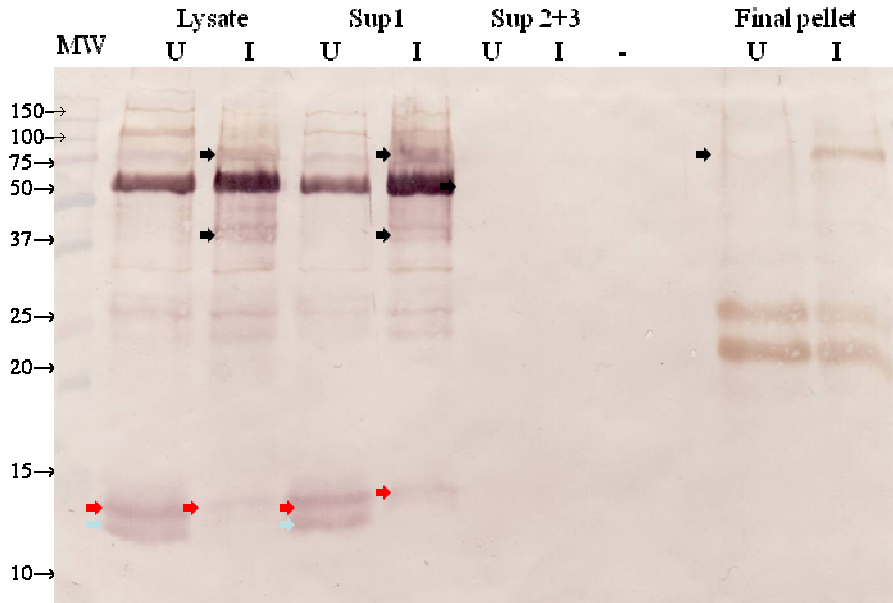
Figure 4.9: Detection of reactivity of the purified IgG from patient sera to nerve proteins. The uninfected and infected nerve lysate and supernatants (sup1, 2, 3) and final IF pellet of nerve protein fractions showed similar reactivity to LL sera (purified IgG). However, there are a few bands that show differential reactivity (such as those indicated with red arrow (in both uninfected and infected nerve but strong reactivity in uninfected), blue arrow (stronger in uninfected) (below 15 kD) and black arrows (high molecular weight stronger in infected).

Finally, another experiment was done to confirm the reactivity of the patient serum
(IgG) antibody to the nerve protein (~15 kD) and to identity this protein. Based on mass
spectrometry data, proteins in the region around 15 kD contained hemoglobin, ConA
family protein, acid binding proteins and myelin P2. Since myelin P2 is known to be
antigenic in other neuropathy diseases, anti-Myelin P2 antibody was tested against the
nerve lysate and compared to the reactivity of leprosy IgG and PAS staining as shown in
Figure 4.10 (A, B).
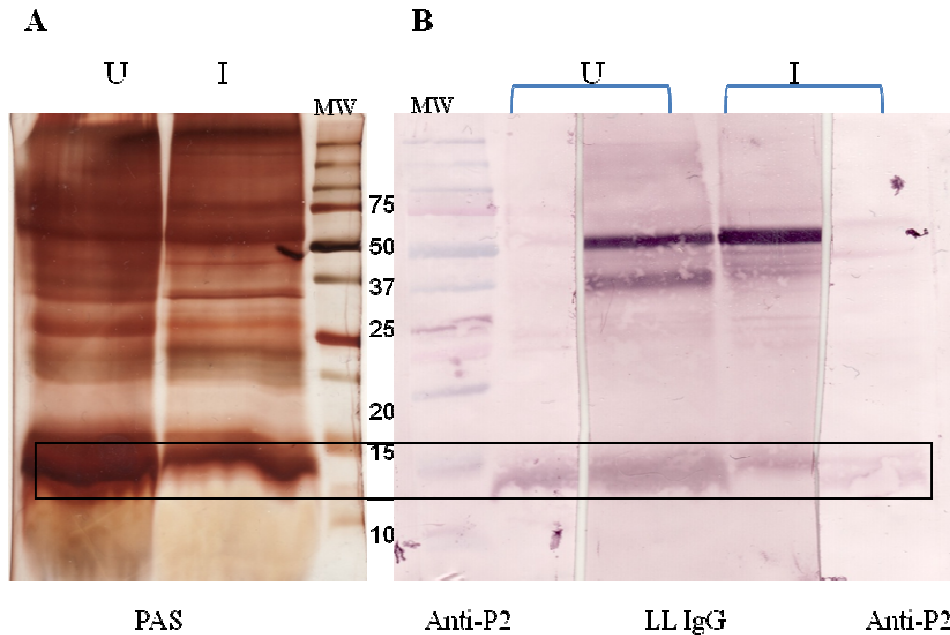
Figure 4.10: **Confirm the reactivity of the patient serum (IgG) antibody to the nerve
protein (~15 kD) in comparison to anti-P2 antibody and PAS stain.** (A) Infected and
uninfected nerve lysate stained with PAS. (B) Western blot for infected and uninfected
nerve separated in a wide lane gel probed with either anti-P2 (1:500) as a primary and anti-
rabbit (1:5000) as secondary or with purified IgG from LL sera as primary (1:500) and

anti-human IgG as secondary antibody. The bands of about 15 kD stained dark by PAS and reacted to anti-myelin P2 and patient IgG antibodies.

Additional confirmation was obtained by using a recombinant purified myelin P2 protein (human) to test the serum of leprosy patients. Several patient sera ranging from low bacterial index (BI), paucibacillary (PB) to high BI multibacillary (MB) were selected and tested. All the sera that were selected showed a reaction to the myelin P2 protein **(Figure 4.11).**
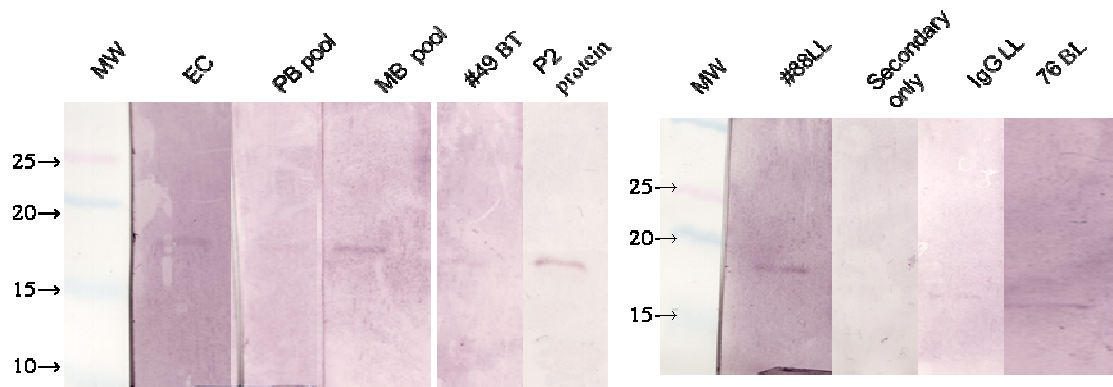
Figure 4.11: **Recombinant myelin P2 protein (200ng/lane) reacted with different leprosy patient serum** as primary antibody (1:1000) (illustrated on top of each strip), secondary is anti-human polyvalent, as control myelin P2 was tested against its antibody, and another control for the secondary antibody only (anti-human polyvalent). All tested serum (Pooled of PB or MB, individual BT, LL and BL and the endemic control tested (EC)) showed reactivity to the myelin P2 protein with different strength/intensities.

4.5. DISCUSSION

Mycobacterium leprae has a unique tropism for the peripheral nervous system (PNS), it grows within Schwann cells (SCs) that surround the axons of the peripheral nerves. Although several mechanisms used by *M. leprae* to invade the host cells have been discovered, mechanisms associated with nerve damage after entry are in question. To understand the host-pathogen interaction in the peripheral nerve that leads to nerve damage, the armadillo leprosy model was used. Proteomics approach was applied to identify differences in infected nerves compared to uninfected armadillo nerves. The first pilot reference protein map of armadillo peripheral nerve (sciatic) was created based on the available armadillo database (2X coverage). Based on the armadillo database, almost all of the proteins identified from the 1D gel profile are peripheral nerve proteins. The predominant peripheral nerve proteins that were identified were myelin P0, myelin P2, periaxin, neurofilaments (NFs), tubulin, vimentin and peripherin. Comparing the 2DE nerve protein profile showed fewer spots in the infected nerves compared to the uninfected. A further humoral study identified increased levels of IgG in infected nerves. In addition, leprosy patient serum was shown to contain antibody against the nerve component (myelin P2).

Peripheral nervous system (PNS) myelin is enriched in glycoproteins and basic proteins **(Garbay B., 2000).** There are more than 45 different proteins found in PNS myelin, however the genes responsible for demyelination in many neuropathies are unknown. The major PNS protein is myelin protein-zero (P0, 28 kD) (50-60%), peripheral

myelin protein 22 (PMP-22 kD), myelin basic protein (MBP) (15%) and myelin P2 account for 10%; both MBP and P2 are localized at the cytoplasmic side. Other high molecular mass glycoproteins present in small amounts are periaxin-170 kD and the 100 kD myelin-associated glycoprotein (MAG).

Myelin P0 a highly conserved protein among species, has a variety of post-translation modifications, such as phosphorylation, acylation in the amino acids 110–119, and glycosylation with a single, nine-sugar chain linked to asparagine 93 **(Garbay B., 2000).** MBP in PNS has four polypeptide bands ranging between 14-21 kD. It has a variety of post-translation modifications such as phosphorylation and methylation and it is one of the major autoantigens in multiple sclerosis. Myelin P2 is a small protein (14 kD), with a high positive charge. It is a member of a family of fatty acid-binding proteins, with a high affinity for oleic acid**,** retinoic acid and retinol. P2 is also an autoantigen in a peripheral autoimmune neuropathy, known as Guillain Barre Syndrome (GBS). Its function is related to stabilizing the myelin membrane dynamics and lipid transport to and from the membrane (**Suresh S., 2010**). A majority of patients with autoimmune diseases such as in chronic inflammatory demyelinating polyneuropathy (CIDP) develop antibody to myelin proteins; P0, P2, or PMP-22 **(Sanvito L., 2009).** Also, antibody to MAP was found in Guillain-Barre Syndrome (GBS) together with elevated antibodies to P2, which were also detected in some patients with CIDP and other neurological diseases (OND) **(Quarles, R H., 1990).** IgG antibody against different peptides of myelin P2 were found to be significant in CIDP patients compared to healthy control. These myelin P2 peptides were found to stimulate production of cytokines such as IL-10 and IL-4 in CIDP patients. In

CIDP disease myelin P2 was found to be a target antigen for both humoral and cellular immunity (**Sanvito L., 2009, Makowaska A., 2008).**

The pathogenesis associated with SC is nerve injury and demyelination. These could be due to axonal damage and disruption of axonal-SCs signals. Another cause is the immune stimulation (autoimmune) that target the myelin proteins, such as in multiple sclerosis and Guillain-Barre Syndrome (GBS). Auto-antibodies have been found not only in chronic diseases, but also in infectious diseases such as Lyme disease that is caused by *Borrelia burgdorferi*. Many post-Lyme disease syndrome (PLS) patients found to have increased levels of anti-neural antibody **(Chandra A., 2010).** Like autoimmune disorders, *M. leprae* causes demyelination of the peripheral nerve that starts by damaging the myelin sheath and decreasing the action-potential conduction velocity (**Rambukkana A., 2004**).

One of the reasons for auto-antibody production during infection is the similarity between pathogen and host components or molecular mimicry. The other theory is the exposure of intracellular nerve antigens during demyelination. Several auto-antibodies were found to be of significant in leprosy patients. For example, some leprosy patients have a high frequency of antibodies against proteins in neural intermediate filaments **(Lefford M., 1989).** Anti-nuclear antibody (ANA), anti-double stranded DNA (dsDNA), anti-single stranded DNA (ssDNA), anti-nuclear antigen (anti-ribonucleoprotein (nRNP), anti-Smith and anti-histone (AHA) have been found to be elevated in LL patients in India (**Paradhan V., 2004).** Anticardiolipin antibodies (aCL) antibodies and anti-β2

glycoprotein I antibodies and anti-β2 glycoprotein I (GPI) antibodies were significantly higher in leprosy patients examined in Brazil **(Ribeiro S., 2011).**

Antibodies to neuronal glycolipids or to glycosphingolipids that are expressed as surface determinants of myelin such as ceramide were studied in India. Significant increase of anti-ceramide IgM antibody was found in MB leprosy patients in comparison to both endemic controls (non-leprosy) and PB leprosy patients (**Singh, K., 2010).** Another anti-glycolipids antibody is anti-sulfatide (cerebroside) IgM subtype that was found to be elevated in MB or lepromatous patients. These two antibodies are associated with various demyelinating peripheral polyneuropathies. The demyelination is caused through inhibition of the synthesis of sulfatide expressed on myelin surface. Auto-antibodies to antigenic epitopes of myelin proteins especially to myelin P2 have been reported in many chronic demyelination diseases **(Rostami A., 1984, Sanvito L., 2009).** However, to our knowledge it has not been previously reported in leprosy patients before.

Comparative proteomic analysis using two-dimensional polyacrylamide gel electrophoresis (2DE) is a powerful tool for identifying changes in the expression pattern of proteins in response to infection. This may lead to biomarker discovery, which can then lead to understanding the pathway and the mechanisms of host-pathogen interaction.

M. leprae is an intracellular pathogen that interacts and replicates inside the host cells in the PNS. As a result of this interaction, it can modify the expression of the host cell proteins. To uncover the bacterial effect on the host nerve proteins, 2DE was used followed

by ESI LC-MS/MS identification of nerve proteins of armadillo PNS. The first goal was to establish a preliminary library of armadillo peripheral nerve protein (new model for nerve damage). The second goal was to compare the protein profiles of infected and uninfected nerves. Using the Ensembl armadillo database, we identified several nerve proteins from both 1D and 2DE gels. Several of the anti-human or mouse antibodies in this study were also found to have cross reactivity to armadillo, such as anti human IgG, anti-IgM, anti human-NF, anti-myelin P2.

Comparing the protein profile between infected and uninfected nerve, we found decreased amount of proteins around 15 kD in infected tissue. One of these proteins could be myelin P2 based on mass spectrometry and antibody testing. Its decrease during infection could be due to nerve demyelination caused by *M. leprae*. The protein bands that were found in uninfected armadillo nerves (in PAS gel) and absent in the infected nerve, could be hemoglobin α and β subunits, ConA family protein, crystallin α, and/or fatty acid binding proteins. Based on mass analysis of the 2D spots around 15 kD, all those proteins have molecular weight of 15 kD and known post-translational modifications. Hemoglobin α and β (15 and 16 kD) a common contamination in the PNS was not separated from myelin P2. Hemoglobin was also found to be glycosylated at the N-terminus of the beta and alpha chain and at certain lysine or valine residue **(Woodi, M., 2009)**, which explains its staining by PAS and ConA. Fatty acids binding proteins transport the fatty acids from the plasma membrane to the cytoplasm by an aqueous diffusion-mediated process. FABP4 is mainly in adipocytes, FABP5 also called psoriasis-associated FABP (PAFABP) is

mainly found in the epidermal, FABP8 also called myelin P2 is predominant in peripheral nervous system **(Chmurzyńska, A., 2006).**

We also found high level of antibodies (IgG, IgM) in infected armadillo tissues. The IgG from the infected tissue was isolated using protein A/G spin column (Pierce, USA) and its identity was confirmed by mass spectrometry. This is in agreement with the correlation between the bacterial load and the humoral immune response **(Touw J., 1982).** However, the target for this antibody has not been confirmed, yet. Several experiments were done using bacterial (*M. leprae* cell lysate) and host components (nerve, liver and spleen lysate) without any success. Moreover, the analysis of the purified antibody (IgG) from infected nerve by mass spectrometry, showed the presence of mycobacterial Ag 65 (hsp 65). The antibody in the infected tissue that could be generated against *M. leprae* antigen could also cross react with other host tissue components. For example, the antibody generated against mycobacterial 65kD- heat shock protein was found to have cross reactivity to the human epidermal cytokeratin **(Rambukkana A., 1992)** and also to human heat shock protein 60 (hsp 60). It was reported that *M. leprae* HSP has up to 50% gene sequence identity with their human analogues (**Njoo D., 2003**). Many studies pointed to the increase of plasma cells and antibodies in leprosy skin lesion especially in the LL form **(Iyer, A. M., 2007, Parkash O.M., 1997).**

Also, the serological study (patient sera) showed the presence of antibodies in the MB, PB sera that recognize proteins migrating at 15 kD. Based on mass spectrometry (1D and 2D analysis) the predominant proteins are myelin P2 (13 kD), hemoglobin (15 kD) and

fatty acid binding proteins (15 kD). Recombinant purified human myelin P2 (18 kD), was recognized by purified IgG from a pool of patient serum, suggesting it is at least one component in this band (15 kD). All these observation could lead to the nerve damage found in leprosy. The detection of the anti-myelin P2 in leprosy (LL) sera (IgG), and the presence of this auto-antibody in other autoimmune neuropathies, strongly suggests the role of this antibody in the pathogenesis (nerve damage) of the disease. The antibody response which occurs in patients with leprosy is generally ineffective against the bacteria. The significance of this response is not clear and could involve reactions to cell debris after apoptosis.

The development of this proteomic map for armadillo, offers a major advance for investigations the mechanisms of leprosy using the only animal model for this disease.

4.6.   FUTURE DIRECTIONS

Further studies are needed to complete the work started here in armadillo proteomic and nerve damage in leprosy. The protein mapping of armadillo nerve proteins should continue to create a master library of the armadillo proteome. Examine and quantify the myelin proteins after myelin enrichment from both uninfected and infected nerve (at different disease stages) to determine which myelin proteins decrease after demyelination. Further analysis of post-translation modification of nerve proteins after enrichment for modified peptides (glycosylated and phosphorylated) is required. Compare uninfected nerve fraction to infected nerve fraction in term of numbers of modified peptides by quantitative-mass spectrometry.

Proteomic analysis of the infected tissues resulted in finding increased immunoglobulin IgG and IgM deposited in the nerve and spleen. Mass spectrometry analysis of purified IgG confirmed the presence of the immunoglobulin together with Ag65 (hsp) from mycobacteria. However, several experiments were done to find the antibody targets such as nerve, *M. leprae* lysates without any success. Further experiments are needed to find the targets for the antibodies (IgM and IgG) in the infected tissues. These experiments include fluorescently labeling the isolated antibodies and testing their reactivity to the infected tissue using immunohistochemistry. Another test is to analyze the reactivity of the purified IgG to different *M. leprae* cell fractions or mycobacterium antigens by Western blot and immunochemistry.

Purified serum IgG from leprosy patients was found to react with different bands (protein) on the 1D gel of the nerve lysate. One of these protein bands was found to be myelin P2 based on mass spectrometry, recognition by myelin P2 antibody and recombinant myelin P2 protein testing. Further experiments could be done to find the identity of other nerve proteins that reacted with the serum. Furthermore, different leprosy patient sera from different group (low and high BI) were found to react to the myelin P2 protein. These preliminary findings of antibodies in the leprosy patients against the nerve major components such as myelin P2 could open a new research area in leprosy. Antibodies generated against *M. leprae* proteins that are homologues to nerve components have been found in leprosy **(Ribeiro S., 2011).**

Further experiments with larger sample (sera) size from different leprosy group (LL, BT, BB and TT) including reaction and non-reaction state and control sera (no leprosy) are needed. These experiments will help to differentiate the frequency of the auto-antibody in these groups. Also, the titer of the auto-antibody found could be tested in these groups using ELISA. Moreover, in a way to demonstrate the relationship between this "auto-antibody" and the nerve injury in leprosy a biological experiment is needed. This could be done through the *in vitro* system such as SCs-neuron co-culture. The experiment will require two cultures infected with *M. leprae*, one treated with the purified IgG antibody from leprosy sera and the other kept as untreated infected culture. The cultures will be examined to determined the rate of de-myelination.

These studies will help in understanding the pathogenesis of leprosy and the nerve damage that occurs in the disease and whether the nerve damage is antibody mediated. It also has significant implication as a diagnostic tool or therapeutic intervention.

References

1. Harboe M, Aseffa A, Leekassa R (2005) Challenges presented by nerve damage in leprosy. Lepr Rev 76: 5-13.

2. Barker LP (2006) *Mycobacterium leprae* interactions with the host cell: recent advances. Indian J Med Res 123: 748-759.

3. Rambukkana A (2000) How does *Mycobacterium leprae* target the peripheral nervous system? Trends in Microbiology 8: 23-28.

4. Suneetha LM, Satish PR, Suneetha S, Job CK, Balasubramanian AS (1997) *M. leprae* binds to a 28-30-kDa phosphorylated glycoprotein of rat peripheral nerve. Int J Lepr Other Mycobact Dis: official organ of the International Leprosy Association 65: 352-356.

5. Suneetha LM, Satish PR, Korula RJ, Suneetha SK, Job CK, et al. (1998) *Mycobacterium leprae* binds to a 25-kDa phosphorylated glycoprotein of human peripheral nerve. Neurochemical research 23: 907-911.

6. Suneetha LM, Singh SS, Vani M, Vardhini D, Scollard D, et al. (2003) *Mycobacterium leprae* binds to a major human peripheral nerve glycoprotein myelin P zero (P0). Neurochemical research 28: 1393-1399.

7. Spierings E, Boer T De, Zulianello L, Ottenhoff TH (2000) Novel mechanisms in the immunopathogenesis of leprosy nerve damage: the role of Schwann cells, T cells and *Mycobacterium leprae*. Immunology and cell biology 78: 349-355.

8. Save MP, Shetty VP, Shetty KT, Antia NH (2004) Alterations in neurofilament protein(s) in human leprous nerves: morphology, immunohistochemistry and Western immunoblot correlative study. Neuropathol Appl Neurobiol 30: 635-650.

9. Pant HC (1988) Dephosphorylation of neurofilament proteins enhances their susceptibility to degradation by calpain. The Biochemical journal 256:665-810.

10. Birdi TJ, Antia NH (2003) Mechanisms involved in peripheral nerve damage in leprosy with special reference to insights obtained from in vitro studies and the experimental mouse model. Int J Lepr Other Mycobact Dis: official organ of the International Leprosy Association 71: 345-354.

11. Spierings E, Vlieger M de, Brand a, Klatser PR, Ottenhoff TH (1999) Antibodies to sulfatide in leprosy and leprosy reactions. Am J Trop Med Hyg 61: 495-499.

12. Singh K, Singh B, Ray PC (2010) Original Article Anti-ceramide antibodies in leprosy : marker for nerve damage. J Infect Dev Ctries 4:378-381.

13. Ribeiro SL, Pereira HL, Silva NP, Souza AW, Sato EI (2011) Anti-β2-glycoprotein I antibodies are highly prevalent in a large number of Brazilian leprosy patients. Acta reumatológica portuguesa: 36: 30-37.

14. Raju R, Devi SK, Mehervani C, Kumar a S, Meena a K, et al. (2011) Antibodies to myelin P0 and ceramide perpetuate neuropathy in long standing treated leprosy patients. Neurochemical research 36: 766-773.

15. Adams JE, Peña MT, Gillis TP, Williams DL, Adams LB, et al. (2005) Expression of nine-banded armadillo (Dasypus novemcinctus) interleukin-2 in E. coli. Cytokine 32: 219-225.

16. Truman RW and Sanchez RM (1993) Armadillos: Models for leprosy. Lab Animal 22: 28-32.

17. Woodi M, Mondal AK, Padmanabhan B, Rajagopalan KP (2009) Analysis Of Protein Posttranslational Modifications By Mass Spectrometry : With Special Reference To Haemoglobin. Consultant 24: 23-29.

18. Rostami A, Brown MJ, Lisak RP, Sumner AJ, Zweiman B, et al. (1984) The role of myelin P2 protein in the production of experimental allergic neuritis. Annals of neurology 16: 680-685.

19. Inglis H R, Csurhes P, McCombe P (2007) Antibody responses to peptides of peripheral nerve myelin proteins P0 and P2 in patients with inflammatory demyelinating neuropathy. J Neurol, Neurosurg Psychiatry 78: 419-422.

20. Chmurzyńska A (2006) The multigene family of fatty acid-binding proteins (FABPs): function, structure and polymorphism. J Appl Genet 47:39-48.

21. Bahk S, Jang J, Choi C , Lee S , Park Z, et al. (2007) Post-Translational Modification of Crystallins in Vitreous Body from Experimental Autoimmune Uveitis of Rats research articles. J Proteome Research 6: 3891-3898.

22. Garbay B, Heape a M, Sargueil F, Cassagne C (2000) Myelin synthesis in the peripheral nervous system. Progress in neurobiology 61: 267-304.

23. Suresh S, Wang C, Nanekar R, Kursula P, Edwardson JM (2010) Myelin basic protein and myelin protein 2 act synergistically to cause stacking of lipid bilayers. Biochemistry 49: 3456-63.

24. Sanvito L, Makowska A, Mahdi-Rogers M, Hadden RDM, Peakman M, et al. (2009) Humoral and cellular immune responses to myelin protein peptides in chronic inflammatory demyelinating polyradiculoneuropathy. J Neurol Neurosurg Psychiatry 80: 333-8.

25. Quarles RH, Ilyas A a, Willison HJ (1990) Antibodies to gangliosides and myelin proteins in Guillain-Barré syndrome. Annals of neurology 27: S48-52.

26. Makowska A, Pritchard J, Sanvito L, Gregson N, Peakman M, et al. (2008) Immune responses to myelin proteins in Guillain-Barré syndrome. J Neurol Neurosurg Psychiatry 79: 664-671.

27. Chandra A, Wormser GP, Klempner MS, Trevino RP, Crow MK, et al. (2010) Anti-neural antibody reactivity in patients with a history of Lyme borreliosis and persistent symptoms. Brain, Behav Immun 24: 1018-1024.

28. Rambukkana A (2004) *Mycobacterium leprae*-induced demyelination: a model for early nerve degeneration. Curr Opin immunol 16: 511-518.

29. Lefford MJ (1989) Anti-neural antibodies in leprosy sera : further characterization of the antigen ~. PoLAR 21: 125-135.

30. Pradhan V, Badakere SS, Shankar Kumar U (2004) Increased incidence of cytoplasmic ANCA (cANCA) and other autoantibodies in leprosy patients from western India. Lepr Rev 75: 50-56.

31. Touw J, Langendijk EM, Stoner GL, Belehu A (1982) Humoral immunity in leprosy: immunoglobulin G and M antibody responses to *Mycobacterium leprae* in relation to various disease patterns. Infect Immun 36: 885-892.

32. Rambukkana A, Das PK, Krieg S, Yong S, Poole ICLE, et al. (1992) Mycobacterial 65,000 MW heat-shock protein shares a carboxy-terminal epitope with human epidermal cytokeratin 1/2. Immunol 77: 267-276.

33. Njoo D, Hu RVP (2003) Detection of shared antigenic determinants between *Mycobacterium leprae* heat shock protein 65 and human heat shock protein 60. Hansen. Int. 28: 31-43.

34. Iyer AM, Mohanty KK, Egmond D van, Katoch K, Faber WR, et al. (2007) Leprosy-specific B-cells within cellular infiltrates in active leprosy lesions. Human pathol 38: 1065-1073.

35. Parkash O, Beuria MK, Girdhar BK, Katoch K, Sengupta U (1997) Efforts in diagnosing early leprosy using serological techniques. J Bioscien 22: 111-116.

CHAPTER 5

Studies on the Effect of *in vitro* Growth Media on Gene Expression and DNA Content in *M. leprae*, and Identification of Genetic Markers Suitable for Measuring Viability of *M. leprae* Using Molecular Methods

This is an ongoing study started in 2003 by Dr. Varalakshmi Vissa, Rama Sakamuri, and Dr. Ramanuj Lahiri. In 2008, I joined the study and my contribution was to test the bacterial viability using molecular approaches. I also participated summarizing the previous experiments that had been done.

5.1. SUMMARY

Mycobacterium leprae, the causative agent of leprosy has never been cultivated *in vitro*. Many studies have been done in making media for culturing the bacteria *in vitro*. The molecular analysis and *in silico* information showed the extreme decay in the *M. leprae* genome and metabolic pathways compared to other mycobacteria. Therefore, researchers have focused on studying metabolic pathways of *M. leprae* in order to address the question of the growth requirements for the *in vitro* conditions.

The first aim of this study was to test and compare the requirement of several nutrients and their concentration for the *in vitro* maintenance of *M. leprae.*The consumption of simple and complex carbon and nitrogen sources in different concentrations and

combinations were tested in a basal medium 7H12 for 3, 7 14 and 21 days. The *M. leprae* metabolic activity was measured as the cumulative release of radiolabled CO_2 in a radiorespirometry assay (RR).

The second aim of this study was to find molecular genetics technique to assess bacterial viability for uncultivable pathogens. This was done by using quantitative real-time PCR (qRT-PCR) to measure RNA levels of *M. leprae* targets including 16S rRNA. Excellent correlation between RR and level of mRNA was noted. The simple addition of 2% glycerol supported *M. leprae* viability up to 21 days, as compared to the basal medium. On the other hand, the addition of thioglycolate, reduced *M. leprae* viability by 3 days.

These experiments provide the first methodology for studying *in vitro* conditions for *M. leprae* viability and growth using RR assay. This finding of useful growth sustaining and inhibitory media using viability testing assays; will have applicability for clinical specimens, physiological study of *M. leprae* metabolism *in vitro* compared to *in vivo*.

5.2. INTRODUCTION

Mycobacterium leprae, the causative agent of leprosy, is one of the major uncultivable pathogenic bacteria. *M. leprae* displays an extremely slow duplication rate, the doubling time in the mouse foot pad on the order of 10-13 days (**Pattyn S., 1977**). It has progressively deteriorating DNA (massive gene decay). This makes *M. leprae* a fragile organism if it is to live without a host (**Cole ST, 2001**), even when provided with nutrients that proven beneficial for other related organisms such as *M. lepraemurium* (**Pattyn S., 1977**).

Many attempts have been done in making media for culturing or maintaining the bacteria *in vitro using* viable *M. leprae* preparations that had been collected from a variety of sources including: patient biopsies, armadillo tissues and mouse foot pad tissue. Molecular analysis and *in silico* information showed an extreme decay in the *M. leprae* genome and metabolic pathways compared to other mycobacteria. Therefore, studies have focused on metabolic pathways of *M. leprae* to address the question of the growth requirements for the *in vitro* conditions.

The cultivation attempts involving tissue culture were started in 1929; following this many attempts were done using embryonic tissues, human or animal fibroblasts, and malignant cells, with little or no success **(Pattyn S., 1977, Hutchinson J., 1987).** In 1960, Shepared found that the footpad of nude mouse is susceptible and supported the multiplication of *M. leprae* within 6-9 months **(Shepard C., 1960).** In 1973, Samuel used human macrophages to grow *M. leprae* and showed the multiplication of the bacilli inside macrophages **(Samuel D., 1973).** Sharp also tried to culture *M. leprae* in macrophages from nude rats and armadillos **(Sharp A., 1984).** Beside tissue cultures, cell-free cultures have been attempted following the discovery of *M. leprae* in 1880 **(Hutchinson J., 1987)**. Different media combinations and growth conditions were used. For example, the egg yolk system has been attempted previously with clinically derived bacilli. Embril *et al*. were able to perform egg-to-egg transfers (six at most), but determined that yolk sac inoculation is not suitable for *M. leprae* **(Embril J., 1954).**

Many attempts in culturing studies have shown the ability of the bacteria to use hydrocarbons (lipids) as a carbon source (direct cholesterol, bovine serum, egg yolk that also contains cholesterol). Kato *et al.* reported culturing of different mycobacteria species including *M. leprae* derived from infected armadillo. They found that medium enriched with 10% serum, cholesterol-lecithin and glycerol supported the growth of *M. leprae* based on acid fast staining test **(Kato L., 1978).** Keto also tried to culture the bacilli extracted from leprosy patients and *M. leprae* infected armadillo specimens into acetone-DMSO-tetradecane medium and kept at 34°C for two months. They found an increase in the culture turbidity, bacterial masses and number of bacilli based on acid-fast stain. This experiment pointed to the importance of hydrocarbons (acetone, DMSO) as a main carbon source and energy for the bacilli **(Kato L., 1983).** It was thought that *M. leprae* may be a microbe-dependent microorganism that required other bacteria to obtain the iron. Therefore, Kato *et al*. attempted to select and culture *M. leprae* from *M. leprae* infected tissues in media containing mycobactin, thioglycolate and lipoic acid **(Kato L., 1985).** Dople *et al* reported limited *in vitro* multiplication of *M. leprae* in primary culture using Dhople-Hanks (DH) and Mahadevan media **(Dhople A, 1988).**

Since *M. leprae* was described as microaerophilic, several attempts were made to culture *M. leprae* in medium with reduced oxidation-reduction conditions **(Ishaque M., 1989).** Ishaque reported two-fold increase in the number of acid-fast bacilli in solid media with egg-yolk under 2.5% O_2 and 10% CO_2, and five-fold increase in the ATP and DNA content after 18 weeks. A similar study looked at the effect of different oxygen

concentrations on the *in vitro* growth of *M. leprae*. Dhople *et al.* found that the optimal growth of *M. leprae* was in tubes with 40-50% free air space **(Dhople A., 1991).**

Group in Japan tried to culture *M. leprae* derived from foot pad of nude mice in Kirchner medium with additional additives such as 10% fetal calf serum and egg-yolk extract with or without media containing adenosine. Their study pointed to increase in ATP production and DNA content at 2 and 4 weeks in medium containing adenosine; however the bacterial count did not change **(Nakamura M., 2001).** These studies pointed to the importance of oxygen at a certain percentage in order for *M. leprae* to grow (*M. leprae* favors lower oxygen tensions). Extra oxygen can lead to accumulation of hydroxide radicals that damage the bacteria. They also pointed to the need for hydrocarbons (lipids) as a carbon source for *M. leprae* growth.

However, all these studies were insufficient to verify the identity of the mycobacteria (*M. leprae* or other) and for the quantification of the growth and viability. They also failed to determine the effect of the medium components or conditions for *M. leprae* growth. The major parameters used to test for *M. leprae* growth and its viability were microscopic examination after acid-fast staining, DNA content of the bacilli, and metabolism (ATP production and [H^3] thymidine uptake).

Understanding the metabolism of the bacteria could provide clues for new components to be used in culturing media. Faulty metabolic pathways have been traced, after

determining *M. leprae*'s genome, the lack of certain biosynthetic pathways such as lipid metabolism pathways were identified **(Cole S., 2001).**

The first challenge of this study was finding media (cell-free culture medium) to maintain and culture *M. leprae in vitro*. Metagrowth database with bioinformatics tools was used **(Ogata H., 2005).** The data were collected from literature, genomic sequence information, metabolic databases and transporter databases. This allowed for identifying the genes which are lost or truncated from major metabolic pathways and suggested additives necessary for the organism to survive under *in vitro* conditions. Providing those metabolic intermediate compounds in the media could then be tested to culture or maintain the viability of the organism.

Different media formulations were made using 7H12 as base with different supplements in different concentrations and combinations from simple carbon sources (glucose, sucrose, sodium thioglycolate, glutamine, glycerol, citric acid, sodium acetate) to more complex mixture (yeast extract, brain heart infusion broth, fetal calf serum, and peptone), and various growth supplements (amino acids and vitamins) or a combination of carbon source and supplements. The *M. leprae* metabolic activity was measured as the cumulative release of radiolabled CO_2 in a radiorespirometry assay (RR).

The second challenge was the ability to differentiate between live versus dead *M. leprae,* which also relates to the uncultivated *M. leprae*. However, many alternative methods have been used to determine bacterial viability. These methods involved testing

the ability of the bacteria to replicate in the mouse foot pad **(Shepard C., 1960).** Other

rapid *in vitro* methods include testing cell integrity (membrane damage) such as

fluorescent staining using LIVE/DEAD BacLight Bacterial Viability Staining (VS) Kit®

(Molecular Probes, Eugene, Oregon,U.S.A) with green Syto9 that can get into intact cells

and bind the DNA and the red propidium iodide (PI) that can get into the cell with

damaged membranes and bind to DNA (**Lahiri R., 2004, 2005**). Another method is one

that depends on testing the metabolic activity of the bacteria using the radiorespirometry

(RR) assay by measuring the rate of oxidation of ^{14}C-palmitate to carbon dioxide by *M.*

leprae. The palmitic acid is incorporated into cells compounds (triglycerol) with the action

of beta-oxidation it produce acetyl coenzyme A, which is oxidized in the Krebs (TCA)

cycle to yield CO_2 **(Franzblau S, 1988)**. Adenosine tri-phosphate (ATP) bioluminescence

assay has also been used for testing *M. leprae* viability **(Agrawal V., 2007).** However,

these assays require large quantities of the bacteria (10^7-10^8).

An alternative method for testing bacterial viability involves molecular methods. With

advance molecular technology and the availability of the mycobacteria genome sequences,

identification of the bacilli and its viability and growth are possible.

In this method the intact DNA sequence could be detected, but the DNA could persist in

killed cells for long time makes this method less sensitive. Another molecular method is by

detection of ribosomal RNA (rRNA) such as 16S rRNA which also has long half-life

(Lavania M., 2008). Detection of 16S rRNA has been the molecular method of choice in

the past for a rapid assessment of mycobacterial viability such as *M. tuberculosis* and *M.*

smegmatis after antimycobacterial drugs which corresponded to the number of CFU (**Van**

249

der Vliet., 1994). 16S rRNA has also been used to assist the viability of *M. leprae* in clinical samples **(Phetsuksiri B., 2006).** However, the detection of 16S rRNA is not directly indicated to the live bacteria; instead it reflects the total metabolic state of bacteria present **(Van der Vliet**., **1994).** Finally, detection of messenger RNA (mRNA) could be the accurate indicator since it is highly labile with short half-life **(Keer J., 2003).** The commonly used techniques for detection of mRNA are reverse transcriptase PCR (RT-PCR) which is a two-stage process; first, the mRNA is transcribed into complementary DNA (cDNA) using random hexanucleotide primers. Second, the cDNA is used as a template for PCR amplification of a specific gene **(Keer J., 2003).** This method has been used to study the viability of *M. tuberculosis* using Ag 85B mRNA as marker **(Hellyer T., 1999).** Also the mRNAs have been used to study *M. leprae* gene expression from clinical biopsy samples **(Williams D., 2003).** Using quantitative real-time PCR (qRT-PCR) Williams et al. developed tools for testing *M. leprae* viability based on expression of sodA, 16S rRNA and correlated to the amount of repetitive element DNA targets (RLEP) from clinical sample **(Martinez A., 2010).**

In this study quantitative RT-PCR assay was used to assess *M. leprae* viability from different cultured media at different time points (0-14 and 21 days) since the doubling time of *M. leprae* is 2 weeks. This is done by testing many gene targets at the level of mRNAs, 16S rRNA (Taqman multiplex assay) compared to the DNA levels of each gene. Excellent correlation between RR reading and level of sodA mRNA was noted. The simple addition of 2% glycerol to NHDP (7H12) media, supported *M. leprae* viability up to 21 days, as

compared to the basal medium (7H12 only). On the other hand, the addition of thioglycolate, reduced *M. leprae* viability within 3 days.

These experiments provide the first methodology for studying *in vitro* conditions for *M. leprae* viability and growth using RR assay and molecular method. This finding of useful growth sustaining and inhibitory media using viability testing assay will have applicability to clinical specimens and the physiological study of *M. leprae* metabolism *in vitro* compared to *in vivo*.

5.3. MATERIALS AND METHODS

5.3.1 *Mycobacterium leprae* cells

M. leprae Thai-53 was isolated from athymic mouse foot pads approximately 6-8 months post infection (at LSU, Baton Rouge by Lahiri R.). The skin was removed aseptically and cells were washed after harvesting and resuspended in 7H9 plus 10 % (v/v) fetal calf serum (**Truman and Krahenbuhl, 2001).** The viability of *M. leprae* cells were enumerated by LIVE/DEAD BacLight method (Molecular Probes) **(Lahiri R., 2005).**

2.3.2 Media preparation

Preparation of the media 7H12B (NHDP)

Solution A: 2.6 g of 7H9 broth (BD Difco Middle Brook), 0.5 g of casitone (Pancreatic digest of casein, Bacto) and autoclaved distaled water up to 500 ml.

Solution B: 1.25 g albumin, from bovine serum (FA free) (Sigma, US), 1.86 g dextrose anhydrous (Sigma, US) and autoclaved water up to 25 ml. The solution was sterilized using 0.2 µm filter. 10 ml of solution B was added to 90 ml of solution A, the medium was mixed and filters sterilized through 0.2 µm membrane, stored at 4°C until used (**Siddiqi S., 1988**).

The vitamin mix supplement and trace mineral supplements were obtained from the American Type Culture Collection (Cat. Nos. MD-VS and MD-TMS). The lipid was a pre made lipid cocktail (contains saturated and unsaturated fatty acids) (Gibco, Cat. No.11905). Amino acid mixtures were purchased in two forms with or without addition of adenine and uracil [all ingredients at 85.6 mg/L with the exception of adenine (21 mg/L) and leucine (173.4 mg/L)] (yeastmedia.com a division of Quality Bioresources).

5.3.3 Supplements

Supplements were selected based on the genome of *M. leprae* (**Cole S., 2001, Vissa V., 2001**) and Metagrowth bioinformatics (**Ogata H., 2005**), which includes a variety of simple carbon sources (glucose, sucrose, sodium thioglycolate, glutamine, glycerol, citric acid, sodium acetate), more complex ones (yeast extract, brain heart infusion broth, fetal calf serum), various mixture of amino acids, various growth supplements such as vitamins, trace minerals and lipids. **Table 5.1** explains the reason for adding each supplement. All media supplements were from Sigma. The supplements were prepared from stock solutions before adding into basic medium to obtain a final concentration and were also filter sterilized with 0.2 µM filters. MilliQ water was used to dilute all solutions, except where

ethanol was required. All the formulations were made into triplicates in 15 ml sterile falcon tubes and one batch of the formulation was kept at 37°C to check for microbial contaminations. For example, thioglycolate was prepared at 10% stock solution, filter sterilized and 0.1% final concentration was used for the media. Glycerol stock of 50% (autoclaved), 2% final was used for the media. The antibiotic rifampicin (Sigma, US) was prepared at 8 mg/ml in DMSO, 2 mg/ml final concentration was used for the media.

Table 5.1: Media supplements with the reason for adding them into the basic media.

	Supplement	Reason
1	Glucose, sucrose, sodium thioglycolate, glutamine, glycerol, citric acid, sodium acetate and dextran	Simple and complex carbon source.
2	D-glucose, glucose 6-phosphate	*M. leprae* lacks the enzymatic step (phosphoglucomutase,pgmA) to convert glucose-1P to glucose-6P
3	Yeast extract, brain heart infusion, fetal Calf serum	Complex carbon and nitrogen source, prolonge ATP production in phosphate buffer (Nakamura M., 1996).
4	Peptone, caesin hydrolysate	Complex Nitrogen source.
5	Vitamin supplements: folic acid, pyridoxine hydrocloride, riboflavin, biotin, thiamin, nicotinic acid, calcium pantothenate, vitamin B12, p-amino benzoic acid, thioctic acid	The bacterium possesses the synthetic genes for vitamin B12 from cobinamide but lacks genes for the precursor synthesis (*cob* genes, required for cobinamide synthesis, have selective deletion).
6	Trace elements: $MgSO_4$, $MnSO_4$, NaCl, $FeSO_4$, Co(No3)2, $CaCl_2$ (anhydrous), $ZnSO_4$, $CuSO_4$, AlK(SO4)2 (anhydrous), H_3BO4, Na_2MoO4, Na_2SeO3 (anhydrous), Na_2WO4, $NiCl_2$	Presence of transporters for ion/proton and metal.
7	Chemically defined lipid cocktail	Synthesis and modification of polyketides.
8	Amino acid mixtures: Myo-inositol, p-aminobenzoic acid, alanine, arginine, aspergine, aspartic acid, cysteine, glutamic acid, glutamine, glycine, histidine, isoleucine, lysine, methionine, phenylalanine, proline, serine, threonine, tryptophan, tyrosine, valine and leucine	Presence of transporters for amino acids.

9	L-methionine, Cysteine, Thiotic acid, Sodium thioglycolate, Sodium metabisulfate	Sulfur source; sulfur transporter genes are inactivated in *M. leprae* genome. Mutations in detoxification genes (encoding peroxidases)
10	Mycobactin	*M. leprae* lacks biosynthetic pathway for siderophore and deficient in iron storage mechanism.
11	Vitamin K (which includes menaquinone)	*M. leprae* has a pathway from the glycolysis to isopentenyl-PP. The required final product after this pathway is not obvious. Vitamin k functions in electron transfer.
12	Ferrous sulfate	Iron and sulfur source, metal supplement
13	Cobalamine	Cobalamine synthesis seems to be disabled in *M. leprae*
14	Trehalose	Trehalose biosynthetic pathway is deficient in *M. leprae*. The *treZ* gene is disrupted.
15	Soluble starch, Sodium pyruvate, DTT, Catalase, nitrate reductase	Detoxification, sequestering agents of toxic free radicals. *M. leprae* lost most of the genes for detoxification of reactive oxygen and nitrogen species such as nitric oxide (NO).
16	N-acetyl glucosamine, D-glucoronic acid	*Mycobacterium scrofulaceum* (causes similar disease as leprosy) can be grown in Ogawa's or Sauton's media enriched with glucuronic acid and N-acetyl-D-glucosamine
17	L-glutamine	Presence of transporters for glutamine . *M. leprae* does not have enzyme (pyruvate carboxylase) to convert pyruvate to oxaloacetate
18	Cyanocobalamine	The biosynthesis of vitamin B12 coenzyme (i.e. cobamamide) is almost absent in *M. leprae*
19	Diaminopimilic acid	Biosynthesis of lysine is deficient, so addition of diaminopimelate helps the bacteria for peptidoglycan synthesis.
20	Hemin	Synthesis of protoheme is missing in *M. leprae*.
21	Glycerol	Glycerol (2%), dextran (1%) and fetal calf serum; prolong ATP production in phosphate buffer (pH 7.0).
22	Acetyl-CoA	The acetyltransferase gene in the pathway from pyruvate to acetyl-CoA is a pseudogene in M. leprae. Also, *M. leprae* lacks acetyl-CoA ligase.
23	Fetal calf serum and egg yolk	Prolonged the ATP production in phosphate buffer (pH 7.0).

5.3.4 Media preparation history

Many experiments were conducted since 2003 to test the effect of different supplements on *M. leprae* viability. First the effects of different carbon sources were tested. The 7H9 medium was used as base and different carbon sources were added (preparation #1): glucose, sucrose, sodium thioglycolate, glutamine, glycerol, citric acid, sodium acetate, yeast extract, brain heart infusion, fetal calf serum. Other additives were added at certain concentration, such as amino acids, trace elements, lipid cocktail and vitamins (**Table 5.2).** Another experiment with different carbon and nitrogen sources were also performed with 7H9 as base (preparation #2): casitone, bovine albumin, dextrose, methionine, cobalamine, thiotic acid, sodium pyruvate, trehalose, soluble starch and all these supplements together. In addition, 1% casitone, 5% bovine albumin and 7.5% dextrose as carbon source was added to make 7H12 or NHDP medium (**Table 5.3).**

The effect of using either carbon source or nitrogen source for energy was tested: using media with carbon source only individually and all (glucose, fructose, sucrose, cholesterol, glutamine, thioglycolate) mixed together. Another set of media contained both carbon and nitrogen sources such as yeast extract, fetal calf serum, brain heart extract and mixture of all of these (preparation #3). In all these media amino acids plus nucleotide mix, vitamin mix, trace elements plus hemin, lipid cocktail and amino acid mix were added individually or in combination (**Table 5.4).**

Another experiment was done to test the effect of using glycerol as a carbon source. Using the 7H12 as a base and 2% glycerol as supplement, different additives were added separately to the each medium. Using the base line (7H12) and different supplements, 22 combinations were made in duplicates (preparation #4); 1- base line medium, 2- base line

medium plus glycerol, the rest of the media have the base line plus glycerol plus other

additives (**Table 5.5).** Moreover, another experiment was carried out to test the effect of

glycerol together with different additives (preparation #5). There were 20 different media

combinations, beside the base line 7H12 and the base line plus glycerol and other additives

(**Table 5.6).** Using the 7H12 base line media, the positive effect of the 2% glycerol and the

negative effect of the sodium thioglycolate (0.1%) were verified in independent experiments

(preparation #6). Two biological replicates with three technical replicates were tested (**Table

5.7).**

Table 5.2: Media preparation #1

Formulation Number	Carbon Source/Mixture	Base medium 7H9 (ml)	Amino Acid Mix Complete (ml)	Vitamin Mix (ml)	Trace Elements (ml)	Lipid Cocktail (ml)	Amino Acid Mix - (Adenine + Uracil) (ml)	Water (ml)	RR 3 days (^{14}C CPM)	RR 7 days (^{14}C CPM)
1	Glucose A 100 µl	1	1.5	**0.5**	0	0	0	6.9	14637	1863
2	Glucose B 100 µl	1	1.5	0	0	0	0	7.4	13474	13318
3	Glucose C 100 µl	1	1.5	0	**0.5**	0	0	6.9	11416	5383
4	Glucose D 100 µl	1	1.5	0	0	**0.5**	0	6.9	13771	6676
5	Glucose E 100 µl	1	1.5	**0.5**	**0.5**	**0.5**	0	5.9	13290	1162
6	Glucose F 100 µl	1	0	**0.5**	**0.5**	**0.5**	**1.5**	5.9	12249	11006
7	Sucrose A 100 µl	1	1.5	**0.5**	0	0	0	6.9	14296	10194
8	Sucrose B 100 µl	1	1.5	0	0	0	0	7.4	12342	5379
9	Sucrose C 100 µl	1	1.5	0	**0.5**	0	0	6.9	12950	6788
10	Sucrose D 100 µl	1	1.5	0	0	**0.5**	0	6.9	13319	3313
11	Sucrose E 100 µl	1	1.5	**0.5**	**0.5**	**0.5**	0	5.9	12651	2169
12	Sucrose F 100 µl	1	0	**0.5**	**0.5**	**0.5**	**1.5**	5.9	14269	6643
13	Sodium Thioglycolate A 100 µl	1	1.5	**0.5**	0	0	0	6.9	10962	46
14	Sodium Thioglycolate B 100 µl	1	1.5	0	0	0	0	7.4	12496	28
15	Sodium Thioglycolate C 100 µl	1	1.5	0	**0.5**	0	0	6.9	6953	46
16	Sodium Thioglycolate D 100 µl	1	1.5	0	0	**0.5**	0	6.9	8973	44
17	Sodium Thioglycolate E 100 µl	1	1.5	**0.5**	**0.5**	**0.5**	0	5.9	7951	35
18	Sodium Thioglycolate F 100 µl	1	0	**0.5**	**0.5**	**0.5**	**1.5**	5.9	12272	484
19	Glutamine A 200 µl	1	1.5	**0.5**	0	0	0	6.7	16547	10469
20	Glutamine B 200 µl	1	1.5	0	0	0	0	7.2	10754	4525
21	Glutamine C 200 µl	1	1.5	0	**0.5**	0	0	6.7	11179	8937
22	Glutamine D 200 µl	1	1.5	0	0	**0.5**	0	6.7	6673	33
23	Glutamine E 200 µl	1	1.5	**0.5**	**0.5**	**0.5**	0	5.7	9384	48

24	Glutamine F 200 µl	1	0	**0.5**	**0.5**	**0.5**	**1.5**	5.7	12999	8609
25	Glycerol A 200 µl	1	1.5	**0.5**	0	0	0	6.7	14397	9621
26	Glycerol B 200 µl	1	1.5	0	0	0	0	7.2	15637	4925
27	Glycerol C 200 µl	1	1.5	0	**0.5**	0	0	6.7	10753	12626
28	Glycerol D 200 µl	1	1.5	0	0	**0.5**	0	6.7	6618	44
29	Glycerol E 200 µl	1	1.5	0.5	0.5	0.5	0	5.7	9822	70
30	Glycerol F 200 µl	1	0	**0.5**	**0.5**	**0.5**	**1.5**	5.7	8032	94
31	Citric Acid E 50 µl	0.5	0.75	0.25	0.25	0.25	0	2.95	72	49
32	Sodium Acetate E 50 µl	0.5	0.75	0.25	0.25	0.25	0	2.95	4690	48
33	Complex Carbon Glucose 50 µl Sucrose 50 µl Sodium Thioglycolate 50 µl Glutamine 50 µl Glycerol 50 µl Citric Acid 50 µl Sodium Acetate 50 µl	0.5	0.75	0.25	0.25	0.25	0	2.65	1532	20999
34	Yeast Extract A 100 µl	1	1.5	**0.5**	0	0	0	6.9	10928	9200
35	Yeast Extract B 100 µl	1	1.5	0	0	0	0	7.4	6070	7830
36	Yeast Extract C 100 µl	1	1.5	0	**0.5**	0	0	6.9	14086	4882
37	Yeast Extract D 100 µl	1	1.5	0	0	**0.5**	0	6.9	6687	78
38	Yeast Extract E 100 µl	1	1.5	0.5	0.5	**0.5**	0	5.9	4557	49
39	Yeast Extract F 100 µl	1	0	**0.5**	**0.5**	**0.5**	**1.5**	5.9	12034	3875
40	Brain Heart Infusion A 100 µl	1	1.5	**0.5**	0	0	0	6.9	15795	10949
41	Brain Heart Infusion B 100 µl	1	1.5	0	0	0	0	7.4	21541	17140
42	Brain Heart Infusion C 100 µl	1	1.5	0	**0.5**	0	0	6.9	15593	14507
43	Brain Heart Infusion D 100 µl	1	1.5	0	0	**0.5**	0	6.9	9431	69
44	Brain Heart Infusion E 100 µl	1	1.5	**0.5**	**0.5**	**0.5**	0	5.9	7830	58
45	Brain Heart Infusion F 100 µl	1	0	**0.5**	**0.5**	**0.5**	**1.5**	5.9	11383	38
46	Fetal Calf Serum A1000 µl	1	1.5	**0.5**	0	0	0	6	13749	8956
47	Fetal Calf Serum B 1000 µl	1	1.5	0	0	0	0	6.5	14778	15786

48	Fetal Calf Serum C 1000 µl	1	1.5	0	**0.5**	0	0	6	15190	10750
49	Fetal Calf Serum D 1000 µl	1	1.5	0	0	**0.5**	0	6	10217	10792
50	Fetal Calf Serum E 1000 µl	1	1.5	**0.5**	**0.5**	**0.5**	0	5	5074	8136
51	Fetal Calf Serum F 1000 µl	1	0	**0.5**	**0.5**	**0.5**	**1.5**	5	4120	11754
52	Peptone E 50µl	0.5	0.75	0.25	0.25	0.25	0	2.95	16650	9267
53	Caesin Hydrolysate E 50µl	0.5	0.75	0.25	0.25	0.25	0	2.95	7521	481
54	Complex Carbon/Nitrogen Yeast Extract 50µl Fetal Calf Serum 50µl Brain Heart Infusion 50µl Peptone 50µl Caesin Hydrolysate 50µl	0.5	0.75	0.25	0.25	0.25	0	2.3	7001	8660
55	Dulbecco's Medium 50µl	0	0	0	0	0	0	0	9023	8879

Table 5.3: Media preparation #2

Formulation number	Formulation	Base medium 7H9	Casitone	Bovine Albumin	Dextrose	Additive	RR 3 days (^{14}C CPM)	RR 7 days (^{14}C CPM)
90	NAHDP (Base)	4.7 mg / ml	1%	5%	7.50%		30263	28720
91	-7H9		1%	5%	7.50%		19972	30884
92	-Casitone	4.7 mg / ml		5%	7.50%		31154	31749
93	-Bovine Albm	4.7 mg / ml	1%		7.50%		32439	22529
94	-Dextrose	4.7 mg / ml	1%	5%			34375	21497
95	+Methionine 1	4.7 mg / ml	1%	5%	7.50%	Methionine 0.01mg/ml	39903	
96	+Methionine 2	4.7 mg / ml	1%	5%	7.50%	Methionine 0.05mg/ml	34805	31600
97	+Methionine 3	4.7 mg / ml	1%	5%	7.50%	Methionine 0.1mg/ml	40103	34100
98	+Mycobactin 1	4.7 mg / ml	1%	5%	7.50%	Mycobactin 0.2mg/ml	42096	26978

99	+Mycobactin 2	4.7 mg / ml	1%	5%	7.50%	Mycobactin 1mg/ml	41165	29754
100	+Mycobactin 3	4.7 mg / ml	1%	5%	7.50%	Mycobactin 2mg/ml	29902	34254
101	+Cobalamine 1	4.7 mg / ml	1%	5%	7.50%	Cobalamine 3ng/ml	35943	41110
102	+Cobalamine 2	4.7 mg / ml	1%	5%	7.50%	Cobalamine 15ng/ml	39671	29308
103	+Cobalamine 3	4.7 mg / ml	1%	5%	7.50%	Cobalamine 75ng/ml	33061	31183
104	+Thiotic Acid 1	4.7 mg / ml	1%	5%	7.50%	Thiotic Acid 0.01mg/ml	26857	11556
105	+Thiotic Acid 2	4.7 mg / ml	1%	5%	7.50%	Thiotic Acid 0.05mg/ml	14702	2538
106	+Thiotic Acid 3	4.7 mg / ml	1%	5%	7.50%	Thiotic Acid 0.1mg/ml	729	154
107	+Trehalose 1	4.7 mg / ml	1%	5%	7.50%	Trehalose 0.02mg/ml	48977	42031
108	+Trehalose 2	4.7 mg / ml	1%	5%	7.50%	Trehalose 0.1mg/ml	35165	30214
109	+Trehalose 3	4.7 mg / ml	1%	5%	7.50%	Trehalose 0.5mg/ml	20119	29100
110	all nutrients	4.7 mg / ml	1%	5%	7.50%	Methionine 0.05mg/ml, Mycobactine 1mg/ml, Cobalamine 15ng/ml, Thiotic Acid 0.05mg/ml, Trehalose 0.1mg/ml	13332	2377
111	all nutrients +ETOH	4.7 mg / ml	1%	5%	7.50%	Methionine 0.05mg/ml, Cobalamine 15ng/ml, Trehalose 0.1mg/ml Ethanol0.20%	52260	
112	soluble starch	2.35mg/ml	0.50%	0.50%	3.75%	Starch 2mg/ml	51704	34604
113	sodium pyruvate	2.35mg/ml	0.50%	0.50%	3.75%	sodium pyruvate 10mg/ml	47394	37847
114	starch + sodium pyruvate	2.35mg/ml	0.50%	0.50%	3.75%	starch 2mg/ml + sodium pyruvate 10mg/ml	32938	38488

Table 5.4: Media preparation #3

Formulation number	Additive	Concentration	Base medium 7H9	Casitone	Bovine Albumin	Dextrose
115	Pyruvate	100mg/ml	4.7mg/ml	1%	5%	7.50%
117	Pyruvate	50mg/ml	4.7mg/ml	1%	5%	7.50%
119	Pyruvate	25mg/ml	4.7mg/ml	1%	5%	7.50%
121	Pyruvate	10mg/ml	4.7mg/ml	1%	5%	7.50%
123	Pyruvate	5mg/ml	4.7mg/ml	1%	5%	7.50%
125	Catalase	100U/ml	4.7mg/ml	1%	5%	7.50%
127	Catalase	200U/ml	4.7mg/ml	1%	5%	7.50%
129	DMSO	1.30%	4.7mg/ml	1%	5%	7.50%
131	DMSO	0.66%	4.7mg/ml	1%	5%	7.50%
133	L-Cysteine	0.05%	4.7mg/ml	1%	5%	7.50%
135	L-Cysteine	0.10%	4.7mg/ml	1%	5%	7.50%
137	Sodium thioglcolate	0.10%	4.7mg/ml	1%	5%	7.50%
139	Sodium thioglcolate	0.05%	4.7mg/ml	1%	5%	7.50%
141	None	none	4.7mg/ml	1%	5%	7.50%
143	Trace elements + Vitamin mix	2% each	4.7mg/ml	1%	5%	7.50%
145	Trace elements + Vitamin mix	5% each	4.7mg/ml	1%	5%	7.50%
147	Fetal Bovine Serum	10%	4.7mg/ml	1%	5%	7.50%
149	Glycerol	2%	4.7mg/ml	1%	5%	7.50%
151	n-Propyl gallate	0.25%	4.7mg/ml	1%	5%	7.50%
153	Sodium metabisulfite + ferrous sulfate	0.25% each	4.7mg/ml	1%	5%	7.50%
155	Potasium permanganate	0.25%	4.7mg/ml	1%	5%	7.50%
157	Pyruvate	50mg/ml	4.7mg/ml	1%	5%	7.50%
158	Pyruvate	10mg/ml	4.7mg/ml	1%	5%	7.50%
159	None	none	4.7mg/ml	1%	5%	7.50%
160	Trace elements + Vitamins	3%	4.7mg/ml	1%	5%	7.50%
161	L-Cysteine	0.05%	4.7mg/ml	1%	5%	7.50%
162	Fetal bovine serum	10%	4.7mg/ml	1%	5%	7.50%
163	Glycerol	2%	4.7mg/ml	1%	5%	7.50%
164	Sodium metabisulfite + ferrous sulfate	0.1% each	4.7mg/ml	1%	5%	7.50%

165	glyceraldehyde	0.25%	4.7mg/ml	1%	5%	7.50%
166	None	none	4.7mg/ml	1%	5%	7.50%
167	Pyruvate	25mg/ml	4.7mg/ml	1%	5%	7.50%

Table 5.5: Media preparation #4

Formulation number	Base medium	Supplement	Additive 1	Additive 2	Additive 3	Additive 4	Additive 5	RR 3 days (^{14}C CPM)	RR 7 days (^{14}C CPM)
1 a, b	NHDP							45007	21200
2 a, b	NHDP	Glycerol (2%)						68699	1999
3 a, b	NHDP		FBS (3%)	Dextran (10%)				74421	29760
4 a, b	NHDP		Glucose (0.1%)	ATP (0.25%)				51842	23930
5 a, b	NHDP		Sucrose (100ul of 10%)	ATP (0.25%)				42186	21611
6 a, b	NHDP	Glycerol (2%)	Fumaric acid (0.1%)					43803	21805
7 a, b	NHDP	Glycerol (2%)	Succinic acid (0.1%)					56647	20094
8 a, b	NHDP	Glycerol (2%)	Diaminopimilic acid (0.1%)					67743	49219
9 a, b	NHDP	Glycerol (2%)	D-Glucoronic acid (0.1%)					59097	61621
10 a, b	NHDP	Glycerol (2%)	N-acetyl Glucosamine (0.1%)					67614	52519
11 a, b	NHDP	Glycerol (2%)	Vitamin Mix (1%)					58206	55429
12 a, b	NHDP	Glycerol (2%)	L-Glutamine (10mM)					62798	58218
13 a, b	NHDP	Glycerol (2%)	DTT (0.1%)					58	43
14 a, b	NHDP	Glycerol (2%)	Sodium acetate (0.1%)					59607	51851
15 a, b	NHDP	Glycerol (2%)	Sodium pyruvate (25mg/ml)					68492	45419
16 a, b	NHDP	Glycerol (2%)	Cynocobalamine (380ug/ml)					63879	49353
17 a, b	NHDP	Glycerol (2%)	Trace elements (1%)					56470	48300
18 a, b	NHDP	Glycerol (2%)	Amino Acid Mix minus A + T (1%)					71139	45730
19 a, b	NHDP	Glycerol (2%)	Amino Acid Mix minus A + T (1%)	Trace elements (1%)	Vitamin Mix (1%)			66711	51381
20 a, b	NHDP	Glycerol (2%)	N-acetyl	D-Glucoronic				75208	49878

			Glucosamine (0.1%)	acid (0.1%)					
21 a, b	NHDP	Glycerol (2%)	Glucose (0.1%)	Amino Acid Mix minus A + T (1%)	Trace elements (1%)	Vitamin Mix (1%)	ATP (0.25%)	44716	18213
22 a, b	NHDP	Glycerol (2%)	Sucrose (0.1%)	Amino Acid Mix minus A + T (1%)	Trace elements (1%)	Vitamin Mix (1%)	ATP (0.25%)	44025	17942

Table 5.6: Media preparation #5

Formulation number	Base medium	Supplement	Additives	RR 3 days (^{14}C CPM)	RR 7 days (^{14}C CPM)
1 a, b	NHDP	0	-	46535	19586
2 a, b	NHDP	Glycerol (2%)	-	48210	36394
3 a, b	NHDP	Glycerol (2%)	Hemin (0.033%)	42319	33119
4 a, b	NHDP	Glycerol (2%)	Non essential Amino Acid Mix solution (1%), Trace elements (1%), Vitamin Mix (1%)	45438	38114
5 a, b	NHDP	Glycerol (2%)	Ribose (0.1%), Trace elements (1%), Vitamin Mix (1%)	45982	34211
6 a, b	NHDP	Glycerol (2%)	N-acetyl Glucosamine (0.1%), D-Glucoronic acid (0.1%)	52644	42189
7 a, b	NHDP	Glycerol (2%)	N-acetyl Glucosamine (0.1%), D-Glucoronic acid (0.1%), Trace elements (1%), Vitamin Mix (1%)	42465	42799
8 a, b	NHDP	Glycerol (2%)	FBS (3%), Dextran (0.1%), Trace elements (1%), Vitamin Mix (1%)	44598	41253
9 a, b	NHDP	Glycerol (2%)	FBS (3%), Dextran (0.1%)	44939	40826
10 a, b	NHDP	Glycerol (2%)	L-Glutamine (100ul of 400mM), Trace elements (1%), Vitamin Mix (1%)	37403	40795
11 a, b	NHDP	Glycerol (2%)	Sodium Thio glycolate (0.1%), Trace elements (1%), Vitamin Mix (1%)	52	80
12 a, b	NHDP	Glycerol (2%)	N-acetyl Glucosamine (0.1%), D-Glucoronic acid (0.1%) , Diaminopimilic acid (100ul of 10%)	47704	41143

13 a, b	NHDP	Glycerol (2%)	Sodium pyruvate (25mg/ml), Trace elements (1%), Vitamin Mix (1%)	35715	40381
14 a, b	NHDP	Glycerol (2%)	Cynocobalamine (0.19mg/ml), Trace elements (1%), Vitamin Mix (1%)	40640	38748
15 a, b	NHDP	Glycerol (2%)	Sodium Thio glycolate (0.1%), FBS (3%), Dextran (0.1%)	58	94
16 a, b	NHDP	Glycerol (2%)	L-Cysteine (0.1%), FBS (3%), Dextran (0.1%)	29133	8733
17 a, b	NHDP	Glycerol (2%)	L-Methionine (0.1%), FBS (3%), Dextran (0.1%)	44420	47666
18 a, b	NHDP	Glycerol (2%)	Trace elements (1%) , Vitamin Mix (1%),	45295	40292
19 a, b	NHDP	Glycerol (2%)	N-acetyl Glucosamine (0.1%), D-Glucoronic acid (0.1%), Diaminopimilic acid (0.1%), Trace elements (1%), Vitamin Mix (1%)	46354	36540
20 a, b	NHDP	Glycerol (2%)	N-acetyl Glucosamine (0.1%) , D-Glucoronic acid (0.1%), Diaminopimilic acid (0.1%), Sodium Thio Glycolate (0.05%), Trace elements (1%), Vitamin Mix (1%), FBS (3%), Dextran (0.1%), Sodium pyruvate (25mg/ml), L-Glutamine (100ul of 400mM), Non essential Amino Acid Mix solution (1%)	31723	20944
21 a, b	NHDP	-	-	39920	22039

Table 5.7: Media preparation #6

Media number	Basal medium	Supplement	RR 3 days (^{14}C CPM)	RR 7 days (^{14}C CPM)
1	NHDP	-	63004	14851
2	NHDP	Glycerol (2%)	64431	35964
3	NHDP	Sodium thioglycolate (0.1%)	58293	2750
4	NHDP	Rifampicin	34905	196

5.3.5 Media inoculation with *M. leprae*

After making all the media with the supplements, 50 µg/ml ampicillin was added into each media from original stock of 100 mg/ml. Media aliquots of 1 ml each were dispensed into 2 ml screw cap tubes and labeled for supplements and time points, triplicate tubes for all the media were made. Each medium was inoculated with 100 µl (1×10^8 live cells). All the inoculated tubes were incubated at 33°C for each time point (0, 3,7,10, 14 and 21 days). For each time point the tubes were centrifuged for 10 min, at 13,000 rpm, the media were removed and 1 ml of RNA later (Qiagen, US) was added, the tubes were mixed and stored for 2 days at 4°C. The tubes were centrifuged after 2 days (13000 rpm for 15 min), RNA later was removed and the cells were stored at -70°C until further processing.

5.3.6 Radiorespirometry (RR) assay

The viability of *M. leprae* in the media was determined first by RR assay that depends on the oxidation of ^{14}C-palmitic acid to $^{14}CO_2$ **(Franzblau S., 1988).** Briefly, 0.1 ml aliquots ($1x10^8$ *M. leprae*) from each media were removed at each time point and suspended in 4.9 ml of 7H12 medium with 1 µci $[^{14}C]$ palmitic acid in a glass vial inserted into liquid scintillation vial lined with filter paper impregnated with NaOH and 2,5-diphenyloxazole. The oxidation of the palmitic acid, an indicator of metabolic activity of *M. leprae* was measured as the cumulative $[^{14}C]$ CO_2 released over 7 days.

5.3.7 Viability staining test

The bacilli were stained using LIVE/DEAD BacLight Bacterial Viability Kit (Molecular Probes) **(Lahiri R., 2005).** *M. leprae* were washed twice with normal saline and incubated for 15 min at room temperature with green Syto9 and the red propidium iodide (PI). The bacteria were washed twice in normal saline, the pellet was re-suspended in 20 µl of 10 % (v/v) glycerol in normal saline and 5 µl of the suspension was placed on a glass slide. The dead and live bacteria were enumerated by direct counting of fluorescent green and red bacilli under a fluorescence microscope. The excitation/ emission maxima are 480 nm/500 nm for Syto9 and 490 nm/635 nm for PI.

5.3.8 RNA extraction and purification

Aliquots of the *M. leprae* cells from different media taken at different time points stored at -70°C were used to extract DNA and RNA using All Prep DNA/RNA and Protein Micro Kit (Qiagen, US). Briefly, *M. leprae* cells were suspended in RLT buffer (600 µl) containing freshly added β-mercaptoethanol (10µl). The suspended cells were disrupted using Lysing Matrix B (0.1-mm silica spheres) (MP biomedical, USA) disrupted at a speed setting of 6 using a Fast Prep-24 (MP biomedical) equipment for 40 sec. The lysates were transferred to an All prep DNA spin column and centrifuged for 30 s at 8000 x *g* (10,000 rpm). The columns were placed in a new collection tubes and stored at 4˚C for later purification. For the RNA purification, one volume of 70% ethanol was added to the flow-through from the DNA column and mixed. Then, the materials were transferred into RNeasy spin columns and centrifuged for 15 s at 8000 x *g* (10,000 rpm). DNase was added to the RNeasy columns to degrade DNA. The columns were washed two times with RPE buffer plus ethanol, spun dry and the RNA was eluted with 50 µl RNase-free water. For the DNA samples the columns were washed two times with AW1 and AW2 buffer and the DNA was eluted with 100 µl of elution buffer.

5.3.9 Reverse transcription (RT-qPCR)

The RNAs extracted from each cell culture were used to prepare cDNA using Reverse Transcriptase enzyme (Invitrogen, US) from random primers after treatment with DNase. Briefly, 22 µl of RNA (~1 µg) from each cell sample was treated with 0.5 µl DNase I (Ambion, USA) and 0.1 volume of 10X DNase I buffer in a total volume of 25 µl, and was incubated at 37˚C for 30 min. DNase inactivation reagent (0.1 volume) was added,

incubated for 2 min at room temperature with mixing. The samples were centrifuged at 10,000 rpm for 2 min and the supernatants were transferred to a new tube. Some of the RNA treated with the DNase (8µl) was used to prepare cDNA using 10 µl of Superscript master mix with reverse transcriptase (Invitrogen) and 1µl of dNTP and random hexamer primers (3 µg/µl) (Invitrogen). *M. leprae* RNAs excluding the reverse transcriptase enzyme were used to look for DNA contamination (RT-). The sample mix of 20 µl was incubated at 42˚C for 90 min. Another method for Reverse transcription (RT-qPCR) was used later, due to fewer steps and less sample manipulation.

QuantiTect Rev. Transcription Kit (Qiagen, US)

The RNA templates (~1 µg) (20 µl of a 50 µl total/per sample) were first treated with gDNA Wipeout Buffer in a total volume of 28 µl for 5 min at 42°C. The sample was split into two reactions, reverse transcriptase plus and minus (RT+ and RT-). Both reactions (final volume of 20 µl) contained Quantiscript RT Buffer, RT Primer Mix (Qiagen). Quantiscript Reverse Transcriptase (1 µl) was added only in the RT+ reaction. Both reactions were incubated for 30 min at 42°C. The reactions were stopped by incubation for 3 min at 95°C.

5.3.10 Multiplex PCR

The DNAs and the RNA (RT+ and RT-) prepared from *M. leprae* were used as templates to amplify gene-specific primers (**Table 5.8**) using multiplex PCR kit (Qiagen, US). Seven genes were from glycerol pathway: *glpK, glpQ1, glpQ2, gpdA1, gpdA2, glpD1* and *glpD2,* the three psudogenes (underlined). Four genes were used for a drug resistance screening study; *rpoB* encoding the β-subunit of RNA polymerase, *folP* encoding

dihydropteroate synthase for folic acid synthesis, *gyrA* and *gyrB* encoding DNA gyrase subunit A and B for DNA replication. One gene was for detoxification encoding superoxide dismutase (*sodA),* two genes *sdhD* and *lldD2* from tricarboxylic acid cycle (TCA) and the *16S rRNA*. The PCR was made with 1 µl of each *M. leprae* cDNA (a total of 20 µl) and DNA (a total of 100 µl) and RT controls were amplified using 0.2 µM of primers combination and multiplex mix in 10 µl total PCRs. The PCR thermal cycle was done with 35- cycles consisting of denaturation 95°C, 1 min followed by annealing between 50-60°C,1 min and extension 72°C,1 min. A final extension step 72°C for 10 min was included. The PCR products were visualized by 2% agarose gel (Invitrogen), stained with ethidium bromide.

Table 5.8: Multiplex PCR primer combinations for amplification of DNA and RNA of panel of *M. leprae* genes. Primer sets for 16 genes (the pseudogenes are underlined) were divided into six combinations to allow detection of each amplicon by 2% agarose gel electrophoresis.

Combination # (pathways)	Gene name (ML number)	Primers sequence	Size (bp)
1 (glycerol pathway and TCA)	*glpK* (ML 1231c)	F 5'-GTGATTTTCGATCATAATGGT-3' R 5'-TGCAATATCTTTAGCTGACAA-3'	150
	glpD1 (ML1777c)	F 5'-GCTCAACGTCGCGTGATCGA-3' R 5'-GAACACGAAGCGGTTGAGC-3'	790
	glpD2 (ML0713)	F 5'-CGGTGCGTTGCGATTA -3' R 5'-GCGCCATCCTCCGAATCG-3'	186
	sdhD (ML0698c)	F 5'-ATGAGCAACTCCGATCTTCAG-3' R 5'-CGTGTGGTCTTTGCGGCTGTA-3'	345
2 (glycerol pathway and TCA)	glpQ2 (ML2571)	F 5'-CCGGTAAGCATGCAGGCG-3' R 5'-ACCATCCCATGGCCCCAA-3'	140
	lldD2 (ML2046)	F 5'-ATTAAACGAGCCCAACAAGC-3' R 5'-GGCGAGAGTGGATAACGAAA-3'	125
	atpα (ML1143)	F 5'-ACAATCTCCGCTGACGA-3' R 5'-CGAAGTCACCAAGTATCACCG-3'	200

3 (drug resistance screening)	*gyrA* (*ML0006*)	F 5'-CCG TAG CCA CGC TAA GTC A-3' R 5'-C CCG GCG AAC CGA AAT TGC-3'	168
	gyrB (*ML0005*)	F 5'-ACTGATCCTCGAAGTTCTGAACTG-3' R 5'-CAATGCCGTAATAATTTGCTTGAA-3'	186
	rpoB (*ML1891c*)	F 5'-CAGGACGTCGAGGCGATCAC-3' R 5'-TCG TCA GCG GTC AAG TA-3'	396
	folP1 (*ML0224*)	F 5'-TTCGTTCTCAGATGGCGGAC-3' R 5'-GCCCACCAGACACATCGTTG-3'	286
4	*sodA* (*ML0072c*)	F 5'-TGAGATCAACGAGATCCACC-3' R 5'-GCCCAGTTTACGACATTCC-3'	408
	16S rRNA	F 5'-AGAGTTTGATCCTGGCTCAGG-3' R 5'-CATCCTGCACCGCAAAAAGCTT-3'	250
5 (glycerol pathway)	*glpQ1* (*ML0074*)	F 5'-GCCTATGAGCTCGCGCTC-3' R 5'-CCAGTCCAGAACCAATGAAAC-3'	220
	gpdA1 (*ML2280c*)	F 5'-AGAACATCTTCGCCATCGTGG-3' R 5'-AGTTGATTGGTACAAGTGACG-3'	160
	gpdA2 (*ML1679c*)	F 5'-GCATGGGGCACTGCACTG-3' R 5'-AGCAATCTCGCTAGCCAG-3'	372
6 (ATP synthesis)	*atpα* (*ML1143*)	F 5'-ACAATCTCCGCTGACGA-3' R 5'-CGAAGTCACCAAGTATCACCG-3'	200
	atpγ (*ML1144*)	F 5'-GAGTCCGCCCGACCCTACGCT-3' R 5'-GCGATTTTGGCGGCGTTCTCA-3'	300

5.3.11 Quantitative Real time PCR (qRT-PCR) (Taqman assay)

Quantitation of gene expression of *M. leprae* genes *sodA, atpα,* and *16S rRNA* was accomplished using Real Time PCR Design Tool for Taqman assay through Integrated DNA Technologies (IDT) (http://www.idtdna.com/Scitools/Applications/RealTimePCR/Default.aspx). The primers and probe (dual-labeled) were designed based on *M. leprae* genome sequence (http://genolist.pasteur.fr/Leproma/) (**Table 5.9**) The level of gene expression was normalized by using DNA-based, real-time PCR assay. The primers and probes were first tested individually to standardize the PCR condition and the efficiency; later on multiplex PCR with three primers sets were set up.

Purified *M. leprae* DNA or cDNA (2 μl) was added to 20 μl PCR mixture total, containing iQ Multiplex Powermix (Bio Rad, US), 400 nM of each primer, and 200 nM of each probe for RNA-based PCR assays. Reaction mixtures were subjected to 95°C for 3 min, and 40 cycles of 95°C for 30 sec and 60°C for 1 min using a Bio-Rad CFX 96 system. The quantity of cDNA and DNA for each gene was based on the cycle threshold (Ct), and with standard curve generated by using different known concentrations of *M. leprae* DNA (NHDP-63) at ten-fold dilution ranging from 10ng-1pg. Each PCR and Taqman assay for each sample was run in triplicate.

Several genes listed in **Table 5.8** were tested for gene expression using the Taqman assay, but due to detection limit (high Ct values) and sensitivity factors only three genes were chosen (**Table 5.9**) at the end to compare the viability of *M. leprae* in different media.

Table 5.9: Taqman assay primers and probes

Gene	Primers and probes sequence of *M. leprae* targets	Product size bp
sodA (ML0072c)	F-5'-CTG GAA CCA CAT ATC TCT GGT GAG -3 R- 5'-CCC AAATGA AAG GCC AGGTTC TTC -3 P- 5'-FAM/AAG GTGTCA ATG ACG CGCTTG CCAAA/3BHQ_1/ 3	167
atpα (ML1143)	F-5'-GAA GAG TAC GTA AGC TCC TTC ACC'3 R-5'-CGT TAT GTT CGT CGA GGT TGA G'3 P-5'- HEX/TGA TGACCC AGG AGCTGC TCG AGT T/3BHQ_1/ 3	175
16S rRNA (MLP000016/rrs)	F- 5'-TGC AAG TCG AAC GGA AAG GTC TCT'3 R- 5'-ACC CAG TTT CCC AAG CTT ATC CCT'3 P -5'-cy5/TA ACA CGT GGG TAA TCT GCC CTG CAC TT/3BHQ_1/ 3	180

5.3.12 Quantitative Real time PCR (qRT-PCR) with pre-amplification

The qRT-PCR was repeated for the final experiment (preparation #6) using the extra step of pre-amplification before the final qRT-PCR. This was done to increase the detection limit (decrease the Ct values) for the quantitative analysis.

Protocol for qRT-PCR with pre-amplification of cDNA

The PCRs was made with 1 µl of each *M. leprae* cDNA (from a starting of 20 µl) and DNA (from a starting of 100 µl) and RT minus controls as templates and were amplified using 0.2 µM of primer combination and multiplex mix in 10 µl total reaction. The PCR step was made using IQ multiplex power mix enzyme with 2 µl template (cDNA) and 200 nM of upper multiplex primer mix and lower multiplex primer mix in a total 25 µl reaction. The PCR cycling condition consists of 95°C for 3 min, and 10 cycles of denaturation at 95°C for 15 sec and annealing at 60°C for 4 min. After the PCR, the reaction product was diluted 1:5 (in TE buffer) and used as template for qPCR. The qPCR mix was made in a 20 µl total consisting of 10 µl of IQ multiplex power mix enzyme, 200 nM of each upper and lower multiplex primer mix, 200 nM of each primer specific probe and 3 µl of the template (diluted PCR product (1:5).

5.3.13 Statistical analysis

The RR data, a representative of three experiments (RR readings) are shown as mean ± SD. The standard curves for each RT-PCR assay and the correlation between the RR, viability staining and RT-PCR were calculated using a linear regression model (Minitab 16).

5.4. RESULTS

5.4.1 Searching for favorable media for *M. leprae* viability and radiorespirometry (RR) results
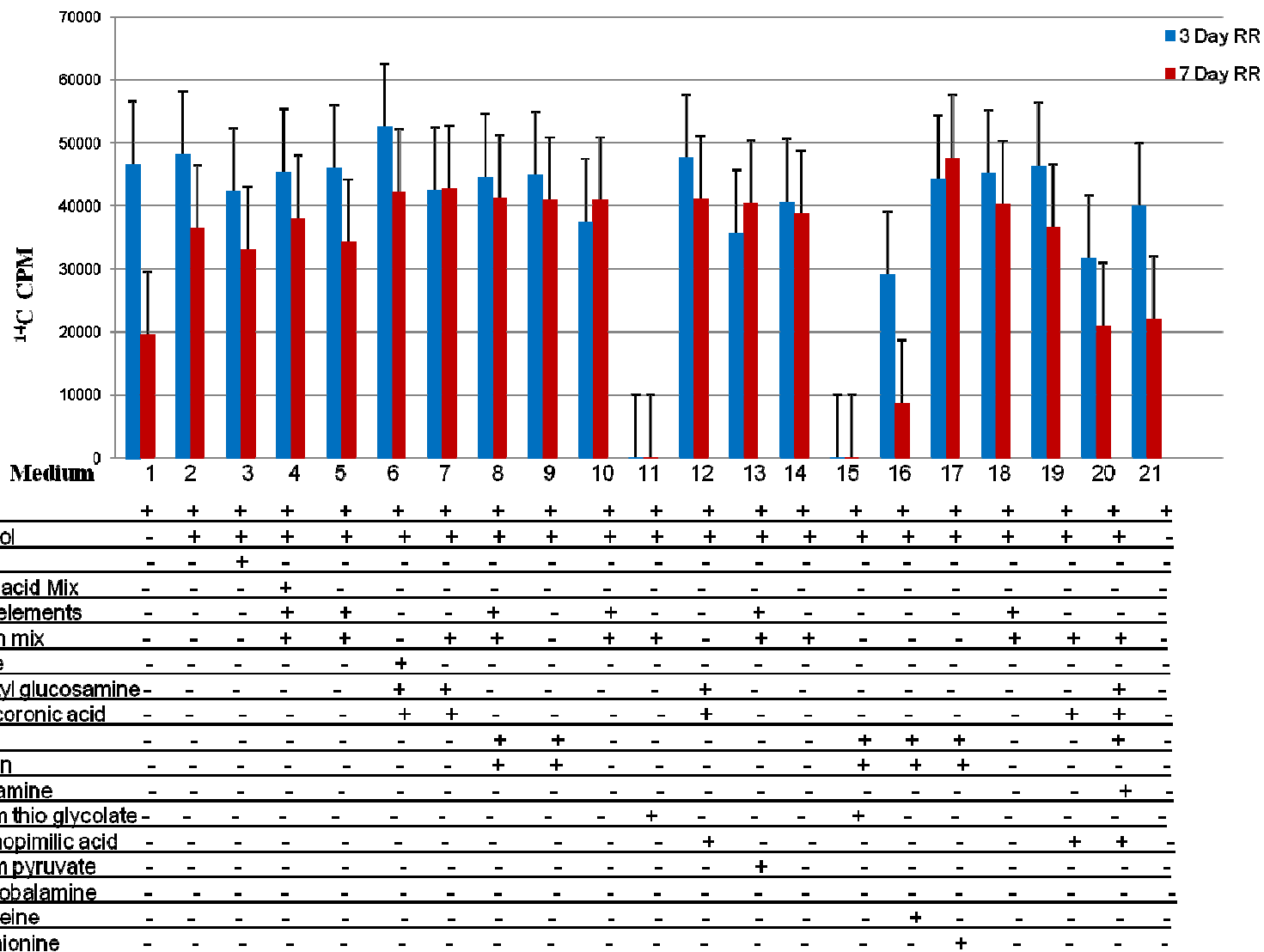
Many experiments (in our lab) have been done to study the effect of different supplements on *M. leprae* viability. Different media formulations were made using 7H9 as base with simple carbon sources (glucose, sucrose, sodium thioglycolate, glutamine, glycerol, citric acid, sodium acetate) to more complex mixture (yeast extract, brain heart infusion broth, fetal calf serum, and peptone) and various growth supplements such as amino acids, vitamins mix and trace elements were added. **Table 5.2** shows the 55 different media formulations that were made and tested. The carbon sources with the addition of amino acid mix were compared to each other and used as the basis (letter B medium) for comparson the effect of adding different supplements (vitamin mix, trace elements, and lipid cocktail). Standard radiorespirometry (RR) was used to rapidly identify formulations that were either deleterious or better than the base media. **Figure 5.1** illustrates the RR results for these carbon sources. The addition of casitone, bovine albumin and dextrose to 7H9 medium, resulted in a medium we called 7H12 or NHDP. The NHDP medium was then modified with addition of different carbon source as shown in **Table 5.3** and **Table 5.4.** The findings from these set of experiments **(Table 5.2-5.4)** showed that 7H12 (NHDP) is an excellent basal medium to support survival of *M. leprae* for one week. Addition of some carbon sources such as methionine, mycobactin and cobalmine and trehalose to NHDP had virtually no effect on improving the RR of *M.*

273

leprae. Of the several formulations tested, glycerol at 2% to the NHDP demonstrated higher *M. leprae* RR activity when compared to the basal NHDP medium, at least up to 7days. The effects of 2% glycerol in the NHDP media plus other supplements were tested as shown in **Table 5.5.** As a result of media formulations trials (**Tables 5.2-5.5**), a new set of experiments (media preparation # 5) were designed for selection of the promising formulations, which have addition of glycerol (**Table 5.6)** The RR values for all media experiments are shown for each **Table (5. (2-6)** and the summary of RR results of all the tested media is illustrated in **Table S5.3.**

7H12 (NHDP) medium was capable of ensuring respiration (viability) up to 7 days. However, the challenge was to prevent the drop in bacterial viability during the second week. Therefore, 7H12 (NHDP) was used as the base and test the effect of specific supplements for a new set of formulations. 21 formulations were made, 2% glycerol was added to these formulations except # 1 and 21 (NHDP only) other formulations (3-20) have different components beside 2% glycerol**.** The new media with 0.1% sodium thioglycolate media # 11 and 15 in **Table 5.6**, showed decrease in viability based on the RR data (**Figure 5.2).** This decrease in respiration could be because the available oxygen may have been reduced to intolerable levels. Glycerol at 2%, was by itself a useful component, capable of enhancing viability *of M. leprae* as seen by RR activity media # 2, **Figure 5.2.** The addition of other additives to NHDP even in the presence of glycerol had virtually no effect on improving *M. leprae* viability in 7H12 (media 3-19 except 11, 15 and 16). Media #16 has beside the NHDP and glycerol, the addition of L-cysteine (0.1%) that showed more than 50% drop in the respiration by 7days.

274
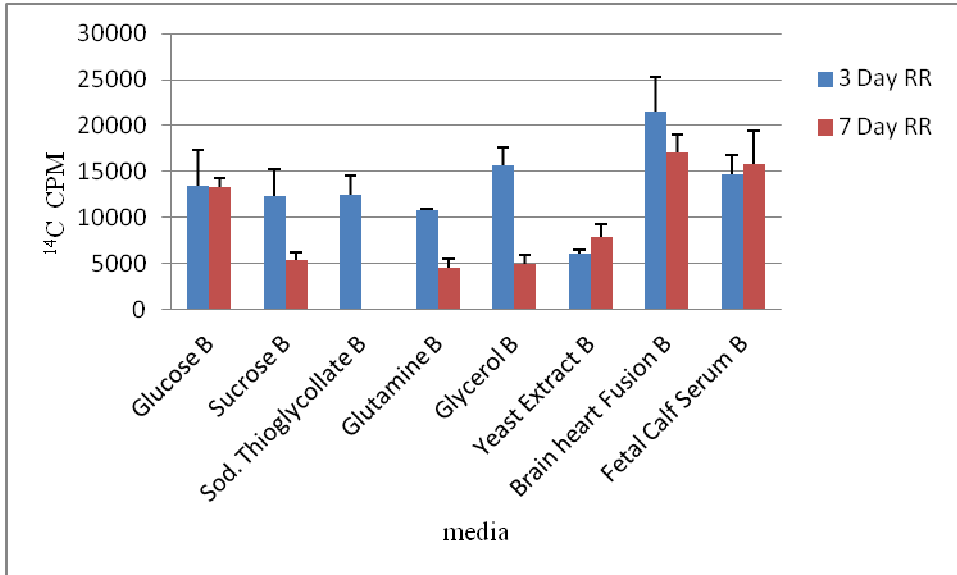
Figure 5.1: **Radiorespirometry (RR) of** *M. leprae* **in 7H9 medium with amino acid mix as supplement (media with letter B in Table 5.2) and with different carbon sources** (glucose, sucrose, sodium thioglycolate, glutamine, glycerol, yeast extract, brain heart fusion, and fetal calf serum) for 3 and 7 days. It showed the positive effect of some compounds like brain heart fusion, and fetal calf serum in maintaining the *M. leprae* respiration by 3 and 7 days. While the media with sodium thioglycolate, showed drop in the *M. leprae* respiration by 7 days.

| Medium	1	2	3	4	5	6	7	8	9	10	11	12	13	14	15	16	17	18	19	20	21
NHDP	+	+	+	+	+	+	+	+	+	+	+	+	+	+	+	+	+	+	+	+	+
Glycerol	-	+	+	+	+	+	+	+	+	+	+	+	+	+	+	+	+	+	+	+	-
Hemin	-	-	+	-	-	-	-	-	-	-	-	-	-	-	-	-	-	-	-	-	-
Amino acid Mix	-	-	-	+	-	-	-	-	-	-	-	-	-	-	-	-	-	-	-	-	-
Trace elements	-	-	-	+	+	-	-	+	-	+	-	-	+	-	-	-	-	-	+	-	-
Vitamin mix	-	-	-	+	+	-	+	+	-	+	+	-	+	+	-	-	-	-	+	+	+
Ribose	-	-	-	-	-	+	-	-	-	-	-	-	-	-	-	-	-	-	-	-	-
N-acetyl glucosamine	-	-	-	-	-	+	+	-	-	-	-	+	-	-	-	-	-	-	-	-	+
D-Glucoronic acid	-	-	-	-	-	+	+	-	-	-	-	+	-	-	-	-	-	-	-	+	+
FBS	-	-	-	-	-	-	-	+	+	-	-	-	-	-	-	+	+	+	-	-	+
Dextran	-	-	-	-	-	-	-	+	+	-	-	-	-	-	-	+	+	+	-	-	-
L-Glutamine	-	-	-	-	-	-	-	-	-	-	-	-	-	-	-	-	-	-	-	-	+
Sodium thio glycolate	-	-	-	-	-	-	-	-	-	-	-	+	-	-	-	+	-	-	-	-	-
Diaminopimilic acid	-	-	-	-	-	-	-	-	-	-	-	+	-	-	-	-	-	-	-	+	+
Sodium pyruvate	-	-	-	-	-	-	-	-	-	-	-	-	+	-	-	-	-	-	-	-	-
Cynocobalamine	-	-	-	-	-	-	-	-	-	-	-	-	-	-	-	-	-	-	-	-	-
L-Cysteine	-	-	-	-	-	-	-	-	-	-	-	-	-	-	-	+	-	-	-	-	-
L-Methionine	-	-	-	-	-	-	-	-	-	-	-	-	-	-	-	-	+	-	-	-	-

Figure 5.2: Radiorespirometry (RR) of *M. leprae* at 3 and 7 days in different media formulations listed in Table 5.6. As seen in previous trials 2% glycerol sustains the RR for up to 7 days (compare # 1 7H12 versus 2-19). Sodium thioglycolate (media number 11 and 15) has a negative influence as early as 3 days.

5.4.2 Molecular method results

The total DNA and RNA were extracted from *M. leprae* cells, incubated in each of the 21 media in **Table 5.6**, using All Prep DNA/RNA Kit. Since mRNA is highly labile with short half-life, it was used as indicator for viable bacteria. The cDNAs were prepared from *M. leprae* cells (mRNAs) by reverse transcriptase PCR. The DNA and cDNA were used as templates in a multiplex PCR to amplify gene specific-primers in different combinations. Several genes were from glycerol pathway **(Figure S5.1)** and TCA pathway. For example, **Figure 5.3 (A-C)** shows the expression (cDNAs) of some genes (combination 1, 3, 5 in **Table 5.8).** The 16S rRNA, and sodA genes were tested individually for some of the media (# 1, 2, 3, 11, 15, 16 and 21) for 3 and 7 days **(Figure 5.3, D, E)**. Moreover, combination 1 and 3 targets were used to test all the cDNA prepared from all the media **(Supplementary Tables).** Based on these gene expression observations from all the tested media, the RT-PCR results from the target messages were found to correlate well with the RR data in **Figure 5.2.**
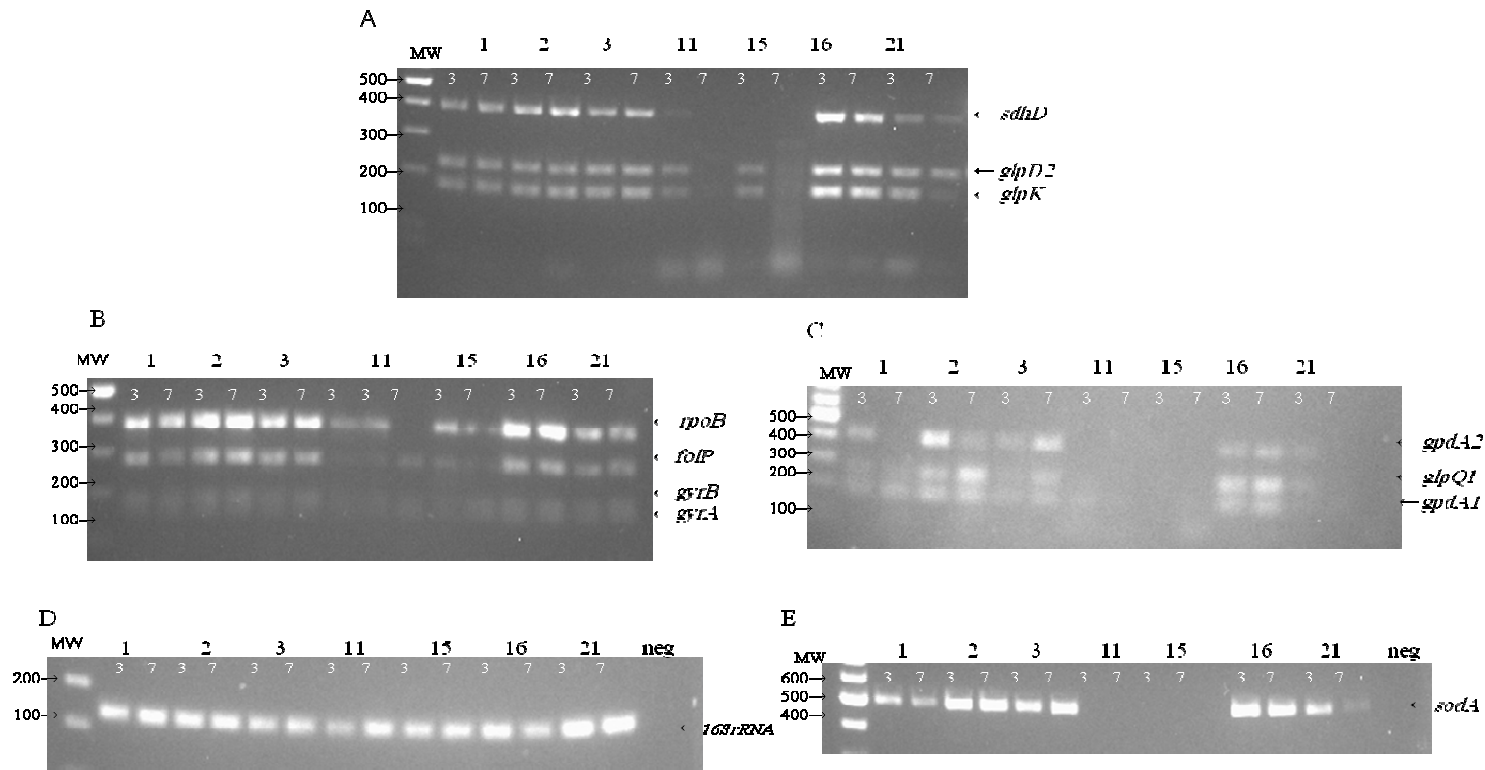
Figure 5.3: Detection of combination 1 (A), combination 3 (B), combination 5(C) and *16 S rRNA* (D), *sodA* (E) gene targets amplified with multiplex PCR. The cDNA from *M. leprae* grown in different media formulations at 3 and 7days was used as template. *M. leprae* grown in media # 11 and 15 have lost the expression of *sdhD* by 3 days and then lost the message for all the targets in combination 1(*sdhD, glpD2 and glpK*) by 7 days. Also, very less amplification of the targets tested was seen for *M. leprae* in media # 11 and 15 in the other combinations (3, 5). The *16S rRNA* was detected in all the tested media, but the *sodA* message was lost for cells in media # 11 and 15 by 3 and 7 days.

278

### 5.4.3 RR and RT-PCR results from the confirmatory experiments

Confirmation experiments for the effect of 2% glycerol on the *M. leprae* viability from 0 to 14 or 21 days were done. Also, to compare the three media formulation NHDP (N), NHDP+ 0.1% thioglycolate (N+T) and NHDP +2% glycerol (N+G), two independent experiments (new *M. leprae* batches) (1 and 2) were done with three technical replicates (the cells were dispensed into three vials and triplicates PCR for each) for different time points, analyzed by the RR assay and the molecular (qRT-PCR) approaches. Rifampicin (a known bactericidal agent) was also used as a negative control to verify the inhibitory effect on bacterial respiration **(Table 5.7).** The RR data of *M. leprae* cells in all the tested media **(Table 5.7)** at 3 and 7 days is shown in **Figure 5.4A** (first experiment) and for 0-21 days in **Figure 5.4B** (second experiment). In comparison to the respiration rate of *M. leprae* in NHDP media, the other media with thioglycolate or rifampicin went down (more than half) by 7 days except for the media containing glycerol which still showed more than 50% activity at 7days and 25% at 21 days.

### Bacterial viability (staining test, VS)

The viability of the bacilli from the second experiment was also tested based on the membrane integrity using LIVE/DEAD BacLight Bacterial Viability Kit as shown in **Figure 5.5**. The results from this method correlate well with the RR data as illustrated in **Figure 5.6**
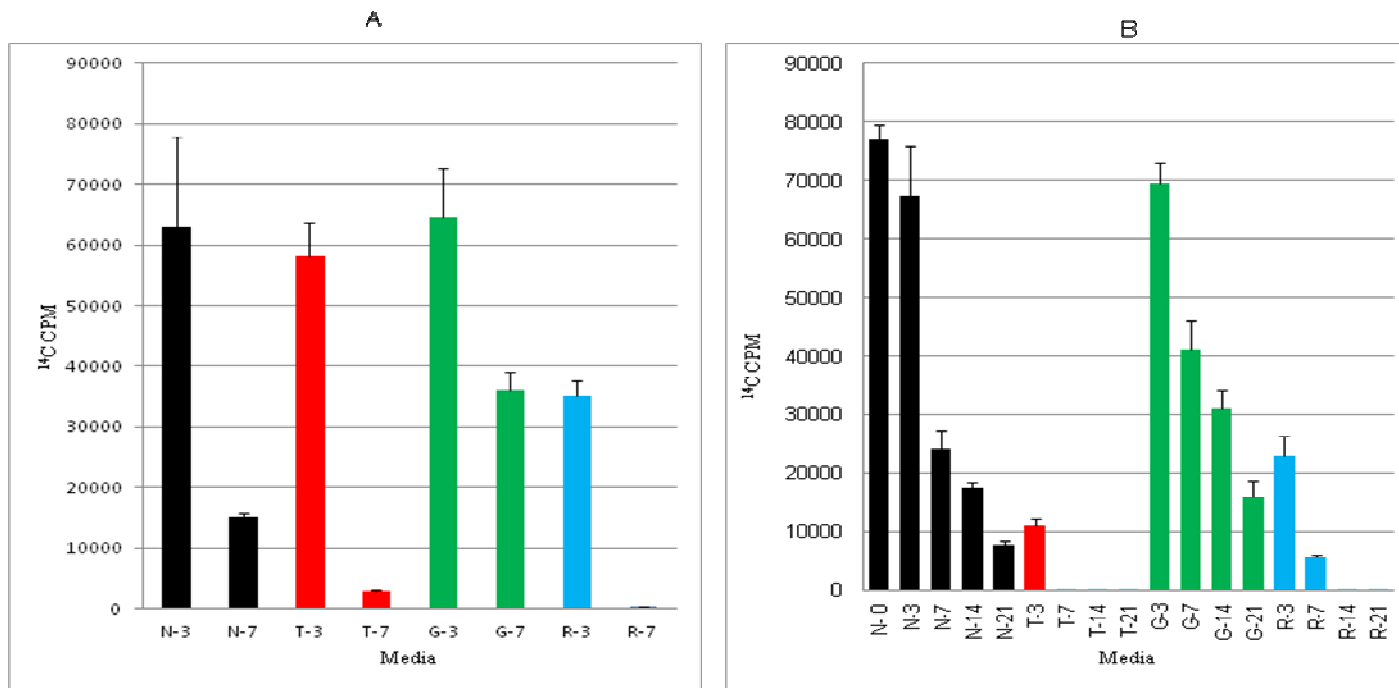
Figure 5.4: **Radiorespirometry (RR) of *M. leprae* (from two independent experiments); comparing of viability in different media.** NHDP (N), 0.1% sodium thioglycolate (T), 2% glycerol, and rifampicin (R) at different time points. A- *M. leprae* RR was tested at 3 and 7 days, B- *M. leprae* RR was tested at 3, 7, 14 and 21 days. In both experiments there was a decrease in the *M. leprae* respiration by 7 days in the media N, T and R. In the G media the decrease was not as dramatic and the respirations continued for up to 21 days. These experiments confirm the effect of 2% glycerol in maintaining *M. leprae* respiration for up to 21days.
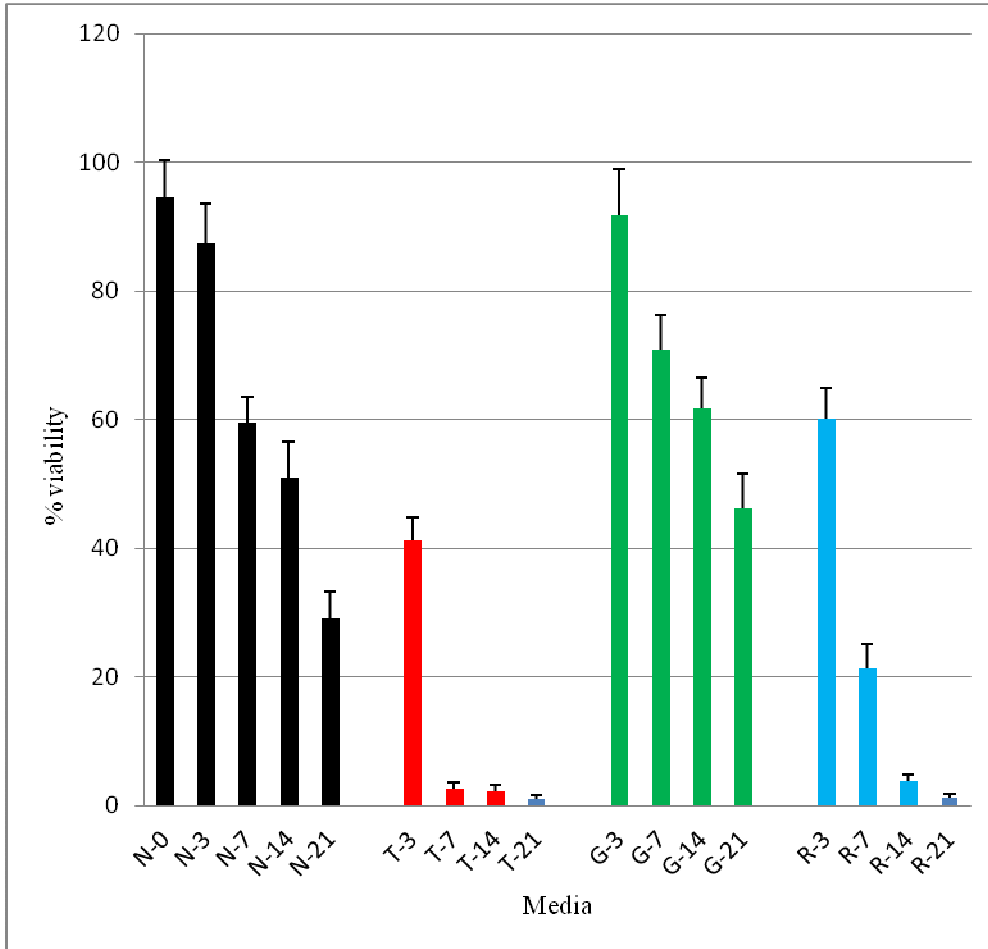
Figure 5.5: **Detection of the bacilli viability using the staining technique (VS).** The *M. leprae* in media containing 0.1%thioglycolate and rifampicin showed a drop in viability (more than half) by 7 days. The *M. leprae* in the basal media (NHDP) showed half the viability by 14 days then the viability dropped, while the NHDP media containing glycerol maintained the viability (~50%) of *M. leprae* to 21 days.

RR = - 9856 + 811.5 %
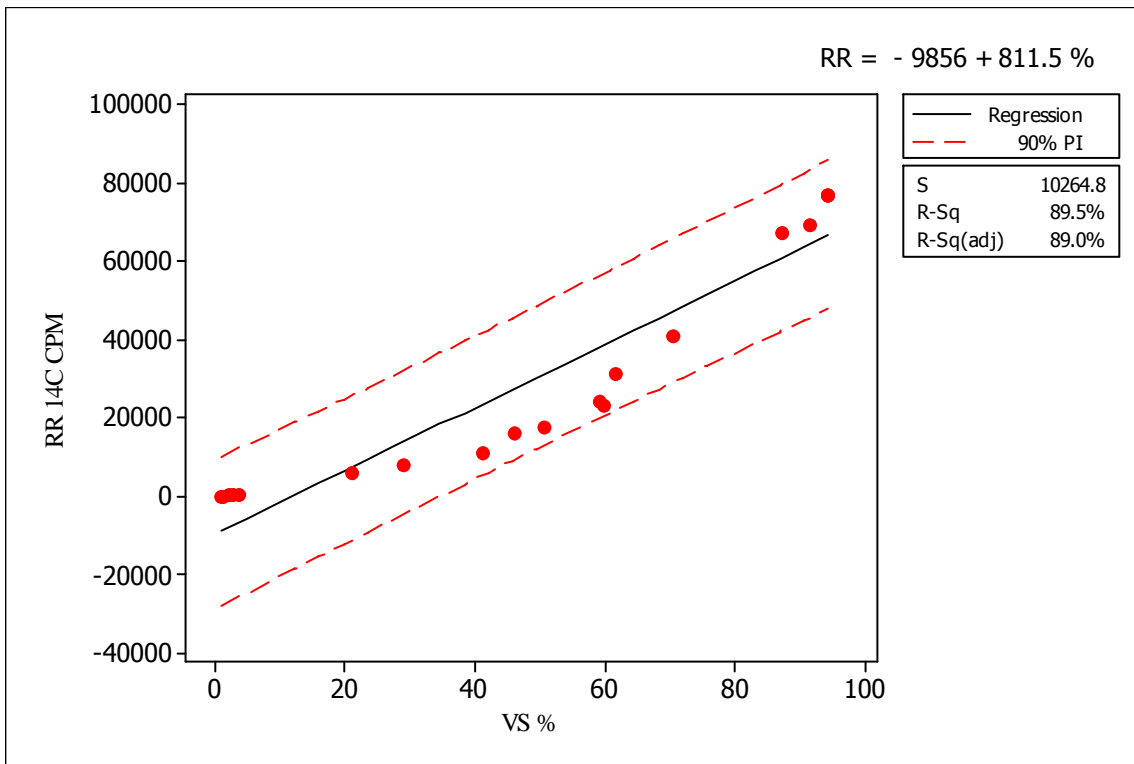
Figure 5.6: Correlation of VS with RR: linear regression model shows the correlation between the cumulative 7day RR counts (CPM) with the percentage of live *M. leprae* as measured by the viability staining (VS) technique. *M. leprae* were obtained from each medium condition and subjected to both assays.

5.3.4 Real-time PCR (RT-PCR)

The RR and VS data correlate with the gene expression of three gene targets tested (*sodA, atp-α* and *16S rRNA*) using the cDNAs (RT+) as template extracted from *M. leprae* grown in all tested media at different time points, shown on agarose gel in **Figure 5.7**. The *M. leprae* DNAs extracted from all cultures were analyzed in parallel to the cDNA to confirm that equal amount of cells were used. This test was also done for the sample in the

second experiment and the same RT-PCR on agarose gel was reproduced for theses

selected media condition (data not shown).
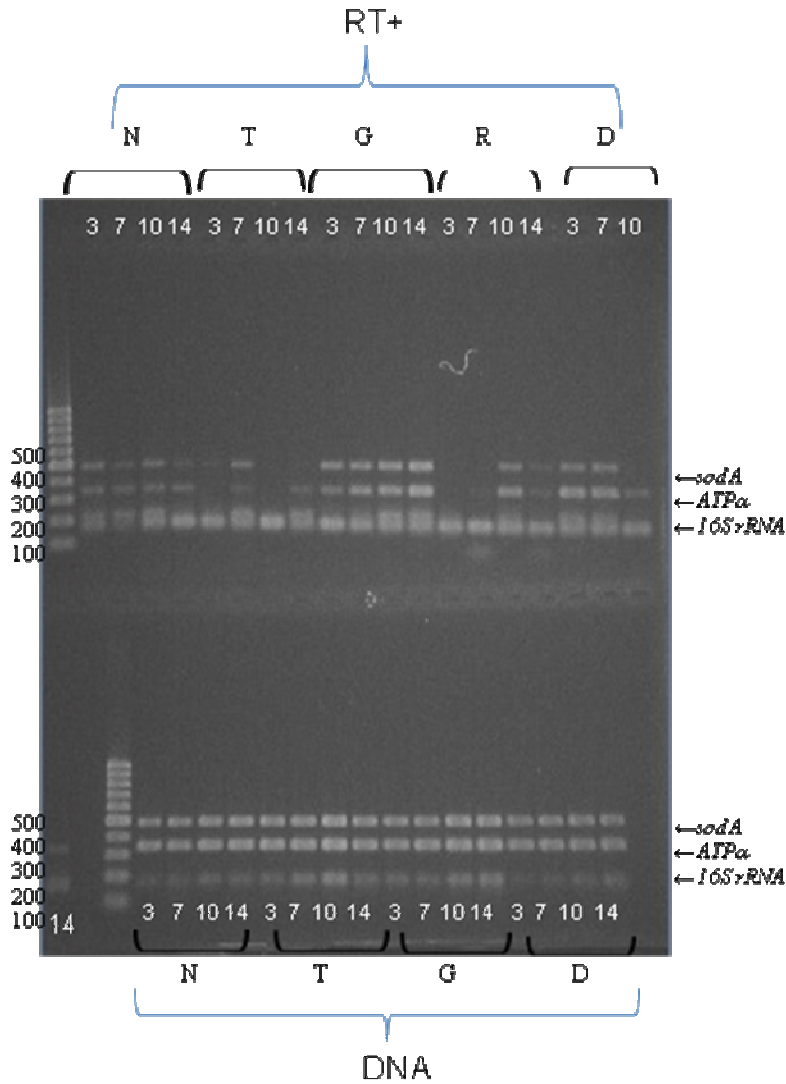
Figure 5.7: **Detection of** *sodA, atp-α* **and** *16S rRNA* **genes by multiplex PCR using**

cDNA (RT+) and DNA templates. *M. leprae* messages for the selected genes were lost or

reduced in tested media, except for *M. leprae* from the media containing 2% glycerol,

which were maintained up to 14 days. The *16S rRNA* was amplified from all tested media

conditions for all the time points (3-14 days).

5.4.5 Quantitative Real-time PCR (qRT-PCR), confirmed the beneficial effect of glycerol and inhibitory effect of thioglycolate on *M. leprae* gene expression

Taqman multiplex RT-PCR using iQ Multiplex Powermix was used to quantify the gene expression of selected genes (*atp-α, sodA* and *16S rRNA*). Two independent experiments were conducted. Three independent cultures and triplicate PCRs were set up for each condition. For the qRT-PCR a standard curve was developed based on 10 fold dilution of *M. leprae* (NHDP-63) DNA (ranging from 10 ng to 1pg). The PCR efficiencies were 96.1% for *sodA*, 100.7% for *atp-α* and 85.0% for *16S rRNA*. The R values were between 0.998 to 0.994 **(Figure 5.8).**

The mRNA levels in different media were compared to the corresponding DNA quantity for each gene. In comparison to *M. leprae* in NHDP and NHDP + thioglycolate, *M. leprae* in NHDP + glycerol medium had more mRNA copies (lower Ct values) for the tested genes up to 14 days (first experiment) or 21 days (second experiment). On other hand, the DNA amounts were similar in all the media for all the genes tested.
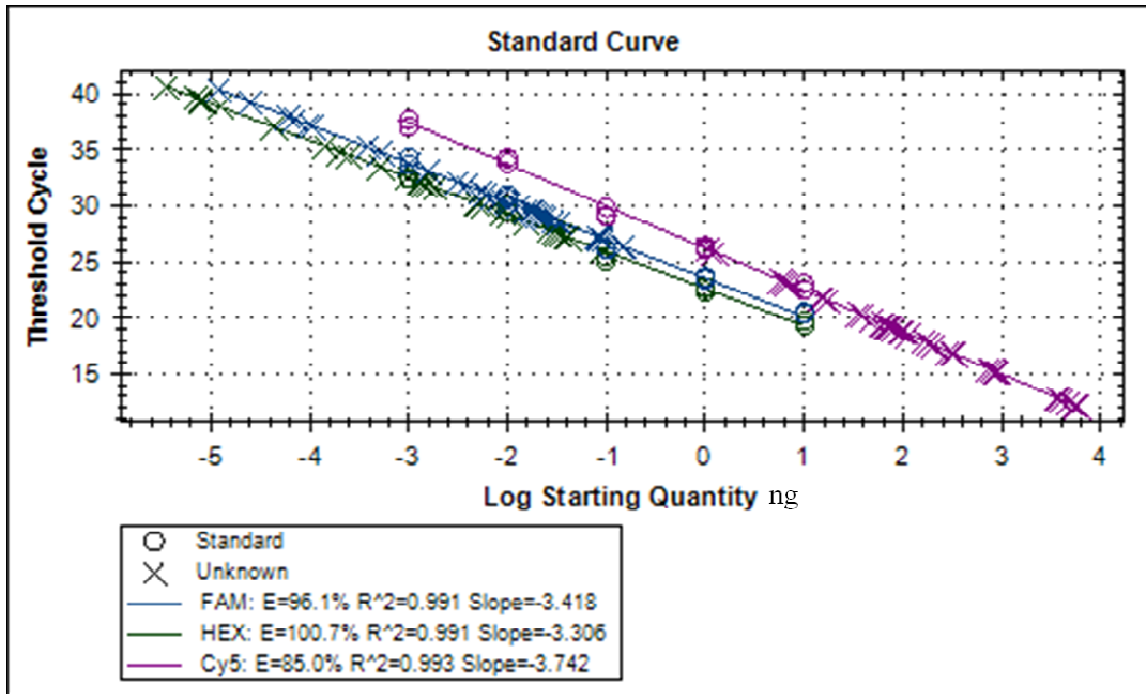
Figure 5.8: RT-PCR standard concentration curves for target genes (*sodA* (FAM), *atp-α* (HEX), *16S rRNA* (Cy5) tested based on 10 fold dilution of *M. leprae* DNA.

Moreover, the Ct values for DNA and cDNA of target genes in each media condition were compared. Unlike the Ct vlaues of the DNA which seems to be stable for all the tagets in all the media, the Ct values of cDNA for all tested genes changes (increased Ct, less mRNA) for NHDP and thioglycolate containing media. However, the cDNA values for the tested genes were more stable in media containing glycerol as shown in **Figure 5.9.** This experiment was also repeated with similar results (data not shown). These results confirmed the role of media containing glycerol in maintaining *M. leprae* viability (respiration and gene expression) up to 21 days, compared to basal medium NHDP and thioglycolate containing medium.

285
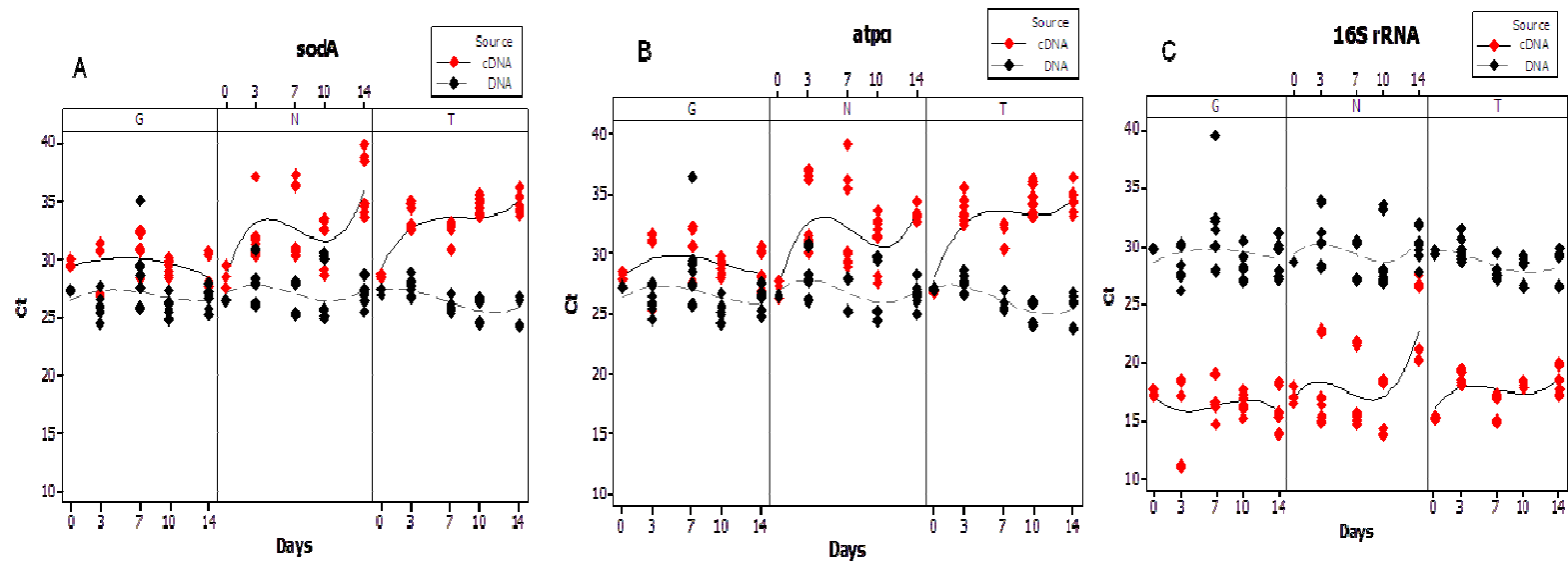
Figure 5.9: **Comparison between DNA and cDNA levels of *M. leprae* grown in three different conditions.** Three targets were tested; A-sodA, B-atp-α and C- 16S rRNA. *M. leprae* grown in the NHDP and the thioglycolate media showed decrease in the expression of all target genes (increase in Ct values) by 10 days, while glycerol media stabilized the gene expression over the time period tested. Each medium was tested in three independent cultures. Triplicate RT-PCRs were run for each independent culture (9 data points for each medium).

Pre-amplification Real-time PCR (qRT-PCR)

Using the pre-amplification step, we were able to use less amounts of the templates. Multiplex qPCR for four genes (*sodA,*

atp-α, gpdA2 and *16S rRNA*) was performed. The effect of different media on cell viability was compared based on the Ct values:

we were able to detect the gene expression until 21 days (**Figure 5.10).**
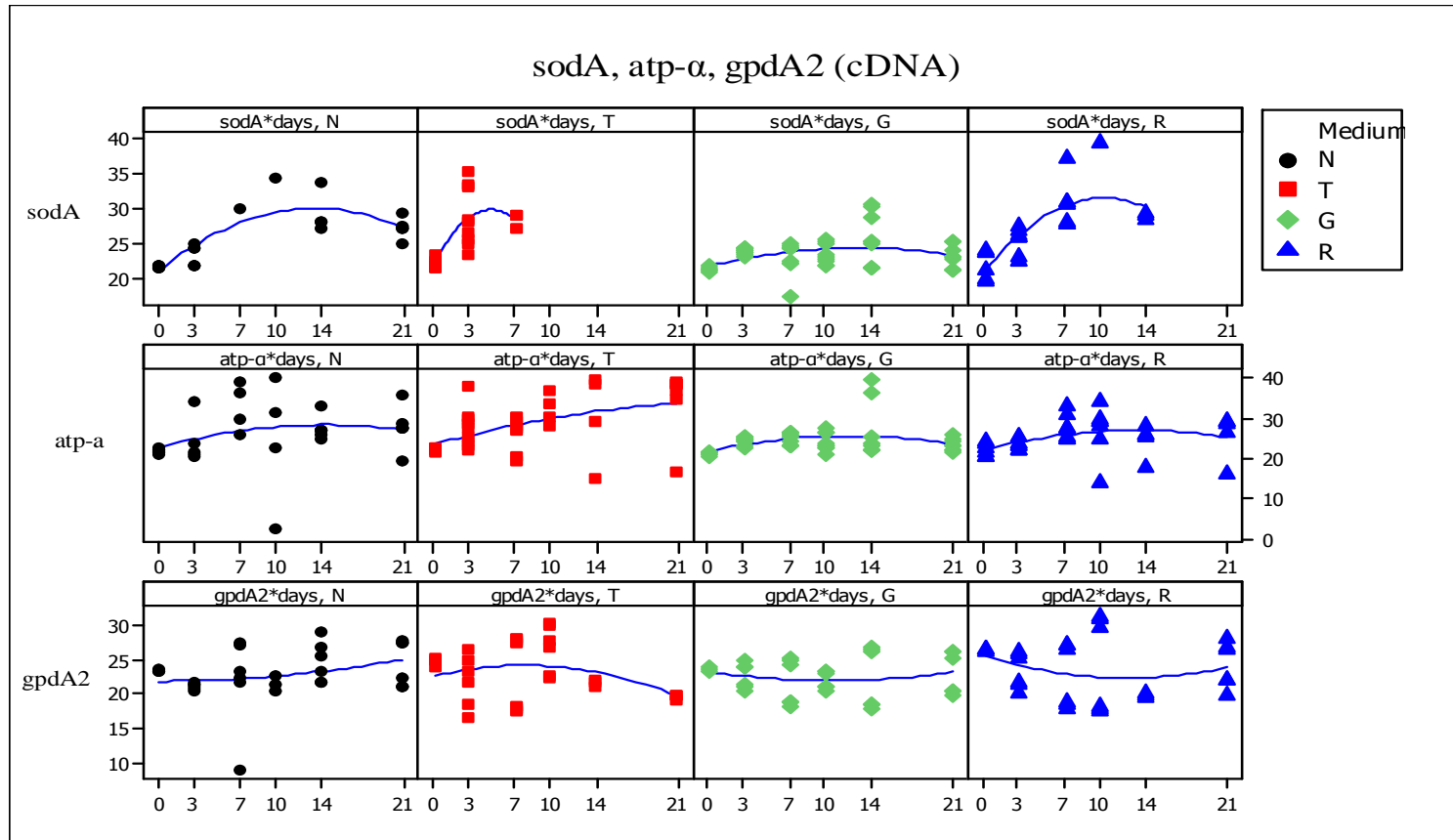
Figure 5.10: Comparison between Ct values of cDNA of *M. leprae* genes *sodA*, *atpα* and *glpdA2* for different media condition; regression cubic fit was used to connect the values. *sodA* mRNA decreased in media containing NHDP (N), rifampicin (R) and the thioglycolate (T), while it was stable for glycerol (G) containing medium up to 21 days. Unlike *sodA*, the expression of other genes (*atpα* and *glpA2*) did not show a distinct change in gene expression between media (the data are more scattered).

Unlike the expression of the *16S rRNA*, the expression of *sodA* seems to change depending on the media condition and time points, which matches the RR and the viability staining results. Therefore, the qRT-PCR results of *sodA* gene expression for all the media and the time points were correlated to the RR (**Figure 5.11**).
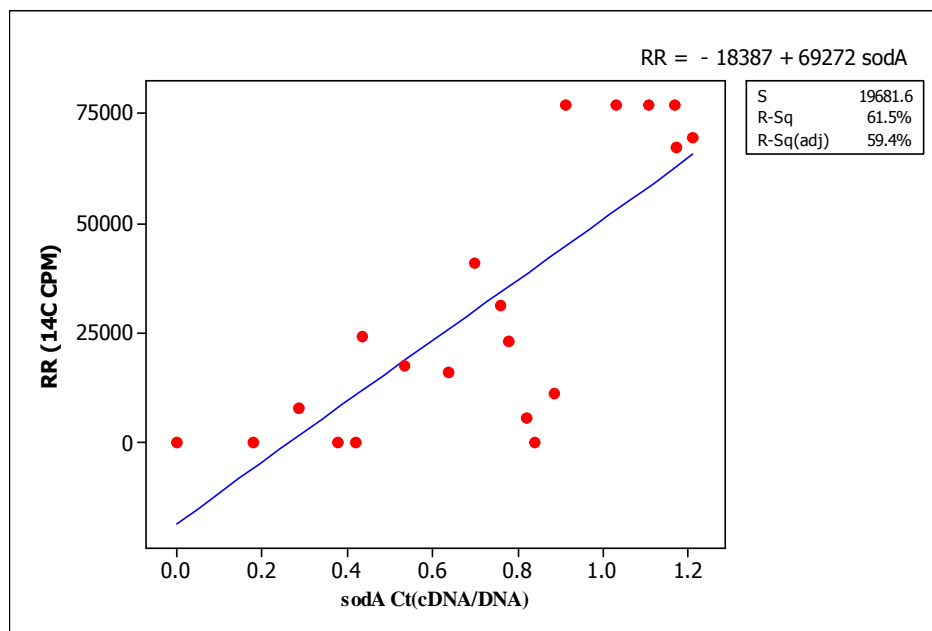
Figure 5.11: **Correlation of *sodA* qRT-PCR Ct (cDNA/DNA) results with the RR for the same sample sets using fitted line plot.** The gene expression of *sodA* is correlate well (r2= 61.9%) with the RR values for each media condition.

5.4.6 Fold change (difference) in gene expression between media condition

The fold change in gene expression (*sodA* and *atpα*) in media containing glycerol in comparison to NHDP (N) or NHDP with thioglycolate (N+T) was calculated using $2^{-\Delta\Delta Ct}$ method. The Ct values for each condition were normalized using the DNA (Ct) for each medium condition. Starting at 7 days there were ~20 fold differences in the level of gene expression in the media containing glycerol (N+G) compared to the base line media N or N + T. This difference continues for 10 and 14 days **(Figure 5.12).**
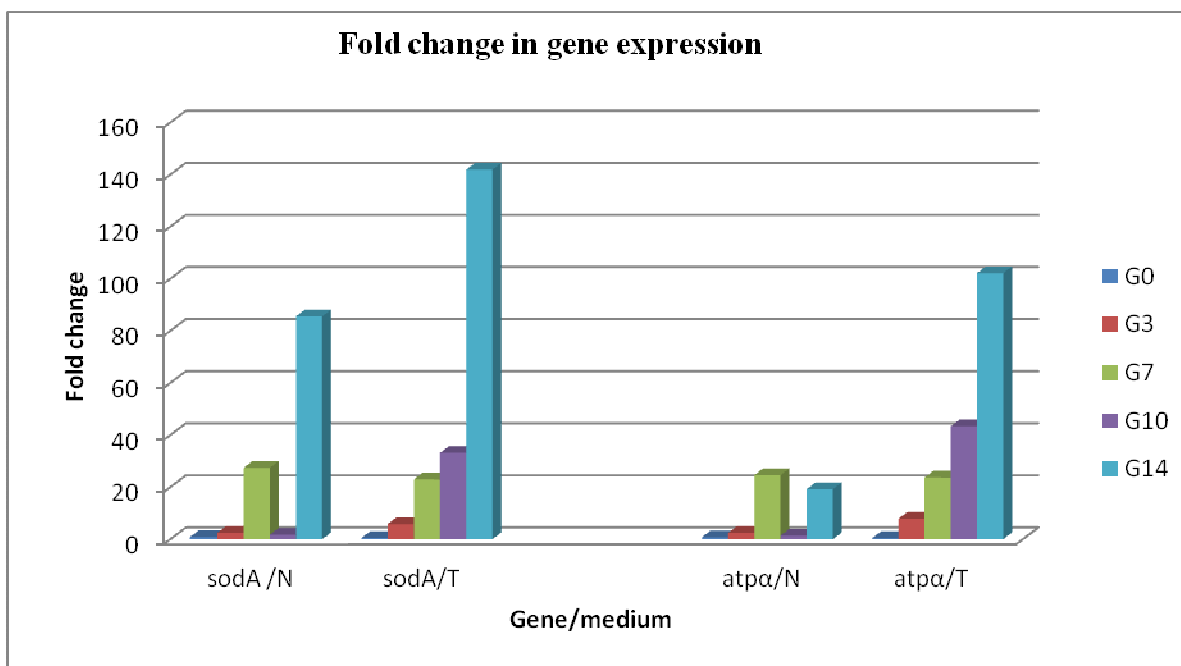
Figure 5.12: Differences in gene expression (*sodA* and *atpα*) in media containing glycerol (G) and thioglycolate (T) and NHDP (N) media.

5.5. DISCUSSION

M. leprae is an obligate intracellular parasite. Previously attempts were made to cultivate *M. leprae* in several types of cultured cells, which this resulted in successful replication on human derived macrophages **(Samuel D., 1973)** and in nervous tissue (Schwann cells) **(Mukherjee R., 1985).** In addition to tissue culture, attempts over a century were also made to cultivate *M. leprae in vitro* using cell-free culture. Many studies claimed cultivation of *M. leprae* **(Nakamura M., 1949, Dhople A., 1988).** However, until now no published paper has produced proof (differentiated from other mycobacteria species) of multiplication of *M. leprae* in artificial media. Other experiments that were done to monitor the bacterial viability during lab tests showed that the bacilli survived for one day at 37ºC, 7 days at 20 ºC to 30 ºC and for 90 days in lyophilized conditions **(Sreevatsa., 1997).** The major criteria used to claim culturing (cell free) of *M. leprae* were based on macroscopic and microscopic examination of the cultured bacilli using acid fast stain and an inability to grow on LJ media. Other criteria that were rarely used in some studies to verify the viability were inoculation into the mouse foot pad **(Pattyn S., 1973, 1977).**

In order to be able to cultivate or maintain *M. leprae in vitro*, the metabolism of the bacilli should be characterized to identify defected metabolic pathways, so that appropriate nutrient are provided. The second step is to verify the viability of the bacilli in the *in vitro* system.

Analysis of the genome sequence of *M. leprae* revealed gene deficiencies in specific metabolic pathways, such as detoxification of reactive oxygen and nitrogen species. *M. leprae* also encodes some metal, amino acid and sugar transporters, but it lacks some enzymatic steps in glycolysis, and the TCA cycle. *M. leprae* is also found to have deficiency in one of the trehalose biosynthesis pathway (Tre Y-Z pathway) and fatty acid biosynthesis (cannot synthesize malonyl-CoA, lacks acetyl-CoA ligase and glutaryl-CoA dehydrogenase and lacks most of the lipase genes). In addition *M. leprae* is missing pathways for thiamine (vitamin B1) and thiamine-PP biosynthesis. The gene for siderophores biosynthesis is also missing. Based on this information, specific culture media (axenic) were designed by adding missing components to the media that could enhance the growth. There were 115 total physical conditions and nutriments assigned by the database (http://www.igs.cnrs-mrs.fr/axenic-cgi/generate_table?Mycobacterium+no+off+off) that were tested in different experiments as listed in **Table 5.2-5.7.**

It has been known that 7H9 broth base formulation supports the growth of several mycobacterial species when supplemented with nutrients such as glycerol, oleic acid, albumin and dextrose, except for *M. bovis* which is inhibited by glycerol **(Keating L., 2005).** The presence of large number of inorganic salts in this medium is essential for the growth of mycobacteria. For example, sodium citrate, when converted to citric acid can hold certain inorganic cations in solution. The albumin protects the cells from toxic free fatty acids. Catalase destroys toxic peroxides that may be present in the medium; dextrose is an energy source; and sodium chloride provides essential electrolytes **(Cohn M., 1968).**

Reducing agents used in some media such as pyruvate, catalase, DMSO, L-cysteine, sodium thioglycolate, ascorbic acid, fetal bovine serum, glycerol, n-propyl gallate, sodium metabisulfite, ferrous sulfate and potassium permanganate, degrade or prevent the formation of oxygen intermediates like hydrogen peroxide and scavenge toxic radicals **(Nebra Y., 2002).** Some reducing agents (DTT, sodium thioglycolate, L-cysteine and glutathione) can protect cell function by; i- induce low-oxidation-reduction potential, ii-provide –SH groups that activate enzymes needed in the electron transport system **(Dhople A., 1991).**

Since *M. leprae* has not been cultivated *in vitro*, it is a challenge to determine bacterial viability. In 1960 Shepard used foot pad of immune-competent mouse (MFP) to cultivate *M. leprae* bacilli. This resulted in six to eight doubling cycles of *M. leprae* after 60-150 days. This technique was successfully used to discriminate between viable (multiplying) and non-viable bacteria. It was also used to monitor antimicrobial activity of a drug against *M. leprae* in mice. Also, it has been used to measure drug susceptibility of *M. leprae* recovered from leprosy patients and studies the efficacy of leprosy treatment in clinical trials. However, due to large cell inoculation needed, long incubation time and a lack of sensitivity and precision of culturing in cell-free medium, this technique has not been used by many laboratories **(Levy L., 2006).**

Because of the limitation of the mouse foot-pad technique, alternatives have been developed such as RR assay **(Franzblau S., 1988).** The RR procedure is based on measuring the metabolic activity of *M. leprae*, which is the ability of the bacteria to

oxidize radiolabeled ^{14}C palmitic acid to generate $^{14}CO_2$ accumulated over 7 days

cumulative counts per minute (CPM). Using the metabolic activity by measuring the $^{14}CO_2$

released in the RR assay has been used to study anti leprosy drug susceptibility **(Hastings R., 1988).** RR assay was found to be correlated well to *M. leprae* grow in the mouse foot pad and can be used as an alternative for MFP technique in many studies **(Truman R., 2001).** Truman *et al* found that *M. leprae* loses viability very quickly after harvest from MFP when stored in liquid medium at 37ºC or 1h in freezing condition **(Truman R., 2001).** Also the RR assay in another study was compared to the percentage of live bacteria using fluorescence viability staining (VS) assay **(Lahiri R., 2005).** However, the RR assay is not very sensitive because it reflects 7 days of metabolic activity beside the expense and the time consuming of the technique and the using of radioactive substances.

Molecular methods could be the key to test the bacterial viability. Unlike DNA and rRNA, it has been demonstrated that there was correlation between detectable mRNA species and bacterial viability **(Hellyer T., 1999, Keer J., 2003).** Comparing media in terms of supporting cells viability using the mRNA and finding a sets of genes as viability markers were the goals of this study.

All the DNAs, RNAs extracted from *M. leprae* inoculated into different media formulation in **Table 5.6** (#1-21) were amplified using primer combination sets **(Table 5.8)**. Media #1 and 21 are the base line media since they only have NHDP media with no additives. The rest of the media have 2% glycerol beside other additives. Some of the media that have sodium thioglycolate (0.1%) such as media #11 and 15 have negative

effect (suppress) on the cells. Thioglycolate is a commonly used reagent for bacteriological research to maintain reducing conditions in media and mediate ADP and ATP formation from inorganic phosphate **(Kato L., 1985).** Sodium thioglycolate media has been used as differential media that can differentiate two distinct patterns of growth based on their relationship to the oxygen either a strictly fermentative type or a facultative anaerobe. (http://www.jlindquist.net/generalmicro/dfnewthiopage.html). The negative effect of reducing agents (Sodium thioglycolate and DTT) on *M. leprae* metabolism has been shown previously by Franzblau in an *in vitro* system **(Franzblau S., 1988).**

    M. leprae DNA in the tested media extracted from all cells was detected from all tested combination sets (data not shown). The expression of different genes from those media **(Figure 5.3)** demonstrated that *M. leprae* in media #11 and 15 have the lowest gene expression except for the 16S rRNA that has longer half-life and high copy number. Comparing the amplification from cDNA prepared from media #1 and 21 (base line) samples to media with the glycerol (2-20 except 11 and 15, 16) it seems that the base line media has a lower expression level (mRNA). For example in **Figure 5.3 B** the intensity of the bands for media #2 and 3 are stronger for all tested combination than that for 1 and 21 media. The expression of the *sodA* and *atps* genes were detected for the cells in all the media except for media # 11 and 15 that have sodium thioglycolate (**Figure 5.3 E).** We conclude that the NHDP with the 2% glycerol is an excellent medium to support survival of *M. leprae* for one week. However, the challenge is to prevent the drop in viability during the second week. This was tested by a second experiment to validate the importance of the glycerol in maintaining the cells for more than 7 days (up to 14 days).

We noticed from the RT-PCR study and the summary **Tables S5. 1** that there are some genes with expression levels that correlate well with the RR and could be used to indicate the stability and viability of the cells. These genes are *sodA, atps, glpK, glpD2* and *glpA2* that can differ between 3 and 7 day samples. We also noticed that *glpA1* has weak expression for some media even through it is pseudogene.

Our data shows a good correlation between the molecular method RT-PCR and the RR assay (**Figure 5.2)** of *M. leprae* grow in different media. We have shown that mRNA is rapidly degraded, which results in detection of only viable bacteria in some media. The qRT-PCR data from medium tested in two independent experiments (biological replicates) with three technical replicates each showed that all tested messages (*sodA, atp-α* and *glpdA2*) and the 16S ribosomal RNA were expressed in the media containing the 2% glycerol for all the time points starting from 0 up to 21 days. On the other hand the same messages fluctuated in media containing only baseline (NHDP) or in media with 0.1% thioglycolate. In fact the mRNA for some genes (particularly s*odA*) were lost or decreased after 7 days. The 16S rRNA showed constant values or slight decrease in case of thioglycolate media.

Many studies have used 16S rRNA as indicator for the bacilli viability, but we show that even cells that have completely lost their viability (by RR and VS) in some media (T, R), the 16S rRNA expression was still detectable by the qRT-PCR with average Ct value ~25-27 in suppressing media containing T or R . Therefore, the correlation between the

cell viability using the RR assay and the expression of the 16S rRNA is very week (**Figure 5.13**).

RR = 27294 + 10.67 cDNA SQ avg 16S rRNA
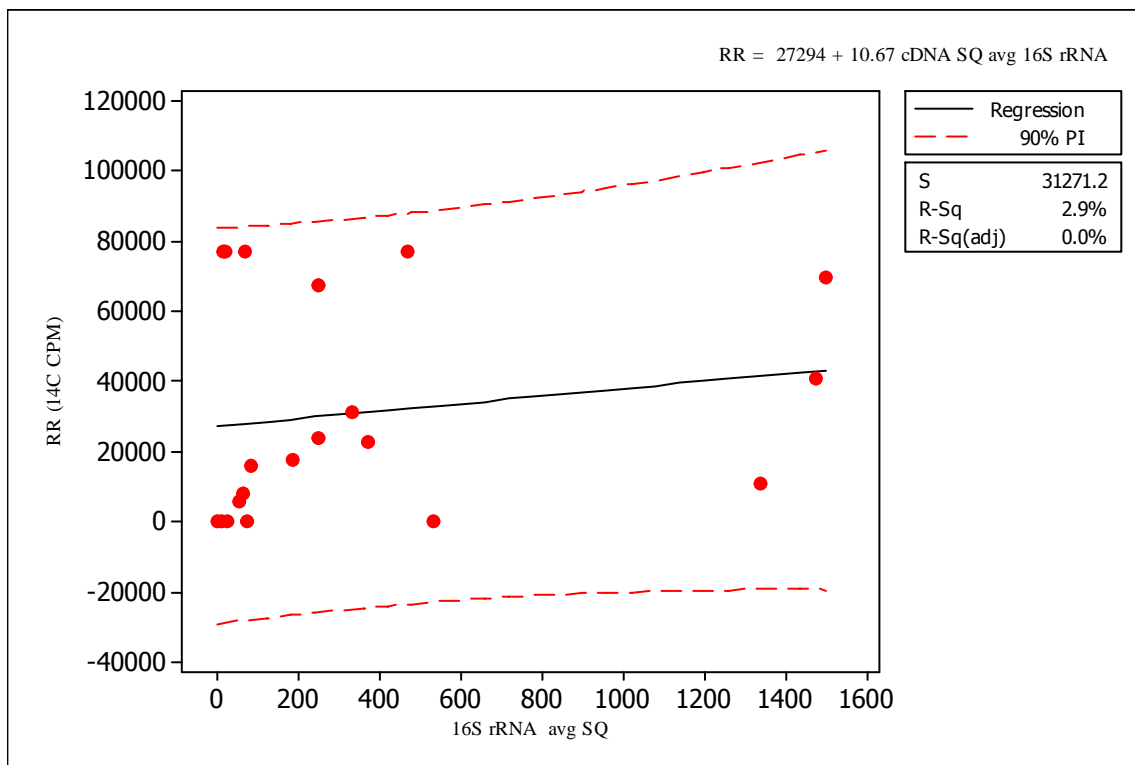
Figure 5.13: Correlation of *16S rRNA* qRT-PCR (SQ) results with the RR values (for the same sample sets) using fitted line plot.

Gene expression of *sodA* was very sensitive in determining the status of the cells in each medium. For example, the bacilli in the media containing the thioglycolate showed significant decline in the expression of soda by 10 days compared to other genes tested. The media containing glycerol showed stability in the gene expression (three targets; *sodA, atp-α* and *glpdA2*) up to 21 days.

In previous studies there was good correlation between membrane integrity (VS) and metabolic activity (RR) in bacilli freshly harvested from the nu/nu MFP, which in turn has been shown to correlate with MFP growth (**Lahiri R., 2004, 2005**). In our study the tested assays; the RR, viability staining (VS), RT-PCR and qRT-PCR can be correlated together in terms of showing the effect of different supplement on the bacterial viability and gene expression. The RR and VS were correlated together in this study and then they were correlated to the gene expression of *sodA* in different media. However, unlike the metabolic assays (RR) and theVS, the qRT-PCR requires fewer bacilli and less time to perform.

It now appears that 2% glycerol enhances the viability of *M. leprae* in these *in vitro* assays. This is statistically significant as seen by RR assay in **Figure 5.4** and RT-qPCR data in **Figure 5.10.** Glycerol is the preferred carbon source for *in vitro* growth of many mycobacterial species, including *M. tuberculosis* (**Ratledge P., and Wheeler P., 1988, Keating L., 2005**). It has been hypothesized that glycerol and its metabolic derivatives can act as precursors in the biosynthesis of lipids and cell wall components. Also, beta-oxidation, glyoxylate shunt and gluconeogenesis pathways have been shown to be upregulated in mycobacteria for *in vivo* growth in macrophages (**Keating L., 2005**).

Supplementary Figure
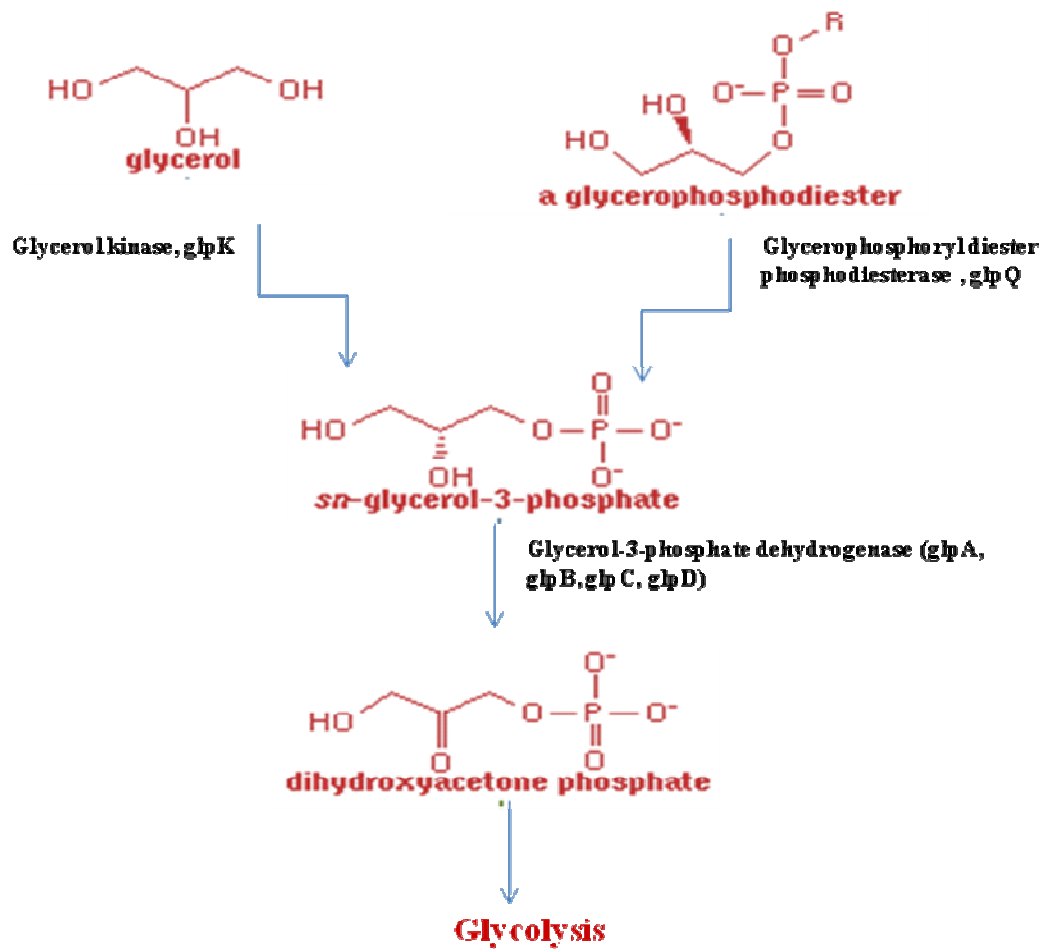
Figure S5.1: Glycerol pathway.

Supplementary Tables

Table S5.1: Summary of gene expression of eight *M. leprae* genes using multiplex PCR (combination1 and 3 primer sets) based on detection on stained agarose gels. In column 1, the numbers refer to media #, followed by 3d or 7d to indicate incubation duration in days.

cDNA Sample	Combination 1				Combination 3			
	glpK	*glpD1*	*glpD2*	*sdhD*	*gyrA*	*gyrB*	*folP*	*rpoB*
1-3d	+*	-	+*	+*	+*	+*	+*	+*
1-7d	+*	-	+*	+*	-	-	-	+*
2-3d	+	-	+	+	+	+	+	+
2-7d	+	-	+	+	+	+	+	+
3-3d	+*	-	+*	+*	+*	+*	+*	+*
3-7d	-	-	-	+*	-	-	-	-
4-3d	+*	-	+*	+*	+	+	+	+
4-7d	+*	-	+*	+*	-	-	+*	+*
5-3d	+	-	+	+	+	+	+	+
5-7d	+	-	+	+	+*	+*	+*	+*
6-3d	+	-	+	+	+	+	+	+
6-7d	+	-	+	+	+*	+*	+*	+*
7-3d	+	-	+	+	+*	+*	+*	+*
7-7d	+	-	+	+	+*	+*	+	+

8-3d	+	-	+	+	+	+*	+	+
8-7d	+	-	+	+	+*	+*	+*	+*
9-3d	+	-	+	+	+	+*	+	+
9-7d	-	-	-	-	+*	+*	+*	+*
10-3d	+	-	+	+	+	+	+	+
10-7d	+*	-	+*	+*	+	+	+	+
11-3d	-	-	-	-	-	-	-	-
11-7d	-	-	-	-	-	-	-	-
12-3d	+	-	+	+	+	+	+	+
12-7d	+*	-	+*	+*	+	+	+	+
13-3d	+	-	+	+	+	+	+	+
13-7d	+*	-	+*	+*	+*	+*	+*	+*
14-3d	+	-	+	+	+	+	+	+
14-7d	+	-	+	+	+	+	+	+
15-3d	+	-	+	+	+	+	+	+
15-7d	-	-	-	-	-	-	-	-
16-3d	+*	-	+*	+*	-	-	+*	+*
16-7d	+*	-	+*	+*	-	-	+*	+*
17-3d	+	-	+	+	+	+	+	+
17-7d	+	-	+	+	+	+	+	+
18-3d	+	-	+	+	+	+	+	+
18-7d	+	-	+	+	+	+	+	+

19-3d	+	-	+	+	+	+	+	+
19-7d	+	-	+	+	+	+	+	+
20-3d	+*	-	+*	+	+	+	+	+
20-7d	+	-	+	+	+	+	+	+
21-3d	+	-	+	+	+	+*	+	+
21-7d	-	-	-	-	-	+*	-	-

+*: weak

The media that show some differences such as media # 1, 2, 3, 11, 15, 16 and 21 have been PCR repeated twice with all combination. All PCR resulted in good expression of the tested genes for the media #2 and 3 (contain glycerol), weak expression for the media #1 and 21 (baseline) and very weak or lost the expression for some genes for the media # 11 and 15 (contain thioglycolate) **(Table 5.5).**

Table S5.2: Summary results (interpretation) of the effect of some media supplements on

M. leprae respiration (RR results) as compare to the base line media (NHDP).

Main carbon source	Additive	Comment
7H9+ Glucose with Amino acid (base line)	Vitamin mix	It showed 7 fold decreased respiration by 7 days compared to the same base line media.
7H9 +Sucrose with Amino acid	Vitamin mix	It showed 2 fold decreased respiration by 7 days compard to the same base line media.
7H9 + Sodium Thioglycolate with Amino acid	Vitamin mix	Suppress the cell respiration by 7days.
7H9+ Glutamine with Amino acid	Vitamin mix	It showed 1.5 fold increased respiration by 3 days and 2.3 fold by 7 days.
7H9 + Glycerol with Amino acid	Vitamin mix	It showed 2 fold decreased respiration level by 7 days.
7H9 + Yeast Extract with Amino acid	Vitamin mix	It showed 1.8 fold increased respiration by 3 days and 1fold by 7 days.
7H9 + Brain Heart Infusion with Amino acid	Vitamin mix	It showed 1.3 fold decreased respiration by 3 days and 1.5 fold by 7 days.
7H9 + Fetal Calf Serum with Amino acid	Vitamin mix	It showed 1.7 fold decreased respiration by 7 days.
7H9+ Glucose with Amino acid (base line)	Trace Elements	It showed 2.4 fold decreased respiration by 7 days.
7H9+ Sucrose with Amino acid (base line)	Trace Elements	No change
7H9 + Sodium Thioglycolate with Amino acid	Trace Elements	It showed 1.7 fold decreased respiration by 3 days, at 7 days no change (respiration stopped)
7H9+ Glutamine with Amino acid mix	Trace Elements	It showed 2 fold increased respiration level by 7 days.
7H9 + Glycerol with Amino acid mix	Trace Elements	It showed 2.5 fold increased respiration by 7 days.
7H9 + Yeast Extract with Amino acid	Trace Elements	It showed 2 fold increased respiration by 3 days, 1.6 fold decrease by 7 days.
7H9 + Brain Heart Infusion with Amino acid	Trace Elements	It showed 1.3 fold decreased respiration by 3 days
7H9 + Fetal Calf Serum with Amino acid	Trace Elements	It showed 1.4 fold decreased respiration by 3 days
7H9+ Glucose with Amino acid (base line)	Lipid Cocktail	It showed 2 fold decreased respiration by 7 days

7H9+ Sucrose with Amino acid (base line)	Lipid Cocktail	It showed 1.6 fold decreased respiration by 7 days
7H9 + Sodium Thioglycolate with Amino acid	Lipid Cocktail	It showed 1.3 fold decreased respiration by 3 days and the respiration stopped by 7 days.
7H9+ Glutamine with Amino acid	Lipid Cocktail	It showed 1.6 fold decreased respiration by 3 days and the respiration stopped by 7 days.
7H9 + Glycerol with Amino acid mix	Lipid Cocktail	It showed 2 fold decreased respiration by 3 days and the respiration stopped by 7 days.
7H9 + Yeast Extract with Amino acid	Lipid Cocktail	No change by 3 days, but by 7 days the respiration stopped.
7H9 + Brain Heart Infusion with Amino acid	Lipid Cocktail	It showed 2 fold decrease respiration by 3 days and the respiration stopped by 7 days.
7H9 + Fetal Calf Serum with Amino acid	Lipid Cocktail	It showed 1.5 fold decrease respiration by 3 and 7 days.
7H9 +Complex carbon	Amino acid mix + vitamin mix + Trace Elements + Lipid Cocktail	It dropped the cell respiration by 3 days and increase (10 fold) the respiration level by 7days
7H9+ complex carbon and nitrogen	Amino acid mix + vitamin mix + Trace Elements + Lipid Cocktail	Dropped the respiration level by 3 days and maintained the same level until 7 days.
7H9 with Casitone+ Bovine Albumin+ Dextrose	Methionine	At 0.01mg/ml, compliantly dropped the respiration by 7 days, at higher con (0.05-.1mg/l) it maintained the cells by 7 days compared to base line media.
7H9 with Casitone+ Bovine Albumin+ Dextrose	Mycobactine	Maintained the cell respiration for 3 and 7 days. No change compared to base line media.
7H9 with Casitone+ Bovine Albumin+ Dextrose	Cobalamine	Maintained the cell respiration for 3 and 7 days. No change compared to base line media.
7H9 with Casitone+ Bovine Albumin+ Dextrose	Thiotic acid	Dropped the cell respiration by 3 and 7 days compared to base line media.
7H9 with Casitone+ Bovine Albumin+ Dextrose	Trehalose	Maintained the cell respiration for 3 and 7 days. No change compared to base line media.
7H9 with Casitone+ Bovine Albumin+ Dextrose	Sodium pyruvate or starch	Maintained the cell respiration for 3 and 7 days. No change compared to base line media.
7H9	FBS + Dextran	Increased the cell respiration level by 3 days and then dropped by more than half the level by 7 days.
7H9	Glucose or Sucrose + ATP	Same as base line media.
7H9 +2% Glycerol	+ Fumaric acid or Succinic acid	Same as base line media.
7H9 +2% Glycerol	Diaminopimilic acid or D-Glucoronic acid or N-acetyl	Maintained the cell respiration for 3 and 7 days better than the base line.

	Glucosamine or Vitamin Mix or L-Glutamine	
7H9 +2% Glycerol	+ Sodium acetate or Sodium pyruvate or Cyanocobalamine or Trace elements or Amino Acid Mix	Maintained the cell respiration for 3 and 7 days better than the base line.
7H9 +2% Glycerol	+ Glucose + Amino Acid Mix + Trace elements + Vitamin Mix + ATP	Same as base line media
7H9 +2% Glycerol	DTT (0.1%)	Suppressed the cell respiration by 3 and 7days.
7H9 + 2% Glycerol	-	Showed better cell respiration by 7 days compared to the base line (NHDP).
7H9 + 2% Glycerol	+ Hemin or Amino Acid Mix or Trace elements + Vitamin Mix or Ribose or N-acetyl Glucosamine + D-Glucoronic acid + Diaminopimilic acid or FBS + Dextran or L-Glutamine or Sodium pyruvate or Cynocobalamine or L-Methionine + FBS + Dextran	Showed the same effect as 7H9 + glycerol only.
7H9 + 2% Glycerol	+ L-Cysteine (0.1%)	Showed decreased the cell respiration level by 3 and 7 days compared to base line.
7H9 + 2% Glycerol	+Sodium Thio Glycolate (0.1%)	Showed immediate dropped the cell respiration level by 3 and 7 days.
7H9 + 2% Glycerol	+ Rifampicin	Showed dropped the cell respiration level by 3 and 7 days.

The red texts are for the media that showed negative effect on the cell respiration.

5.6. FUTURE DIRECTIONS

We have shown the ability of *M. leprae* to be maintained in artificial media for 21 days using the molecular method. However, it is not clear whether the cells are doubling (replicating) or not. Further experiments are necessary to determine replication of the bacilli in these media.

Since *M. leprae* has not been cultivated *in vitro*, the gene expression profile either from artificial media or through interaction with the host has never been defined. Further experiments that could be done in this area are to compare the gene expression profile of *M. leprae* from the *in vitro* source (e.g. NHDP + glycerol) against the *M. leprae* from infected tissues (armadillo or patient). This experiment will facilitate identifying the virulence genes and pathways used during the infection. This also will help in understanding the mechanisms and the pathogenesis of leprosy. Furthermore, the lipidome profile *of M. leprae* purified from armadillo infected tissue has been studied (this thesis research). Further study of *M. leprae* lipidome derived from the *in vitro* culture (this study) will facilitate identifying the missing pathways *in vitro* compared to *in vivo* condition.

Another useful experiment that could be done based on this *in vitro* trial is to characterize the whole genome sequencing of *M. leprae* (transcriptome) based on the mRNA prepared from *M. leprae* grown in the media trials. The bacterial metabolite could also be analyzed to identify the pathway that is used by the *M. leprae* in each media conditi

References

1. Pattyn SR (1977) The problem of cultivation of *Mycobacterium leprae*: a review with criteria for evaluating recent experimental work. Leprosy in India 49: 80-95.

2. Pattyn SR (1973) The problem of cultivation of Mycobacterium leprae. A review with criteria for evaluating recent experimental work. Bulletin of the World Health Organization 49: 403-10.

3. Cole ST, Eiglmeier K, Parkhill J, James KD, Thomson NR, et al. (2001) Massive gene decay in the leprosy bacillus. Nature 409: 1007-1011.

4. Hutchinson James (1987) The in vitro cultivation of *Mycobacterium leprae.*

5. Charles B, Shepard C (1960) The experimental disease that follows the injection of human leprosy bacilli into foot-pads of mice. JEM 112: 445-454.

6. Samuel DR, Godal T, Myrvang B, Song YK (1973) Behavior of *Mycobacterium leprae* in human macrophages in vitro. Infection and immunity 8: 446-449.

7. Sharp AK, Banerjee DK (1984) Attempts at cultivation of *Mycobacterium leprae* in macrophages from susceptible animal hosts. Int J Lepr Other Mycobact Dis: Official organ of the International Leprosy Association 52: 189-197.

8. Kato L (1978) Cholesterol, a factor which is required for growth of mycobacteria from leprous tissues. Int J Lepr Other Mycobact Dis: official organ of the International Leprosy Association 46:133-143.

9. Kato L (1983) In vitro cultivation of Mycobacterium X from *Mycobacterium leprae*-infected tissues in acetone-dimethylsulfoxide-tetradecane medium. Int J Lepr Other Mycobact Dis: official organ of the International Leprosy Association 51: 77-83.

10. Kato L (1985) A culture medium for cultivation of mycobacteria, probably *Mycobacterium leprae* from *Mycobacterium leprae* infected tissues. Indian J lepr 57: 728-738.

11. Dhople a M, Green KJ, Osborne LJ (1988) Limited in vitro multiplication of *Mycobacterium leprae*. Annales de l'Institut Pasteur. Microbiol 139:213-223.

12. Ishaque M (1989) Direct evidence for the oxidation of palmitic acid by host-grown *Mycobacterium leprae*. Res. MicrobioL 140:83-93.

13. Dhople AM, Lamoureux LC (1991) Factors influencing the in vitro growth of *Mycobacterium leprae*: effect of oxygen. Microbiol Immunol 35:507-514.

14. Nakamura M, Matsuoka M (2001) Limited ATP generation in cells of Mycobacterium leprae Thai-53 strain in enriched Kirchner liquid medium containing adenosine. Int J Lepr Other Mycobact Dis: official organ of the International Leprosy Association 69:13-20.

15. Ogata H, Claverie J-M (2005) Metagrowth: a new resource for the building of metabolic hypotheses in microbiology. Nucleic acids research 33: D321-4.

16. Lahiri R (2005) Application of a viability-staining method for *Mycobacterium leprae* derived from the athymic (nu/nu) mouse foot pad. J Med Microbiol 54: 235-242.

17. Lahiri, R., Randhawa B, and Krahenbuhl J (2004) Application of a viability-staining method for *Mycobacterium leprae* derived from the athymic (nu/nu) mouse foot pad. J. Medical Microbiol. 54:235-242.

18. Franzblau SG (1988) Oxidation of palmitic acid by *Mycobacterium leprae* in an axenic medium. J Clin Microbiol 26:18-21.

19. Franzblau SG, Biswas AN, Jenner P, Colston MJ (1992) Double-blind evaluation of BACTEC and Buddemeyer-type radiorespirometric assays for in vitro screening of antileprosy agents. Leprosy review 63: 125-33.

20. Agrawal VP, Shetty VP (2007) Comparison of radiorespirometric budemeyer assay with ATP assay and mouse foot pad test in detecting viable *Mycobacterium leprae* from clinical samples. Indian J. Med Microbiol. 25: 358-363.

21. Lavania M, Katoch K, Katoch VM, Gupta AK, Chauhan DS, et al. (2008) Detection of viable *Mycobacterium leprae* in soil samples: insights into possible sources of transmission of leprosy. Infect Genet Evol. 8: 627-631.

22. Van der Vliet GM, Schepers P, Schukkink R A, Van Gemen B, and Klatser P R (1994) Assessment of mycobacterial viability by RNA amplification. Antimicrob Agents Chemother 38:1959-1965.

23. Phetsuksiri B, Rudeeaneksin J, Supapkul P, Wachapong S, Mahotarn K, et al. (2006) A simplified reverse transcriptase PCR for rapid detection of *Mycobacterium leprae* in skin specimens. FEMS Immunol Medical Microbiol 48:319-328.

24. Keer, J, and Birch L (2003) Molecular methods for the assessment of bacterial viability. J. Microbiol. Methods. 53:175-183.

25. Hellyer TJ, Desjardin LE, Hehman GL, Cave MD, Eisenach KD (1999) Quantitative Analysis of mRNA as a Marker for Viability of *Mycobacterium*

tuberculosis Quantitative Analysis of mRNA as a Marker for Viability of *Mycobacterium tuberculosis*. J. Clin Microbiol 37:290-295.

26. Williams DL, Oby-Robinson S, Pittman TL, Scollard DM (2003) Purification of *Mycobacterium leprae* RNA for gene expression analysis from leprosy biopsy specimens. Bio Techniques 35:534-536.

27. Martinez a. N, Lahiri R, Pittman TL, Scollard D, Truman R, et al. (2010) Molecular Determination of *Mycobacterium leprae* Viability by Use of Real-Time PCR. J Clin Microbiol 48:346-346.

28. Truman, R. W. and Krahenbuhl, J. L. (2001). Viable *M. leprae* as a research reagent. Int J Lepr Other Mycobact Dis 69:1–12.

29. Lahiri R (2005) Application of a viability-staining method for Mycobacterium leprae derived from the athymic (nu/nu) mouse foot pad. Journal of Medical Microbiology 54: 235-242.

30. Siddiqi SH, Libonati JP, Carter ME, Hooper NM, Baker JF, et al. (1988) Enhancement of Mycobacterial Growth in Middlebrook 7H12 Medium by Polyoxyethylene Stearate. Current Microbiology 17: 105-110.

31. Vissa VD, Brennan PJ (2001) Minireview The genome of *Mycobacterium leprae*: a minimal mycobacterial gene set. Genome Biology 2: 1-8.

32. Mukherjee R, Antia NH (1985) Intracellular multiplication of leprosy-derived mycobacteria in Schwann cells of dorsal root ganglion cultures. J Clin Microbiol 21:808-14.

33. Nakamura K (1949) Studies on cultivation of the leprosy bacillus. Hawaii Med J 8:265.

34. Sreevatsa, Katoch K (1997) Viability of *M. leprae* while undergoing laboratory procedures. Indian J Lepr 69: 353-359.

35. Keating L a, Wheeler PR, Mansoor H, Inwald JK, Dale J, et al. (2005) The pyruvate requirement of some members of the *Mycobacterium tuberculosis* complex is due to an inactive pyruvate kinase: implications for in vivo growth. Molecular Microbiol 56:163-174.

36. Cohn ML, Waggoner RF, and McClatchy JK (1968) The 7H11 medium for the cultivation of mycobacteria. Am. Rev. Resp. Dis. 98:295-296.

37. Nebra Y, Jofre J, Blanch AR (2002) The effect of reducing agents on the recovery of injured Bifidobacterium cells. J Microbiol Methods 49:247-254.

38. Levy L, Ji B (2006) The mouse foot-pad technique for cultivation of *Mycobacterium leprae*. Lepr Rev 77:5-24.

39. Hastings RC, Gillis TP, Krahenbuhl JL, Franzblau SG (1988) Leprosy. Clin Microbial Rev 1:330-348.

40. Wheeler PR, Ratledge C (1988) Use of Carbon Sources for Lipid Biosynthesis in a Comparison with Other Pathogenic Mycobacteria. J. Gen Microbiol 134: 2111-2121.

CHAPTER 6

6.1. Final summary

M. leprae is an intracellular and uncultivable pathogenic bacterium. It has a massive reduction in its genome compared to other mycobacteria. It is highly dependent and acquires host resources in order to survive, replicate or persist. It has evolved different mechanisms to adhere and survive inside human cells. It uses the host genetic background to manipulate the immune system for long form survival. The clinical forms of leprosy (lepromatous versus tuberculoids) could also relay on unknown host or bacterial factors. These factors can be investigated to understand the pathogenicity of the disease and the development of sensitive and specific diagnosis of leprosy.

The absence of knowledge about the host-bacterial interaction and a disease biomarker lead to late diagnosis and nerve damage in leprosy. Understanding the molecular machinery used by *M. leprae* during interactions with the host and the pathogenesis of leprosy will add new ways of interfering with pathogenic bacteria and facilitate new diagnostic approach, therapy and vaccine.

Many approaches could be used to study host-pathogen interaction such as genetic (up regulation of specific genes), biochemical (protein regulation). Recently, metabolomics of both host and pathogen become interesting to know more about the disease mechanisms. Such approaches were used to uncover the mechanism(s) of host-pathogen interactions in leprosy, a spectral disease (different clinical forms). There are many factors (host or

bacterial) that modulate the range of clinical outcomes from susceptible to resistant. Therefore, unbiased broad based screening assays 'omics' such as metabolomic, lipidomic, and proteomic, methods were used to identify the host or bacterial factors that contribute to leprosy.

Omics are emerging as powerful technologies to understand the phenotypic changes in disease at many areas at the protein, lipid and genome level. Mass spectrometry based 'omics' is a rapidly growing technique that can be used to detect many molecules in complex biological samples. This technique can be applied for biomarker discovery and lead to direct clinical applications including aiding diagnosis, monitoring the progression of a disease, and monitoring treatment efficacy.

The metabolome of leprosy patient sera were examined using the non-targeted metabolomics approaches to identify circulatory biomarkers (Chapter 2). This resulted in identification of certain features that were increased in the high BI patients. The chemical analysis by MS/MS was used to uncover the nature of these significant features that were identified as PUFAs. The main PUFAs that increased in these patients were n-6 (AA) and n-3 (EPA and DHA).

Lipid has been linked to many chronic diseases (diabetes, obesity, atherosclerosis, Alzheimer), since lipid has many functions in cells. Also, analysis of host/pathogen lipids is not something new. However, the new approach of liquid chromatography and mass spectrometry added new aspect for lipidomics. Mass spectrometry electrospray ionization

(ESI) with Q-TOF coupled with reversed-phase column is a great tool to study intact complex lipid and offers high resolution, accurate mass and tandem mass spectrometric data.

Lipids are the major carbon source for nutrition during the growth of *Mycobacterium* spp. *M. leprae* has been shown to induce lipid droplet formation through up-regulation of lipid intake and expression of host lipid metabolism genes **(Cruz D., 2008).** *M. leprae* creates a lipid-rich phagosome in macrophage or SCs with lipid droplets that is favorable for its survival **(Mattos KA, 2011).**

The availability of animal models for leprosy such as armadillo and gene knockout mice (nude mice), facilitated several genetic, metabolic, proteomic and antigenic studies of the bacillus and host interaction. The pathogenesis of the disease was also established using the only animal model for leprosy, the armadillo. The availability of partial annotated genome for this animal enabled further investigation. Lipidomics approach allowed detection, characterization and quantification of many different classes of complex lipids (eukaryotic system and also the mycobacteria) from tissue samples. Such an approach leads to understanding the biological activities of compounds during the disease state and their pathways. Comparative lipidomic profiling of the host (armadillo) tissues during normal and infected state is an important aspect for therapeutic interventions. The lipid profiles of infected armadillo tissues (nerve, liver and spleen) showed increased levels of triacylglycerols (TAGs) with mono- and di-unsaturated fatty acids compared to uninfected tissues. Furthermore, the expression of genes involved in the synthesis of these

FAs and TAG (SCD9, ELOVL5 and DGAT) confirmed our findings. These genes were found to be up-regulated in the infected tissue (Chapter 3).

All these lipids (PUFAs and TAGs with unsaturated fatty acids) that were found in the lepromatous form of the disease either in the armadillo or the human sera can induce the anti-inflammatory phenotype. The combined gene expression and lipidomics analyses revealed that *M. leprae* induces significant changes in the expression of multiple genes (TAG and FA synthesis) controlling inflammatory pathways through changing the lipid profile in *M. leprae* rich environment.

Moreover, the proteome profile of armadillo infected nerve was contrasted to the uninfected nerve. The data from these experiments pointed to changes in the infected nerve protein profiles (mainly decrease in the amount of myelin components (myelin P2), increase in the level of antibodies (IgG and IgM) in the infected nerves and the present of antibodies to nerve components (myelin P2) in the lepromatous leprosy sera (Chapter 4).

All these findings support the phenotype found during leprosy infection, especially in the lepromatous form of the disease. This include peripheral nerve demyelination; increased antibody production, modulated host lipid metabolism and induction of anti-inflammatory response that facilitate bacterial survival and nerve injury.

The in-ability to cultivate *M. leprae in vitro*, affects many aspects of understanding the pathological mechanisms of leprosy. However, the growth of *M. leprae* in mouse footpads also provides viable bacilli for testing the growth of the bacilli *in vitro*.

Therefore, a trial study was conducted to maintain the viability of *M. leprae* in different artificial media (Chapter 5). The viability of the bacteria was determined through RR assay and gene expression analysis of several mRNAs and ribosomal RNA.

The project aimed to maintain and culture *M. leprae* in artificial media by providing different supplements with simple and complex carbon and nitrogen sources that are missing in the bacteria biosynthetic pathways. After several trials with different supplements and concentrations, 7H12 media with 2% glycerol was found to be a good nutritional source to maintain *M. leprae* up to two weeks based on the RR and qRT-PCR data. It was previously shown that glycerol is the preferred carbon source for *in vitro* growth of many mycobacteria. Glycerol and its metabolic derivatives can act as precursors in the biosynthesis of lipids and cell wall components. On the other hand, 7H12 media containing reducing agent such as L-cysteine or DTT or thioglycolate 0.1% suppress *M. leprae* respiration starting at 3 days.

These new metabolomic, lipidomic and proteomic approaches suggest biomarkers of infection and pathogenesis in leprosy, which could be further investigated to provide mechanism of action. These biomarkers could also be applied to clinical diagnostic assay. In order to use these biomarkers for diagnosis of leprosy, further studies should be done. These studies involve monitor the change in the level and the type of these biomarkers at

different stages of the disease before and after MDT treatment. This will help in answering

the question of whether these markers are connected to the disease progression.